Translocator Protein 18 kDa: from Biomarker to Function

Meredith Kyla Loth

Submitted in partial fulfillment of the
requirements for the degree of
Doctor of Philosophy
under the Executive Committee
of the Graduate School of Arts and Sciences

COLUMBIA UNIVERSITY

2018

DISSERTATION ABSTRACT

Translocator Protein 18 kDa: from Biomarker to Function

Meredith K. Loth

Translocator Protein 18 kDa (TSPO) is a protein that is expressed at low levels in the brain, but upon brain injury or inflammation, increases its expression in the areas of the brain specific to injury. In this way, TSPO can be used as a biomarker of brain inflammation and injury. TSPO is primarily expressed in two cell types, microglia and astrocytes, and is used as a marker of reactive gliosis in various brain pathologies. Currently, there is a paucity of knowledge on the function(s) of TSPO in glial cells. Recent studies using conditional and global TSPO knockout mice have questioned the role of TSPO in translocating cholesterol across the outer mitochondrial membrane as the first step in steroidogenesis.

In the brain, microglia and astrocytes exhibit distinct spatial and temporal patterns of TSPO upregulation. These differential patterns are not well characterized across disease models and in particular, are poorly characterized in the early stages of disease, prior to behavioral and clinical disease manifestations. Importantly, these distinct patterns of TSPO upregulation may indicate different functions of TSPO in microglia and astrocytes.

We examined TSPO levels in a neurodegenerative transgenic mouse model of Sandhoff disease and longitudinally compared TSPO levels to behavioral manifestations of disease and other neuropathological endpoints (neurodegeneration, reactive gliosis, ganglioside accumulation). This study confirmed TSPO upregulation prior to neurodegeneration in a brain region-dependent and disease course-dependent way. In brain regions with increased TSPO levels, there was a differential pattern of glial cell activation with astrocytes being activated earlier than microglia during the progression of disease. Immunofluorescent confocal imaging confirmed that TSPO

colocalizes with both microglia and astrocyte markers, but the glial source of the TSPO response differs by brain region and age in SD mice.

We next wanted to gain insight into the function of TSPO in microglia. We previously demonstrated that TSPO ligands (TSPO-L) (1-100 nM) induced intracellular ROS production which was abrogated by NADPH oxidase (NOX2) inhibitors, thereby indicating an association between TSPO and NOX2. To further elucidate the relationship between TSPO and NOX, we determined the source of ROS production resulting from microglia exposure to TSPO-L. Intracellular and extracellular ROS production was inhibited by NOX inhibitors, but not by a mitochondria permeability transition pore inhibitor, indicating that the source of ROS production is from NOX and not from mitochondria. These findings were confirmed using the mitochondria specific ROS probe MitoSOX.

To further explore the TSPO-NOX2 association, we used 3 molecular approaches to examine protein-protein interactions under unstimulated or stimulated conditions (100 ng/mL lipopolysaccharide (LPS) for 18 hours) in primary microglia. 1) Co-immunoprecipitation (co-IP) revealed that the NOX2 subunits, $gp91^{phox}$ (gp91) and $p22^{phox}$ (p22), co-IP with TSPO supporting a protein-protein interaction. TSPO's association with gp91 and p22 decreased with activation, but TSPO's association with VDAC, a mitochondrial protein, remained constant. These findings suggest that microglia activation changes the dynamics of the TSPO-NOX2 interaction. 2) Confocal imaging and colocalization analysis of TSPO/gp91 or TSPO/p22 immunofluorescence confirmed that TSPO colocalizes with both NOX subunits. Under stimulated conditions, TSPO associated with gp91 and TSPO associated with p22, exhibit significantly decreased colocalization with VDAC suggesting a movement from the mitochondria to other cellular compartments. 3) Duolink Proximity Ligation Assay confirmed that TSPO interacts with p22, gp91 and VDAC. Our

results suggest a novel TSPO-gp91-p22 interaction with VDAC in primary microglia that is disrupted by microglia activation and may be involved with redox homeostasis with significant implications for a new understanding of TSPO glial cell biology.

In summary, the present studies have strengthened the use of TSPO as a preclinical biomarker, confirmed its specific spatiotemporal upregulation in two cell types and have provided a new potential function of TSPO in microglia that has the possibility to revolutionize the TSPO field and to inform neurotoxicity assessments and neurological disease treatments.

.

TABLE OF CONTENTS

List of Charts, Graphs, & Illustrations

List of Abbreviations

AD	Alzheimer's disease
ALS	Amyotrophic Lateral Sclerosis
ANT	Adenine Nucleotide Translocator
ANOVA	Analysis Of Variance
AP-1	Activating Protein-1
ATP	Adenosine 5'-Triphosphate
BDNF	Brain-Derived Neurotrophic Factor
Bmax	Maximal number of binding sites
Bcl-2	B-cell lymphoma 2
CA2	Cornu Ammonis
Ca2+	Calcium ion
CBR	Central Benzodiazepine Receptor
CCR	CC Chemokine Receptor
CD	Cluster of Differentiation
cDNA	Complementary DNA
CGD	Chronic Granulomatous Disease
Cl-	Chlorine ion
CNS	Central Nervous System
CO2	Carbon Dioxide
COX-2	Cyclooxygenase-2
CR	Complement Receptor
CRAC	Cholesterol Recognition/interaction Amino acid Consensus

CREB	cAMP Response Element-Binding
CT	Computed Tomography
CXCR	CXC Chemokine Receptor
DAB	3,3'-Diaminobenzidine
DALY	Disability-Adjusted Life Years
DAPI	4,6-Diamidino-2-Phenylindole
DBI	Diazepam Binding Inhibitor
DHE	Dihydroethidium
DMEM	Dulbecco's Modified Eagle Medium
DMSO	Dimethyl Sulfoxide
DNA	Deoxyribonucleic Acid
DPA-713	N,N-Diethyl-2-[2-(4-Methoxyphenyl)-5,7-Dimethyl-Pyrazolo [1,5-a]Pyrimidin-3-yl]-Acetamide
DPI	Diphenyleneiodonium
EAE	Experimental autoimmune encephalitis
EGTA	Ethylene glycol-bis(beta-aminoethyl ether)-N, N, N', N'-tetraacetic acid
ELISA	Enzyme Linked Immunosorbent Assay
ER	Endoplasmic Reticulum
ERK 1/2	Extracellular Signal Regulated Kinases
FAD	Flavin Adenine Dinucleotide
FBS	Fetal Bovine Serum
GABA	Gamma Aminbutyric Acid
GBD	Global Burden of Disease

GFAP	Glial Fibrillary Acidic Protein
GM-CSF	Granulocyte/Macrophage Colony Stimulating Factor
GPx	Glutathione peroxidase
GRx	Glutaredoxin
GR	Glutathione reductase
GSH	γ-glutamylcysteinyl glycine
GSSG	Glutathione disulfide
H2DCFDA	2',7'-Dichlorohydrofluorescein Diacetate
HBSS	Hank's Balanced Salt Solution
HD	Huntington's disease
Het	Heterozygous
HEXB	β subunit of β-Hexosaminidase
HIV	Human Immunodeficiency Virus
HPLC	High Performance Liquid Chromatography
HRP	Horseradish Peroxidase
IFN-γ	Interferon-gamma
IKK	IκB Kinase
IL	Interleukin
IL-1β	Interleukin-1 type-I beta receptor
IMM	Inner Mitochondrial Membrane
iNOS	Inducible Nitric Oxide Synthase
IodoDPA-713	Iodinated form of N,N-Diethyl-2-[2-(4-Methoxyphenyl)-5,7-Dimethyl-Pyrazolo[1,5-a]Pyrimidin-3-yl]-Acetamide

IP	Immunoprecipitation
IRAK	IL-1 receptor-associated kinase 4
K+	Potassium ion
kDa	KiloDalton
Ki	Dissociation constant for inhibition
KO	Knockout
LAMP-2	Lysosomal-associated membrane glycoprotein 2
LPS	Lipopolysaccharide
MAC-1	Macrophage 1 Antigen
MAM	Mitochondrial Associated Membrane
MAPK	Mitogen-Activated Protein Kinase
mGluR	Metabotropic Glutamate Receptors
MHC II	Major Histocompatibility Complex Type II molecules
MOI	Multiplicity of Infection
MPTP	Mitochondrial Permeability Transition Pore
MR	Magnetic Resonance
mRNA	Messenger RNA
MS	Multiple Sclerosis
Na+	Sodium ion
NADPH	Nicotinamide Adenine Dinucleotide Phosphate
NF-κB	Nuclear Factor-kappa B
NGF	Nerve Growth Factor
NMDA	N-Methyl-D-aspartic acid

NO	Nitric Oxide
NOX	NADPH oxidase
Nrf2	Nuclear factor erythroid 2 related factor 2
NT	Neurotrophin
OMM	Outer Mitochondrial Membrane
P450scc	Cytochrome P-450 Side Chain Cleavage Enzyme
PAMPs	Pathogen Associated Molecular Patterns
PBR	Peripheral Benzodiazepine Receptor
PBS	Phosphate Buffered Saline
PD	Parkinson's disease
PET	Positron Emission Tomography
PFA	Paraformaldehyde
PI3K	Phosphatidylinositol 3-Kinase
PIP3	Phosphatidylinositol-3,4,5-Triphosphate
PIP2;7	Aquaporin PIP2;7
PK11195	1-(2-chlorophenyl)-N-methyl-(1-methypropyl)-3-isoquinoline carboxamine
PKA	Protein Kinase A
PKC	Protein Kinase C
PLA	Proximity Ligation Assay
PMA	Phorbol-12-Myristate 13-Acetate
PMN	Polymorphonuclear neutrophils
PND	Post Natal Day

PpIX	Protoporphryin IX
PRR	Pattern Recognition Receptors
PVDF	Polyvinylidene fluoride
qRT-PCR	Quantitative Real Time-Polymerase Chain Reaction
RNA	Ribonucleic Acid
RNS	Reactive Nitrogen Species
Ro5-4864	7-Chloro-5-(4-Chlorophenyl)-1-Methyl-1,3-Dihydrobenzo[e][1,4]Diazepin-2-one
ROS	Reactive Oxygen Species
RPM	Revolutions Per Minute
SD	Sandhoff Disease
SEM	Standard Error of the Mean
SF	Sulforaphane
SH3	src Homology Domain
SOD	Superoxide Dismutase
SPECT	Single Photon Emission Computed Tomography
SR	Scavenger Receptor
StAR	Steroidogenic Acute Regulatory Protein
TBI	Traumatic Brain Injury
TBS	Tris-Buffered Saline
TEM	Transmission Electron Microscopy
TGF-β	Transforming Growth Factor-Beta
TLR	Toll-Like Receptor

TNF	Tumor Necrosis Factor
Trx	Thioredoxin
TSPO	Translocator Protein (18-kDa)
TTN	Triakontatetraneuropeptide
VDAC	Voltage-Dependent Anion Channel
WHO	World Health Organization
WT	Wildtype

Acknowledgements

I would like to thank my advisor and mentor, Dr. Tomás Guilarte for helping me grow and mature into a competent, independent, and critical thinking scientist. Without his encouragement, guidance, support, and knowledge I may not have chosen to pursue a PhD and discovered how much I truly love being a research scientist: a career where it is always encouraged to ask questions, find out how things work, and discover the truth underneath. Dr. Guilarte's high expectations, passion for science, commitment to his lab and research, continuous stream of ideas, and willingness to ask questions and challenge the status quo have all inspired me and greatly contributed to my growth and development as a scientist.

I would like to thank my dissertation committee: Dr. Joseph H. Graziano, Dr. Diane B. Re, Dr. Kim Tieu, and Dr. Jeremy W. Chambers for their time, input, and expertise. Thank you Dr. Graziano for giving me my first opportunity to work in a wet bench lab during my MPH and encouraging me to continue working in a lab after I finished my MPH. It was your lecture in the EHS core in September 2008 during my masters that planted the seed about doing basic science research.You make being a PI look easy, and your continuous and everpresent support throughout my academic journey has been much appreciated. Thank you Dr. Re for your whole hearted support in so many areas of my career. The efficiency, passion, and persistence with which you attack your research career is inspiring, and the warmth and grace you emanate in your professional relationships is refreshing. Thank you Dr. Tieu for always asking questions that help me think of and frame my research in new ways, being willing to challenge me to find new methods to answer research questions and ensuring I am truly measuring what the technique claims. Thank you Dr. Chambers for your open door policy and accessibility; for always being willing to discuss scientific results, ideas, or life lessons; and for cultivating an environment where I can freely express new

ideas regardless of how developed they may or may not be. I appreciate each and every one of you and the multititude of ways you have all supported me on this journey.

Thank you to all of the members of the Guilarte lab whom I have overlapped with, past and present, for their support, commraderie, and willingness to share knowledge and lend a hand: Jennifer Dziedzic, Kirstie Stansfield, Judy Choi, Barbara Soares, Katerina Mancevska, Chun Zhou, Sara Guariglia, Kalynda Gonzales, Meredith Wagner, Vrinda Kalia, Sasha Alikhan, Kristen Ruby, Tania Das, Christina Chung, Jonathan Jacobs, Nada Zaidan, Ingrid Reverte, Juan Perez, Deborah Brooks, Jingyoung Lee, Damaris Albores, Vanessa Nunes de Paiva, Lisa Prince, Mailen Fernandez, Diana Rodriguez, and Diana Azzam. A special thanks to our lab manager, Jennifer Dziedzic, for her willingness to always be an ear to listen, her patience with my questions, my go-to for double checking experimental design, and general aid, love, and support in navigating life in the Guilarte Lab. A special thanks to Dr. Kirstie Stansfield for her approachability as a scientist, her patience with me especially when I was new to the lab, showing me it's possible to multitask like a machine in lab, for the numerous techniques she taught me, and for always being a source of support, encouragement, and knowledge. A special thanks to Dr. Judy Choi for the in depth, thorough and personal training she gave me in handing off the TSPO project. Her patience, thoroughness, and eye for detail allowed me to progress all the more quickly. A special thanks to Dr. Barbara Soares a fellow PhD student in the lab, for always being ready to share a laugh, wizard voice, sass, or wisdom and for so often acting in small ways to be thoughtful, supportive, or make someone laugh. A special thanks to Dr. Kalynda Gonzales for her continuous support in so many different ways including being a companion for the long, late hours in the lab; her high standard of ethics, scientific rigor, and justice; her willingness to ask questions and help others prepare and improve; her infectious passion and enthusiasm for what she does; for making networking look

easy and always using her network to help others get to new places. A special thanks to Juan Perez for generating beautiful microglia cultures for a year for me to work with and giving me back hours of my life to move the research forward faster. And for his easy going attitude and refereshing conversations that made less than pleasnt lab tasks fun. A special thanks to Deborah Brooks for her attention to detail, general support, and for taking the time, energy, and initiative to share her expertise in order to keep the TSPO colony going and ensure the project continuously moves forward.

Thank you to former members of the TSPO project: Judy Choi, MingKai Chen, Anthony Kuhlmann, Jennifer Dziedzic, Chun Zhou, Sara Guariglia, Juan Perez, Deborah Brooks, Vrinda Kalia, Nada Zaidan, Sasha Alikhan, Christina Chung, Jonathan Jacobsen, Meredith Wagner, Vanessa Nunes de Paiva, and Diana Azzam. Whether through your papers, research, optimization of protocols, tissue collection, and microglia generation or through allowing me to teach you, you have all contributed to the basis of this research, moved the project forward, and it is upon your shoulders which I stand.

Thank you to all of those whom I have met along my scientific journey whom have helped me grow by training me, sharing ideas and asking questions including the Tieu Lab (Martin Helley, Carolina Sportelli, Rebecca Fan, and Jennifer Pinnell), the Chambers Lab (Monica Rodriguez, Arlet Acanda de la Rocha, Iru Paudel, and Tony); and Radhika Pradhan, Adnan Divjan, Vesna Slavkovich, Olgica Balac.

Thank you to the Columbia University EHS faculty and students for your knowledge, wisdom, and mentoring. I have learned from each and every one of you.

Thank you to both the Columbia University and Florida International University staff, whose everyday activities make all the research we do possible: Marie Alvarez, Ilka Pinero,

Katherine Martes, and Kenny Ferrieras who order lab supplies. The animal staff particularly Dr. Horatiu Vinerean and Dr. Kevin Prestia as the head veterinarians. The administration including: Nina Kulacki, Lee Marsi, Bernice Ramos Perez, Nancy Loiacono, Melissa Rivera, Andy Kim, and others at Columbia University, and Angel Ruiz, Julian Alarcon, MaryAnn Campos Gato, Anet Saumell, Miriam Tamargo-Ludwig, Maggie Romera, Norma Balladares, Adriana Trespalacios, Connie Ricardo, Darcy Cosano, Ashley Cole, Ileana Perez, and Katie Boulos at Florida International University.

And of course, a huge thank you for those outside of the lab. To my Florida family: Mark and Wendy Murnan; Dan, Lisa, Michael, and Daniel Gonzales; Mary Cuellar; Todd and Juliette Stokes; Gladys Strom; Tim, Gina, and Jenna Johnson; Jeremy Dziedzic; thank you all for the love and support the last two years and providing such a nurturing environment in which to finish up the last 2 years of my PhD.

A huge thank you to my New York City family: Caitlin McKee, Leone Price, Missie Anand, Ambika Anand, Patti DeMatteo, Rother Schlager, Gracie & MacBain, Richard Remigio, Whitney Cowell, Christopher Ovanez. You have all made the journey easier, better, more fun, and inspired me and kept me sane in different ways.

A huge thank you to my family who has been there from the beginning with their unconditional love, unwaivering support, listening ears, and sage advice: my parents, Walter and Diane Loth; my sisters, Kara and Amanda; and my brother in law Patrick and niece and nephew Lily and Benjamin Zielinski. Thank you all for being bright spots in this journey and helping me achieve a major life goal.

And finally, a huge thank you to two of my favorites and teammates for life, Greg and PJ Gonzales. You guys have supported me in every way imaginable, and I am so blessed to have you both on my team.

Dedication

This research is dedicated to anyone that can benefit from these scientific advances, whether they help inform those who are exposed to neurotoxicants, or those with a neurodegenerative disorder. May these advances expand and improve your treatment options, lessen your time to diagnosis, and help future scientists garner more knowledge and generate better solutions to inform researchers, physicians, and public health policy.

Chapter 1: Introduction & Background

INTRODUCTION

Burden of neurological disorder to public health

In 2006, the WHO estimated that neurological disorders affect as many as a billion people worldwide, and that this number is only expected to increase. This is a statistic that is relevant to all as neurological disorders do not discriminate: they can affect any age, gender, race, and socioeconomic status. Further, there are a wide variety of etiologies for neurological disorders, including genetic and environmental factors, as well as interactions between those genetic and environmental factors, thereby increasing the likelihood one can be affected by a neurological disorder.

Global burden of disease (GBD) can be measured in multiple ways, including in terms of mortality, morbidity, and disability. In 1993 a GBD study conducted by the WHO, the World Bank and the Harvard Public School of Public Health, determined that while many neurological disorders or injuries caused little to no direct deaths (mortality), they were major causes of disability or years of healthy life lost (DALYs), and therefore still a major contributor of burden of disease. Specifically, neurological disorders contributed to 92 million DALYs worldwide in 2005 and this is expected to increase to 103 million DALYs by 2030. Additionally, the burden of neurological disorders is expected to increase by the year 2030 regardless of income. Therefore, there is a demand to reduce the burden of neurological disorders. Reducing the burden of neurological diseases can be accomplished through multiple methods including but not limited to raising awareness, taking precaution, or getting treatment to delay the progression of disease, as most neurological disorders are currently incurable.

Reactive gliosis: a hallmark response to brain injury

Brain injury can occur through multiple modalities including stroke, ischemia, traumatic brain injury, neurotoxicant exposure, or various neurodegenerative diseases. Still, regardless of the type or mechanism of brain injury, the archetypal response of glial cells is reactive gliosis where both microglia and astrocytes become reactive and undergo morphological changes, increase proliferation, and modulate growth factor and cytokine release (Chen & Guilarte 2008; McNeela et al 2018; Maeda et al 2007). Reactive gliosis generally has a graded morphological response that is associated with the degree of damage in various forms of brain pathology (Raivich et al 1999). Acutely, reactive gliosis provides a mechanism for limiting the progression of injury. Following chronic activation, the ability of reactive gliosis to limit injury or disease progression decreases and, in some cases, transitions into a harmful state (McNeela et al 2018).). Glial cell activation occurs not only at the sites of primary injury, but also at secondary sites (Chen and Guilarte, 2008) given that as microglia are activated, they can recruit bystanding microglia to become phagocytes, recruit leukocytes and monocytes from the periphery, and eventually astrocytes to become reactive (Raivich et al 1999).

Historically, assessment of reactive gliosis was only possible through postmortem autopsy or invasive biopsies. However, with the advent of positron emission tomography (PET) imaging and *in vivo* imaging techniques, we are able to image specific proteins and biomarkers within the living and active brain. To this end, translocator protein 18 kDa (TSPO) is located exclusively in glial cells in the brain parenchyma and has been used as a sensitive biomarker of reactive gliosis and inflammation associated with a variety of brain insults including chemical-induced neurotoxicity (Kuhlmann and Guilarte 1997, 1999, 2000; Guilarte et al 2003; Chen and Guilarte 2006; Chen et al 2004), ischemia (Gerhard et al 2000); TBI (Coughlin et al 2015, 2017); and

multiple neurodegenerative diseases with an inflammatory component such as Alzheimer's disease, Parkinson's disease, amyotrophic lateral sclerosis (ALS), multiple sclerosis, Zika virus, et cetera. (Zimmer et al 2014; Gerard et al 2006; Zurcher et al 2014; Politis et al 2012; Kuszpit et al 2017). Increased TSPO expression during injury is predominately localized to glial cells, suggesting a role of TSPO in reactive gliosis. Because of the high degree of sensitivity and specificity of increased TSPO levels during brain injury, TSPO has been used as a biomarker to identify injured brain regions, track the progression of injury/ disease, and monitor recovery and efficacy of therapies and treatments. TSPO distribution can also be visualized and quantified both *ex vivo* using receptor autoradiography and *in vivo* using PET and single photon emission computed tomography (SPECT) imaging with the high affinity and specific TSPO ligands that are available and can be radiolabeled (Chen and Guilarte, 2008). These characteristics make TSPO it a powerful tool in assessing neurotoxicity and neurodegenerative disease progression and recovery.

TSPO Background

Translocator protein 18 kDa (TSPO) was discovered in 1977 by Braestrup and Squires. At the time, TSPO was referred to as the peripheral benzodiazepine receptor (PBR) as it was described as a high affinity benzodiazepine binding site in rat peripheral tissue, specifically the kidney (Braestrup & Squires, 1977). The objective of the original experiment by Braestrup and Squires was to find the brain receptor for benzodiazepines using [^{3}H]-diazepam. In using kidney membrane preparations as their negative control for the central-type benzodiazepine receptor (CBR), they observed high levels of [^{3}H]-diazepam specific binding, specifically within the mitochondrial fraction of the kidney (Braestrup & Squires 1977). Thus, even in from its nascence, the TSPO field has been filled with surprises, contradictions, and, enigmas.

Subsequent studies showed that TSPO/PBR and CBR differ in their pharmacological properties. CBR binds benzodiazepines with high affinity (nM) and mediates anxiolytic and anticonvulsant properties of benzodiazepines. CBR is able to inhibit the firing of action potentials by coupling to the γ-aminobutyric acid $(GABA)_A$ receptor on the plasma membrane and modulate the $GABA_A$-regulated opening of Cl^- channels (Tallman et al., 1978). While TSPO also binds to the benzodiazepine valium with high affinity, there is a distinction between the ligands to which these two receptors can bind. 7-chloro-5-(4-chlorophenyl)-1-methyl-1,3-dihydrobenzo[e][1,4]diazepin-2-one (Ro5-4864) is a derivative of valium that binds to TSPO at nanomolar concentrations but to CBR at low affinity (uM concentrations). Conversely, clonazepam binds with low affinity (uM) to TSPO, but with high affinity (nM) to CBR (Schoemaker et al., 1981). TSPO also demonstrates anatomical, structural, and functional differences from CBR, which will be discussed later on in this chapter.

TSPO was originally named peripheral benzodiazepine receptor. However, in 2006, researchers collaborated to rename the protein (Papadopoulos et al 2006). PBR was considered to be a misnomer for several reasons. First, multiple other ligands besides benzodiazepines had been identified in their ability to bind to TSPO including 1-(2-chlorophenyl)-N-methyl-(1-methypropyl)-3-isoquinoline carboxamine (PK11195) (Benavides et al 1983), cholesterol (Lacapere et al 2001; Bernassau et al 1993), and protoporphyrin IX (Taketani et al 1995; Vanhee et al 2011). Additionally, as TSPO had been demonstrated to be in the central nervous system (CNS) in addition to peripheral organs, peripheral was no longer accurate. Finally, it was determined that as TSPO translocated cholesterol, its new name could partially reflect this function.

TSPO Biology & Physiology

TSPO Structure

The crystal structure of TSPO has been partially resolved in two different species of bacteria: *Bacillus cereus* (Guo et al 2015) *a*nd *Rhodobacter sphaeroides* (Li et al 2015), and in one species of rodent *Mus. musculus* (Jaremko et al 2014). TSPO is a protein consisting of 5 transmembrane helices and 169 amino acids. In several studies, this protein is determined to be at the outer mitochondrial membrane (OMM) with the C-terminus outside of the OMM and the N-terminus in the intermembrane space between the OMM and the inner mitochondrial membrane (IMM). Loops 1 and 3 are extra-mitochondrial and loops 2 and 4 are intra-mitochondrial (Jaremko et al 2014) (Figure 1.1 A). Multiple binding sites and domains have been identified within the structure of TSPO including the binding sites for: synthetic ligands (PK11195, Ro5-4864), porphyrin, cholesterol (Cholesterol Recognition Amino acid Consensus, CRAC), and diazepam binding inhibitor (DBI) (Alho et al 1991; Murail et al 2008; Vanhee et al 2011; Selvaraj et al 2017) (See Figure 1.1B for selected binding sites).

TSPO homologs exists in the animal kingdom in bacteria, insects, and mammals (Yeliseev et al 2000; Selveraj et al 2015), as well as in plants including the well-studied *Arabidopsis thaliana* (Guillaumot et al 2009) and other plants such as *Solanum tuberosum* (Corsi et al 2004). Two notable exceptions to the evolutionary conservation of TSPO are *Escherichia coli* and *Saccharomyces cerevisiae* (Liu et al 2014). The human TSPO sequence shares homologies with the following species: 33% *R. sphaeroides*; 43% *Drosophila melanogaster*; and 81% *Mus musculus*. Not only is TSPO structurally conserved across species, but TSPO is also functionally conserved in some cases (Yeliseev, Kruegar, & Kaplan, 1997). In expressing rat TSPO in TspO^{-} *R. sphaeroides*, rat TSPO was able to perform the functions of this bacterial TspO: to negatively

regulate photosynthesis genes in response to oxygen. Further specificity was demonstrated by antagonizing this effect with the TSPO ligand PK11195.

TSPO: monomers, dimers, and oligomers

There is evidence that the structure of TSPO can exist either as a monomer, homodimer (Lacapere et al 2001; Jaipuria et al 2017) or high level oligomer (Delavoie et al 2003; Teboul et al 2012; Jaipuria et al 2017). Lacapere and colleagues demonstrated that monomeric TSPO is associated with both PK11195 and cholesterol binding. Providing further supporting evidence for the association of monomeric TSPO with cholesterol binding, Jaipuria et al demonstrated that cholesterol binding to the CRAC motifs of a TSPO homodimer, leads to structural changes in the protein and induces dissociation of the monomers. The separation of the TSPO homodimer exposes a GxxxG binding motif that provides TSPO monomers an interface to interact with itself (this is the interface where TSPO homodimers associate) or with other proteins, as the GxxxG motif has been identified as a motif that is sufficient to mediate dimerization and has substantial oligomerization potential (Brosig & Langosch 1998; Russ & Engleman 2000). Further, the oligomeric status of TSPO varies across cell types. Molecular weights of multiples 18 kDa have been identified in various cell types including testicular Leydig cells, breast cancer cells, murine macrophages, and brain tissue (Delavoie et al 2003; Loth, unpublished data).

TSPO oligomeric state also varies across species as was noted in Teboul et al 2012 in the single particle analysis of transmission electron microscopy (TEM). That is, image analysis suggested the presence of four monomers for mammalian TSPO as compared to a dimer for bacterial TSPO. Several studies have reported a functional dimer for bacteria (Korkhov et al 2010; Yeliseev & Kaplan 2000) whereas monomers and polymers have been described as functional units for mammalian species (Lacapere et al 2001; Delavoie et al 2003).

Additionally, Delavoie and colleagues provided evidence that during periods of increased ROS expression, the equilibrium of TSPO binding shifts towards forming polymeric TSPO (Delavoie et al 2003). This would indicate that in pathological conditions that are associated with high levels of ROS, the equilibrium of TSPO would shift towards forming oligomers. Taken together, these data indicate that TSPO polymerization is an ongoing, dynamic process that may be partially regulated by ligand binding such as cholesterol as well as by ROS. The functional implications of TSPO's oligomeric state remain to be fully ascertained.

TSPO Subcellular Localization

TSPO has been shown to be predominantly at the outer mitochondrial membrane (OMM) in multiple types of tissues and cells: rat adrenal glands, (Anholt et al 1986), testis, lung, kidney, heart, liver, and skeletal muscle (Antkiewicz-Michlauk et al 1988; O"Beirne et al 1990). Additionally, immune electron microscopy studies in our lab have indicated TSPO is at the OMM in primary murine microglia (See Chapter 4, Figure 11). Subcellular fractionation studies also confirmed the OMM in that digitonin treatment of rat adrenal mitochondria released TSPO and monamine oxidase, (a marker of the OMM), but not cytochrome oxidase, a marker of the inner mitochondrial membrane (IMM) (Anholt et al 1986). Notably, other studies in the guinea pig lung, have supported TSPO's localization to the IMM (Mukherjee & Das 1989) through TSPO binding sites that were associated with the IMM marker, succinic dehydrogenase. Furthermore, Mukherjee & Das observed a decrease in Ro binding to the mitochondrial membrane under hypotonic conditions and not under isotonic conditions, which they concluded suggests the location of the receptors is inside the mitochondria. Additionally, in immunoprecipitation studies, TSPO has been shown to be associated with VDAC, an OMM protein (McEnery et al 1998; Gatliffe et al 2014; Loth et al 2018, see Chapter 4). Moreover, immunohistochemical studies of TSPO with confocal

microscopy and electron microscopy have confirmed the localization of TSPO to the outer mitochondrial membrane and other subcellular compartments such as the mitochondrial associated membrane (MAM) and plasma membrane (Bribes et al, 2004; Chapter 4, Figure 11).

However, other studies have indicated subcellular localizations of TSPO that are non-mitochondrial. In some cases this occur within the same cell type, and in other cases this is across cell types. For example, Olsen et al 1988 reported TSPO in erythrocytes, which are cells which exude their mitochondria prior to leaving the bone marrow. The authors hypothesize that TSPO in this case is localized to the plasma membrane (Olsen et al 1988). Neutrophils also express TSPO, but have lower levels of mitochondria due to the apparent decrease of mitochondrial content along the granulocyte differentiation pathway (Woods & Williams 1996). TSPO is thought to be at the plasma membrane in neutrophils for this reason, as well as based on the experiment by Zavala et al 1991 where in exposing live, intact neutrophils to a TSPO antibody, neutrophils released an oxidative burst. Additionally, in the mouse adrenal cortex, Oke et al 1992 determined through confocal microscopy and 3-D reconstruction that in cells from the zona fasciculate, there was TSPO cell surface staining. In addition to the plasma membrane, TSPO has been suggest to be the nuclei and perinuclear areas from human breast tumor biopsies, breast tumor cell lines, and glial cells after injury (Marangos et al 1982; Schoemaker at al 1983; Hardwick et al., 1999; Kuhlmann and Guilarte, 2000). The demonstration of a subset of TSPO at various subcellular locations (such as the plasma membrane) could account for the multiple functions attributed to TSPO and the actions of TSPO ligands that do not appear to be related to mitochondrial function.

TSPO Tissue Distribution

TSPO is expressed throughout the body, particularly in steroidogenic endocrine producing tissues (Papadopoulos et al 1997; De Souza et al 1985; Anholt et al 1986) and in tissues essential

for lipid metabolism such as white and brown adipose tissue, gonads, adrenal glands, and lung (Selvaraj et al 2015; Tu et al 2016). TSPO is also found in the kidney, heart, platelets (Shoemaker et al 1981; Tu et al 2014) as well as in the liver, heart, and muscle (Marangos et al 1982; Fairweather et al 2014) and in macrophages, monocytes, bone marrow, spleen (Tu et al 2014).

TSPO is also found in the brain, however, in physiological conditions, basal TSPO levels are low, except for ependymal cells that line the ventricles, the choroid plexus, and the olfactory bulb (Cosenza-Nashat et al 2009; Gehlert et al 1983; Benavides et al 1983; Weissman et al 1984). Upon brain injury or inflammation, TSPO upregulates in both microglia and astrocytes, though the temporal response differs in these two cell types (Chen & Guilarte 2008; Loth et al 2016; Notter et al 2018; Lavisse et al 2012; Maeda et al 2007; Wang et al 2014; Cosenza-Nashat et al 2009; Kuhlmann & Guilarte 2000)). Additionally, data demonstrating TSPO upregulation in vascular endothelial cells in the brain in response to injury has recently been demonstrated (Notter et al 2018; Cosenza-Nashat et al 2009). The data regarding if TSPO is expressed in neurons is conflicting. Initially neuronal TSPO was observed in rodents, but not in humans (Weissman et al 1984; Karchewski et al 2004). Cosenza-Nashat et al 2009 published a paper indicating neuronal staining of TSPO. However their antibody absorption studies raised some question as to whether the antibody was specific. However, the antibodies in question have been validated by immunoblotting and subcellular localization confirmed by electron microscopy (Bribes et al 2004; Dussossoy et al 1996). Given their staining was punctate which they say is indicative of mitochondrial distribution and that different mammalian isoforms of TSPO exist (Zhang et al 2006; Lin et al 1993; Costa et al 2006), they speculate that possible that the neuronal form represents a different isoform or a structurally related molecule that is not yet identified (Cosenza-Nashat et al 2009).

TSPO's ubiquity in several types in tissue, both in physiological and pathological states, suggests pleiotropic functionality. Perhaps this is also why so much conflicting data and/or why so many different functions have been attributed TSPO.

TSPO Physiological Functions

Over the last several decades, TSPO has had several proposed functions (See Figure 1.3) However, the further science progresses, the more questions are raised about TSPO's physiology in both health and diseased states. Currently, the function of TSPO is one of the most fiercely debated topics within the field. As the attributed functions of TSPO are numerous, here we will primarily focus on those functions most relevant to the function of TSPO in the brain. It is important to note that several of early studies examining TSPO function use extremely high concentrations of TSPO ligands. Despite the fact that these ligands have nM affinity, researchers were often using uM or higher concentrations for function studies, and thus many of the early studies may not in fact be mediated by TSPO, but are simply off target effects of high ligand concentrations.

Steroidogenesis. One of the most well-studied functions of TSPO is its role in steroidogenesis. In order for steroidogenesis to occur, cholesterol must enter the mitochondria for P450scc to convert cholesterol to pregnenolone, the precursor of all steroids Traditionally, TSPO was thought to translocate cholesterol across the outer mitochondrial membrane (OMM) as the first step in steroidogenesis (Papadopoulos et al 1997, 2006). In this way, TSPO was thought to modulate steroidogenesis and contribute to the translocation of cholesterol being the rate limiting step in steroidogenesis (Privalle et al 1983). Early studies supported this hypothesis in multiple ways. First, TSPO's localization at the OMM (Anholt et al 1986), as well as the high affinity with which TSPO can bind cholesterol (Lacapere et al 2001) and the identification of a cholesterol

specific binding domain (cholesterol recognition amino sequence, CRAC) at the C-terminus, all supported TSPO's putative role in translocating cholesterol (Li et al 1998). Further *in vitro* studies demonstrated increases in steroid production after exposure to the TSPO ligands PK11195 or Ro5-4864 in both murine adrenal cells (Mukhin et al 1989) and Leydig cells (Papadopoulos et al 1990). Additionally, the fact that TSPO's transmembrane domains form a pore-like structure in which the interior is lined with hydrophobic residues, also supported TSPO's putative ability to translocate cholesterol (Korkhov et al 2010; Jaremko et al 2014).

However, in recent years multiple groups have generated TSPO knockout (KO) mice, both global and conditional, that have no impairments in steroidogenesis (Tu et al 2014; Morohaku et al 2014; Wang et al 2016; Banati et al 2014). Tu and colleagues demonstrate that PK11195's effect on steroidogenesis is merely an off target effect and not mediated through TSPO. When they expose both TSPO WT and TSPO KO Leydig cells to increasing concentrations of PK11195, dose-dependent increases in progesterone production are documented in both cell types, indicating that this effect is not modulated by TSPO. In Morohaku's study, there were no differences Leydig cell TSPO KO in serum testosterone, seminal vesical weight or testis weight as compared to wildtype. In the global TSPO KO mice, no differences were seen in steroid biosynthesis, fertility, or circulating adrenal or gonadal steroid levels (Banati et al 2014). The debate among the groups continues as to the role of TSPO in steroidogenesis. Some are attributing the conflicting studies to differences in the genetic background of the mice strains, whereas others explain the mutually exclusive results as there being either an adaptive or compensatory mechanism to impairments in steroidogenesis (McNeela et al 2018). Or perhaps the differing results can be attributed to the age of the animals, as in a recent paper by Barron and colleagues, they observed subtle steroidogenic abnormalities (reduced total steroidogenic output, particularly progesterone, corticosterone, and

androgen) in male TSPO knockout mice that were exacerbated with aging (Barron et al 2018). Interestingly, deletion of TSPO was also once considered to be embryonic lethal (Papadopoulos et al 1997), but again the generation of global TSPO KO mice has called this conclusion into question. Given that TSPO KO animals are able to survive in the new models and have a normal length lifespan, this again points towards the potential explanation of how the genetic background of a mouse can have a major effect on experimental results.

Cell survival and apoptosis via the mitochondrial permeability transition pore. Several studies have suggested a role of TSPO in apoptosis. This theory began with studies in rat cardiac tissue and human glioblastoma cell lines that demonstrated that exposure of TSPO-ligands lead to swelling of the mitochondria, a collapse in mitochondrial membrane potential, and a decrease in cell viability (Chelli et al 2001; Kugler et al 2008; Costa et al 2015). Additionally, both PK11195 and Ro5—4864 are used as chemotherapy coadjuvants in an effort to decrease cell proliferation (Walter et al 2005; Mukhopadhyay et al 2010; Sanidrian et al 2007; Hirsh et al 1998; Decaudin et al 2002). However, other studies using C6 glioma cells or human colorectal cancer cell lines demonstrated that knocking down TSPO reduced cell death by decreasing the number of apoptotic cells and increasing cell proliferation (Levin et al 2005; Shoukrun et al 2008). Also, in a correlation analysis of TSPO, expression was positively associated with tumor malignancy grade and the proliferative index as determined by MIB-1/Ki-67 immunocytochemistry (Miettinen et al 1995). And in human breast cancer cell lines, highest amounts of both TSPO and mitochondria were found in cell lines with high mitotic activity, and TSPO expression correlated inversely with cell doubling time and positively with Ki-67 expression (Beinlich et al 2000). Based on these studies, TSPO's association with the mitochondrial permeability transition pore (mPTP) was suggested by Veenman and colleagues in 2008 as well as Sileikyte and colleagues in 2010.

The mPTP is described as a nonspecific pore that opens in response to mitochondrial stress, specifically an increase in permeability of the inner mitochondrial membrane (Galluzzi et al 2009) This pore allows the passage of molecules < 1.5 kDa, and ultimately functions to decouple oxidative phosphorylation (Halestrap et al 1999) which in turn ruptures the outer mitochondrial membrane, and releases apoptosis stimulating factors, thereby regulating cell death (Pastorino et al 1996; Larochette et al 1999). However, as the field evolves, several studies have challenged the involvement of TSPO with mPTP (Sileikyte et al 2014; Bernadi et al 2013; Baines et al 2007; Krauskopf et al 2006; Kokoszka et al 2004). These studies propose that the mPTP involves other mitochondrial components, but is independent of TSPO as evidenced by TSPO null mitochondria demonstrating no differences in the controls of pore function.

Immunomodulation: pro-inflammatory vs. anti-inflammatory. TSPO's use as a biomarker of brain inflammation is particularly well studied. At baseline, TSPO is at very low levels in the brain neuropil. After exposure to toxic chemical stress (endogenous [ROS etc] or exogenous [neurotoxicants etc.]) or physical stress (head trauma), TSPO is upregulated in brain areas specific to the injury, by glial cells (Chen & Guilarte 2008; Gulyas et al 2012; Lavisse et al 2012; Cagnin et al 2001a and b; Gerhard et al 2006 a and b; Coughlin et al 2015 and 2017; Zimmer et al 2014; Zurcher et al 2015; Politis et al 2012; Pavese et al 2006). These observations have led to the development of positron emission tomography (PET) radiotracers for brain imaging. TSPO-PET imaging represent a unique and valuable tool in that it provides a window to assess active brain disease and can be used to track the effect of a therapeutic intervention's ability to decrease inflammation or potentially even to aid in diagnosis of neurological diseases given the regional specificity TSPO expression demonstrates.

However, despite this extensive history for use as a biomarker of neuroinflammation, little is known about TSPO's function at the molecular level or how TSPO contributes to inflammation. Studies have shown both pro and anti-inflammatory effects of TSPO upregulation and/or TSPO-ligand exposure. At the *in vitro* level, multiple studies have shown that knocking down TSPO in microglia prolongs LPS induced proinflammatory cytokine release, whereas overexpression TSPO leads to the converse (Bae et al 2014). Wilms et al 2003 had a similar finding in that exposing microglia to TSPO ligands decreased LPS-induced proinflammatory cytokine release. Choi et al 2011 found that when microglia are activated with either LPS or ATP, TSPO ligands reduced pro-inflammatory genes expression and cytokine release, and thus may have therapeutic potential. Bae and colleagues (2014) hypothesize that this decrease in inflammatory response is mediated through the attenuation of the nuclear factor-κB pathway, and through an increase in alternatively activated M2 stage related genes, but this remains to be confirmed. Zhao and colleagues (Zhao et al 2011) also have some initial data with the TSPO ligand Vinpocetine that supports this initial hypothesis as they demonstrated that Vinpocetine exposure inhibited production of nitric oxide and IL-1β, IL-6, and TNF-α, as well as the expression of NF-κB and AP-1 in LPS-stimulated microglia. This indicates that Vinpocetine has an anti-inflammatory effect by partly targeting NF-kappaB/AP-1 within BV-2 cells, a microglial cell line in which doubts have been raised regarding how synchronous its responses are compared to primary microglia (Hausler et al, 2002; de Jong et al., 2008; Horvath et al., 2008).

Additionally, *in vivo* studies suggest that TSPO overexpression or TSPO ligand exposure decreases cellular signs of reactive gliosis in LPS, kainic acid, or quinolinic acid exposed rodents (Ryu et al 2005; Veiga et al 2005; Leaver et al 2012; Wang et al 2016). Together, these studies suggest that TSPO upregulation in inflammation represents an adaptive response to mitigate and/or

resolve inflammation. Furthermore, it will be critical to assess the role of each glial cell type (i.e., microglia and astrocytes) and how each contributes to the inflammatory process. Studies examining not only the individual response of each cell type, but also the cross-talk between microglia and astrocytes in inflammation across time will be important in assessing TSPO's role in inflammation.

Mitochondrial respiration and cellular energy production. With the advent of TSPO KO mice, TSPO's role in oxygen consumption and indirectly energy production is being examined. In both microglia (Banati et al 2014) and fibroblasts (Zhao et al 2016) cultured from TSPO KO mice, these investigations observed decreased rates of oxygen consumption and production of adenosine triphosphate (ATP). Additionally, overexpression of TSPO in T-cells increased ATP production and motility (Liu et al 2017). Yet, TSPO's role in mitochondrial respiration and energy production appears to be cell specific because while positive results are seen in fibroblasts, microglia, and T-cells, the opposite is observed in Leydig cells (Tu et al 2016) and certain liver cells (Sileikyte et al 2014).

Regulation of redox process and oxidative stress. The role of TSPO in the regulation of redox homeostasis and in responses to oxidative stress is being examined by multiple groups (Guilarte et al 2016; Carayon et al 1996; Zeno et al 2012; Banati et al 2014; Liu et al 2014; Guo et al 2015). This appears to be another condition where the cell type, time point examined, physiological vs. pathological state, and oligomeric composition generate variable data in regards to the role of TSPO. For example, within the data produced by our lab, TSPO ligands induce an increase in ROS production in primary microglia (Choi et al 2011). Yet, TSPO ligands also induce the translocation of Nrf2, a transcription factor that upon activation, translocates to the nucleus in order to bind to antioxidant response element (ARE) and induce the expression of various

cytoprotective genes, presumably in order to protect itself from the ROS that it is generating (Loth et al 2018, in preparation; See Chapter 3). Taken together, these data indicate that TSPO is maintaining redox homeostasis.

However, in other studies using vascular endothelial cells, overexpression and pharmacological activation of TSPO have been demonstrated to inhibit ROS production, specifically mitochondrial ROS production (Joo et al 2012 and 2015). In an astrocyte cell line, cells that were metabolically injured via glucose deprivation had less free radical production, maintenance of mitochondrial function, improved cell viability, and less nuclear fragmentation when also exposed to Ro5-4864 (Baez et al 2017). Of note, these cells were exposed to ligand concentrations of 10nM, 100 nM, 1 uM, or 10 uM, and lower concentrations of ligand were associated with the improved cell viability, less nuclear fragmentation, and lower ROS production as measured by DHE, whereas higher concentrations of the ligand actually exacerbated effects observed due to glucose deprivation. Furthermore, TSPO deletion in Leydig cells increased ROS production (Tu et al 2015). As indicated previously, Delavoie's et al 2003 found that oligomeric TSPO was preferentially expressed during periods of increased ROS expression.

One distinction regarding TSPO's relationship with ROS production that is made by Veenman et al 2016 is that with short durations of TSPO ligand exposures and low concentrations of ligands, ROS production is enhanced. This is in contrast with the reduction of ROS production induced by long durations of TSPO ligand exposures, and/or the application of high concentrations of TSPO ligands. However, it is important to note that at these high concentrations of TSPO ligands, we may be observing off target effects as opposed to effects truly mediated by TSPO. Therefore, examining both long and short term exposures to physiologically relevant

concentrations of TSPO ligands will be critical in assessing the role of TSPO in ROS production, and whether or not there is indeed this hormetic relationship between TSPO and ROS.

Heme biosynthesis. Multiple groups have noted that protoporphyrin IX/heme is an endogenous ligand for TSPO (Verma et al 1987; Snyder et al 1987; Vanhee et al 2011; Li et al 2015; Taketani et al 1995; Veenman et al 2016). Several groups have examined heme biosynthesis and whether TSPO plays a role (Ginter et al 213; Rampon et al 2009; Taketani et al 1995; Vanhee et al 2011; Gemelli et al 2014; Wendler et al 2003) given that protoporphyrin IX is the precursor to heme. Specifically, Vanhee and colleagues (2011) have demonstrated that in *Arabidopsis thaliana*, TSPO can bind heme both *in vivo* and *in vitro*. Additionally, various point mutations altered whether or not heme binds and if TSPO degrades heme, thereby suggesting that heme binding regulates TSPO degradation in *A. thaliana*. The authors suggest that TSPO plays a role in heme scavenging given that abscisic acid-dependent TSPO induction was accompanied by an increase in unbound heme levels, and downregulation of TSPO was associated with the return to steady state levels of unbound heme. In bacterial TspO, Ginter and colleagues (2013) demonstrate that TSPO degrades porphyrin in a light and oxygen dependent manner, and this reaction can be inhibited by PK11195 or specific point mutations of conserved residues. The authors hypothesize that bacterial TspO mediates porphyrin catabolism with the consumption of reactive oxygen species, and this is potentially a function conserved across species.

Calcium signaling. TSPO has also been implicated in calcium signaling in various contexts. In a neuronal cell line, TSPO deregulates mitochondrial Ca(2+) signaling thereby leading to an increase in the cytosolic Ca(2+) pools that in turn activate NOX5 (the Ca(2+)-dependent NADPH oxidase) and serve to increase ROS (Gatliffe et al 2017). The authors demonstrate that the inhibition of mitochondrial Ca(2+) uptake by TSPO is a result of the phosphorylation of the

voltage-dependent anion channel (VDAC1) by the protein kinase A (PKA), which is recruited to the mitochondria, in complex with the Acyl-CoA binding domain containing 3 (ACBD3). Whether these studies are actually indicative of what is happening in the brain remains to be determined as TSPO is not typically expressed in neurons, and these studies were performed in a neuronal cell line, SH-SY5Y cells. Additionally, studies examining PK11195 have shown that this ligand may be apoptotic in some contexts through changing cellular Ca2+ homeostasis. Campanella et al 2008 demonstrated in HeLa cells that PK11195 increased ER Ca2+ and amplifyied IP(3) which served to induce Ca2+ transients in mitochondria and cytosol. The authors hypothesize that PK 11195 is acting on Bcl-2 given that Bcl-2 modulates Ca2+ in the opposite way: Bcl-2 overexpression reduces Ca2+ in the ER and impairs mitochondrial and cytosolic Ca2+ thereby inhibiting apoptosis. Furthermore, in rat heart mitochondria, TSPO has been demonstrated to modulate Ca2+ transport through VDAC. Tamse and colleagues tested the hypothesis if the endogenous ligand hemin (protoporphyrin IX) to TSPO modified VDAC conductance. They demonstrated that initially, hemin reduced the calcium uptake rate in a dose-dependent manner. However, subsequent to this inhibitory effect on calcium influx, hemin facilitated mitochondrial permeability transition (MPT) as evidenced by greater calcium release following calcium loading. When hemin (protoporphyrin IX) binds to TSPO, it induced the closure of VDAC-TSPO-ANT (adenine nucleotide translocator) complex, indicating another potential way in which TSPO affects Ca2+ signaling and in this case, VDAC conductance.

TSPO ligands & therapeutic potential

Multiple studies have shown that TSPO ligands have the potential to exert neuroprotective effects in various models of injury and neuroinflammation. However, depending on the injury or disease, the ligand that is neuroprotective varies. For example, administration of Ro5-4864 in a

mouse model of AD reversed neuropathology and improved behavioral outcomes, whereas administration of PK11195 only reduced levels of soluble β-amyloid (Barron et al 2013). Administration of Ro5-4684 also decreased reactive gliosis and neuronal death in the hilus of the hippocampus in male rats when administered prior to exposure to kainic acid, a well-known neurotoxicant that targets the hippocampus (Veiga et al 2005). Ro5-4864 also prevented mitochondrial-mediated apoptosis of neurons in a rat model of cortical injury (Soustiel et al 2008) and reduced the severity of diabetic neuropathy (Giatti et al 2009). In most of these studies, PK11195 either showed no effect (Veiga et al 2005; Soustiel et al 2008) or counteracted the effects elicited by Ro5-4864 (Mills et al 2005; Lacor et al 1999). On the other hand, administration of PK11195 but not Ro5-4864 reduced microglial activation in the hippocampus of LPS-injected male rats (Veiga et al 2007). PK11195 also reduced microglial activation and expression of pro-inflammatory cytokines and iNOS in the striatum of quinolinic acid-injected male rats (Ryu et al 2005) and attenuated kainic acid-induced seizures and hyperactivity in male rats (Veenman et al 2002). In addition, *in vitro* data demonstrated that PK11195 rescued motor neuron death in both a familial model of ALS, as well as in a humanized model of sporadic ALS, indicating a potential common therapeutic target for sporadic and familial ALS. Furthermore, preliminary *in vivo* data of PK administration in a mouse model of ALS improved Rotarod performance and neuroscore in females (Obis et al 2018, in preparation).

Etifoxine, a clinically approved drug for treating anxiety in humans and identified as a TSPO ligand reduced the number of macrophages at lesion, promoted axonal regeneration, and improved motor functions after peripheral nerve injury in rat (Girard et al., 2008). In a mouse model of MS (EAE), administration of etifoxine attenuated EAE severity when administered before the development of clinical signs and also improved symptomatic recovery when

administered at the peak of the disease (Daugherty et al 2013). The authors determined this by the decreased inflammatory pathology in the lumbar spinal cord, as well as the decrease in peripheral immune cell infiltration into the spinal cord.

Thus, it appears that TSPO ligand administration has therapeutic potential, but ligands have differential effects. Each ligand will need to be independently evaluated in each disease and injury model in both sexes before being used clinically to improve outcomes. Additionally, whether or not each ligand is actually working through modulating TSPO will need to be determined using TSPO KO technology. Many of the above studies have not measured TSPO levels, and therefore this could again be another circumstance in which off target effects of TSPO are being observed.

Microglia: the Guardians of the CNS

Microglia constitute around 10% of the total number of cells in the adult central nervous system (CNS), with their density varying across brain regions (Mittelbronn et al 2001). Substantia nigra typically has the highest density of microglia (12%), while the cortex and corpus callosum have some of the lower densities (5%). Microglia were first discovered by Pio del Rio-Hortega in 1920 and described as "a unique cell type differing in morphology from other glia and neurons." (Block et al 2007). Indeed, microglia are morphologically and developmentally distinct from other cell types in the CNS. They leave the yolk sac between embryonic day 8.5-9.0 and enter the blood stream (Ginhoux et al 2010), and thus are erythromyeloid in origin, unlike the rest of the CNS (Matcovitch-Natan et al 2016). They are maintained via self-renewal in the healthy CNS and not from progenitors in bone marrow where precursors for macrophages typically originate from (Ajami et al 2007).

Microglia are often referred to as the macrophages of the CNS, with their main perceived role being to react to injury, infection, or pathology. However, part of this perception of their sole function stems from the fact that functions of microglia are not noticed unless they stop performing their physiological functions including general maintenance and clearing cellular debris (Beyer et al 2000). Research over the last several years has revealed other distinct roles for microglia including sculpting the structure of the CNS, refining neuronal circuitry and network connectivity (Barron 19995; Milligan et al 991), and contributing to plasticity (Salter & Beggs 2014). Additionally, microglia play a role in cell survival in terms of immune surveillance, clearance capabilities and maintenance of local homeostasis (Casan & Peri 2015). In this way, microglia are viewed as instructive in physiological conditions, as opposed to reactive as they are viewed following injury or infection or in pathological conditions. For our purposes here, we will primarily focus on microglia's role and function in inflammation and redox homeostasis.

In a healthy brain, microglia are perceived to be in a resting, non-activated state. However, microglia are hardly "resting" in the normal brain. *In vivo* imaging studies with two-photon microscopy and time-lapse imaging in mice expressing fluorescently-labeled microglia have shown that microglia possess highly mobile ramifications that are constantly surveying their environment and are capable of *de novo* formation, extension, and withdrawal. Microglia possess a lattice-like pattern of adjacent, non-overlapping territories that are capable of responding to injury and mobilizing towards the site of injury in less than 30 seconds (Davalos et al 2005; Nimmerjahn et al 2005). Thus, in order to maintain brain homeostasis, microglia must be constantly and actively surveilling the microenvironment. When there is a more widespread threat (injury, infection, or disease), they adopt a stimulus-dependent phenotype that includes

cytoskeletal rearrangements to allow for morphological changes, stereotypic transcriptional alterations, and proliferation (Salter & Beggs 2014).

Microglia activation

Microglia activation can be neurotoxic or neuroprotective, depending on the prior state of the brain and injury progression. During a CNS insult, microglia can change from a surveying state to an activated state through a series of morphological and functional changes (Town et al 2005). Depending on the insult and the current cytokine milieu, microglia will adopt either a pro-inflammatory M1 state typically viewed as classical activation or a pro-survival M2 state typically viewed as alternative activation. While generally viewed as an oversimplification of phenotypes in microglia, the M1/M2 nomenclature is still commonly used to classify microglial responses, despite the fact these phenotypes most likely occur across a continuum (Aguzzi et al 2013). Notably, the "resting" state of microglia is referred to as M0 and is characterized by TGFβ, making it distinct from other tissue macrophages (Hickman et al 2013; Butovsky et al 2014). Most chronic pathological conditions are characterized by a lack of balance among the various activation states of microglia. For example, a predominantly M1 phenotype is characterized by excessive ROS production and neuroinflammation, whereas a prolonged M2 phenotype can negatively affect immune defense and can contribute to tumorigenesis in gliomas (Cherry et al 2014; Hu et al 2015; Komohara et al 2008).

Much of the research regarding microglia has focused on their effector functions in which they are cytotoxic and drive the neuroinflammation that accompanies many forms of acute or chronic neuropathology. This includes release of pro-inflammatory cytokines, arachidonic acid derivatives, excitatory neurotransmitters, proteinases and ROS. ROS production by microglia in particular has been implicated in many neurodegenerative diseases as a major cause of neuronal

dysfunction, damage, and cell death through oxidative damage or disruption of neuronal redox signaling circuits (Block et al 2007; Gao et al 2012).

In the early stages of injury, microglia are able to undergo morphological changes in which their processes become hyper-ramified and hypertrophic (Hanisch and Kettenmann, 2007; Streit et al, 1999). Microglia are able to produce and release neurotrophic factors such as nerve growth factor (NGF), brain-derived neurotrophic factor (BDNF), and neurotrophin-3 and -4 (NT-3 and NT-4) to support injured neurons (Elkabes et al., 1996; Block and Hong 2005; Hanisch and Kettenmann 2007). If the injured neurons are repaired, then it is possible that microglia can revert back to a healthy resting state (Streit et al., 1999). If injury is significant or persistent, then microglia can undergo further activation. It is upon this "chronic" activation that microglia tend to release neurotoxic factors such as ROS that are can damage nearby neurons and other glial cells such as oligodendrocytes and astrocytes. Prolonged microglia activation can ultimately result in the breakdown of the blood brain barrier resulting in the infiltration of invading monocytes from the periphery (Kreutzberg, 1996).

Oxidant production in microglia. Oxidant generation helps contribute to cell homeostasis via the regulation of specific redox-dependent pathways (Holmstrom & Finkel 2014). ROS have various potential sources, both exogenous such as radiation, or drugs, and endogenous such as mitochondria, peroxisomes, ER, and various enzymes including xanthine oxidase, nitric oxide synthetase, cytochrome P450's, and NADPH oxidase (Brieger et al 2012). In particular, the family of NADPH oxidases are a major source of oxidants used in intracellular and intercellular signaling (Sorce & Krasue 2009; Lambeth & Neish 2014; Nayernia et al 2014). As mononuclear phagocytic cells, microglia express high levels of superoxide producing NADPH oxidases, and NADPH oxidase (NOX) and intracellular ROS together are critical for the regulation of microglia

activation. Physiologically, the ROS generated from NOX is important for host defense and redox signaling circuits in order to determine the various activation phenotypes of microglia. Of the various sources of ROS in a cell, NOX is the only source with the specific and exclusive task of producing ROS and is the fundamental source of ROS in the body. Pathologically, over-production or dysregulation of ROS-derived NOX are implicated in various neurological diseases where there is direct oxidative tissue damage that results in neuron loss or dysfunction.

The NOX family consists of seven isoforms, NOX1-5 and DUOX1-2. All NOX family members are transmembrane electron carriers that use cytosolic NADPH as an electron donor to transport electrons through flavin adenine dinucleotide (FAD) and membrane-embedded hemes to reduce oxygen to superoxide. NOX4 is the only exception to this as it produces H_2O_2. Cellular expression of NOX isoforms varies across cell types, both in the body and in the CNS. Of these isoforms, NOX2 (also known as $gp91^{phox}$) is highly expressed in microglia both in humans and rodents (Sorce et al 2014). NOX1 and NOX4 have been documented in microglia, but there are multiple conflicting results within the literature with a lack of specific antibodies being cited for the conflicting data (Haslund-Vinding et al 2016).

In its resting state, NOX2 has 3 cytosolic subunits ($p47^{phox}$, $p67^{phox}$, $p40^{phox}$) the G-protein Rac. There are also two membrane bound subunits $gp91^{phox}$ (NOX2) and $p22^{phox}$, which are collectively referred to as flavocytochrome b_{558} (See Figure 1.4). The membrane in the case of Cytb558 can refer to either the plasma membrane or vesicle membranes. As documented by Ejlerskov, Cytb558 can be stored in small vesicles (<100 nm) through clathrin-mediated endocytosis. Additionally, NOX2 has also been shown to be associated with lipid rafts (cholesterol-enriched membrane microdomains) in a cholesterol-

dependent manner. These lipid rafts potentially play a role in creating a platform for NOX2 mobility and signaling (Vilhardt & van Deurs 2004).

In its activated state, the 3 cytosolic subunits translocate to Cytb558. The rate limiting step of activation is the phosphorylation of p47^{phox}. p47 ^{phox} has *src*-homology (SH3) domains that in the resting state are hidden due to internal interactions with the polybasic region C-terminal to the SH3 domains from residues 286-340 (Leusen et al 1996; Ago et al 1999; Huang & Kleinberg 1999; Boussetta et al 2010). However, the auto inhibited region is revealed when various serine residues from 303 to 379 become phosphorylated, typically through PKC, and thus induce a conformational change that disrupts the SH3 domain and C-terminus internal binding. This disruptions allows p47 ^{phox} to translocate to Cytb558 and bind to the proline rich regions of phosphorylated p22 ^{phox} with its own SH3 domain (See Figure 1.4; Faust et al 1995; Ago et al 1999; Huang & Kleinberg 1999; Sumimoto 2008; Lewis et al 2010; Boussetta et al 2010). p47 ^{phox} is further stabilized by its interactions with gp91^{phox} (Rastogi et al 2017). Once bound, p47 ^{phox} allows for the electron transfers to proceed from FAD to the heme groups in Cytb558 in order to reach oxygen (DeLeo et al 1995). The transfer of electrons from NADPH to FAD requires p67 ^{phox}, which is often referred to as the activator subunit (Leusen et al 1996) as well as Rac1/2 (Diebold & Bokoch 2001).

Receptor-mediated NOX activation in microglia.

Microglia, as the "professional" phagocytes in the brain, have an array of surface sensing receptors that allow them to rapidly respond to changes in the environment. These pattern recognition receptors (PRRs) are expressed constitutively to aid in the recognition and binding of pathogen-associated molecular patterns (PAMPs). Below are some examples of PRRs in which NOX expression and ROS generation have been implicated in signaling and/or disease.

Toll-like receptors (TLR). Microglia express TLRs in their non-activated state and alter TLR expression levels when they are activated. (Block et al 2007). At least 12 members of the TLR family have been identified in mammals that recognize PAMPs from bacteria, fungi, parasites, viruses, and self (the host (Akira et al 2009)). For example, TLR4 is traditionally viewed as the LPS receptor as it recognizes the cell wall of this Gram-negative bacteria. In this way, TLRs often contribute to neuropathology due to their association with disease-related molecules such as amyloid β (Jana et al 2008), mutant SOD1 (Liu et al 2009), α-synuclein (Codolo et al 2013), gangliosides (Jou et al 2006), and oxidized phospholipids (Imai et al 2008). In several of the cases listed, NOX and ROS production are upregulated by the binding of the ligands to TLRs (Imai et al 2008; Liu et al 2009; Codolo el al 2013), and it has been suggested that TLR's rely on NOX activity to initiate signaling. For example, ROS derived from NOX can aid in the regulation of partitioning of lipid rafts to the membrane or help in the assembly of signaling complexes (Nakahira et al 2006; Yang et al 2008). Additionally, TLRs can aid in priming the cell to be hyperresponsive and prime NOX2 by recruiting cytosolic phox proteins to the membrane by initiating phosphorylation of p47 (DeLeo et al 1998; Dang et al 2006). Further TLR signaling is also capable of activating IL-1 receptor-associated kinase 4 (IRAK4), which is also capable of phosphorylating p47 on several residues (Pacquelet et al 2007). Notably, IRAK4-deficient neutrophils are unable to activate NOX2 (Picard et al 2003).

Complement receptor 3 (CR3; CD 11b/CD18; MAC-1, macrophage antigen complex I). CR3 can function as both an adhesion molecule and a PRR that recognizes a diverse set of ligands. It is essential for phagocytosis and aids in mediating the activation of phagocytes in response to various stimuli (Le Cabec et al 2002). In macrophages and neutrophils, CR3 is associated with activation of a respiratory burst (Le Cabec et al 2002) and its expression is partially

regulated by NOX 2 (Roy et al 2008). Relatedly, while LPS does bind to TLR4, it also binds to CR3, and it is this LPS binding to CR3 that stimulates NOX activity in microglia (Qin et al 2005; Pei et al 2007). Additionally, binding of α-synuclein aggregates to CR3 induces NOX-derived ROS in microglia (Zhang et al 2005). Given that CR3 is upregulated in neurodegenerative diseases (it is often used as a marker for microglia activation), this receptor could represent a mechanism of microglial-derived oxidative stress during inflammation-mediated neurodegeneration (Roy et al 2008).

Ionotropic & metabotropic purinergic receptors. Both ionotropic P2X and metabotropic P2Y purinergic receptors are essential for microglial motility, migration, and phagocytosis, as these receptors are involved in the regulation of the microglial actin cytoskeleton (Haslund-Vinding et al 2016). In regards to ROS production, multiple groups have noted that ATP stimulation of P2X7 receptor induces ROS production in microglia (Choi et al 2011; Mead et al 2012; Parvathenani et al 2003). However, the direct association between P2X7 and NOX activity has not been fully confirmed. P2X receptors are coupled to nonselective cation channels and are permeable to K^+, Na^+, and Ca^{2+} (Skaper et al., 2010), and thus calcium entry is required for signaling and ROS production to occur following ATP stimulation in microglia (Kim et al 2007). Increases in intracellular calcium have also been associated with increases in NOX activity through various pathways including ERK1/2 (Apolloni et al 2013), p38MAPK, and PI3K dependent pathways (Parvathenani et al 2003). In addition, activation of microglial purinergic receptors has been implicated in various neurodegenerative diseases including ALS, AD, and PD (Parvathenani et al 2003). For example, in P2X7 or P2Y receptor deficient microglia, Aβ mediated and α-synuclein mediated microglia activation is decreased Kim et al 2007). It has been hypothesized that this decrease in microglial activation can be attributed to alpha-synuclein not binding to the

P2X7 receptor, and thus not signaling through PI3K, and thereby limiting NOX activation (Jiang et al 2015).

Activation of neurotransmitter receptors. Given their role in surveying their surrounding environment, microglia express a fair number of neurotransmitter receptors, both in their activated and non-activated states (Kettenmann et al 2013). Multiple neurotransmitters can induce NOX2 production in microglia. One of the first identified was glutamate through induction of the NMDAR (Girouard et al 2009), but since then agonists for glutamate metabotropic (mGlu3), $GABA_A$, P2X7, and mGlu5 have all been identified as activating NOX in microglia (Mead et al 2012). These neurotransmitters had differential effects in that NOX activation with glutamate receptor agonists was neurotoxic, and NOX activation by GABA or purinergic receptors was neuroprotective. Relatedly, NMDA receptor stimulation was also accompanied by an increase in pro-inflammatory cytokines and ROS, that were identified as toxic to neurons (Kaindl et al 2012).

Scavenger receptors (CD36). Scavenger receptors are a group of PRRs that are responsible for recognition of modified lipoproteins and multiple polyanionic ligands in order to initiate intracellular signaling for defense against bacterial pathogens (Block et al 2007). Activation of scavenger receptors appears to result in the increased production and release of reactive oxygen species (Bianca et al 1999; Coraci et al., 2002; Husemann et al., 2002), and CD36 in particular is essential for NOX-mediated oxidant production in Aβ activated microglia and for free radical production and tissue injury in cerebral ischemia (Cho et al 2005; Bianca et al 1999). CD36's interaction with surface receptors CD47 and integrin α6β1 also points to its involvement in oxidant production, as all 3 are required for binding, signaling, and oxidant production (Bamberger et al 2003). In some instances, CD36 can act as a coreceptor for TLRs as is the case

in CNS ischemia where CD36 is required for the development of vascular oxidative stress (Cho et al 2005).

Therapeutic potential of NOX inhibitors. NOX activity is involved in a large array of neurodegenerative and neuroinflammatory diseases including: Alzheimer's disease (AD), stroke, traumatic brain injury (TBI), Parkinson's disease (PD), amyotrophic lateral sclerosis (ALS), Huntington's disease (HD), multiple sclerosis (MS) (Ma et al 2017). In addition, NOX has been demonstrated to mediate inflammation-related neurotoxicity in the following models: LPS (Qin et al 2004); rotenone (Gao et al 2004); DEP (diesel exhaust particles; Block et al 2004); paraquat (Wu et al 2005); MPTP (Gao et al 2003; Wu et al 2003); Aβ (Qin et al 2002); substance P (Block et al 2006); thrombin (Choi et al 2005); and α-synuclein (Zhang et al 2005). Given that NOX activity is involved in several diseases and neurotoxic exposures, many groups are interested in developing NOX inhibitors, specifically those geared towards microglial NOX2 activity. Due to the ways in which microglia can cause neuronal damage due to the ROS they generate, NADPH oxidase may represent an attractive therapeutic target for neurodegenerative diseases in which microglia are involved. In their 2017 review, Ma and colleagues review the current status of preclinical studies examining the neuroprotective effects of NOX inhibition, both genetic and pharmacological, in AD, stroke, TBI, PD, ALS, HD, MS. While several of these studies have been informative and promising, the authors attribute the lack of translatable results to the clinic to three main factors: the timing of application; determining the optimal treatment window; and the acute and/or chronic nature of disease models. For example, most studies have initiated NOX inhibition either prior to or in the early phases of disease or injury. Not many studies have examined NOX inhibition later in the disease process, which is the more realistic scenario within a clinical condition. Additionally, assessing the optimal treatment window in neurodegenerative

disease is challenging given that these diseases take several years, and sometimes decades, to develop. Therefore, it is critical to examine NOX inhibition both in acute and chronic models.

Redox signaling in microglia. Given that microglia are able to produce superoxide and NO, they are in close proximity to the reactive reaction products such as H_2O_2 and peroxynitrite that can cause oxidative damage. Therefore, microglia must possess sufficient antioxidative defense systems in order to protect themselves and to maintain redox homeostasis. Microglia contain high cellular concentrations of GSH (γ-glutamylcysteinyl glycine) and express and upregulate several antioxidant enzymes including: MnSOD (super oxide dismutase), Cu/ZnSOD, GPx (glutathione peroxidase) GR (glutathione reductase), and catalase (Dringen 2005).

Redox status. GSH is highly expressed in microglial cells as compared to neurons, astrocytes, and oligodendrocytes (Dringen 2005). GSH content has been demonstrated to decrease with age (Njie et al 2012), but certain compounds such as docosahexaenoic acid can increase total GSH content in microglia and limit proinflammatory cytokine production (Pettit et al 2013). GSH functions to scavenge superoxide in two ways: either directly through coupling to GSSG or through various enzyme catalyzed reactions. These enzymes include GSH peroxidase (GPx) which oxidizes GSH, and glutaredoxin (GRx) which reduces oxidized cysteine residues (Vilhardt et al 2017). Microglia have been shown to have the highest GPx activity in the brain in both rats and humans (Lindenau et al 1998; Power & Blumbergs 2009). GPx expression increases directly in response to oxidative stress (Wang et al 2015).

GSH and NOX2 derived ROS appear to have an inverse relationship, as GSH is consumed in the process of scavenging for superoxide. Won et al 2015 found that not only could increasing GSH levels by supplementing with N-acetyl cysteine protect again oxidative stress, but also that GSH depletion was prevented by blocking superoxide production during reperfusion.

Additionally, blocking superoxide production with the NOX inhibitor apocynin increased GSH content. Also, p47 KO mice did not show any change in either ROS production or GSH content in a model of ischemia-reperfusion, again supporting that inhibition of a functional NOX2 complex prevents GSH depletion. The exact nature of GSH and NOX in microglia is not currently fully understood: whether the two physically interact or if NOX regulates GSH synthesis through another means by acting on cysteine levels or import of cystine into the cell.

In order to synthesize GSH, cysteine must be available as it the precursor. The reducing conditions of the cytosol favor cysteine, but the extracellular environment is more oxidized and thus favors cystine. Therefore, importing cystine into the cell is critical for GSH synthesis. Both microglia and astrocytes use xc- cystine-glutamate exchanger (xCT; SLC7A11) for this purpose (Bannai 1984; McBean 2002). The import of cystine is coupled with the outward flow of glutamate. This pairing with glutamate moving down its concentration gradient provides the driving force for cystine import (Bannai 1984; McBean 2002). However, microglial release of glutamate and upregulation of xCT has been linked to various neurological diseases including HIV, EAE, and AD (Gupta et al 2010; Savchenko et al 2013; Evonuk et al 2015). Still, upregulation of xCT is regulated by Nrf2 which also upregulates enzymes to catalyze the formation of GSH to help minimize microglial glutamate induced toxicity (Shih et al 2003).

Thioredoxins (Trx) function to reduce protein disulphides to free thiols, and GSH peroxidases function to oxidize GSH. Trx protects proteins by reducing oxidized cysteine residues and using electrons from NADPH, peroxides and hydrogen peroxide. One of the genes Nrf2 upregulates in response to oxidative stress is Trx (Vilhardt et al 2017). Currently little is known about the actions of Trx in microglia, except that Trx activation is often associated with conditions

that cause microglia activation such as LPS, Aβ peptide, and IL-1β (Wang et al 2007; Zhang et al 2010; Sharma et al 2007).

NOX2-mediated redox signaling.

NF-κB. The transcription factor nuclear factor kappaB is known to be a redox-sensitive factor**.** NF-κB is often viewed as a pivotal switch in microglia adapting the M1 proinflammatory phenotype. Under basal conditions, NF-κB is inactive in the cytosol due to its binding with IkB. However, due to an increase oxidants, IkB will release the catalytic NF-κB subunits to allow it to translocate into the nucleus to induce the expression of various proinflammatory genes in microglia (Rojo et al 2014). Oxidants in this case can either act directly on IkB or through activation of redox sensitive upstream kinases. This increase in transcriptional activity of the NF-κB p65/p50 dimer is often associated with MAP kinases downstream of NOX activation and oxidant production in microglia (Pawate et al 2004). While NF-κB is not essential for acquisition of the M1 phenotype (Taetzxch et al 2015), constitutively active NF-κB in microglia will drive these cells to a proinflammatory state that results in motor neuron death in ALS *in vitro* models (Frakes et al 2014). Additionally, microglia exposed to H2O2 showed altered NF-κB p50 protein-protein interactions and augmented late-stage TNFα expression, indicating that H2O2 impairs NF-κB p50 function and prolongs amplified M1 activation. In this model DNA binding decreased when NF-κB p50 was oxidized, and this DNA binding could be restored through addition of the reducing enzyme thioredoxin (Kabe et al 2005).

Nrf2. Nrf2 (is nuclear factor erythroid 2 related factor 2) is considered the master regulator of antioxidant responses, as upon its translocation to the nucleus, it binds to genes in the antioxidant response element (ARE) to upregulate cytoprotective genes such as HO-1 and other antioxidant proteins. Under basal conditions, Nrf2 is bound to Kelch-like ECH-associated protein (KEAP1).

Nrf2 is continuously ubiquinated and degraded by the proteasome. However, when the cysteine residues in KEAP1 are oxidized, it releases Nrf2 where it is subsequently translocated to the nucleus (Niture et al 2014; Ma et al 2013). Thus, inherent with M1 induction and increased NOX2 activity, there is a level of Nrf2 activation and induction of an antioxidant response that occurs. Previous studies have shown that NOX2 activity is an upstream and essential regulator in Nrf2/Keap1 signaling (Sekhar et al 2003). Additionally, Nrf2 deficient macrophages have an increased NOX2 superoxide production, TLR4 signaling, and IkB inactivation, resulting in a prolonged inflammatory response (Kong et al 2010). Relatedly, induction of HO-1 through a Nrf2 dependent mechanism by activing a7-nAchR in oxygen and glucose deprived microglia cultures, also inhibited NOX activity.

Oxidant production and control of that oxidant production (redox signaling) are of critical importance in all cell types, but especially within microglia, cells who produce oxidants as one of their main functions. ROS can have a wide range of effects and their rapid production and transient nature are exploited by cells for efficient and reversible signaling. The chemical reactivity of ROS allows both cytotoxic effects against pathogens and selective chemical modifications to biomolecules in order to regulate various enzymatic functions. The ubiquitous theme of NOX activation by environmental stresses likely led to coevolved responses in which redox-dependent cellular signaling pathways are hardwired into hermetic and cytoprotective systems. It is when these responses are no longer balanced that the relationship with ROS becomes problematic and deleterious. Microglia, as guardians of the CNS and major oxidant producers, are charged with balancing this delicate relationship both intracellularly and extracellularly across the brain.

SUMMARY

As previously stated, TSPO is a biomarker of brain injury and inflammation that is used in preclinical and clinical studies to detect a wide range of brain pathologies. However, there is a lack of knowledge on the function of TSPO in microglia and astrocytes, the two cell that express and upregulate TSPO as a result of injury. Recent studies using TSPO knockout mice have questioned the long-held view that TSPO transports cholesterol into the mitochondria for steroid synthesis. In the brain, microglia and astrocytes exhibit distinct spatial and temporal patterns of TSPO upregulation, indicating a potentially different function of TSPO in microglia and astrocytes.

Additionally, TSPO expression prior to clinical expression of diseases has not been fully investigated. Many studies are cross-sectional in nature and thus assess TSPO levels when the disease is already in the active clinical stage. There is a need to assess TSPO expression not only in the progression of clinically active disease, but also in the early non-symptomatic stages of disease.

The main goal of the proposed studies is to address some of the key questions regarding TSPO biology and function in microglia and TSPO's trajectory of upregulation in relation to various neuropathological and behavioral endpoints.

Specific Aim #1: To examine TSPO levels in a neurodegenerative transgenic mouse model of Sandhoff disease and longitudinally compare TSPO levels to behavioral manifestations of disease and other neuropathological endpoints (neurodegeneration, reactive gliosis, ganglioside accumulation). This study will aim to see how early in time TSPO can be used as a biomarker and will track the cellular source of the TSPO signal and how it varies across brain regions. We will measure TSPO levels *ex vivo* using quantitative receptor autoradiography and

immunohistochemistry, as well as *in vivo* using SPECT with the novel TPSO ligand [^{125}I]-IodoDPA-713.

Specific Aim #2: To examine the source of TSPO-ligand (TSPO-L) induced reactive oxygen species (ROS) production in primary microglia. This study will examine other potential sources of TSPO-L induced ROS and aim to follow up on the finding that TSPO-L induced ROS production can be abrogated with NADPH oxidase inhibitors. Additionally, we will assess the effect of TSPO-L on the redox sensitive transcription factor nuclear factor erythroid 2 related factor (Nrf2).

Specific Aim #3: To determine if TSPO is interacting with NADPH oxidase (NOX2) in primary microglia. These studies will build off of the finding that TSPO is associated with NOX2 in microglia and aim to determine if there is a direct protein-protein interaction and/or functional interaction. These studies will employ multiple methods to assess if these proteins are interacting including: immunoprecipitation, proximity ligation assay, and immunofluorescence and colocalization analyses.

A.

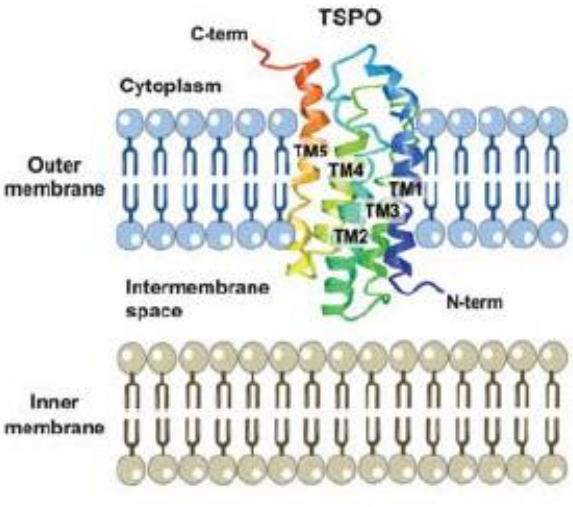

B.

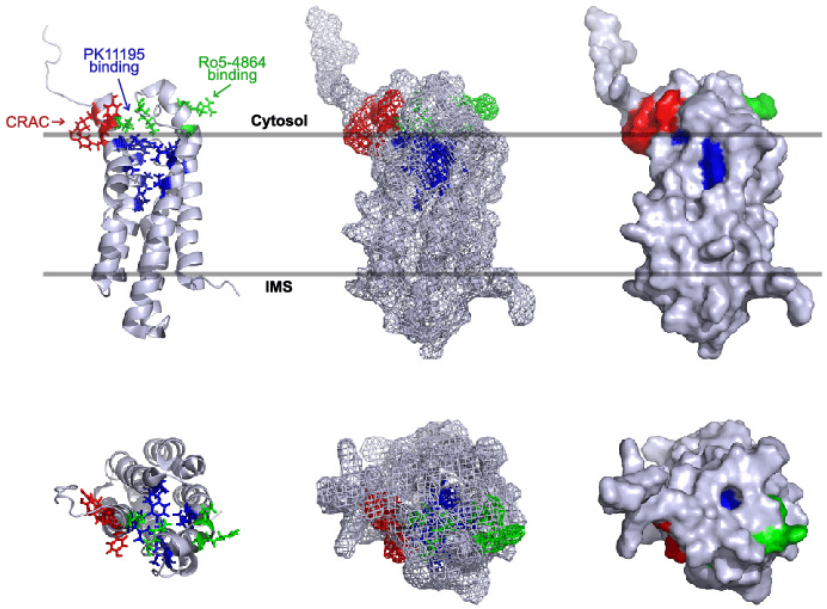

Figure 1.1. Structure of TSPO including indication of cholesterol, PK11195, and Ro5-4864 binding sites. The binding sites for cholesterol, PK, and Ro have been determined to be separate and distinct from one another. Previously the CRAC motif (residues 147-159) was thought to line the inside of a hydrophobic pore that would allow cholesterol to bind and translocate. However, higher resolution NMR models demonstrated that the CRAC domain is actually on the outer edge of TSPO, facing the membrane environment (Jaremko et al 2014). PK actually has a binding pocket that involves several key residues Ala23, Val26, Leu49, Ala50, Ile52, Trp107, Ala110, Leu114, Ala147, and Leu150, none of which involve CRAC motif amino acid side chains (Jaremko et al 2014). The binding site for Ro is more lateral than that for PK and involves the residues Glu29, Arg32, Lys39, and Val154 (Farges et al 1994). (Image 1A taken from Notter et al 2018 and 1B taken from Selvaraj et al 2017).

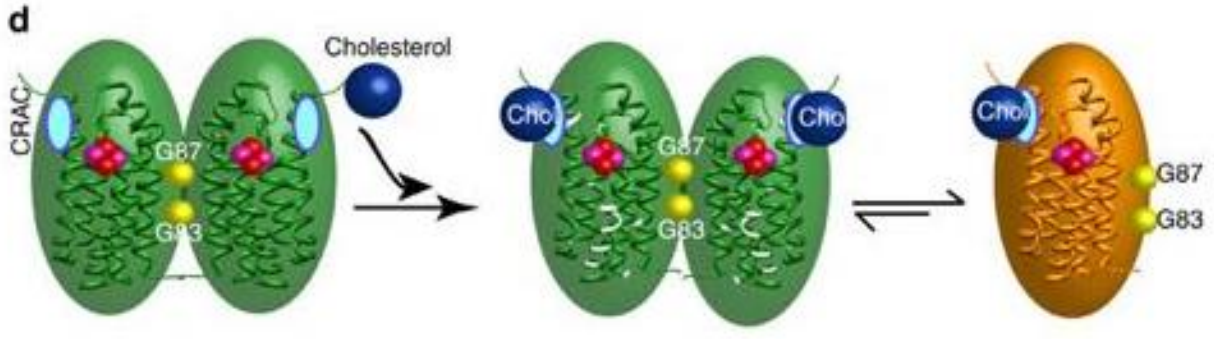

Figure 1.2. TSPO monomer & dimer. Proposed model of TSPO homodimer dissociation (Image taken from Jaipuria et al 2017).

TSPO-Associated Functions in Animals, Plants, and Bacteria		
Animals	**Plants**	**Bacteria**
Mitochondrial membrane potential transition		Interactions with large membrane channels
Transport of porphyrin intermediates	Translocation of tetrapyrrole intermediates	Transport of porphyrin intermediates
Heme metabolism	Tetrapyrrole metabolism	Heme metabolism
ROS generation	Oxidative stress	ROS generation
Programmed cell death	Cell death	Induction of apoptosis in eukaryotes
Mitochondrial protein transport		
Mitochondrial metabolism		Anaerobic and aerobic metabolism
Mitochondrial cholesterol transport		Cholesterol binding
Steroidogenesis		
Nuclear gene expression		Gene expression
Cell cycle	Cell cycle	Cell cycle
Cell growth		Cell growth
Cell proliferation		
Cell migration		
Cell adhesion		Adhesion
Cell differentiation		
Embryonic development	Seed and plant development	
Endocrinological function		
Reproduction		
Stress response	Stress response	Stress response
Immune response	Response to pathogens	
Inflammatory response		
Glial activation		
Response to brain disease and injury		
Emotional health		
Mental health		
Cardiovascular health		
Homeostasis	Homeostasis	Homeostasis
Life span of multicellular organisms		

Figure 1.3. Table summarizing the attributed functions to TSPO across phylogeny. (Image taken from Veenman et al 2016).

A.

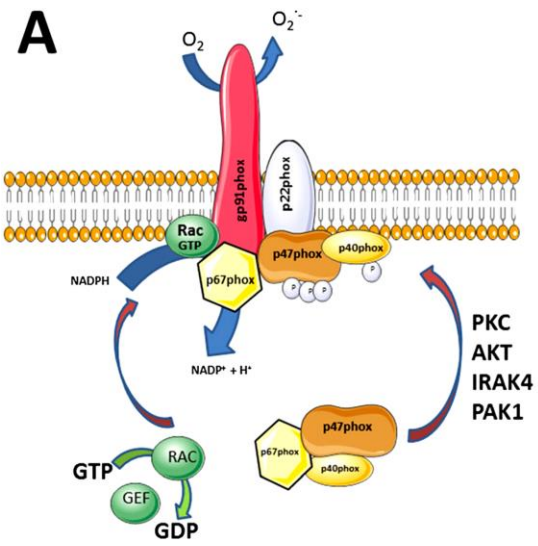

B.

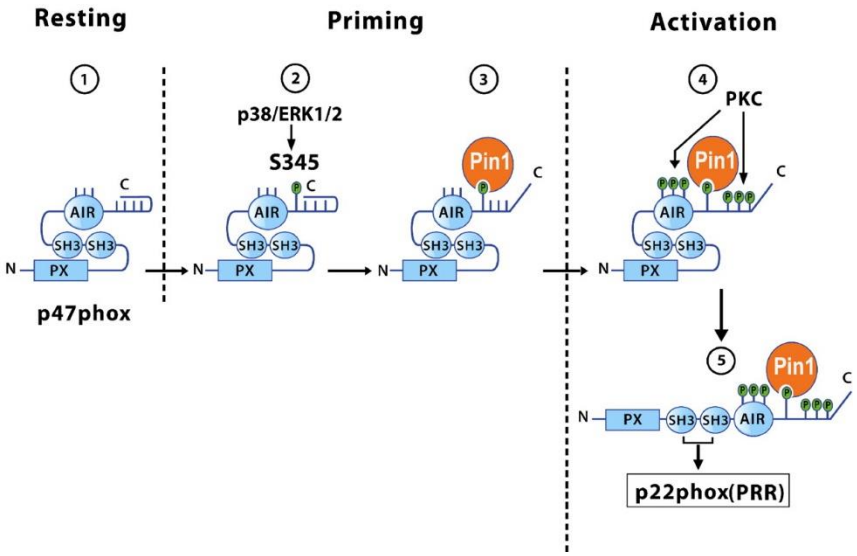

Figure 1.4. NOX2 Activation & p47 ^{phox} Phosphorylation

A. NADPH oxidase (NOX2) is activated through the translocation of 3 cytosolic subunits to the its 2 membrane bound subunits (Image taken from Hashlund-Vinding et al 2016).

B. p47 ^{phox} is phosphorylated at multiple sites in order to reveal its SH3 domains that allow it to bind to the proline rich region of p22^{phox} (Image taken from Boussetta et al 2010).

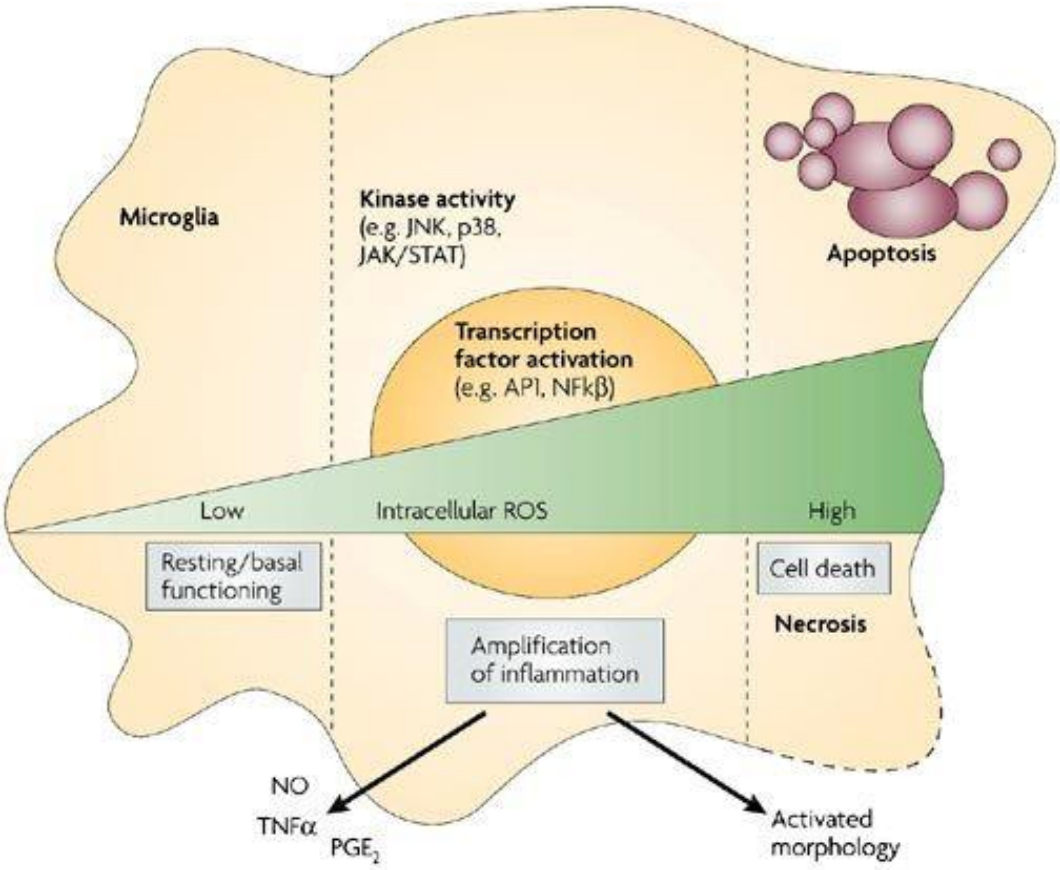

Figure 1.5 Intracellular ROS levels regulate microglial activation

The degree of ROS in microglia controls which transcription factors are activated and if ROS are being used for redox signaling purposes, or if as ROS levels increases, they initiate transcription factors to induce activation of the microglia. If ROS levels become too high, microglia induce cell death either through apoptosis or necrosis (Image taken from Block et al 2007).

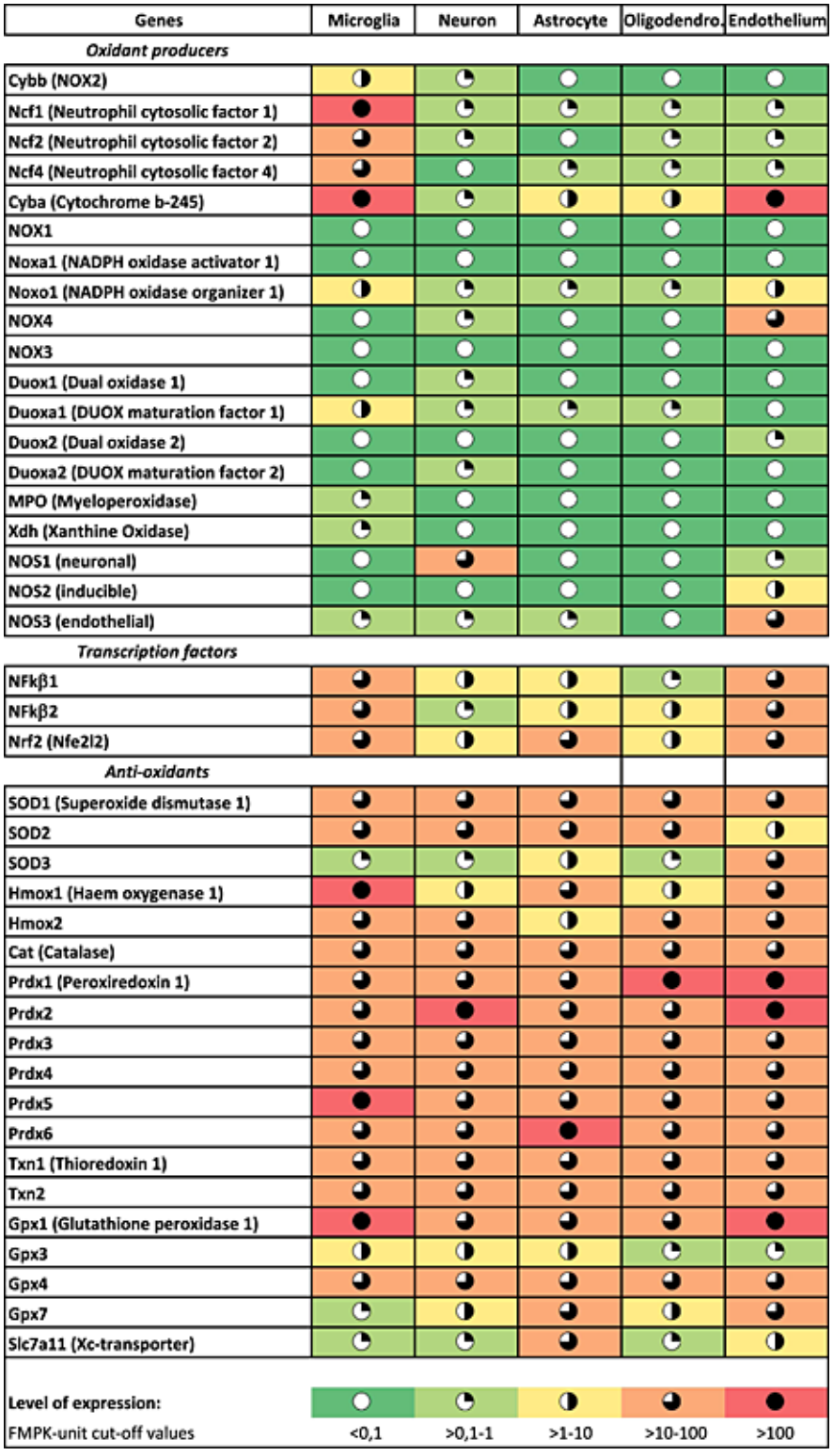

Figure 1.6. Expression of selected oxidant and anti-oxidant related genes from an adult mouse in the cerebral cortex. (Image taken from Zhang et al 2014 and Vilhardt et al 2017).

REFERENCES

Ago, T., Kuribayashi, F., Hiroaki, H., Takeya, R., Ito, T., Kohda, D., & Sumimoto, H. (2003). Phosphorylation of p47phox directs phox homology domain from SH3 domain toward phosphoinositides, leading to phagocyte NADPH oxidase activation. *Proc Natl Acad Sci U S A, 100*(8), 4474-4479. doi:10.1073/pnas.0735712100

Ago, T., Nunoi, H., Ito, T., & Sumimoto, H. (1999). Mechanism for phosphorylation-induced activation of the phagocyte NADPH oxidase protein p47(phox). Triple replacement of serines 303, 304, and 328 with aspartates disrupts the SH3 domain-mediated intramolecular interaction in p47(phox), thereby activating the oxidase. *J Biol Chem, 274*(47), 33644-33653.

Aguzzi, A., Barres, B. A., & Bennett, M. L. (2013). Microglia: scapegoat, saboteur, or something else? *Science, 339*(6116), 156-161. doi:10.1126/science.1227901

Ajami, B., Bennett, J. L., Krieger, C., Tetzlaff, W., & Rossi, F. M. (2007). Local self-renewal can sustain CNS microglia maintenance and function throughout adult life. *Nat Neurosci, 10*(12), 1538-1543. doi:10.1038/nn2014

Alho, H., Harjuntausta, T., Schultz, R., Pelto-Huikko, M., & Bovolin, P. (1991). Immunohistochemistry of diazepam binding inhibitor (DBI) in the central nervous system and peripheral organs: its possible role as an endogenous regulator of different types of benzodiazepine receptors. *Neuropharmacology, 30*(12B), 1381-1386.

Anholt, R. R., De Souza, E. B., Oster-Granite, M. L., & Snyder, S. H. (1985). Peripheral-type benzodiazepine receptors: autoradiographic localization in whole-body sections of neonatal rats. *J Pharmacol Exp Ther, 233*(2), 517-526.

Anholt, R. R., Pedersen, P. L., De Souza, E. B., & Snyder, S. H. (1986). The peripheral-type benzodiazepine receptor. Localization to the mitochondrial outer membrane. *J Biol Chem, 261*(2), 576-583.

Antkiewicz-Michaluk, L., Guidotti, A., & Krueger, K. E. (1988). Molecular characterization and mitochondrial density of a recognition site for peripheral-type benzodiazepine ligands. *Mol Pharmacol, 34*(3), 272-278.

Apolloni, S., Parisi, C., Pesaresi, M. G., Rossi, S., Carri, M. T., Cozzolino, M., . . . D'Ambrosi, N. (2013). The NADPH oxidase pathway is dysregulated by the P2X7 receptor in the SOD1-G93A microglia model of amyotrophic lateral sclerosis. *J Immunol, 190*(10), 5187-5195. doi:10.4049/jimmunol.1203262

Awad, M., & Gavish, M. (1987). Binding of [3H]Ro 5-4864 and [3H]PK 11195 to cerebral cortex and peripheral tissues of various species: species differences and heterogeneity in peripheral benzodiazepine binding sites. *J Neurochem, 49*(5), 1407-1414.

Babior, B. M. (2000). Phagocytes and oxidative stress. *Am J Med, 109*(1), 33-44.

Bae, K. R., Shim, H. J., Balu, D., Kim, S. R., & Yu, S. W. (2014). Translocator protein 18 kDa negatively regulates inflammation in microglia. *J Neuroimmune Pharmacol, 9*(3), 424-437. doi:10.1007/s11481-014-9540-6

Baez, E., Guio-Vega, G. P., Echeverria, V., Sandoval-Rueda, D. A., & Barreto, G. E. (2017). 4'-Chlorodiazepam Protects Mitochondria in T98G Astrocyte Cell Line from Glucose Deprivation. *Neurotox Res, 32*(2), 163-171. doi:10.1007/s12640-017-9733-x

Baines, C. P., Kaiser, R. A., Sheiko, T., Craigen, W. J., & Molkentin, J. D. (2007). Voltage-dependent anion channels are dispensable for mitochondrial-dependent cell death. *Nat Cell Biol, 9*(5), 550-555. doi:10.1038/ncb1575

Bamberger, M. E., Harris, M. E., McDonald, D. R., Husemann, J., & Landreth, G. E. (2003). A cell surface receptor complex for fibrillar beta-amyloid mediates microglial activation. *J Neurosci, 23*(7), 2665-2674.

Banati, R. B., Middleton, R. J., Chan, R., Hatty, C. R., Kam, W. W., Quin, C., . . . Liu, G. J. (2014). Positron emission tomography and functional characterization of a complete PBR/TSPO knockout. *Nat Commun, 5*, 5452. doi:10.1038/ncomms6452

Bannai, S. (1984). Induction of cystine and glutamate transport activity in human fibroblasts by diethyl maleate and other electrophilic agents. *J Biol Chem, 259*(4), 2435-2440.

Bannai, S. (1984). Transport of cystine and cysteine in mammalian cells. *Biochim Biophys Acta, 779*(3), 289-306.

Barron, A. M., Garcia-Segura, L. M., Caruso, D., Jayaraman, A., Lee, J. W., Melcangi, R. C., & Pike, C. J. (2013). Ligand for translocator protein reverses pathology in a mouse model of Alzheimer's disease. *J Neurosci, 33*(20), 8891-8897. doi:10.1523/JNEUROSCI.1350-13.2013

Barron, A. M., Ji, B., Kito, S., Suhara, T., & Higuchi, M. (2018). Steroidogenic abnormalities in translocator protein knockout mice and significance in the aging male. *Biochem J, 475*(1), 75-85. doi:10.1042/BCJ20170645

Batoko, H., Veljanovski, V., & Jurkiewicz, P. (2015). Enigmatic Translocator protein (TSPO) and cellular stress regulation. *Trends Biochem Sci, 40*(9), 497-503. doi:10.1016/j.tibs.2015.07.001

Beinlich, A., Strohmeier, R., Kaufmann, M., & Kuhl, H. (2000). Relation of cell proliferation to expression of peripheral benzodiazepine receptors in human breast cancer cell lines. *Biochem Pharmacol, 60*(3), 397-402.

Benavides, J., Quarteronet, D., Imbault, F., Malgouris, C., Uzan, A., Renault, C., . . . Le Fur, G. (1983). Labelling of "peripheral-type" benzodiazepine binding sites in the rat brain by using [3H]PK 11195, an isoquinoline carboxamide derivative: kinetic studies and autoradiographic localization. *J Neurochem, 41*(6), 1744-1750.

Bender, A. S., & Norenberg, M. D. (1998). Effect of benzodiazepines and neurosteroids on ammonia-induced swelling in cultured astrocytes. *J Neurosci Res, 54*(5), 673-680.

doi:10.1002/(SICI)1097-4547(19981201)54:5<673::AID-JNR12>3.0.CO;2-P

Bernardi, P. (2013). The mitochondrial permeability transition pore: a mystery solved? *Front Physiol, 4*, 95. doi:10.3389/fphys.2013.00095

Bianca, V. D., Dusi, S., Bianchini, E., Dal Pra, I., & Rossi, F. (1999). beta-amyloid activates the O-2 forming NADPH oxidase in microglia, monocytes, and neutrophils. A possible inflammatory mechanism of neuronal damage in Alzheimer's disease. *J Biol Chem, 274*(22), 15493-15499.

Block, M. L., & Hong, J. S. (2005). Microglia and inflammation-mediated neurodegeneration: multiple triggers with a common mechanism. *Prog Neurobiol, 76*(2), 77-98. doi:10.1016/j.pneurobio.2005.06.004

Block, M. L., Wu, X., Pei, Z., Li, G., Wang, T., Qin, L., . . . Veronesi, B. (2004). Nanometer size diesel exhaust particles are selectively toxic to dopaminergic neurons: the role of microglia, phagocytosis, and NADPH oxidase. *FASEB J, 18*(13), 1618-1620. doi:10.1096/fj.04-1945fje

Block, M. L., Zecca, L., & Hong, J. S. (2007). Microglia-mediated neurotoxicity: uncovering the molecular mechanisms. *Nat Rev Neurosci, 8*(1), 57-69. doi:10.1038/nrn2038

Boussetta, T., Gougerot-Pocidalo, M. A., Hayem, G., Ciappelloni, S., Raad, H., Arabi Derkawi, R., . . . El-Benna, J. (2010). The prolyl isomerase Pin1 acts as a novel molecular switch for TNF-alpha-induced priming of the NADPH oxidase in human neutrophils. *Blood, 116*(26), 5795-5802. doi:10.1182/blood-2010-03-273094

Braestrup, C., & Squires, R. F. (1977). Specific benzodiazepine receptors in rat brain characterized by high-affinity (3H)diazepam binding. *Proc Natl Acad Sci U S A, 74*(9), 3805-3809.

Bribes, E., Carriere, D., Goubet, C., Galiegue, S., Casellas, P., & Simony-Lafontaine, J. (2004). Immunohistochemical assessment of the peripheral benzodiazepine receptor in human tissues. *J Histochem Cytochem, 52*(1), 19-28. doi:10.1177/002215540405200103

Brieger, K., Schiavone, S., Miller, F. J., Jr., & Krause, K. H. (2012). Reactive oxygen species: from health to disease. *Swiss Med Wkly, 142*, w13659. doi:10.4414/smw.2012.13659

Brosig, B., & Langosch, D. (1998). The dimerization motif of the glycophorin A transmembrane segment in membranes: importance of glycine residues. *Protein Sci, 7*(4), 1052-1056. doi:10.1002/pro.5560070423

Butovsky, O., Jedrychowski, M. P., Moore, C. S., Cialic, R., Lanser, A. J., Gabriely, G., . . . Weiner, H. L. (2014). Identification of a unique TGF-beta-dependent molecular and functional signature in microglia. *Nat Neurosci, 17*(1), 131-143. doi:10.1038/nn.3599

Caballero, B., Veenman, L., Bode, J., Leschiner, S., & Gavish, M. (2014). Concentration-dependent bimodal effect of specific 18 kDa translocator protein (TSPO) ligands on cell death processes induced by ammonium chloride: potential implications for neuropathological effects due to hyperammonemia. *CNS Neurol Disord Drug Targets, 13*(4), 574-592.

Caballero, B., Veenman, L., & Gavish, M. (2013). Role of mitochondrial translocator protein (18 kDa) on mitochondrial- related cell death processes. *Recent Pat Endocr Metab Immune Drug Discov, 7*(2), 86-101.

Cagnin, A., Brooks, D. J., Kennedy, A. M., Gunn, R. N., Myers, R., Turkheimer, F. E., . . . Banati, R. B. (2001). In-vivo measurement of activated microglia in dementia. *Lancet, 358*(9280), 461-467. doi:10.1016/S0140-6736(01)05625-2

Cagnin, A., Myers, R., Gunn, R. N., Lawrence, A. D., Stevens, T., Kreutzberg, G. W., . . . Banati, R. B. (2001). In vivo visualization of activated glia by [11C] (R)-PK11195-PET following herpes encephalitis reveals projected neuronal damage beyond the primary focal lesion. *Brain, 124*(Pt 10), 2014-2027.

Campanella, M., Szabadkai, G., & Rizzuto, R. (2008). Modulation of intracellular Ca2+ signalling in HeLa cells by the apoptotic cell death enhancer PK11195. *Biochem Pharmacol, 76*(11), 1628-1636. doi:10.1016/j.bcp.2008.09.034

Carayon, P., Portier, M., Dussossoy, D., Bord, A., Petitpretre, G., Canat, X., . . . Casellas, P. (1996). Involvement of peripheral benzodiazepine receptors in the protection of hematopoietic cells against oxygen radical damage. *Blood, 87*(8), 3170-3178.

Caron, E., & Hall, A. (1998). Identification of two distinct mechanisms of phagocytosis controlled by different Rho GTPases. *Science, 282*(5394), 1717-1721.

Casano, A. M., & Peri, F. (2015). Microglia: multitasking specialists of the brain. *Dev Cell, 32*(4), 469-477. doi:10.1016/j.devcel.2015.01.018

Chelli, B., Falleni, A., Salvetti, F., Gremigni, V., Lucacchini, A., & Martini, C. (2001). Peripheral-type benzodiazepine receptor ligands: mitochondrial permeability transition induction in rat cardiac tissue. *Biochem Pharmacol, 61*(6), 695-705.

Chen, J. C., Ho, F. M., Pei-Dawn Lee, C., Chen, C. P., Jeng, K. C., Hsu, H. B., . . . Lin, W. W. (2005). Inhibition of iNOS gene expression by quercetin is mediated by the inhibition of IkappaB kinase, nuclear factor-kappa B and STAT1, and depends on heme oxygenase-1 induction in mouse BV-2 microglia. *Eur J Pharmacol, 521*(1-3), 9-20. doi:10.1016/j.ejphar.2005.08.005

Chen, M. K., & Guilarte, T. R. (2008). Translocator protein 18 kDa (TSPO): molecular sensor of brain injury and repair. *Pharmacol Ther, 118*(1), 1-17. doi:10.1016/j.pharmthera.2007.12.004

Cherry, J. D., Olschowka, J. A., & O'Banion, M. K. (2014). Neuroinflammation and M2 microglia: the good, the bad, and the inflamed. *J Neuroinflammation, 11*, 98. doi:10.1186/1742-2094-11-98

Cho, S., Park, E. M., Febbraio, M., Anrather, J., Park, L., Racchumi, G., . . . Iadecola, C. (2005). The class B scavenger receptor CD36 mediates free radical production and tissue injury in cerebral ischemia. *J Neurosci, 25*(10), 2504-2512. doi:10.1523/JNEUROSCI.0035-05.2005

Choi, J., Ifuku, M., Noda, M., & Guilarte, T. R. (2011). Translocator protein (18 kDa)/peripheral benzodiazepine receptor specific ligands induce microglia functions consistent with an activated

state. *Glia, 59*(2), 219-230. doi:10.1002/glia.21091

Codolo, G., Plotegher, N., Pozzobon, T., Brucale, M., Tessari, I., Bubacco, L., & de Bernard, M. (2013). Triggering of inflammasome by aggregated alpha-synuclein, an inflammatory response in synucleinopathies. *PLoS One, 8*(1), e55375. doi:10.1371/journal.pone.0055375

Colton, C. A., & Gilbert, D. L. (1987). Production of superoxide anions by a CNS macrophage, the microglia. *FEBS Lett, 223*(2), 284-288.

Coraci, I. S., Husemann, J., Berman, J. W., Hulette, C., Dufour, J. H., Campanella, G. K., . . . El-Khoury, J. B. (2002). CD36, a class B scavenger receptor, is expressed on microglia in Alzheimer's disease brains and can mediate production of reactive oxygen species in response to beta-amyloid fibrils. *Am J Pathol, 160*(1), 101-112.

Corsi, L., Avallone, R., Geminiani, E., Cosenza, F., Venturini, I., & Baraldi, M. (2004). Peripheral benzodiazepine receptors in potatoes (Solanum tuberosum). *Biochem Biophys Res Commun, 313*(1), 62-66.

Cosenza-Nashat, M., Zhao, M. L., Suh, H. S., Morgan, J., Natividad, R., Morgello, S., & Lee, S. C. (2009). Expression of the translocator protein of 18 kDa by microglia, macrophages and astrocytes based on immunohistochemical localization in abnormal human brain. *Neuropathol Appl Neurobiol, 35*(3), 306-328. doi:10.1111/j.1365-2990.2008.01006.x

Costa, B., Da Pozzo, E., Giacomelli, C., Taliani, S., Bendinelli, S., Barresi, E., . . . Martini, C. (2015). TSPO ligand residence time influences human glioblastoma multiforme cell death/life balance. *Apoptosis, 20*(3), 383-398. doi:10.1007/s10495-014-1063-3

Costa, B., Salvetti, A., Rossi, L., Spinetti, F., Lena, A., Chelli, B., . . . Martini, C. (2006). Peripheral benzodiazepine receptor: characterization in human T-lymphoma Jurkat cells. *Mol Pharmacol, 69*(1), 37-44. doi:10.1124/mol.105.015289

Coughlin, J. M., Wang, Y., Minn, I., Bienko, N., Ambinder, E. B., Xu, X., . . . Pomper, M. G. (2017). Imaging of Glial Cell Activation and White Matter Integrity in Brains of Active and Recently Retired National Football League Players. *JAMA Neurol, 74*(1), 67-74. doi:10.1001/jamaneurol.2016.3764

Coughlin, J. M., Wang, Y., Munro, C. A., Ma, S., Yue, C., Chen, S., . . . Pomper, M. G. (2015). Neuroinflammation and brain atrophy in former NFL players: An in vivo multimodal imaging pilot study. *Neurobiol Dis, 74*, 58-65. doi:10.1016/j.nbd.2014.10.019

Cox, J. A., Jeng, A. Y., Sharkey, N. A., Blumberg, P. M., & Tauber, A. I. (1985). Activation of the human neutrophil nicotinamide adenine dinucleotide phosphate (NADPH)-oxidase by protein kinase C. *J Clin Invest, 76*(5), 1932-1938. doi:10.1172/JCI112190

Dang, P. M., Elbim, C., Marie, J. C., Chiandotto, M., Gougerot-Pocidalo, M. A., & El-Benna, J. (2006). Anti-inflammatory effect of interleukin-10 on human neutrophil respiratory burst involves inhibition of GM-CSF-induced p47PHOX phosphorylation through a decrease in ERK1/2 activity. *FASEB J, 20*(9), 1504-1506. doi:10.1096/fj.05-5395fje

Daugherty, D. J., Chechneva, O., Mayrhofer, F., & Deng, W. (2016). The hGFAP-driven conditional TSPO knockout is protective in a mouse model of multiple sclerosis. *Sci Rep, 6*, 22556. doi:10.1038/srep22556

Daugherty, D. J., Selvaraj, V., Chechneva, O. V., Liu, X. B., Pleasure, D. E., & Deng, W. (2013). A TSPO ligand is protective in a mouse model of multiple sclerosis. *EMBO Mol Med, 5*(6), 891-903. doi:10.1002/emmm.201202124

Davalos, D., Grutzendler, J., Yang, G., Kim, J. V., Zuo, Y., Jung, S., . . . Gan, W. B. (2005). ATP mediates rapid microglial response to local brain injury in vivo. *Nat Neurosci, 8*(6), 752-758. doi:10.1038/nn1472

de Jong, E. K., de Haas, A. H., Brouwer, N., van Weering, H. R., Hensens, M., Bechmann, I., . . . Biber, K. (2008). Expression of CXCL4 in microglia in vitro and in vivo and its possible signaling through CXCR3. *J Neurochem, 105*(5), 1726-1736. doi:10.1111/j.1471-4159.2008.05267.x

De Souza, E. B., Anholt, R. R., Murphy, K. M., Snyder, S. H., & Kuhar, M. J. (1985). Peripheral-type benzodiazepine receptors in endocrine organs: autoradiographic localization in rat pituitary, adrenal, and testis. *Endocrinology, 116*(2), 567-573. doi:10.1210/endo-116-2-567

Decaudin, D., Castedo, M., Nemati, F., Beurdeley-Thomas, A., De Pinieux, G., Caron, A., . . . Poupon, M. F. (2002). Peripheral benzodiazepine receptor ligands reverse apoptosis resistance of cancer cells in vitro and in vivo. *Cancer Res, 62*(5), 1388-1393.

Delavoie, F., Li, H., Hardwick, M., Robert, J. C., Giatzakis, C., Peranzi, G., . . . Papadopoulos, V. (2003). In vivo and in vitro peripheral-type benzodiazepine receptor polymerization: functional significance in drug ligand and cholesterol binding. *Biochemistry, 42*(15), 4506-4519. doi:10.1021/bi0267487

DeLeo, F. R., Renee, J., McCormick, S., Nakamura, M., Apicella, M., Weiss, J. P., & Nauseef, W. M. (1998). Neutrophils exposed to bacterial lipopolysaccharide upregulate NADPH oxidase assembly. *J Clin Invest, 101*(2), 455-463. doi:10.1172/JCI949

Diebold, B. A., & Bokoch, G. M. (2001). Molecular basis for Rac2 regulation of phagocyte NADPH oxidase. *Nat Immunol, 2*(3), 211-215. doi:10.1038/85259

Domazet-Loso, T., & Tautz, D. (2008). An ancient evolutionary origin of genes associated with human genetic diseases. *Mol Biol Evol, 25*(12), 2699-2707. doi:10.1093/molbev/msn214

Doorduin, J., de Vries, E. F., Dierckx, R. A., & Klein, H. C. (2008). PET imaging of the peripheral benzodiazepine receptor: monitoring disease progression and therapy response in neurodegenerative disorders. *Curr Pharm Des, 14*(31), 3297-3315.

Dringen, R. (2005). Oxidative and antioxidative potential of brain microglial cells. *Antioxid Redox Signal, 7*(9-10), 1223-1233. doi:10.1089/ars.2005.7.1223

Dussossoy, D., Carayon, P., Feraut, D., Belugou, S., Combes, T., Canat, X., . . . Casellas, P. (1996). Development of a monoclonal antibody to immuno-cytochemical analysis of the cellular

localization of the peripheral benzodiazepine receptor. *Cytometry, 24*(1), 39-48. doi:10.1002/(SICI)1097-0320(19960501)24:1<39::AID-CYTO5>3.0.CO;2-D

Ejlerskov, P., Christensen, D. P., Beyaie, D., Burritt, J. B., Paclet, M. H., Gorlach, A., . . . Vilhardt, F. (2012). NADPH oxidase is internalized by clathrin-coated pits and localizes to a Rab27A/B GTPase-regulated secretory compartment in activated macrophages. *J Biol Chem, 287*(7), 4835-4852. doi:10.1074/jbc.M111.293696

Elkabes, S., DiCicco-Bloom, E. M., & Black, I. B. (1996). Brain microglia/macrophages express neurotrophins that selectively regulate microglial proliferation and function. *J Neurosci, 16*(8), 2508-2521.

Evonuk, K. S., Baker, B. J., Doyle, R. E., Moseley, C. E., Sestero, C. M., Johnston, B. P., . . . DeSilva, T. M. (2015). Inhibition of System Xc(-) Transporter Attenuates Autoimmune Inflammatory Demyelination. *J Immunol, 195*(2), 450-463. doi:10.4049/jimmunol.1401108

Fairweather, D., Coronado, M. J., Garton, A. E., Dziedzic, J. L., Bucek, A., Cooper, L. T., Jr., . . . Guilarte, T. R. (2014). Sex differences in translocator protein 18 kDa (TSPO) in the heart: implications for imaging myocardial inflammation. *J Cardiovasc Transl Res, 7*(2), 192-202. doi:10.1007/s12265-013-9538-0

Fairweather, D., Coronado, M. J., Garton, A. E., Dziedzic, J. L., Bucek, A., Cooper, L. T., Jr., . . . Guilarte, T. R. (2014). Sex differences in translocator protein 18 kDa (TSPO) in the heart: implications for imaging myocardial inflammation. *J Cardiovasc Transl Res, 7*(2), 192-202. doi:10.1007/s12265-013-9538-0

Fan, J., Campioli, E., Midzak, A., Culty, M., & Papadopoulos, V. (2015). Conditional steroidogenic cell-targeted deletion of TSPO unveils a crucial role in viability and hormone-dependent steroid formation. *Proc Natl Acad Sci U S A, 112*(23), 7261-7266. doi:10.1073/pnas.1502670112

Farges, R., Joseph-Liauzun, E., Shire, D., Caput, D., Le Fur, G., & Ferrara, P. (1994). Site-directed mutagenesis of the peripheral benzodiazepine receptor: identification of amino acids implicated in the binding site of Ro5-4864. *Mol Pharmacol, 46*(6), 1160-1167.

Faust, L. R., el Benna, J., Babior, B. M., & Chanock, S. J. (1995). The phosphorylation targets of p47phox, a subunit of the respiratory burst oxidase. Functions of the individual target serines as evaluated by site-directed mutagenesis. *J Clin Invest, 96*(3), 1499-1505. doi:10.1172/JCI118187

Finkel, T. (2011). Signal transduction by reactive oxygen species. *J Cell Biol, 194*(1), 7-15. doi:10.1083/jcb.201102095

Frakes, A. E., Ferraiuolo, L., Haidet-Phillips, A. M., Schmelzer, L., Braun, L., Miranda, C. J., . . . Kaspar, B. K. (2014). Microglia induce motor neuron death via the classical NF-kappaB pathway in amyotrophic lateral sclerosis. *Neuron, 81*(5), 1009-1023. doi:10.1016/j.neuron.2014.01.013

Galluzzi, L., Blomgren, K., & Kroemer, G. (2009). Mitochondrial membrane permeabilization in neuronal injury. *Nat Rev Neurosci, 10*(7), 481-494. doi:10.1038/nrn2665

Gao, H. M., Hong, J. S., Zhang, W., & Liu, B. (2002). Distinct role for microglia in rotenone-induced degeneration of dopaminergic neurons. *J Neurosci, 22*(3), 782-790.

Gao, H. M., Jiang, J., Wilson, B., Zhang, W., Hong, J. S., & Liu, B. (2002). Microglial activation-mediated delayed and progressive degeneration of rat nigral dopaminergic neurons: relevance to Parkinson's disease. *J Neurochem, 81*(6), 1285-1297.

Gao, H. M., Liu, B., & Hong, J. S. (2003). Critical role for microglial NADPH oxidase in rotenone-induced degeneration of dopaminergic neurons. *J Neurosci, 23*(15), 6181-6187.

Gao, H. M., Zhou, H., & Hong, J. S. (2012). NADPH oxidases: novel therapeutic targets for neurodegenerative diseases. *Trends Pharmacol Sci, 33*(6), 295-303. doi:10.1016/j.tips.2012.03.008

Gatliff, J., & Campanella, M. (2012). The 18 kDa translocator protein (TSPO): a new perspective in mitochondrial biology. *Curr Mol Med, 12*(4), 356-368.

Gatliff, J., & Campanella, M. (2016). TSPO: kaleidoscopic 18-kDa amid biochemical pharmacology, control and targeting of mitochondria. *Biochem J, 473*(2), 107-121. doi:10.1042/BJ20150899

Gatliff, J., East, D., Crosby, J., Abeti, R., Harvey, R., Craigen, W., . . . Campanella, M. (2014). TSPO interacts with VDAC1 and triggers a ROS-mediated inhibition of mitochondrial quality control. *Autophagy, 10*(12), 2279-2296. doi:10.4161/15548627.2014.991665

Gatliff, J., East, D. A., Singh, A., Alvarez, M. S., Frison, M., Matic, I., . . . Campanella, M. (2017). A role for TSPO in mitochondrial Ca(2+) homeostasis and redox stress signaling. *Cell Death Dis, 8*(6), e2896. doi:10.1038/cddis.2017.186

Gehlert, D. R., Yamamura, H. I., & Wamsley, J. K. (1983). Autoradiographic localization of 'peripheral' benzodiazepine binding sites in the rat brain and kidney using [3H]RO5-4864. *Eur J Pharmacol, 95*(3-4), 329-330.

Gemelli, C., Dongmo, B. M., Ferrarini, F., Grande, A., & Corsi, L. (2014). Cytotoxic effect of hemin in colonic epithelial cell line: involvement of 18 kDa translocator protein (TSPO). *Life Sci, 107*(1-2), 14-20. doi:10.1016/j.lfs.2014.04.026

Gerhard, A., Pavese, N., Hotton, G., Turkheimer, F., Es, M., Hammers, A., . . . Brooks, D. J. (2006). In vivo imaging of microglial activation with [11C](R)-PK11195 PET in idiopathic Parkinson's disease. *Neurobiol Dis, 21*(2), 404-412. doi:10.1016/j.nbd.2005.08.002

Gerhard, A., Trender-Gerhard, I., Turkheimer, F., Quinn, N. P., Bhatia, K. P., & Brooks, D. J. (2006). In vivo imaging of microglial activation with [11C](R)-PK11195 PET in progressive supranuclear palsy. *Mov Disord, 21*(1), 89-93. doi:10.1002/mds.20668

Ginhoux, F., Greter, M., Leboeuf, M., Nandi, S., See, P., Gokhan, S., . . . Merad, M. (2010). Fate mapping analysis reveals that adult microglia derive from primitive macrophages. *Science, 330*(6005), 841-845. doi:10.1126/science.1194637

Ginter, C., Kiburu, I., & Boudker, O. (2013). Chemical catalysis by the translocator protein (18 kDa). *Biochemistry, 52*(21), 3609-3611. doi:10.1021/bi400364z

Girouard, H., Wang, G., Gallo, E. F., Anrather, J., Zhou, P., Pickel, V. M., & Iadecola, C. (2009). NMDA receptor activation increases free radical production through nitric oxide and NOX2. *J Neurosci, 29*(8), 2545-2552. doi:10.1523/JNEUROSCI.0133-09.2009

Guilarte, T. R., Kuhlmann, A. C., O'Callaghan, J. P., & Miceli, R. C. (1995). Enhanced expression of peripheral benzodiazepine receptors in trimethyltin-exposed rat brain: a biomarker of neurotoxicity. *Neurotoxicology, 16*(3), 441-450.

Guilarte, T. R., Loth, M. K., & Guariglia, S. R. (2016). TSPO Finds NOX2 in Microglia for Redox Homeostasis. *Trends Pharmacol Sci, 37*(5), 334-343. doi:10.1016/j.tips.2016.02.008

Guillaumot, D., Guillon, S., Deplanque, T., Vanhee, C., Gumy, C., Masquelier, D., . . . Batoko, H. (2009). The Arabidopsis TSPO-related protein is a stress and abscisic acid-regulated, endoplasmic reticulum-Golgi-localized membrane protein. *Plant J, 60*(2), 242-256. doi:10.1111/j.1365-313X.2009.03950.x

Gulyas, B., Toth, M., Schain, M., Airaksinen, A., Vas, A., Kostulas, K., . . . Halldin, C. (2012). Evolution of microglial activation in ischaemic core and peri-infarct regions after stroke: a PET study with the TSPO molecular imaging biomarker [((11))C]vinpocetine. *J Neurol Sci, 320*(1-2), 110-117. doi:10.1016/j.jns.2012.06.026

Guo, Y., Kalathur, R. C., Liu, Q., Kloss, B., Bruni, R., Ginter, C., . . . Hendrickson, W. A. (2015). Protein structure. Structure and activity of tryptophan-rich TSPO proteins. *Science, 347*(6221), 551-555. doi:10.1126/science.aaa1534

Gupta, S., Knight, A. G., Gupta, S., Knapp, P. E., Hauser, K. F., Keller, J. N., & Bruce-Keller, A. J. (2010). HIV-Tat elicits microglial glutamate release: role of NAPDH oxidase and the cystine-glutamate antiporter. *Neurosci Lett, 485*(3), 233-236. doi:10.1016/j.neulet.2010.09.019

Gut, P., Zweckstetter, M., & Banati, R. B. (2015). Lost in translocation: the functions of the 18-kD translocator protein. *Trends Endocrinol Metab, 26*(7), 349-356. doi:10.1016/j.tem.2015.04.001

Halestrap, A. P. (2009). What is the mitochondrial permeability transition pore? *J Mol Cell Cardiol, 46*(6), 821-831. doi:10.1016/j.yjmcc.2009.02.021

Hancock, J. T., Desikan, R., & Neill, S. J. (2001). Role of reactive oxygen species in cell signalling pathways. *Biochem Soc Trans, 29*(Pt 2), 345-350.

Hanisch, U. K., & Kettenmann, H. (2007). Microglia: active sensor and versatile effector cells in the normal and pathologic brain. *Nat Neurosci, 10*(11), 1387-1394. doi:10.1038/nn1997

Haslund-Vinding, J., McBean, G., Jaquet, V., & Vilhardt, F. (2017). NADPH oxidases in oxidant production by microglia: activating receptors, pharmacology and association with disease. *Br J Pharmacol, 174*(12), 1733-1749. doi:10.1111/bph.13425

Hausler, K. G., Prinz, M., Nolte, C., Weber, J. R., Schumann, R. R., Kettenmann, H., & Hanisch, U. K. (2002). Interferon-gamma differentially modulates the release of cytokines and chemokines in lipopolysaccharide- and pneumococcal cell wall-stimulated mouse microglia and macrophages. *Eur J Neurosci, 16*(11), 2113-2122.

Haynes, S. E., Hollopeter, G., Yang, G., Kurpius, D., Dailey, M. E., Gan, W. B., & Julius, D. (2006). The P2Y12 receptor regulates microglial activation by extracellular nucleotides. *Nat Neurosci, 9*(12), 1512-1519. doi:10.1038/nn1805

Hickman, S. E., Kingery, N. D., Ohsumi, T. K., Borowsky, M. L., Wang, L. C., Means, T. K., & El Khoury, J. (2013). The microglial sensome revealed by direct RNA sequencing. *Nat Neurosci, 16*(12), 1896-1905. doi:10.1038/nn.3554

Hirsch, T., Decaudin, D., Susin, S. A., Marchetti, P., Larochette, N., Resche-Rigon, M., & Kroemer, G. (1998). PK11195, a ligand of the mitochondrial benzodiazepine receptor, facilitates the induction of apoptosis and reverses Bcl-2-mediated cytoprotection. *Exp Cell Res, 241*(2), 426-434. doi:10.1006/excr.1998.4084

Hoffmann, M. H., & Griffiths, H. R. (2018). The dual role of ROS in autoimmune and inflammatory diseases: Evidence from preclinical models. *Free Radic Biol Med*. doi:10.1016/j.freeradbiomed.2018.03.016

Holmstrom, K. M., & Finkel, T. (2014). Cellular mechanisms and physiological consequences of redox-dependent signalling. *Nat Rev Mol Cell Biol, 15*(6), 411-421. doi:10.1038/nrm3801

Horvath, R. J., Nutile-McMenemy, N., Alkaitis, M. S., & Deleo, J. A. (2008). Differential migration, LPS-induced cytokine, chemokine, and NO expression in immortalized BV-2 and HAPI cell lines and primary microglial cultures. *J Neurochem, 107*(2), 557-569. doi:10.1111/j.1471-4159.2008.05633.x

Hu, X., Leak, R. K., Shi, Y., Suenaga, J., Gao, Y., Zheng, P., & Chen, J. (2015). Microglial and macrophage polarization-new prospects for brain repair. *Nat Rev Neurol, 11*(1), 56-64. doi:10.1038/nrneurol.2014.207

Huang, J., & Kleinberg, M. E. (1999). Activation of the phagocyte NADPH oxidase protein p47(phox). Phosphorylation controls SH3 domain-dependent binding to p22(phox). *J Biol Chem, 274*(28), 19731-19737.

Husemann, J., Loike, J. D., Anankov, R., Febbraio, M., & Silverstein, S. C. (2002). Scavenger receptors in neurobiology and neuropathology: their role on microglia and other cells of the nervous system. *Glia, 40*(2), 195-205. doi:10.1002/glia.10148

Imai, Y., Kuba, K., Neely, G. G., Yaghubian-Malhami, R., Perkmann, T., van Loo, G., . . . Penninger, J. M. (2008). Identification of oxidative stress and Toll-like receptor 4 signaling as a key pathway of acute lung injury. *Cell, 133*(2), 235-249. doi:10.1016/j.cell.2008.02.043

Innamorato, N. G., Lastres-Becker, I., & Cuadrado, A. (2009). Role of microglial redox balance in modulation of neuroinflammation. *Curr Opin Neurol, 22*(3), 308-314.

doi:10.1097/WCO.0b013e32832a3225

Jaipuria, G., Leonov, A., Giller, K., Vasa, S. K., Jaremko, L., Jaremko, M., . . . Zweckstetter, M. (2017). Cholesterol-mediated allosteric regulation of the mitochondrial translocator protein structure. *Nat Commun, 8*, 14893. doi:10.1038/ncomms14893

Jana, M., Palencia, C. A., & Pahan, K. (2008). Fibrillar amyloid-beta peptides activate microglia via TLR2: implications for Alzheimer's disease. *J Immunol, 181*(10), 7254-7262.

Jaremko, L., Jaremko, M., Giller, K., Becker, S., & Zweckstetter, M. (2014). Structure of the mitochondrial translocator protein in complex with a diagnostic ligand. *Science, 343*(6177), 1363-1366. doi:10.1126/science.1248725

Jaremko, M., Jaremko, L., Giller, K., Becker, S., & Zweckstetter, M. (2016). Backbone and side-chain resonance assignment of the A147T polymorph of mouse TSPO in complex with a high-affinity radioligand. *Biomol NMR Assign, 10*(1), 79-83. doi:10.1007/s12104-015-9642-y

Jayakumar, A. R., Panickar, K. S., & Norenberg, M. D. (2002). Effects on free radical generation by ligands of the peripheral benzodiazepine receptor in cultured neural cells. *J Neurochem, 83*(5), 1226-1234.

Jeohn, G. H., Kong, L. Y., Wilson, B., Hudson, P., & Hong, J. S. (1998). Synergistic neurotoxic effects of combined treatments with cytokines in murine primary mixed neuron/glia cultures. *J Neuroimmunol, 85*(1), 1-10.

Jezek, P., & Hlavata, L. (2005). Mitochondria in homeostasis of reactive oxygen species in cell, tissues, and organism. *Int J Biochem Cell Biol, 37*(12), 2478-2503. doi:10.1016/j.biocel.2005.05.013

Jiang, T., Hoekstra, J., Heng, X., Kang, W., Ding, J., Liu, J., . . . Zhang, J. (2015). P2X7 receptor is critical in alpha-synuclein--mediated microglial NADPH oxidase activation. *Neurobiol Aging, 36*(7), 2304-2318. doi:10.1016/j.neurobiolaging.2015.03.015

Joo, H. K., Lee, Y. R., Kang, G., Choi, S., Kim, C. S., Ryoo, S., . . . Jeon, B. H. (2015). The 18-kDa Translocator Protein Inhibits Vascular Cell Adhesion Molecule-1 Expression via Inhibition of Mitochondrial Reactive Oxygen Species. *Mol Cells, 38*(12), 1064-1070. doi:10.14348/molcells.2015.0165

Joo, H. K., Lee, Y. R., Lim, S. Y., Lee, E. J., Choi, S., Cho, E. J., . . . Jeon, B. H. (2012). Peripheral benzodiazepine receptor regulates vascular endothelial activations via suppression of the voltage-dependent anion channel-1. *FEBS Lett, 586*(9), 1349-1355. doi:10.1016/j.febslet.2012.03.049

Jou, I., Lee, J. H., Park, S. Y., Yoon, H. J., Joe, E. H., & Park, E. J. (2006). Gangliosides trigger inflammatory responses via TLR4 in brain glia. *Am J Pathol, 168*(5), 1619-1630. doi:10.2353/ajpath.2006.050924

Kabe, Y., Ando, K., Hirao, S., Yoshida, M., & Handa, H. (2005). Redox regulation of NF-kappaB activation: distinct redox regulation between the cytoplasm and the nucleus. *Antioxid Redox*

Signal, 7(3-4), 395-403. doi:10.1089/ars.2005.7.395

Kaindl, A. M., Degos, V., Peineau, S., Gouadon, E., Chhor, V., Loron, G., . . . Gressens, P. (2012). Activation of microglial N-methyl-D-aspartate receptors triggers inflammation and neuronal cell death in the developing and mature brain. *Ann Neurol, 72*(4), 536-549. doi:10.1002/ana.23626

Kang, G., Kong, P. J., Yuh, Y. J., Lim, S. Y., Yim, S. V., Chun, W., & Kim, S. S. (2004). Curcumin suppresses lipopolysaccharide-induced cyclooxygenase-2 expression by inhibiting activator protein 1 and nuclear factor kappab bindings in BV2 microglial cells. *J Pharmacol Sci, 94*(3), 325-328.

Karchewski, L. A., Bloechlinger, S., & Woolf, C. J. (2004). Axonal injury-dependent induction of the peripheral benzodiazepine receptor in small-diameter adult rat primary sensory neurons. *Eur J Neurosci, 20*(3), 671-683. doi:10.1111/j.1460-9568.2004.03530.x

Kaspar, J. W., Niture, S. K., & Jaiswal, A. K. (2009). Nrf2:INrf2 (Keap1) signaling in oxidative stress. *Free Radic Biol Med, 47*(9), 1304-1309. doi:10.1016/j.freeradbiomed.2009.07.035

Kettenmann, H., Kirchhoff, F., & Verkhratsky, A. (2013). Microglia: new roles for the synaptic stripper. *Neuron, 77*(1), 10-18. doi:10.1016/j.neuron.2012.12.023

Kim, S. Y., Moon, J. H., Lee, H. G., Kim, S. U., & Lee, Y. B. (2007). ATP released from beta-amyloid-stimulated microglia induces reactive oxygen species production in an autocrine fashion. *Exp Mol Med, 39*(6), 820-827. doi:10.1038/emm.2007.89

Kokoszka, J. E., Waymire, K. G., Levy, S. E., Sligh, J. E., Cai, J., Jones, D. P., . . . Wallace, D. C. (2004). The ADP/ATP translocator is not essential for the mitochondrial permeability transition pore. *Nature, 427*(6973), 461-465. doi:10.1038/nature02229

Komohara, Y., Ohnishi, K., Kuratsu, J., & Takeya, M. (2008). Possible involvement of the M2 anti-inflammatory macrophage phenotype in growth of human gliomas. *J Pathol, 216*(1), 15-24. doi:10.1002/path.2370

Kong, X., Thimmulappa, R., Kombairaju, P., & Biswal, S. (2010). NADPH oxidase-dependent reactive oxygen species mediate amplified TLR4 signaling and sepsis-induced mortality in Nrf2-deficient mice. *J Immunol, 185*(1), 569-577. doi:10.4049/jimmunol.0902315

Korkhov, V. M., Sachse, C., Short, J. M., & Tate, C. G. (2010). Three-dimensional structure of TspO by electron cryomicroscopy of helical crystals. *Structure, 18*(6), 677-687. doi:10.1016/j.str.2010.03.001

Krauskopf, A., Eriksson, O., Craigen, W. J., Forte, M. A., & Bernardi, P. (2006). Properties of the permeability transition in VDAC1(-/-) mitochondria. *Biochim Biophys Acta, 1757*(5-6), 590-595. doi:10.1016/j.bbabio.2006.02.007

Kreutzberg, G. W. (1996). Microglia: a sensor for pathological events in the CNS. *Trends Neurosci, 19*(8), 312-318.

Kugler, W., Veenman, L., Shandalov, Y., Leschiner, S., Spanier, I., Lakomek, M., & Gavish, M. (2008). Ligands of the mitochondrial 18 kDa translocator protein attenuate apoptosis of human glioblastoma cells exposed to erucylphosphohomocholine. *Cell Oncol, 30*(5), 435-450.

Kugler, W., Veenman, L., Shandalov, Y., Leschiner, S., Spanier, I., Lakomek, M., & Gavish, M. (2008). Ligands of the mitochondrial 18 kDa translocator protein attenuate apoptosis of human glioblastoma cells exposed to erucylphosphohomocholine. *Cell Oncol, 30*(5), 435-450.

Kuhlmann, A. C., & Guilarte, T. R. (1997). The peripheral benzodiazepine receptor is a sensitive indicator of domoic acid neurotoxicity. *Brain Res, 751*(2), 281-288.

Kuhlmann, A. C., & Guilarte, T. R. (1999). Regional and temporal expression of the peripheral benzodiazepine receptor in MPTP neurotoxicity. *Toxicol Sci, 48*(1), 107-116.

Kuhlmann, A. C., & Guilarte, T. R. (2000). Cellular and subcellular localization of peripheral benzodiazepine receptors after trimethyltin neurotoxicity. *J Neurochem, 74*(4), 1694-1704.

Kuszpit, K., Hollidge, B. S., Zeng, X., Stafford, R. G., Daye, S., Zhang, X., . . . Bocan, T. M. (2018). [(18)F]DPA-714 PET Imaging Reveals Global Neuroinflammation in Zika Virus-Infected Mice. *Mol Imaging Biol, 20*(2), 275-283. doi:10.1007/s11307-017-1118-2

Lacapere, J. J., Delavoie, F., Li, H., Peranzi, G., Maccario, J., Papadopoulos, V., & Vidic, B. (2001). Structural and functional study of reconstituted peripheral benzodiazepine receptor. *Biochem Biophys Res Commun, 284*(2), 536-541. doi:10.1006/bbrc.2001.4975

Lambeth, J. D., & Neish, A. S. (2014). Nox enzymes and new thinking on reactive oxygen: a double-edged sword revisited. *Annu Rev Pathol, 9*, 119-145. doi:10.1146/annurev-pathol-012513-104651

Larochette, N., Decaudin, D., Jacotot, E., Brenner, C., Marzo, I., Susin, S. A., . . . Kroemer, G. (1999). Arsenite induces apoptosis via a direct effect on the mitochondrial permeability transition pore. *Exp Cell Res, 249*(2), 413-421. doi:10.1006/excr.1999.4519

Lavisse, S., Guillermier, M., Herard, A. S., Petit, F., Delahaye, M., Van Camp, N., . . . Escartin, C. (2012). Reactive astrocytes overexpress TSPO and are detected by TSPO positron emission tomography imaging. *J Neurosci, 32*(32), 10809-10818. doi:10.1523/JNEUROSCI.1487-12.2012

Le Cabec, V., Carreno, S., Moisand, A., Bordier, C., & Maridonneau-Parini, I. (2002). Complement receptor 3 (CD11b/CD18) mediates type I and type II phagocytosis during nonopsonic and opsonic phagocytosis, respectively. *J Immunol, 169*(4), 2003-2009.

Le Fur, G., Guilloux, F., Rufat, P., Benavides, J., Uzan, A., Renault, C., . . . Gueremy, C. (1983). Peripheral benzodiazepine binding sites: effect of PK 11195, 1-(2-chlorophenyl)-N-methyl-(1-methylpropyl)-3 isoquinolinecarboxamide. II. In vivo studies. *Life Sci, 32*(16), 1849-1856.

Leaver, K. R., Reynolds, A., Bodard, S., Guilloteau, D., Chalon, S., & Kassiou, M. (2012). Effects of translocator protein (18 kDa) ligands on microglial activation and neuronal death in the quinolinic-acid-injected rat striatum. *ACS Chem Neurosci, 3*(2), 114-119. doi:10.1021/cn200099e

Lee, S. C., Liu, W., Dickson, D. W., Brosnan, C. F., & Berman, J. W. (1993). Cytokine production by human fetal microglia and astrocytes. Differential induction by lipopolysaccharide and IL-1 beta. *J Immunol, 150*(7), 2659-2667.

Leusen, J. H., Verhoeven, A. J., & Roos, D. (1996). Interactions between the components of the human NADPH oxidase: intrigues in the phox family. *J Lab Clin Med, 128*(5), 461-476.

Levin, E., Premkumar, A., Veenman, L., Kugler, W., Leschiner, S., Spanier, I., . . . Gavish, M. (2005). The peripheral-type benzodiazepine receptor and tumorigenicity: isoquinoline binding protein (IBP) antisense knockdown in the C6 glioma cell line. *Biochemistry, 44*(29), 9924-9935. doi:10.1021/bi050150s

Levonen, A. L., Landar, A., Ramachandran, A., Ceaser, E. K., Dickinson, D. A., Zanoni, G., . . . Darley-Usmar, V. M. (2004). Cellular mechanisms of redox cell signalling: role of cysteine modification in controlling antioxidant defences in response to electrophilic lipid oxidation products. *Biochem J, 378*(Pt 2), 373-382. doi:10.1042/BJ20031049

Lewis, E. M., Sergeant, S., Ledford, B., Stull, N., Dinauer, M. C., & McPhail, L. C. (2010). Phosphorylation of p22phox on threonine 147 enhances NADPH oxidase activity by promoting p47phox binding. *J Biol Chem, 285*(5), 2959-2967. doi:10.1074/jbc.M109.030643

Li, F., Liu, J., Zheng, Y., Garavito, R. M., & Ferguson-Miller, S. (2015). Protein structure. Crystal structures of translocator protein (TSPO) and mutant mimic of a human polymorphism. *Science, 347*(6221), 555-558. doi:10.1126/science.1260590

Li, H., & Papadopoulos, V. (1998). Peripheral-type benzodiazepine receptor function in cholesterol transport. Identification of a putative cholesterol recognition/interaction amino acid sequence and consensus pattern. *Endocrinology, 139*(12), 4991-4997. doi:10.1210/endo.139.12.6390

Li, Y., & Trush, M. A. (1998). Diphenyleneiodonium, an NAD(P)H oxidase inhibitor, also potently inhibits mitochondrial reactive oxygen species production. *Biochem Biophys Res Commun, 253*(2), 295-299. doi:10.1006/bbrc.1998.9729

Liao, H., Bu, W. Y., Wang, T. H., Ahmed, S., & Xiao, Z. C. (2005). Tenascin-R plays a role in neuroprotection via its distinct domains that coordinate to modulate the microglia function. *J Biol Chem, 280*(9), 8316-8323. doi:10.1074/jbc.M412730200

Lin, D., Chang, Y. J., Strauss, J. F., 3rd, & Miller, W. L. (1993). The human peripheral benzodiazepine receptor gene: cloning and characterization of alternative splicing in normal tissues and in a patient with congenital lipoid adrenal hyperplasia. *Genomics, 18*(3), 643-650.

Lindenau, J., Noack, H., Asayama, K., & Wolf, G. (1998). Enhanced cellular glutathione peroxidase immunoreactivity in activated astrocytes and in microglia during excitotoxin induced neurodegeneration. *Glia, 24*(2), 252-256.

Liu, B., Gao, H. M., Wang, J. Y., Jeohn, G. H., Cooper, C. L., & Hong, J. S. (2002). Role of nitric oxide in inflammation-mediated neurodegeneration. *Ann N Y Acad Sci, 962*, 318-331.

Liu, B., & Hong, J. S. (2003). Role of microglia in inflammation-mediated neurodegenerative diseases: mechanisms and strategies for therapeutic intervention. *J Pharmacol Exp Ther, 304*(1), 1-7. doi:10.1124/jpet.102.035048

Liu, G. J., Middleton, R. J., & Banati, R. B. (2017). Subcellular distribution of the 18kDa translocator protein and transcript variant PBR-S in human cells. *Gene, 613*, 45-56. doi:10.1016/j.gene.2017.02.035

Liu, G. J., Middleton, R. J., Hatty, C. R., Kam, W. W., Chan, R., Pham, T., . . . Banati, R. B. (2014). The 18 kDa translocator protein, microglia and neuroinflammation. *Brain Pathol, 24*(6), 631-653. doi:10.1111/bpa.12196

Liu, G. J., Middleton, R. J., Kam, W. W., Chin, D. Y., Hatty, C. R., Chan, R. H., & Banati, R. B. (2017). Functional gains in energy and cell metabolism after TSPO gene insertion. *Cell Cycle, 16*(5), 436-447. doi:10.1080/15384101.2017.1281477

Liu, Y., Hao, W., Dawson, A., Liu, S., & Fassbender, K. (2009). Expression of amyotrophic lateral sclerosis-linked SOD1 mutant increases the neurotoxic potential of microglia via TLR2. *J Biol Chem, 284*(6), 3691-3699. doi:10.1074/jbc.M804446200

Loth, M. K., Choi, J., McGlothan, J. L., Pletnikov, M. V., Pomper, M. G., & Guilarte, T. R. (2016). TSPO in a murine model of Sandhoff disease: presymptomatic marker of neurodegeneration and disease pathophysiology. *Neurobiol Dis, 85*, 174-186. doi:10.1016/j.nbd.2015.11.001

Maeda, J., Higuchi, M., Inaji, M., Ji, B., Haneda, E., Okauchi, T., . . . Suhara, T. (2007). Phase-dependent roles of reactive microglia and astrocytes in nervous system injury as delineated by imaging of peripheral benzodiazepine receptor. *Brain Res, 1157*, 100-111. doi:10.1016/j.brainres.2007.04.054

Marangos, P. J., Patel, J., Boulenger, J. P., & Clark-Rosenberg, R. (1982). Characterization of peripheral-type benzodiazepine binding sites in brain using [3H]Ro 5-4864. *Mol Pharmacol, 22*(1), 26-32.

Matcovitch-Natan, O., Winter, D. R., Giladi, A., Vargas Aguilar, S., Spinrad, A., Sarrazin, S., . . . Amit, I. (2016). Microglia development follows a stepwise program to regulate brain homeostasis. *Science, 353*(6301), aad8670. doi:10.1126/science.aad8670

McBean, G. J. (2002). Cerebral cystine uptake: a tale of two transporters. *Trends Pharmacol Sci, 23*(7), 299-302.

McEnery, M. W. (1992). The mitochondrial benzodiazepine receptor: evidence for association with the voltage-dependent anion channel (VDAC). *J Bioenerg Biomembr, 24*(1), 63-69.

McEnery, M. W., Snowman, A. M., Trifiletti, R. R., & Snyder, S. H. (1992). Isolation of the mitochondrial benzodiazepine receptor: association with the voltage-dependent anion channel and the adenine nucleotide carrier. *Proc Natl Acad Sci U S A, 89*(8), 3170-3174.

McNeela, A. M., Bernick, C., Hines, R. M., & Hines, D. J. (2018). TSPO regulation in reactive

gliotic diseases. *J Neurosci Res, 96*(6), 978-988. doi:10.1002/jnr.24212

Miettinen, H., Kononen, J., Haapasalo, H., Helen, P., Sallinen, P., Harjuntausta, T., . . . Alho, H. (1995). Expression of peripheral-type benzodiazepine receptor and diazepam binding inhibitor in human astrocytomas: relationship to cell proliferation. *Cancer Res, 55*(12), 2691-2695.

Min, K. J., Pyo, H. K., Yang, M. S., Ji, K. A., Jou, I., & Joe, E. H. (2004). Gangliosides activate microglia via protein kinase C and NADPH oxidase. *Glia, 48*(3), 197-206. doi:10.1002/glia.20069

Mittelbronn, M., Dietz, K., Schluesener, H. J., & Meyermann, R. (2001). Local distribution of microglia in the normal adult human central nervous system differs by up to one order of magnitude. *Acta Neuropathol, 101*(3), 249-255.

Morgan, S. C., Taylor, D. L., & Pocock, J. M. (2004). Microglia release activators of neuronal proliferation mediated by activation of mitogen-activated protein kinase, phosphatidylinositol-3-kinase/Akt and delta-Notch signalling cascades. *J Neurochem, 90*(1), 89-101. doi:10.1111/j.1471-4159.2004.02461.x

Morohaku, K., Pelton, S. H., Daugherty, D. J., Butler, W. R., Deng, W., & Selvaraj, V. (2014). Translocator protein/peripheral benzodiazepine receptor is not required for steroid hormone biosynthesis. *Endocrinology, 155*(1), 89-97. doi:10.1210/en.2013-1556

Moss, D. W., & Bates, T. E. (2001). Activation of murine microglial cell lines by lipopolysaccharide and interferon-gamma causes NO-mediated decreases in mitochondrial and cellular function. *Eur J Neurosci, 13*(3), 529-538.

Mukherjee, S., & Das, S. K. (1989). Subcellular distribution of "peripheral type" binding sites for [3H]Ro5-4864 in guinea pig lung. Localization to the mitochondrial inner membrane. *J Biol Chem, 264*(28), 16713-16718.

Mukhin, A. G., Papadopoulos, V., Costa, E., & Krueger, K. E. (1989). Mitochondrial benzodiazepine receptors regulate steroid biosynthesis. *Proc Natl Acad Sci U S A, 86*(24), 9813-9816.

Mukhopadhyay, S., Guillory, B., Mukherjee, S., & Das, S. K. (2010). Antiproliferative effect of peripheral benzodiazepine receptor antagonist PK11195 in rat mammary tumor cells. *Mol Cell Biochem, 340*(1-2), 203-213. doi:10.1007/s11010-010-0419-4

Murail, S., Robert, J. C., Coic, Y. M., Neumann, J. M., Ostuni, M. A., Yao, Z. X., . . . Lacapere, J. J. (2008). Secondary and tertiary structures of the transmembrane domains of the translocator protein TSPO determined by NMR. Stabilization of the TSPO tertiary fold upon ligand binding. *Biochim Biophys Acta, 1778*(6), 1375-1381. doi:10.1016/j.bbamem.2008.03.012

Nakahira, K., Kim, H. P., Geng, X. H., Nakao, A., Wang, X., Murase, N., . . . Choi, A. M. (2006). Carbon monoxide differentially inhibits TLR signaling pathways by regulating ROS-induced trafficking of TLRs to lipid rafts. *J Exp Med, 203*(10), 2377-2389. doi:10.1084/jem.20060845

Nayernia, Z., Jaquet, V., & Krause, K. H. (2014). New insights on NOX enzymes in the central

nervous system. *Antioxid Redox Signal, 20*(17), 2815-2837. doi:10.1089/ars.2013.5703

Nimmerjahn, A., Kirchhoff, F., & Helmchen, F. (2005). Resting microglial cells are highly dynamic surveillants of brain parenchyma in vivo. *Science, 308*(5726), 1314-1318. doi:10.1126/science.1110647

Njie, E. G., Boelen, E., Stassen, F. R., Steinbusch, H. W., Borchelt, D. R., & Streit, W. J. (2012). Ex vivo cultures of microglia from young and aged rodent brain reveal age-related changes in microglial function. *Neurobiol Aging, 33*(1), 195 e191-112. doi:10.1016/j.neurobiolaging.2010.05.008

Notter, T., Coughlin, J. M., Sawa, A., & Meyer, U. (2018). Reconceptualization of translocator protein as a biomarker of neuroinflammation in psychiatry. *Mol Psychiatry, 23*(1), 36-47. doi:10.1038/mp.2017.232

Novak, M. L., & Koh, T. J. (2013). Macrophage phenotypes during tissue repair. *J Leukoc Biol, 93*(6), 875-881. doi:10.1189/jlb.1012512

Novo, E., & Parola, M. (2008). Redox mechanisms in hepatic chronic wound healing and fibrogenesis. *Fibrogenesis Tissue Repair, 1*(1), 5. doi:10.1186/1755-1536-1-5

O'Beirne, G. B., Woods, M. J., & Williams, D. C. (1990). Two subcellular locations for peripheral-type benzodiazepine acceptors in rat liver. *Eur J Biochem, 188*(1), 131-138.

Oke, B. O., Suarez-Quian, C. A., Riond, J., Ferrara, P., & Papadopoulos, V. (1992). Cell surface localization of the peripheral-type benzodiazepine receptor (PBR) in adrenal cortex. *Mol Cell Endocrinol, 87*(1-3), R1-6.

Owen, D. R., Narayan, N., Wells, L., Healy, L., Smyth, E., Rabiner, E. A., . . . Moore, C. S. (2017). Pro-inflammatory activation of primary microglia and macrophages increases 18 kDa translocator protein expression in rodents but not humans. *J Cereb Blood Flow Metab, 37*(8), 2679-2690. doi:10.1177/0271678X17710182

Pacquelet, S., Johnson, J. L., Ellis, B. A., Brzezinska, A. A., Lane, W. S., Munafo, D. B., & Catz, S. D. (2007). Cross-talk between IRAK-4 and the NADPH oxidase. *Biochem J, 403*(3), 451-461. doi:10.1042/BJ20061184

Papadopoulos, V., Amri, H., Boujrad, N., Cascio, C., Culty, M., Garnier, M., . . . Drieu, K. (1997). Peripheral benzodiazepine receptor in cholesterol transport and steroidogenesis. *Steroids, 62*(1), 21-28.

Papadopoulos, V., Baraldi, M., Guilarte, T. R., Knudsen, T. B., Lacapere, J. J., Lindemann, P., . . . Gavish, M. (2006). Translocator protein (18kDa): new nomenclature for the peripheral-type benzodiazepine receptor based on its structure and molecular function. *Trends Pharmacol Sci, 27*(8), 402-409. doi:10.1016/j.tips.2006.06.005

Papadopoulos, V., & Lecanu, L. (2009). Translocator protein (18 kDa) TSPO: an emerging therapeutic target in neurotrauma. *Exp Neurol, 219*(1), 53-57.

doi:10.1016/j.expneurol.2009.04.016

Papadopoulos, V., Mukhin, A. G., Costa, E., & Krueger, K. E. (1990). The peripheral-type benzodiazepine receptor is functionally linked to Leydig cell steroidogenesis. *J Biol Chem, 265*(7), 3772-3779.

Parvathenani, L. K., Tertyshnikova, S., Greco, C. R., Roberts, S. B., Robertson, B., & Posmantur, R. (2003). P2X7 mediates superoxide production in primary microglia and is up-regulated in a transgenic mouse model of Alzheimer's disease. *J Biol Chem, 278*(15), 13309-13317. doi:10.1074/jbc.M209478200

Pastorino, J. G., Simbula, G., Yamamoto, K., Glascott, P. A., Jr., Rothman, R. J., & Farber, J. L. (1996). The cytotoxicity of tumor necrosis factor depends on induction of the mitochondrial permeability transition. *J Biol Chem, 271*(47), 29792-29798.

Pavese, N., Gerhard, A., Tai, Y. F., Ho, A. K., Turkheimer, F., Barker, R. A., . . . Piccini, P. (2006). Microglial activation correlates with severity in Huntington disease: a clinical and PET study. *Neurology, 66*(11), 1638-1643. doi:10.1212/01.wnl.0000222734.56412.17

Pawate, S., Shen, Q., Fan, F., & Bhat, N. R. (2004). Redox regulation of glial inflammatory response to lipopolysaccharide and interferongamma. *J Neurosci Res, 77*(4), 540-551. doi:10.1002/jnr.20180

Pettit, L. K., Varsanyi, C., Tadros, J., & Vassiliou, E. (2013). Modulating the inflammatory properties of activated microglia with Docosahexaenoic acid and Aspirin. *Lipids Health Dis, 12*, 16. doi:10.1186/1476-511X-12-16

Picard, C., Puel, A., Bonnet, M., Ku, C. L., Bustamante, J., Yang, K., . . . Casanova, J. L. (2003). Pyogenic bacterial infections in humans with IRAK-4 deficiency. *Science, 299*(5615), 2076-2079. doi:10.1126/science.1081902

Polazzi, E., Gianni, T., & Contestabile, A. (2001). Microglial cells protect cerebellar granule neurons from apoptosis: evidence for reciprocal signaling. *Glia, 36*(3), 271-280.

Politis, M., Giannetti, P., Su, P., Turkheimer, F., Keihaninejad, S., Wu, K., . . . Piccini, P. (2012). Increased PK11195 PET binding in the cortex of patients with MS correlates with disability. *Neurology, 79*(6), 523-530. doi:10.1212/WNL.0b013e3182635645

Power, J. H., & Blumbergs, P. C. (2009). Cellular glutathione peroxidase in human brain: cellular distribution, and its potential role in the degradation of Lewy bodies in Parkinson's disease and dementia with Lewy bodies. *Acta Neuropathol, 117*(1), 63-73. doi:10.1007/s00401-008-0438-3

Privalle, C. T., Crivello, J. F., & Jefcoate, C. R. (1983). Regulation of intramitochondrial cholesterol transfer to side-chain cleavage cytochrome P-450 in rat adrenal gland. *Proc Natl Acad Sci U S A, 80*(3), 702-706.

Qin, L., Li, G., Qian, X., Liu, Y., Wu, X., Liu, B., . . . Block, M. L. (2005). Interactive role of the toll-like receptor 4 and reactive oxygen species in LPS-induced microglia activation. *Glia, 52*(1),

78-84. doi:10.1002/glia.20225

Qin, L., Liu, Y., Cooper, C., Liu, B., Wilson, B., & Hong, J. S. (2002). Microglia enhance beta-amyloid peptide-induced toxicity in cortical and mesencephalic neurons by producing reactive oxygen species. *J Neurochem, 83*(4), 973-983.

Qin, L., Liu, Y., Wang, T., Wei, S. J., Block, M. L., Wilson, B., . . . Hong, J. S. (2004). NADPH oxidase mediates lipopolysaccharide-induced neurotoxicity and proinflammatory gene expression in activated microglia. *J Biol Chem, 279*(2), 1415-1421. doi:10.1074/jbc.M307657200

Rampon, C., Bouzaffour, M., Ostuni, M. A., Dufourcq, P., Girard, C., Freyssinet, J. M., . . . Vriz, S. (2009). Translocator protein (18 kDa) is involved in primitive erythropoiesis in zebrafish. *FASEB J, 23*(12), 4181-4192. doi:10.1096/fj.09-129262

Rastogi, R., Geng, X., Li, F., & Ding, Y. (2016). NOX Activation by Subunit Interaction and Underlying Mechanisms in Disease. *Front Cell Neurosci, 10*, 301. doi:10.3389/fncel.2016.00301

Repalli, J. (2014). Translocator protein (TSPO) role in aging and Alzheimer's disease. *Curr Aging Sci, 7*(3), 168-175.

Richards, J. G., & Mohler, H. (1984). Benzodiazepine receptors. *Neuropharmacology, 23*(2B), 233-242.

Rojo, A. I., McBean, G., Cindric, M., Egea, J., Lopez, M. G., Rada, P., . . . Cuadrado, A. (2014). Redox control of microglial function: molecular mechanisms and functional significance. *Antioxid Redox Signal, 21*(12), 1766-1801. doi:10.1089/ars.2013.5745

Roy, A., Jana, A., Yatish, K., Freidt, M. B., Fung, Y. K., Martinson, J. A., & Pahan, K. (2008). Reactive oxygen species up-regulate CD11b in microglia via nitric oxide: Implications for neurodegenerative diseases. *Free Radic Biol Med, 45*(5), 686-699. doi:10.1016/j.freeradbiomed.2008.05.026

Rupprecht, R., Papadopoulos, V., Rammes, G., Baghai, T. C., Fan, J., Akula, N., . . . Schumacher, M. (2010). Translocator protein (18 kDa) (TSPO) as a therapeutic target for neurological and psychiatric disorders. *Nat Rev Drug Discov, 9*(12), 971-988. doi:10.1038/nrd3295

Russ, W. P., & Engelman, D. M. (2000). The GxxxG motif: a framework for transmembrane helix-helix association. *J Mol Biol, 296*(3), 911-919. doi:10.1006/jmbi.1999.3489

Ryu, J. K., Choi, H. B., & McLarnon, J. G. (2005). Peripheral benzodiazepine receptor ligand PK11195 reduces microglial activation and neuronal death in quinolinic acid-injected rat striatum. *Neurobiol Dis, 20*(2), 550-561. doi:10.1016/j.nbd.2005.04.010

Salter, M. W., & Beggs, S. (2014). Sublime microglia: expanding roles for the guardians of the CNS. *Cell, 158*(1), 15-24. doi:10.1016/j.cell.2014.06.008

Santidrian, A. F., Cosialls, A. M., Coll-Mulet, L., Iglesias-Serret, D., de Frias, M., Gonzalez-Girones, D. M., . . . Gil, J. (2007). The potential anticancer agent PK11195 induces apoptosis

irrespective of p53 and ATM status in chronic lymphocytic leukemia cells. *Haematologica, 92*(12), 1631-1638. doi:10.3324/haematol.11194

Savchenko, V. L. (2013). Regulation of NADPH oxidase gene expression with PKA and cytokine IL-4 in neurons and microglia. *Neurotox Res, 23*(3), 201-213. doi:10.1007/s12640-012-9327-6

Sawada, M., Kondo, N., Suzumura, A., & Marunouchi, T. (1989). Production of tumor necrosis factor-alpha by microglia and astrocytes in culture. *Brain Res, 491*(2), 394-397.

Schoemaker, H., Bliss, M., & Yamamura, H. I. (1981). Specific high-affinity saturable binding of [3H] R05-4864 to benzodiazepine binding sites in the rat cerebral cortex. *Eur J Pharmacol, 71*(1), 173-175.

Schoemaker, H., Boles, R. G., Horst, W. D., & Yamamura, H. I. (1983). Specific high-affinity binding sites for [3H]Ro 5-4864 in rat brain and kidney. *J Pharmacol Exp Ther, 225*(1), 61-69.

Schoemaker, H., Morelli, M., Deshmukh, P., & Yamamura, H. I. (1982). [3H]Ro5-4864 benzodiazepine binding in the kainate lesioned striatum and Huntington's diseased basal ganglia. *Brain Res, 248*(2), 396-401.

Schultz, R., Pelto-Huikko, M., & Alho, H. (1992). Expression of diazepam binding inhibitor-like immunoreactivity in rat testis is dependent on pituitary hormones. *Endocrinology, 130*(6), 3200-3206. doi:10.1210/endo.130.6.1597138

Schwartz, M., & Baruch, K. (2014). The resolution of neuroinflammation in neurodegeneration: leukocyte recruitment via the choroid plexus. *EMBO J, 33*(1), 7-22. doi:10.1002/embj.201386609

Sekhar, K. R., Crooks, P. A., Sonar, V. N., Friedman, D. B., Chan, J. Y., Meredith, M. J., . . . Freeman, M. L. (2003). NADPH oxidase activity is essential for Keap1/Nrf2-mediated induction of GCLC in response to 2-indol-3-yl-methylenequinuclidin-3-ols. *Cancer Res, 63*(17), 5636-5645.

Selvaraj, S., Bloomfield, P. S., Cao, B., Veronese, M., Turkheimer, F., & Howes, O. D. (2018). Brain TSPO imaging and gray matter volume in schizophrenia patients and in people at ultra high risk of psychosis: An [(11)C]PBR28 study. *Schizophr Res, 195*, 206-214. doi:10.1016/j.schres.2017.08.063

Selvaraj, V., & Stocco, D. M. (2015). The changing landscape in translocator protein (TSPO) function. *Trends Endocrinol Metab, 26*(7), 341-348. doi:10.1016/j.tem.2015.02.007

Selvaraj, V., Stocco, D. M., & Tu, L. N. (2015). Minireview: translocator protein (TSPO) and steroidogenesis: a reappraisal. *Mol Endocrinol, 29*(4), 490-501. doi:10.1210/me.2015-1033

Serhan, C. N., & Savill, J. (2005). Resolution of inflammation: the beginning programs the end. *Nat Immunol, 6*(12), 1191-1197. doi:10.1038/ni1276

Sharma, V., Mishra, M., Ghosh, S., Tewari, R., Basu, A., Seth, P., & Sen, E. (2007). Modulation of interleukin-1beta mediated inflammatory response in human astrocytes by flavonoids: implications in neuroprotection. *Brain Res Bull, 73*(1-3), 55-63.

doi:10.1016/j.brainresbull.2007.01.016

Shih, A. Y., Johnson, D. A., Wong, G., Kraft, A. D., Jiang, L., Erb, H., . . . Murphy, T. H. (2003). Coordinate regulation of glutathione biosynthesis and release by Nrf2-expressing glia potently protects neurons from oxidative stress. *J Neurosci, 23*(8), 3394-3406.

Shoukrun, R., Veenman, L., Shandalov, Y., Leschiner, S., Spanier, I., Karry, R., . . . Gavish, M. (2008). The 18-kDa translocator protein, formerly known as the peripheral-type benzodiazepine receptor, confers proapoptotic and antineoplastic effects in a human colorectal cancer cell line. *Pharmacogenet Genomics, 18*(11), 977-988. doi:10.1097/FPC.0b013e3283117d52

Sileikyte, J., Blachly-Dyson, E., Sewell, R., Carpi, A., Menabo, R., Di Lisa, F., . . . Forte, M. (2014). Regulation of the mitochondrial permeability transition pore by the outer membrane does not involve the peripheral benzodiazepine receptor (Translocator Protein of 18 kDa (TSPO)). *J Biol Chem, 289*(20), 13769-13781. doi:10.1074/jbc.M114.549634

Sileikyte, J., Petronilli, V., Zulian, A., Dabbeni-Sala, F., Tognon, G., Nikolov, P., . . . Ricchelli, F. (2011). Regulation of the inner membrane mitochondrial permeability transition by the outer membrane translocator protein (peripheral benzodiazepine receptor). *J Biol Chem, 286*(2), 1046-1053. doi:10.1074/jbc.M110.172486

Snyder, S. H., Verma, A., & Trifiletti, R. R. (1987). The peripheral-type benzodiazepine receptor: a protein of mitochondrial outer membranes utilizing porphyrins as endogenous ligands. *FASEB J, 1*(4), 282-288.

Sorce, S., & Krause, K. H. (2009). NOX enzymes in the central nervous system: from signaling to disease. *Antioxid Redox Signal, 11*(10), 2481-2504. doi:10.1089/ARS.2009.2578

Sorce, S., Nuvolone, M., Keller, A., Falsig, J., Varol, A., Schwarz, P., . . . Aguzzi, A. (2014). The role of the NADPH oxidase NOX2 in prion pathogenesis. *PLoS Pathog, 10*(12), e1004531. doi:10.1371/journal.ppat.1004531

Starosta-Rubinstein, S., Ciliax, B. J., Penney, J. B., McKeever, P., & Young, A. B. (1987). Imaging of a glioma using peripheral benzodiazepine receptor ligands. *Proc Natl Acad Sci U S A, 84*(3), 891-895.

Stolk, J., Hiltermann, T. J., Dijkman, J. H., & Verhoeven, A. J. (1994). Characteristics of the inhibition of NADPH oxidase activation in neutrophils by apocynin, a methoxy-substituted catechol. *Am J Respir Cell Mol Biol, 11*(1), 95-102. doi:10.1165/ajrcmb.11.1.8018341

Streit, W. J., Walter, S. A., & Pennell, N. A. (1999). Reactive microgliosis. *Prog Neurobiol, 57*(6), 563-581.

Sumimoto, H. (2008). Structure, regulation and evolution of Nox-family NADPH oxidases that produce reactive oxygen species. *FEBS J, 275*(13), 3249-3277. doi:10.1111/j.1742-4658.2008.06488.x

Taetzsch, T., Levesque, S., McGraw, C., Brookins, S., Luqa, R., Bonini, M. G., . . . Block, M. L.

(2015). Redox regulation of NF-kappaB p50 and M1 polarization in microglia. *Glia, 63*(3), 423-440. doi:10.1002/glia.22762

Taketani, S., Kohno, H., Furukawa, T., & Tokunaga, R. (1995). Involvement of peripheral-type benzodiazepine receptors in the intracellular transport of heme and porphyrins. *J Biochem, 117*(4), 875-880.

Tallman, J. F., Thomas, J. W., & Gallager, D. W. (1978). GABAergic modulation of benzodiazepine binding site sensitivity. *Nature, 274*(5669), 383-385.

Tamse, C., Lu, X., Mortel, E., Cabrales, E., Feng, W., & Schaefer, S. (2008). The peripheral benzodiazepine receptor modulates Ca2+ transport through the VDAC in rat heart mitochondria. *Journal of Clinical and Basic Cardiology, 11*(1), 24-29.

Teboul, D., Beaufils, S., Taveau, J. C., Iatmanen-Harbi, S., Renault, A., Venien-Bryan, C., . . . Lacapere, J. J. (2012). Mouse TSPO in a lipid environment interacting with a functionalized monolayer. *Biochim Biophys Acta, 1818*(11), 2791-2800. doi:10.1016/j.bbamem.2012.06.020

Thannickal, V. J., & Fanburg, B. L. (2000). Reactive oxygen species in cell signaling. *Am J Physiol Lung Cell Mol Physiol, 279*(6), L1005-1028. doi:10.1152/ajplung.2000.279.6.L1005

Torres, S. R., Frode, T. S., Nardi, G. M., Vita, N., Reeb, R., Ferrara, P., . . . Farges, R. C. (2000). Anti-inflammatory effects of peripheral benzodiazepine receptor ligands in two mouse models of inflammation. *Eur J Pharmacol, 408*(2), 199-211.

Town, T., Nikolic, V., & Tan, J. (2005). The microglial "activation" continuum: from innate to adaptive responses. *J Neuroinflammation, 2*, 24. doi:10.1186/1742-2094-2-24

Tremblay, M. E., Stevens, B., Sierra, A., Wake, H., Bessis, A., & Nimmerjahn, A. (2011). The role of microglia in the healthy brain. *J Neurosci, 31*(45), 16064-16069. doi:10.1523/JNEUROSCI.4158-11.2011

Tu, L. N., Morohaku, K., Manna, P. R., Pelton, S. H., Butler, W. R., Stocco, D. M., & Selvaraj, V. (2014). Peripheral benzodiazepine receptor/translocator protein global knock-out mice are viable with no effects on steroid hormone biosynthesis. *J Biol Chem, 289*(40), 27444-27454. doi:10.1074/jbc.M114.578286

Tu, L. N., Zhao, A. H., Hussein, M., Stocco, D. M., & Selvaraj, V. (2016). Translocator Protein (TSPO) Affects Mitochondrial Fatty Acid Oxidation in Steroidogenic Cells. *Endocrinology, 157*(3), 1110-1121. doi:10.1210/en.2015-1795

Tu, L. N., Zhao, A. H., Stocco, D. M., & Selvaraj, V. (2015). PK11195 effect on steroidogenesis is not mediated through the translocator protein (TSPO). *Endocrinology, 156*(3), 1033-1039. doi:10.1210/en.2014-1707

Vanhee, C., Zapotoczny, G., Masquelier, D., Ghislain, M., & Batoko, H. (2011). The Arabidopsis multistress regulator TSPO is a heme binding membrane protein and a potential scavenger of porphyrins via an autophagy-dependent degradation mechanism. *Plant Cell, 23*(2), 785-805.

doi:10.1105/tpc.110.081570

Veenman, L., Bode, J., Gaitner, M., Caballero, B., Pe'er, Y., Zeno, S., . . . Gavish, M. (2012). Effects of 18-kDa translocator protein knockdown on gene expression of glutamate receptors, transporters, and metabolism, and on cell viability affected by glutamate. *Pharmacogenet Genomics, 22*(8), 606-619. doi:10.1097/FPC.0b013e3283544531

Veenman, L., & Gavish, M. (2006). The peripheral-type benzodiazepine receptor and the cardiovascular system. Implications for drug development. *Pharmacol Ther, 110*(3), 503-524. doi:10.1016/j.pharmthera.2005.09.007

Veenman, L., Gavish, M., & Kugler, W. (2014). Apoptosis induction by erucylphosphohomocholine via the 18 kDa mitochondrial translocator protein: implications for cancer treatment. *Anticancer Agents Med Chem, 14*(4), 559-577.

Veenman, L., Shandalov, Y., & Gavish, M. (2008). VDAC activation by the 18 kDa translocator protein (TSPO), implications for apoptosis. *J Bioenerg Biomembr, 40*(3), 199-205. doi:10.1007/s10863-008-9142-1

Veenman, L., Vainshtein, A., Yasin, N., Azrad, M., & Gavish, M. (2016). Tetrapyrroles as Endogenous TSPO Ligands in Eukaryotes and Prokaryotes: Comparisons with Synthetic Ligands. *Int J Mol Sci, 17*(6). doi:10.3390/ijms17060880

Veiga, S., Azcoitia, I., & Garcia-Segura, L. M. (2005). Ro5-4864, a peripheral benzodiazepine receptor ligand, reduces reactive gliosis and protects hippocampal hilar neurons from kainic acid excitotoxicity. *J Neurosci Res, 80*(1), 129-137. doi:10.1002/jnr.20430

Veiga, S., Carrero, P., Pernia, O., Azcoitia, I., & Garcia-Segura, L. M. (2007). Translocator protein 18 kDa is involved in the regulation of reactive gliosis. *Glia, 55*(14), 1426-1436. doi:10.1002/glia.20558

Verma, A., Nye, J. S., & Snyder, S. H. (1987). Porphyrins are endogenous ligands for the mitochondrial (peripheral-type) benzodiazepine receptor. *Proc Natl Acad Sci U S A, 84*(8), 2256-2260.

Vilhardt, F., Haslund-Vinding, J., Jaquet, V., & McBean, G. (2017). Microglia antioxidant systems and redox signalling. *Br J Pharmacol, 174*(12), 1719-1732. doi:10.1111/bph.13426

Vilhardt, F., & van Deurs, B. (2004). The phagocyte NADPH oxidase depends on cholesterol-enriched membrane microdomains for assembly. *EMBO J, 23*(4), 739-748. doi:10.1038/sj.emboj.7600066

Walter, R. B., Pirga, J. L., Cronk, M. R., Mayer, S., Appelbaum, F. R., & Banker, D. E. (2005). PK11195, a peripheral benzodiazepine receptor (pBR) ligand, broadly blocks drug efflux to chemosensitize leukemia and myeloma cells by a pBR-independent, direct transporter-modulating mechanism. *Blood, 106*(10), 3584-3593. doi:10.1182/blood-2005-02-0711

Wang, H., Zhai, K., Xue, Y., Yang, J., Yang, Q., Fu, Y., . . . He, W. (2016). Global Deletion of

TSPO Does Not Affect the Viability and Gene Expression Profile. *PLoS One*, *11*(12), e0167307. doi:10.1371/journal.pone.0167307

Wang, M., Wang, X., Zhao, L., Ma, W., Rodriguez, I. R., Fariss, R. N., & Wong, W. T. (2014). Macroglia-microglia interactions via TSPO signaling regulates microglial activation in the mouse retina. *J Neurosci, 34*(10), 3793-3806. doi:10.1523/JNEUROSCI.3153-13.2014

Wang, Q., Chuikov, S., Taitano, S., Wu, Q., Rastogi, A., Tuck, S. J., . . . Mao-Draayer, Y. (2015). Dimethyl Fumarate Protects Neural Stem/Progenitor Cells and Neurons from Oxidative Damage through Nrf2-ERK1/2 MAPK Pathway. *Int J Mol Sci, 16*(6), 13885-13907. doi:10.3390/ijms160613885

Wang, W., Zhang, L., Zhang, X., Xue, R., Li, L., Zhao, W., . . . Li, Y. (2016). Lentiviral-Mediated Overexpression of the 18 kDa Translocator Protein (TSPO) in the Hippocampal Dentate Gyrus Ameliorates LPS-Induced Cognitive Impairment in Mice. *Front Pharmacol, 7*, 384. doi:10.3389/fphar.2016.00384

Wang, X., Svedin, P., Nie, C., Lapatto, R., Zhu, C., Gustavsson, M., . . . Mallard, C. (2007). N-acetylcysteine reduces lipopolysaccharide-sensitized hypoxic-ischemic brain injury. *Ann Neurol, 61*(3), 263-271. doi:10.1002/ana.21066

Weissman, B. A., Skolnick, P., & Klein, D. C. (1984). Regulation of "peripheral-type" binding sites for benzodiazepines in the pineal gland. *Pharmacol Biochem Behav, 21*(6), 821-824.

Wilms, H., Claasen, J., Rohl, C., Sievers, J., Deuschl, G., & Lucius, R. (2003). Involvement of benzodiazepine receptors in neuroinflammatory and neurodegenerative diseases: evidence from activated microglial cells in vitro. *Neurobiol Dis, 14*(3), 417-424.

Won, S. J., Kim, J. E., Cittolin-Santos, G. F., & Swanson, R. A. (2015). Assessment at the single-cell level identifies neuronal glutathione depletion as both a cause and effect of ischemia-reperfusion oxidative stress. *J Neurosci, 35*(18), 7143-7152. doi:10.1523/JNEUROSCI.4826-14.2015

Woods, M. J., & Williams, D. C. (1996). Multiple forms and locations for the peripheral-type benzodiazepine receptor. *Biochem Pharmacol, 52*(12), 1805-1814.

Woods, M. J., Zisterer, D. M., & Williams, D. C. (1996). Two cellular and subcellular locations for the peripheral-type benzodiazepine receptor in rat liver. *Biochem Pharmacol, 51*(10), 1283-1292.

Wu, X. F., Block, M. L., Zhang, W., Qin, L., Wilson, B., Zhang, W. Q., . . . Hong, J. S. (2005). The role of microglia in paraquat-induced dopaminergic neurotoxicity. *Antioxid Redox Signal, 7*(5-6), 654-661. doi:10.1089/ars.2005.7.654

Yang, C. S., Shin, D. M., Lee, H. M., Son, J. W., Lee, S. J., Akira, S., . . . Jo, E. K. (2008). ASK1-p38 MAPK-p47phox activation is essential for inflammatory responses during tuberculosis via TLR2-ROS signalling. *Cell Microbiol, 10*(3), 741-754. doi:10.1111/j.1462-5822.2007.01081.x

Yasin, N., Veenman, L. Gavish, M. (2015, December 20-22, 2015). *Regulation of nuclear gene expression by PK 11195, a ligand specific for*

the 18 kDa mitochondrial translocator protein (TSPO). Paper presented at the Annual Meeting of the Israel Society for Neuroscience,, Eiliat, Israel.

Yeliseev, A. A., & Kaplan, S. (1995). A sensory transducer homologous to the mammalian peripheral-type benzodiazepine receptor regulates photosynthetic membrane complex formation in Rhodobacter sphaeroides 2.4.1. *J Biol Chem, 270*(36), 21167-21175.

Yeliseev, A. A., & Kaplan, S. (2000). TspO of rhodobacter sphaeroides. A structural and functional model for the mammalian peripheral benzodiazepine receptor. *J Biol Chem, 275*(8), 5657-5667.

Yeliseev, A. A., Krueger, K. E., & Kaplan, S. (1997). A mammalian mitochondrial drug receptor functions as a bacterial "oxygen" sensor. *Proc Natl Acad Sci U S A, 94*(10), 5101-5106.

Zavala, F., Masson, A., Brys, L., de Baetselier, P., & Descamps-Latscha, B. (1991). A monoclonal antibody against peripheral benzodiazepine receptor activates the human neutrophil NADPH-oxidase. *Biochemical and Biophysical Research Communications, 176*(3), 1577-1583. doi:https://doi.org/10.1016/0006-291X(91)90468-M

Zeno, S., Veenman, L., Katz, Y., Bode, J., Gavish, M., & Zaaroor, M. (2012). The 18 kDa mitochondrial translocator protein (TSPO) prevents accumulation of protoporphyrin IX. Involvement of reactive oxygen species (ROS). *Curr Mol Med, 12*(4), 494-501.

Zeno, S., Zaaroor, M., Leschiner, S., Veenman, L., & Gavish, M. (2009). CoCl(2) induces apoptosis via the 18 kDa translocator protein in U118MG human glioblastoma cells. *Biochemistry, 48*(21), 4652-4661. doi:10.1021/bi900064t

Zhang, K., Demeure, O., Belliard, A., Goujon, J. M., Favreau, F., Desurmont, T., . . . Hauet, T. (2006). Cloning, sequencing, and chromosomal localization of pig peripheral benzodiazepine receptor: three different forms produced by alternative splicing. *Mamm Genome, 17*(10), 1050-1062. doi:10.1007/s00335-006-0022-x

Zhang, L., Yu, H., Zhao, X., Lin, X., Tan, C., Cao, G., & Wang, Z. (2010). Neuroprotective effects of salidroside against beta-amyloid-induced oxidative stress in SH-SY5Y human neuroblastoma cells. *Neurochem Int, 57*(5), 547-555. doi:10.1016/j.neuint.2010.06.021

Zhao, A. H., Tu, L. N., Mukai, C., Sirivelu, M. P., Pillai, V. V., Morohaku, K., . . . Selvaraj, V. (2016). Mitochondrial Translocator Protein (TSPO) Function Is Not Essential for Heme Biosynthesis. *J Biol Chem, 291*(4), 1591-1603. doi:10.1074/jbc.M115.686360

Zhao, J., Moore, A. N., Redell, J. B., & Dash, P. K. (2007). Enhancing expression of Nrf2-driven genes protects the blood brain barrier after brain injury. *J Neurosci, 27*(38), 10240-10248. doi:10.1523/JNEUROSCI.1683-07.2007

Zhao, Y. Y., Yu, J. Z., Li, Q. Y., Ma, C. G., Lu, C. Z., & Xiao, B. G. (2011). TSPO-specific ligand

vinpocetine exerts a neuroprotective effect by suppressing microglial inflammation. *Neuron Glia Biol, 7*(2-4), 187-197. doi:10.1017/S1740925X12000129

Zimmer, E. R., Leuzy, A., Benedet, A. L., Breitner, J., Gauthier, S., & Rosa-Neto, P. (2014). Tracking neuroinflammation in Alzheimer's disease: the role of positron emission tomography imaging. *J Neuroinflammation, 11*, 120. doi:10.1186/1742-2094-11-120

Zurcher, N. R., Loggia, M. L., Lawson, R., Chonde, D. B., Izquierdo-Garcia, D., Yasek, J. E., . . . Atassi, N. (2015). Increased in vivo glial activation in patients with amyotrophic lateral sclerosis: assessed with [(11)C]-PBR28. *Neuroimage Clin, 7*, 409-414. doi:10.1016/j.nicl.2015.01.009

Chapter 2: TSPO in a murine model of Sandhoff disease: presymptomatic marker of neurodegeneration and disease pathophysiology

Reprinted with permission: Loth, M. K., Choi, J., McGlothan, J. L., Pletnikov, M. V., Pomper, M. G., & Guilarte, T. R. (2016). TSPO in a murine model of Sandhoff disease: presymptomatic marker of neurodegeneration and disease pathophysiology. Neurobiol Dis, 85, 174-186. doi:10.1016/j.nbd.2015.11.001

ABSTRACT

Translocator protein (18 kDa), formerly known as the peripheral benzodiazepine receptor (PBR), has been extensively used as a biomarker of active brain disease and neuroinflammation. TSPO expression increases dramatically in glial cells, particularly in microglia and astrocytes, as a result of brain injury, and this phenomenon is a component of the hallmark response of the brain to injury. In this study, we used a mouse model of Sandhoff disease (SD) to assess the longitudinal expression of TSPO as a function of disease progression and its relationship to behavioral and neuropathological endpoints. Focusing on the presymptomatic period of the disease, we used *ex vivo* [^{3}H]DPA-713 quantitative autoradiography and *in vivo* [^{125}I]IodoDPA-713 small animal SPECT imaging to show that brain TSPO levels markedly increase prior to physical and behavioral manifestation of disease. We further show that TSPO upregulation coincides with early neuronal GM2 ganglioside aggregation and is associated with ongoing neurodegeneration and activation of both microglia and astrocytes. In brain regions with increased TSPO levels, there is a differential pattern of glial cell activation with astrocytes being activated earlier than microglia during the progression of disease. Immunofluorescent confocal imaging confirmed that TSPO colocalizes with both microglia and astrocyte markers, but the glial source of the TSPO response differs by brain region and age in SD mice. Notably, TSPO colocalization with the astrocyte marker GFAP was greater than with the microglia marker, Mac-1. Taken together, our findings have significant implications for understanding TSPO glial cell biology and for detecting neurodegeneration prior to clinical expression of disease.

Key Words: Translocator protein 18 kDa; TSPO; Sandhoff disease; biomarker; microglia; astrocytes; neurodegeneration

Short Title: TSPO in Sandhoff mice

1. INTRODUCTION

Sandhoff disease (SD) is an autosomal recessive disorder characterized by a deficiency in the lysosomal enzyme β-hexosaminidase, which leads to the accumulation of gangliosides and glycolipids, specifically GM2 and GA2 (Jeyakumar et al., 2002; Mahuran et al., 1999). Because gangliosides are expressed at high levels in the central nervous system (CNS), the brain is one of the most affected organs (Jeyakumar et al., 2002). Ganglioside accumulation in the brain ultimately leads to progressive and widespread neurodegeneration and motor impairments (Wada et al., 2000). In humans, the onset of the infantile form of SD occurs around 6 months of age with symptoms such as motor weakness, early blindness, macroencephaly, and seizures. Symptoms progress rapidly, and death occurs between 3 to 5 years of age (Maegawa et al., 2006).

β-hexosaminidase is formed by the dimerization of two subunits, α- and β-subunits to form β-hexosaminidase A (αβ) or two β subunits to form β-hexosaminidase B (ββ). In the mouse model of SD, the gene encoding for the β subunit of β-hexosaminidase (*Hexb*) is disrupted, resulting in the deficiency of both β-hexosaminidase A and B (Yamanaka et al., 1994). This deficiency leads to impaired degradation and subsequent accumulation of GM2 and GA2 gangliosides in neurons (Sango et al., 1995; Jeyakumar et al., 2002; Mahuran et al., 1999), resulting in severe neurodegeneration in the brain (Wada et al., 2000). Sandhoff (*Hexb* KO) mice exhibit spastic and reduced hind limb movements with progressive motor deficits starting at 3 months of age (Sango et al. 1995). The life span of SD mice is approximately 5 months of age as the mice lose the ability to move and are unable to retrieve food or water (Sango et al., 1995; Tifft and Proia, 1997; Jeyakumar et al., 2002). Histopathological studies have shown that excess storage of glycolipids in lysosomes leads to neuronal apoptosis in the cerebellum, brainstem, spinal cord, trigeminal ganglion, retina, and thalamus in SD mice (Sango et al., 1995; Wada et al., 2000). Tissues from

humans diagnosed with SD have also shown neurodegeneration in spinal cord, cerebral cortex, and thalamus (Huang et al., 1997; Wada et al., 2000). Thus, the mouse model of SD shares many of the clinical symptoms and neuropathology as the human form of the disease.

Previous work has shown that microglia become activated in both the mouse model and in human cases of SD (Wada et al., 2000; Visigalli et al., 2009) and that microglial activation appears to precede neuronal degeneration. Furthermore, cDNA microarray analysis has shown increased TSPO gene expression in the SD mice (Wada et al, 2000), and using PET imaging, uptake of [$_{11}$C]-PK11195, a TSPO-specific ligand, was higher in SD mice at 4 months of age compared to wildtype (Visigalli et al., 2009). However, a longitudinal assessment of TSPO expression as a function of disease progression using behavioral and neuropathological endpoints has not been investigated. Furthermore, it has been previously reported that [$_{11}$C]-PK11195 PET imaging shows significant non-specific binding and poor brain uptake (Boutin et al., 2007; Endres et al., 2009), and thus, better ligands are needed for *in vivo* TSPO PET/SPECT studies.

DPA-713, also known as *N*,*N*-diethyl-2-[2-(4[methoxy-phenyl)-5,7-dimethylpyrazolo[1,5-a]pyrimidin-3-yl]-acetamide, is a pyrazolo-pyrimidine that is 10-fold less lipophilic than PK11195 but with twice the affinity for TSPO (Wang et al., 2009). [$_{11}$C]DPA-713 PET imaging has been performed in a rodent model of brain injury and in a human study with higher signal-to-noise ratios than [$_{11}$C]-PK11195 (Doorduin et al., 2009; Endres et al., 2009). [$_{125}$I]IodoDPA-713 is a novel TSPO-specific radioligand that has been previously used to detect TSPO *in vivo* in a mouse model of lung inflammation (Wang et al., 2009), but it is unknown whether [$_{125}$I]IodoDPA-713 can be used to detect *in vivo* TSPO binding in the brain. In this study, we used [$_{3}$H]DPA713 and [$_{125}$I]IodoDPA-713 to assess the progression of TSPO expression in SD mouse model in a longitudinal fashion. The goal of this study was to examine how early in disease progression TSPO

levels increased in relation to: 1) neuronal GM2 ganglioside accumulation, 2) activation of microglia and astrocytes, 3) neurodegenerative changes based on silver staining, and 4) behavioral expression of disease focusing on the presymptomatic phase of the disease.

2. MATERIALS AND METHODS

2.1. *Animal care and use statement*

All animal studies were reviewed and approved by both Columbia University Medical Center and the Johns Hopkins University Animal Care and Use Committee. Studies were conducted in accordance with the Guide for Care and Use of Laboratory Animals as stated by the United States National Institutes of Health.

2.2. *Animal model and tissue preparation*

Mice heterozygous for *Hexb* were generously donated by Dr. Richard Proia (National Institute of Kidney & Digestive Diseases, Bethesda, MD). Wildtype (*Hexb* +/+) or SD (*Hexb* -/-) mice were euthanized at 1, 1.5, 2, or 3 months of age by either decapitation to obtain freshfrozen brain tissue for receptor autoradiography or by transcardiac perfusion for immunohistochemistry. Fresh frozen brains were stored at -80°C. For transcardiac perfusion, animals were deeply anesthetized with pentobarbital (100 mg/kg body weight) and perfused with 4% paraformaldehyde (PFA) in 0.1M phosphate buffer (pH 7.4 at 4°C). Perfused brains were post-fixed overnight in the same fixative, cryoprotected with 25% sucrose for 48 h, flash-frozen in dry-ice-cooled isopentane, and stored at -80°C.

2.3. *Behavioral assessment*

2.3.1. ***Motor skill***

Motor skill was measured using the rotarod apparatus (Columbus Instrument, Columbus, OH). The latency time the mouse remained on the rod at accelerating speeds was recorded. Each mouse was trained for 5 min at a speed of 4 RPM. Training was followed by a 30-min rest period in the home cage. Mice were then placed back on the rotarod for three trials. Each trial began at 4 RPM and accelerated every 30s by 4 RPM to a maximum of 40 RPM. Trials were separated by a 10-min rest period. Mice were tested for 3 consecutive days.

2.3.2. *Locomotor activity*

Mice were placed in open field activity chambers with infrared beams (San Diego Instruments Inc., San Diego, CA) for 1 h. During this time, horizontal activity and rearing were automatically recorded.

2.4. *Quantitative receptor autoradiography*

Fresh frozen brains were sectioned at 20 μm on a freezing cryostat (Leica, Nussloch, Germany) in the horizontal plane. Brain sections were thaw-mounted onto poly-L-lysine-coated slides (Sigma-Aldrich, St. Louis, MO) and stored at -20°C. [^{3}H]DPA-713 autoradiography was used to assess TSPO levels in multiple brain regions. Adjacent brain sections were used as follows: slides were thawed and warmed on a slide warmer at 37°C for 30 min and prewashed for 5 min in 50 mM Tris-HCl buffer (pH 7.4) at room temperature. Slides were incubated in a buffer containing 1.0 nM [^{3}H]DPA-713 for 30 min at room temperature. For non-specific binding, adjacent sections were incubated in the presence of 10 μM racemic PK11195. Slides were washed twice for 3 min each in 4°C buffer and dipped twice in 4°C deionized water. Sections were apposed to Kodak Bio-Max MR films with tritium microscales for 4 weeks (GE Healthcare, Piscataway, NJ). Images were acquired and quantified using the MCID software (InterFocus Imaging Ltd, Cambridge, England).

2.5. *Immunohistochemistry*

Brain sections from PFA-perfused animals were sectioned at 40 μm using a freezing microtome (Leica SM2000R; Leica Microsystems, Wetzlar, Germany). Sections were stored in cryoprotectant consisting of 50% glycerol in 0.05M phosphate buffer at -20°C. Sections were washed with Tris-buffered saline for 30 min. For GFAP and Mac-1 (CD11b) immunohistochemistry, sections were pre-treated with 0.6% H_2O_2 in TBS for 10 min and blocked with a 5% normal goat serum and 0.2% Triton X-100 solution for 1 h. Sections were incubated with rabbit anti-GFAP antibody (1:1000, Dako Z-0334, Carpinteria, CA) or rat anti-CD11b antibody (1:250, BD PharMingen 553308, San Diego, CA) at 4°C overnight. After washing with TBS, sections were incubated with the appropriate biotinylated secondary antibodies (1:200, Vector, Burlingame, CA) for 1 h. This was followed by an incubation in ABC elite, an avidin-biotin-horseradish peroxidase (HRP) complex (Vector) for 30 min. Immunoreactivity was visualized with a 0.25 mg/mL 3,3'-diaminobenzidine (DAB) (Sigma) and 0.03% H_2O_2 solution. Sections were mounted on slides, dehydrated in increasing concentrations of ethanol, and coverslipped using Permount media (Sigma). For double and triple labeling immunofluorescence, sections were washed with TBS for 60 min and then blocked in 5% normal donkey serum with 0.2% Triton X-100 solution for 1 h. Sections were incubated in primary antibodies diluted in blocking solution overnight at 4°C using the following dilutions: rat anti-Mac-1 (1:250, BD Pharmingen 553308), rabbit anti-TSPO (1:500, Abcam ab109497), mouse anti-GFAP (1:2000, Millipore MAB3402), rabbit anti-GM2 (1:500, Millipore 345759), or mouse anti-NeuN (1:1000, Chemicon MAB377). After washing in TBS, sections were incubated with appropriate secondary antibodies (1:500, AlexaFluor488, AlexaFluor594, AlexaFluor647; Molecular Probes, Carlsbad, CA) diluted in a 2% normal donkey serum with 0.1% Triton X-100 at room temperature for 1 h.

Following another series of washes in TBS, sections were mounted onto slides in ProLong Gold DAPI mounting media (Molecular Probes).

2.6. *Silver staining for neuronal degeneration*

Free-floating sections from PFA-perfused animals were further fixed in 4% PFA in 0.1M phosphate buffer for 48 h before staining. Silver staining was performed using the FD Neurotech NeuroSilver Kit (Ellicott City, MD) according to manufacturer's instructions.

2.7. *[^{125}I]IodoDPA-713 small animal SPECT/CT for dynamic in vivo imaging of TSPO*

An X-SPECT small-animal SPECT/CT system (Gamma Medica-Ideas, Northridge, CA) was used for image acquisition. Each mouse was anesthetized with isofluorane prior to imaging. About 1-2 mCi of [^{125}I]IodoDPA-713 was injected into each mouse via intravenous injection, and images were acquired immediately after injection. The SPECT projection data were acquired using 2 low-energy, high-resolution parallel-hole collimators with a radius of rotation of 4.65 cm (spatial resolution, 1.6 mm). The tomographic data were acquired in 64 projections over 360° at 20 s per projection. After tomography, CT was acquired in 512 projections to allow anatomic coregistration. Data were reconstructed using the ordered subsets-expectation maximization algorithm and analyzed using AMIDE software (free software provided by SourceForge). A time activity curve of the [^{125}I]IodoDPA713 uptake was generated for each mouse. Three mice per genotype were scanned for this study. For the blocking study, nonradioactive IodoDPA-713 (20 μM) was intravenously co-injected with [^{125}I]IodoDPA-713, and images were acquired immediately after [^{125}I] injection. Ligands were synthesized according to the methods described in Wang et al., 2009.

2.8. *Imaging and image analysis*

Immunohistochemistry sections stained using DAB were examined using an Olympus BX51 microscope (Proscan II, Prior, Rockland, MA) linked to an Olympus DP70 camera. Highresolution imaging and contrast microscopy using oil immersion and 40x (numerical apertures 1.00) and 100x (numerical aperture 1.35) were used. Immunofluorescently-labeled tissue was imaged at 60x or 96x magnification using a laser scanning confocal microscope (Fluoview FV10i, Olympus, Center Valley, PA), utilizing the FV10 image software. All tissues stained under the same conditions were imaged using the same scanning parameters on the same day. Five to six confocal stacks of each brain region were obtained for each age and genotype for each experimental condition. Confocal stacks were projected into single images using the maximum fluorescence. All images were analyzed using Metamorph Offline (Molecular Devices, Downingtown, PA). The threshold level was kept at the same level for analysis in images obtained from the same experiment. For colocalization analyses, gray scale images at each wavelength were used to examine the area of colocalized pixels of both wavelengths to calculate the percent colocalization of their signals. Percent colocalization was calculated as previously described by Stansfield, et al., 2012. For GM2 and NeuN association analyses, GM2 aggregates and NeuN positive cells were counted using FV10i software.

2.9. *Statistical analysis*

Repeated measure analysis of variance (ANOVA) was used for comparison of weekly body and brain weights across time between wildtype and Sandhoff mice. Student's t-test was used for comparison between wildtype and Sandhoff mice for SPECT imaging, rotarod test, horizontal activity, and rearing activity within each age group due to the fact that animals were euthanized at each age and that the rotarod and activity cages were different across institutions. Therefore, for each age, we normalized the SD results to age-matched wildtype mice. The Bonferroni method

was used to correct for multiple comparisons (p = 0.0125). A 1-way analysis of variance (ANOVA) was used for comparison between wildtype and SD mice across the 4 ages for the quantitative receptor autoradiography, and a 2-way analysis of variance was used for colocalization analyses. ANOVA with *p* values < 0.05 was considered significant, and these data were further subjected to *post hoc* LSD analysis.

3. RESULTS

3.1 Brain and body weights of wildtype (WT) and Sandhoff disease (SD) mice

The body weights of mice were taken weekly starting at 6 weeks and ending at 13 weeks (3 months, the oldest age used in this study) when brains were extracted. Following extraction, the brain weights of WT and SD mice (i.e., *Hexb* knockout) were measured at 3 months of age. Brain weights were not significantly different between WT (425.0 ± 15.1 mg) and SD mice (448.4 ± 20.3 mg) (n = 13 per group. Data are presented as mean ± s.e.m.). Figure 1A shows that the body weight gain differences between WT and SD mice were not significantly different [$F_{(1,25)}$=0.12, p=0.7295; n = 13 per group] up to 3 months of age.

3.2 Progression of motor function deficits

Previous studies have documented the progressive decline in motor function in SD mice beginning at 3 months of age (Sango et al., 1995). Here, we sought to characterize the motor coordination and grip strength of SD mice as a function of age focusing on the presymptomatic phase of the disease. This was done in order to compare the TSPO response in relation to the behavioral manifestation of disease. Figure 1B shows that at 1, 1.5, or 2 months, WT and SD mice showed no significant differences in motor skills as assessed by rotarod performance (Fig. 1B; $t_{(16)}$=0.349, p=0.731; $t_{(14)}$=1.223, p=0.240; $t_{(17)}$=0.761, p=0.457 for 1, 1.5, and 2 months,

respectively; n=10-13 mice). However, at 3 months, SD mice expressed a dramatic decrease in latency time, demonstrating decreased motor coordination and reduced grip strength (Fig. 1B; $t_{(27)}$=5.131, p<0.001).

We also assessed locomotor activity using activity chambers, specifically examining horizontal activity and rearing (ability to stand on hind legs). At 3 months of age, SD mice had a lower level of rearing activity compared to age-matched WT mice, indicating motor impairments (Fig. 1D; $t_{(26)}$=3.405, p=0.0022; n=9-14 mice). Statistically significant differences in horizontal activity were not seen between WT and SD mice within each age group (Fig. 1C). However, at all ages, horizontal activity and rearing appeared to be lower in SD mice compared to agematched WT mice (Figs 1C and D). The latter findings suggests that the generation of *Hexb*(-/-) animals affects horizontal activity and rearing at an age when GM2 ganglioside aggregation or neurodegeneration are absent, i.e., 1 month of age (see section 2.3.1 and 2.3.3). Therefore, we inferred that the difference in horizontal and rearing behavior in SD mice is not associated with disease-induced neurodegeneration but is instead associated with a genotype effect of SD mice.

3.3 Longitudinal assessment of TSPO in relation to neuropathology

We assessed the age-dependent progression of neuropathology in SD mice by examining several pathological endpoints including 1) neuronal ganglioside aggregation (GM_2 immunohistochemistry), 2) brain injury and inflammation using TSPO levels (quantitative receptor autoradiography and *in vivo* imaging), 3) ongoing neurodegeneration using silver staining, and 4) reactive gliosis with microglia and astrocyte markers using immunohistochemistry. These studies were performed in the thalamus, brainstem, and cerebellum because they are the brain regions most severely affected in SD mice (Huang et al., 1997; Sango et al., 1995; Wada et al., 2000). We should note that we also assessed TSPO levels in other brain regions such as the

hippocampus and cerebral cortex (including orbital, motor, and somatosensory cortex) and found no effect, showing the regional specificity of the TSPO response, and not a global inflammatory response (Supplementary Figs. 1A and B). However, see section 2.3.3.

3.3.1 Longitudinal assessment of neuronal aggregation of GM2 gangliosides

To determine the age at which neuronal ganglioside aggregation begins in this mouse model, we stained for GM2 gangliosides at each of the four different ages (1, 1.5, 2, and 3 months) in both WT and SD mice. We stained for GM2 instead of GA2 as GM2 precedes GA2 in the ganglioside catabolic process in mice (Phaneuf et al., 1996; Jeyakumar et al., 2002). We costained for GM2-positive gangliosides and NeuN-positive neurons and counted the number of neurons that contained GM2 aggregates in different brain regions. In the thalamus, we observed neuronal GM2 ganglioside aggregation beginning at 1.5 months, peaking at 2 months, and subsiding at 3 months of age, possibly due to neuronal loss (Fig. 2A; $F_{(4,14)}=18.825$; $p < 0.001$). Significant accumulation of neuronal GM2 ganglioside aggregation was not observed in the brainstem or cerebellum until 2 months of age (Fig. 3A; $F_{(4,14)}=8.711$; $p = 0.003$ for brainstem and Fig. 4A; $F_{(4,14)}=22.150$; $p < 0.001$ for cerebellum). The level of GM2 ganglioside aggregation at 3 months of age remained similar to levels observed at 2 months in these two brain regions. This suggests that there is a regional and temporal specific accumulation of gangliosides and that one of the first brain regions affected by this disease is the thalamus.

3.3.2 Age-dependent analysis of brain TSPO levels using [^{3}H]DPA-713 quantitative autoradiography

We examined TSPO levels in different brain regions in SD mice as a function of age to determine the association between the initiation of GM2 ganglioside aggregation (the primary initiating event that leads to neuronal degeneration) and the TSPO response to this neuronal injury.

We performed [^{3}H]DPA-713 TSPO autoradiography and analyzed 5 brain regions: the cerebral cortex (including the orbital, motor, and somatosensory cortex), hippocampus, thalamus (ventral posteromedial thalamic nucleus), brainstem (parvicellular reticular nucleus), and cerebellum (deep cerebellar nuclei) in age-matched WT and SD mice. In WT mice, we found no significant differences in [^{3}H]DPA-713 binding to TSPO as a function of age for any of the brain regions examined; thus, we combined the [^{3}H]DPA-713 binding data for WT mice from each age and brain region (thalamus: $F_{(3,34)}=0.066$; $p=0.978$; brainstem: $F_{(3,29)}=0.110$; $p=0.954$; cerebellum: $F_{(3,32)}=0.027$; $p = 0.994$; hippocampus: $F_{(3,34)}=0.153$; $p=0.927$; cortex: $F_{(3,33)}=0.128$; $p=0.943$; n=9-14/age group). In the thalamus of SD mice, TSPO levels measured using [^{3}H]DPA-713 autoradiography were markedly elevated relative to WT beginning at 1.5 months of age (Fig. 2B). TSPO levels progressively increased as a function of age in SD mice, reaching nearly 5-fold higher levels relative to WT at 3 months of age (Fig. 2B; $F_{(4, 62)}=139.144$; $p < 0.001$). It should be noted that the earliest significant increase in TSPO levels in the thalamus occurred at 1.5 months of age, a time when there was minimal, non-significant GM2 ganglioside aggregation in neurons (Fig. 2A and B). Therefore, the TSPO response in the thalamus was measured at the earliest age when GM2 ganglioside aggregation was observed.

In the brainstem, we observed a significant increase in TSPO binding beginning at 2 months of age with further increases at 3 months of age (Fig. 3B; $F_{(4,53)}=13.002$; $p < 0.001$). The significant increase in TSPO levels in the brainstem coincided with a significant increase in neuronal GM2 accumulation in this brain region. In the cerebellum, TSPO binding was significantly elevated only at 3 months in SD mice as compared to WT and all other ages (Fig. 4B; $F_{(4,59)}=6.692$; $p < 0.001$). This was in contrast to the significant ganglioside accumulation seen in the cerebellum at 2 months. It is possible that the TSPO glial response in the deep cerebellar nuclei

may require a greater amount of time than in other brain regions. Additionally, we found no statistically significant differences in TSPO binding in the hippocampus or the orbital, motor, and somatosensory cortex at any age (Supplementary Figs. 1A and B; $F_{(4,62)}=0.559$; $p=0.693$ for hippocampus and $F_{(4,60)}=1.191$; $p=0.324$ for cortex).

3.3.3 Longitudinal assessment of neurodegeneration

To assess the relationship between TSPO expression and neurodegeneration in the SD mouse brain, we used silver staining as a means to evaluate ongoing neurodegeneration. At 1 month of age, SD mice showed no significant silver accumulation in the thalamus (Fig. 2C), cerebellum (Fig. 4C) or brainstem (Fig. 3C) compared to WT. At 1.5 months, there was significant silver accumulation in the thalamus of SD mice compared to WT. At 2 and 3 months, SD mice showed robust silver accumulation in the thalamus (Fig. 2C) and in both the brainstem (Fig. 3C) and cerebellum (Fig. 4C). The cerebral cortex (including the orbital, motor, and somatosensory cortex) exhibited minimal silver accumulation by 3 months (Supplementary Fig 2A). Collectively, these results indicate that TSPO expression increases in brain areas undergoing neurodegeneration. It is notable that we detected significant and selective neurodegeneration in the CA2 region of the hippocampus beginning at 1.5 months and increasing with disease progression (Fig. 5A). This is in contrast to the fact that we did not detect increased TSPO levels or glial cell activation via quantitative autoradiography or immunohistochemistry in the CA2 region of the hippocampus at any age. These findings suggest that the CA2 region of the hippocampus is not able to mount a glial/TSPO response to ongoing neurodegeneration. Further studies are needed in order to understand this unusual and unexpected finding.

3.3.4 Longitudinal assessment of reactive gliosis

Another aspect of this study was to determine the cellular sources of the TSPO response in SD mouse brain. It is known that increased TSPO expression in the injured brain is associated with both microglia and astrocyte activation (Chen and Guilarte, 2008; Chen et al. 2004; Consenza-Nashat et al., 2009; Raghavendra et al., 2000; Veenman and Gavish 2000; Venneti et al., 2004). Thus, we performed immunohistochemistry using Mac-1 as a microglia marker and GFAP as an astrocyte marker. Wildtype mice exhibit morphologically normal microglia and astrocytes at all ages examined. On the other hand, in the thalamus of SD mice, microglia activation was first observed at 1.5 months of age, peaked at 2 months of age, and decreased at 3 months of age (Fig. 2D). In both the cerebellum and brainstem, SD mice expressed a progressive age-dependent increase in Mac-1 labeling with maximal activation at 3 months relative to WT (Figs. 3D and 4D for cerebellum and brainstem, respectively). Neither the cortex nor the hippocampus showed activated microglia as demonstrated by Mac-1 labeling (Supplementary Fig. 2B and Fig. 5B).

For astrocytes, we found that in the thalamus, brainstem, cerebellum, and cerebral cortex of SD mice, there was an increased number of astrocytes and increased GFAP levels at all ages relative to WT (Fig. 2E, 3E, 4E, and Supplementary Fig. 2C for thalamus, brainstem, cerebellum, and cortex respectively). Therefore, it appears that in SD mice, astrocytosis occurs very early in time and prior to microglia activation. In all brain regions examined in SD mice, activated astrocytes were observed as early as 1 month of age (Fig. 2E, 3E, 4E, and Supplementary Fig. 2C). Astrocyte activation became more pronounced with disease progression in the regions of the brain that exhibited increasing levels of TSPO as the disease progresses, i.e., the thalamus, brainstem, and cerebellum. The astrocytes in the cerebral cortex, which did not show increased TSPO levels with disease progression, demonstrated an increase in number based on GFAP immunohistochemistry; however, these astrocytes did not appear to be hypertrophic. In contrast,

GFAP staining was seen throughout the entire hippocampus in both WT and SD mice (Fig. 5C) as is normal for this brain region.

3.4 In vivo TSPO imaging using [^{125}I]IodoDPA-713 SPECT

We used [^{125}I]IodoDPA-713 small animal SPECT imaging to measure TSPO expression *in vivo* in SD mice. Small animal SPECT images were co-registered with small animal CT to select the appropriate brain regions for analysis. There was a higher brain uptake of [^{125}I]IodoDPA-713 in the SD mouse compared to WT (Fig. 6A). Time-activity curves in the thalamus showed that SD mice had higher uptake of [^{125}I]IodoDPA-713 than WT mice across all time points (data not shown). Quantitative analysis of the SPECT imaging showed a trend of increased uptake of [^{125}I]IodoDPA-713 in the thalamus, cerebellum, and brainstem with a statistically significant increase of [^{125}I]IodoDPA713 uptake in thalamus at 2 months ($t_{(4)}$=2.81, p=0.0484) and in the brainstem at 3 months ($t_{(6)}$=3.263, p=0.0172) compared to WT (Fig. 6B). To determine that the [^{125}I]IodoDPA713 brain uptake was selective for TSPO, we used a pharmacological block in SD mice using nonradioactive IodoDPA713 (20 μM), resulting in complete blockade of [^{125}I]IodoDPA713 uptake in the brain of SD mouse (Fig. 6A). These findings indicate that the increased [^{125}I]IodoDPA713 in the mouse brain is directly related to increased TSPO brain levels.

3.5 Temporal TSPO expression in glial cell types

An important aspect in understanding the TSPO response to brain injury is to determine the cellular sources of the TSPO response since both microglia and astrocytes express and increase TSPO levels following injury (Chen and Guilarte, 2008; Chen and Guilarte, 2006; Kuhlmann and Guilarte, 2000; Maeda et al., 2007; Vowinckel et al., 1997). In Figures 2, 3, and 4, we show the temporal pattern of TSPO expression and the activation of microglia and astrocytes in SD mice. However, this data does not show the temporal expression of TSPO within each glial cell type. In

order to understand the contribution of microglia and astrocytes to the TSPO signal during the course of neurodegeneration obtained by [$_{3}$H]DPA-713 receptor autoradiography and [$_{125}$I]DPA-713 small animal SPECT, we performed triple-labeled immunohistochemistry and confocal imaging of TSPO with Mac-1 and GFAP.

Figure 7 depicts triple-labeled immunofluorescent confocal images of TSPO, Mac-1, and GFAP in both WT and SD mice. Triple-labeled immunofluorescent confocal imaging confirmed that TSPO colocalized with both microglia and astrocytes in the thalamus (Fig. 7A-C), brainstem, and cerebellum. We also measured the percent colocalization of TSPO with Mac-1 and TSPO with GFAP in the thalamus (Figs. 7B and 7C), brainstem (Figs. 8A and B), and cerebellum (Figs. 9A and B) at the various ages. In the thalamus, the percent colocalization between TSPO and Mac-1 followed a similar pattern in both WT and SD mice with a more pronounced effect in the SD mice (Fig. 7B). The percent colocalization between TSPO and Mac-1 increased with age in both WT and SD mice and peaked at 2 months (Fig. 7B; 2-way ANOVA: Age: $F_{(3,27)}$=4.386; p=0.016. Genotype: $F_{(1,27)}$=10.740; p=0.004. Age x Genotype: $F_{(3,27)}$=2.106; p< 0.132. n=3–4 mice per age group and genotype). In the brainstem and cerebellum, percent colocalization patterns of TSPO and Mac-1 mirrored those seen in the thalamus with levels of percent colocalization being highest in the thalamus (Figs. 8A and 9A).

The percent colocalization between TSPO and GFAP differed significantly between WT and SD mice, partially due to the low signal of both proteins in the WT mice. In SD mice, we observed high levels of colocalization in the thalamus beginning at 1.5 months and remaining elevated until 3 months of age (Fig. 7C; 2-way ANOVA: Age: $F_{(3,29)}$=2.122; p=0.126. Genotype: $F_{(1,29)}$= 41.309; p < 0.001. Age x Genotype: $F_{(3,29)}$= 4.136; p = 0.018. 1-way ANOVA: $F_{(7,29)}$=8.401; p < 0.001. n=3–4 per age group and genotype). Similarly, the temporal progression of TSPO and

GFAP colocalization observed in the brainstem mirrored what was observed in the thalamus (Fig. 8B). In the cerebellum, we observed high levels of TSPO and GFAP colocalization beginning at 1.5 month of age and remained elevated throughout the progression of disease (Fig. 9B). In all regions and at all ages examined, TSPO colocalization with astrocytes was greater than its colocalization with microglia.

4. DISCUSSION

The present work provides novel information on the relationship between the TSPO response to the initiation and progression of neurodegeneration and glial cell activation during the presymptomatic phase of disease in SD mice. The SD mouse provides a well-characterized animal model of neurodegeneration where the initiating pathological event (aggregation of GM2 ganglioside) can be assessed and the magnitude and temporal course of the TSPO response can be compared to neuronal GM2 aggregation, as well as pathological and behavioral endpoints. Based on the *ex vivo* [^{3}H]DPA-713 quantitative autoradiography and *in vivo* [^{125}I]IodoDPA-713 small animal SPECT imaging, we were able to map the regional TSPO expression in the SD mouse brain as a function of age and pathology. Our findings indicate that the thalamus is the brain region where the earliest increases in GM2 ganglioside aggregation and TSPO expression occur, and that these increases occur prior to physical and behavioral manifestation of disease. Additionally, the magnitude of the TSPO response markedly increases as a function of age as neurodegeneration progresses. Our finding that the thalamus is one of the earliest affected brain regions is consistent with other studies using this animal model (Maegawa et al., 2006) and in the clinical setting with patients that express the disease (Kumar et al., 2014, Wu et al., 2013, Saouab et al., 2011, Yun et al., 2005).

Importantly, the regional expression of TSPO in the SD brain was consistent with affected (thalamus, brainstem, and cerebellum) brain regions. The finding that increased TSPO expression in the thalamus occurs with the first observable evidence of GM2 aggregation and prior to behavioral manifestation of disease strongly suggests that TSPO can be used for the early detection of neurodegenerative disease and to assess its progression. These characteristic make TSPO an ideal biomarker to assess the effectiveness of therapeutic interventions by tracking the TSPO signal during the presymptomatic stage of the disease.

It is notable that we were not able to detect an increase in TSPO or glial cell activation in the CA2 region of the hippocampus in SD mice despite significant and progressive neurodegeneration measured by silver staining. To our knowledge, this pathology has not been described previously in either the SD mouse model or in human postmortem tissue from SD subjects. As previously noted, one possibility for this discrepancy could be related to the fact that the CA2 region of the hippocampus is a very small area and the methods used do not have sufficient spatial resolution to detect a TSPO or glial response. Studies using emulsion autoradiography with resolution at the cellular level could be useful to provide an explanation to this question. Alternatively, it is possible that the CA2 region is unique from other brain regions and is not able to mount a TSPO/glial response to injury. For example, a study by Kipp et al., demonstrated that astrocytes cultured from different brain areas not only have differences in cytokine profile expression and capacity in basal unstimulated conditions, but also have regional and temporal specific patterns of activation and cytokine upregulation in response to an inflammatory stimuli, such as LPS (Kipp et al., 2008). Taken together, these findings suggest that glial cell activation and thus the TSPO response to injury is likely to differ by brain region and one cannot assume that different types of injuries will generate the same TSPO/glial cell response.

Progressive reactive gliosis is known to occur in this mouse model of SD as demonstrated in the present study and by other studies (Myerowitz et al., 2002; Wada et al., 2000; Kyrkanides et al., 2005; Kyrkanides et al., 2007). However, no previous study has examined the age dependent activation of both microglia and astrocytes. Here, we established the regional and temporal pattern of microglia and astrocyte activation over the course of disease progression with astrocyte activation occurring earlier in time than microglial activation and confirm that both microglia and astrocytes are the source of the observed TSPO response although they express different temporal profiles (Figs. 2, 3, and 4).

To further understand the function of TSPO and its role in the SD process, we first confirmed that both microglia and astrocytes expressed TSPO with specific regional and temporal patterns. Notably, in this neurodegenerative animal model, TSPO exhibited a higher degree of colocalization with astrocytes than with microglia, which is different with has been previously observed in other brain injury models (Chen and Guilarte, 2008; Cosenza-Nashat M et al. 2009). The greater degree of TSPO expression and colocalization with astrocytes in the SD mouse brain may be related to the early (i.e., 1 month) and sustained progression of astrocytosis present in several brain regions examined. The early astrocytic response occurred before the upregulation of TSPO and before neurodegeneration as assessed by silver staining, indicating that the generation of the SD mouse by knocking out the HexB gene may alter astrocyte physiology. This is consistent with the fact that abnormal growth patterns in astrocytes cultured from SD mice have been documented (Kawishima et al., 2009). Specifically, these studies found significantly faster rates of proliferation, increased ERK phosphorylation, and decreased Akt phosphorylation in astrocytes cultured from SD mice compared to WT. Another study found that despite conditionally expressing β-hexosaminidase in neurons from SD mice, the number of GFAP-positive astrocytes

did not decrease and GFAP gene expression remained elevated, whereas the number of MHC-II and CD45 positive cells and gene expression levels decreased as a result of expressing β hexosaminidase in neurons from SD mice (Kyrkanides et al., 2012). These results suggest that the early proliferation response of the astrocytes is independent of GM2 aggregation in neurons and that there is likely a disruption of neuron-astrocyte signaling. Taken together, these studies suggest that SD mice may have abnormally-functioning astrocytes, potentially explaining the early degree of GFAP expression and hypertorphy observed in the present study. However, it is important to note that despite the early activation of astrocytes, the TSPO signal does not increase until later in the disease process. This finding suggests that the TSPO increase in activated astrocytes starting at 1.5 months in the thalamus is the result of injury due to the disease, and not due to alterations in astrocyte physiology observed as early as 1 month of age.

In the present study, we used the second-generation TSPO ligand DPA-713 in the tritiated and iodinated forms for TSPO autoradiography and *in vivo* imaging using small animal SPECT. Overall, one advantage of using [^{3}H]DPA-713 for TSPO autoradiography studies is the fact that there is virtually no background; thus, a very high signal to noise ratio. Furthermore, using the [^{125}I]IodoDPA-713 allows for *in vivo* SPECT imaging studies in which a single synthesis can be used for multiple studies due to the relatively long half-life of ^{125}I. Recent work has shown that [^{125}I]IodoDPA-713 can be used for imaging TSPO in the lungs using small animal SPECT (Wang et al., 2009; Ordonez et al., 2015). Our current study is the first to demonstrate *in vivo* [^{125}I]IodoDPA-713 small animal SPECT imaging in the brain, with results similar to those measured with [^{3}H]DPA-713 autoradiography despite the fact that [^{125}I]IodoDPA-713 small animal SPECT does not have the same degree of spatial resolution as [^{3}H]DPA-713

autoradiography. Our findings strengthen the use of [^{125}I]IodoDPA-713 as an attractive radioligand for TSPO imaging using small animal SPECT.

Overall, we have shown that the regional expression of TSPO in SD mice is brain region-specific and depends on the age of the SD animal as disease progresses with the thalamus providing the earliest signal of disease based on TSPO expression and other markers of neurodegeneration. Therefore, it is possible that PET, SPECT, or magnetic resonance imaging techniques (if developed) of brain TSPO could serve as an early indicator of brain pathology in the clinical setting. However, while PET and SPECT imaging of TSPO may be useful in the clinical setting as they provide real-time information of ongoing brain inflammation and injury, the potential risks of radiation exposure in children expressing the disease must be taken into consideration. From a translational perspective, the present work sets the stage to determine if TSPO expression in peripheral cells could serve as a surrogate marker for TSPO levels in the brain. For example, using this progressive animal model of SD, one can examine the relationship between increases in TSPO expression in the CNS and those in TSPO-expressing peripheral cells such as platelets, monocytes, and macrophages. The discovery of an early peripheral biomarker of CNS disease would be a significant advance for clinical use.

ACKNOWLEDGMENTS: The authors acknowledge the Johns Hopkins Broadway Research Building Animal Facility Behavioral Core for the use of the open field chambers and rotarod apparatus and the Johns Hopkins MRB Molecular Imaging Center for the assistance with the SPECT imaging and Haoafan Wang for the synthesis of [^{125}I]IodoDPA-713. We would like to thank Fatima Alikhan and Christina Chung for their technical assistance. This work is in partial fulfillment of doctoral degree requirements for JC and ML. This work was supported by NIEHSES007062 to TRG, NIEHS Center grant ES009089, NCI-CA92871 and GE/NFL Head Health Challenge to MGP. JC was supported by NIEHS T32 ES07141.

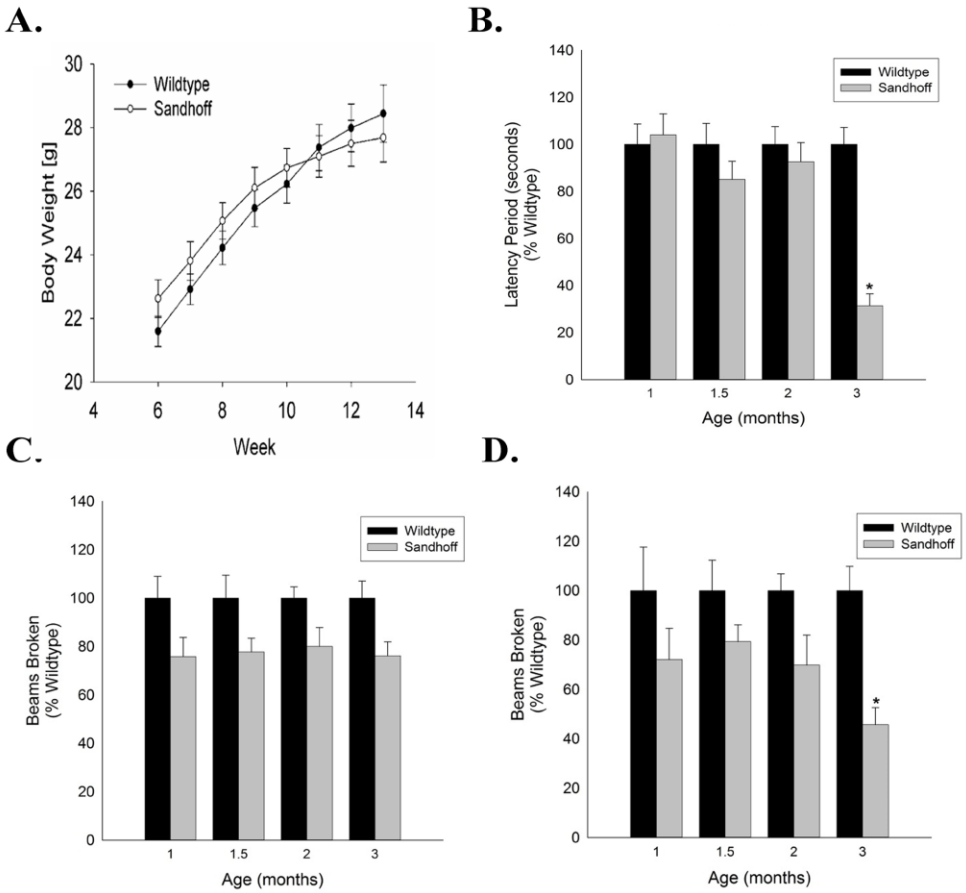

FIGURE 1. **Characterization of Sandhoff Mice.** A) Weekly bodyweights of wildtype and Sandhoff mice from 6 to 13 weeks of age (3months of age). There was no significant difference of body weight between wildtype and Sandhoff mice at any age (Repeated ANOVA. p=0.7295). Data is expressed as the mean of the body weights per week ± SEM. n=13 for both wildtype and Sandhoff mice. B) Wildtype and SD mice show no significant differences in motor skills as assessed by rotarod performance at 1, 1.5, or 2months of age. However, at 3 months of age, SD mice expressed a dramatic decrease in latency time demonstrating their decreased motor coordination and reduced grip strength. Data is expressed as mean ± SEM. n=10–13mice per group. C) Horizontal activity and D) rearing of WT and SD mice were measured for 1 h using the open field activity chamber at each of the 4 ages. When correcting for multiple comparisons, a significant difference between age-matched 3monthwildtype and SD mice was seen for rearing activity (t=3.405; p=0.0022). No significant differences were seen in horizontal activity when applying the Bonferroni method to correct for multiple comparisons. Data is expressed as mean ± SEM. n = 9–14 mice per group.

FIGURE 2

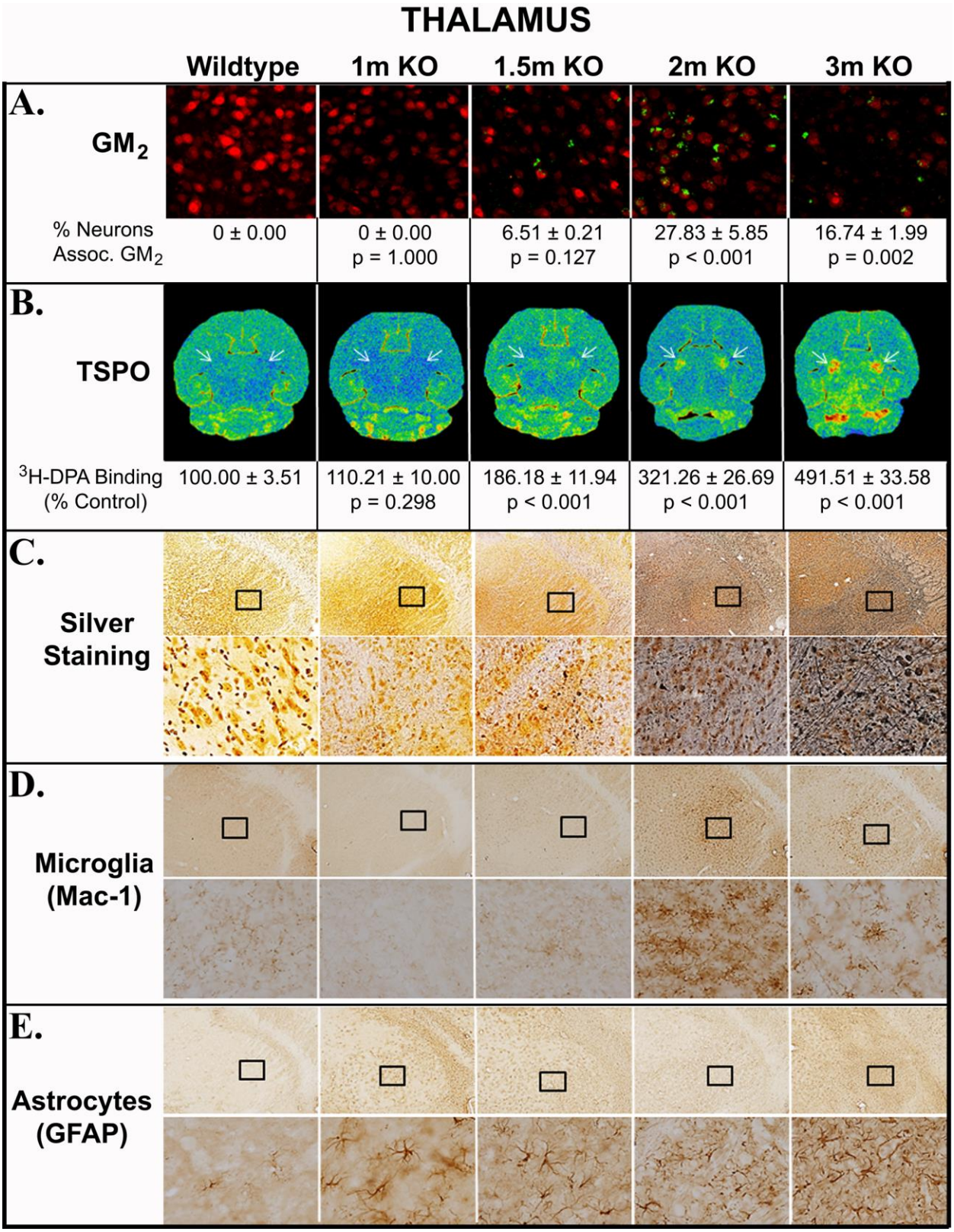
THALAMUS
Wildtype
1m KO
1.5m KO
2m KO
3m KO
A.
GM2
% Neurons Assoc. GM2
0 ± 0.00
0 ± 0.00 p = 1.000
6.51 ± 0.21 p = 0.127
27.83 ± 5.85 p < 0.001
16.74 ± 1.99 p = 0.002
B.
TSPO
3H-DPA Binding (% Control)
100.00 ± 3.51
110.21 ± 10.00 p = 0.298
186.18 ± 11.94 p < 0.001
321.26 ± 26.69 p < 0.001
491.51 ± 33.58 p < 0.001
C.
Silver Staining
D.
Microglia (Mac-1)
E.
Astrocytes (GFAP)

FIGURE 2. TSPO levels and neuropathology of Sandhoff disease mice in the thalamus. A) GM2 ganglioside aggregation (green) in neurons stained with NeuN (red). Representative images show increasing GM2 aggregates with age in SD mice as compared to WT. GM2 aggregation begins at 1.5months and reaches significant levels by 2months ($F_{4,14} = 18.825$; $p < 0.001$). B) TSPO levels measured by [3H]DPA-713 quantitative autoradiography progressively increased as a function of age in SD mice. TSPO levels were significantly increased beginning at 1.5 months, the earliest age at which GM2 aggregation is observed, and increased with age ($F_{4, 62} = 139.144$; $p < 0.001$). C) Representative horizontal brain photomicrographs of active neurodegeneration as detected with silver staining. The top row represents low magnification images with the boxes indicating the area of which the high magnification images in the bottom row were generated. At 1month, SD mice show no significant silver accumulation in the thalamus compared to WT. At 1.5months, there is slight silver accumulation in the thalamus in SD mice compared to WT, and at 2 and 3months, SD mice show robust silver accumulation in the fiber tracks of the thalamus. D)Microglia activation as indicated byMac-1 labeling occurs as early as 1.5 months, with 2 month SD mice exhibiting the highest levels of Mac-1 labeling. E) Activated astrocytes are observed as early as 1 month of age in SD mice, and activation becomes more pronounced with age and disease progression.

FIGURE 3

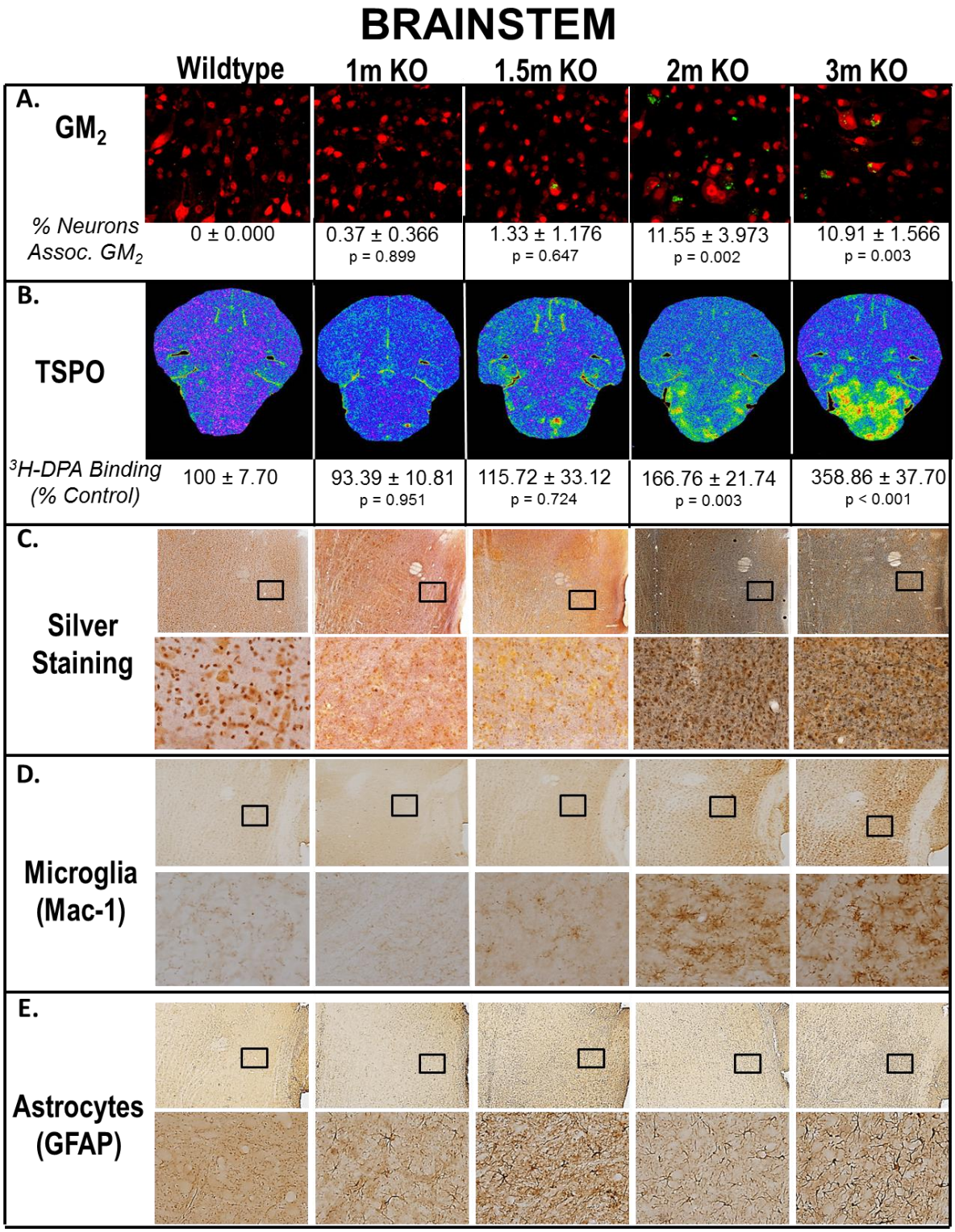
BRAINSTEM
Wildtype
1m KO
1.5m KO
2m KO
3m KO
A.
GM2
% Neurons Assoc. GM2
0 ± 0.000
0.37 ± 0.366
p = 0.899
1.33 ± 1.176
p = 0.647
11.55 ± 3.973
p = 0.002
10.91 ± 1.566
p = 0.003
B.
TSPO
3H-DPA Binding (% Control)
100 ± 7.70
93.39 ± 10.81
p = 0.951
115.72 ± 33.12
p = 0.724
166.76 ± 21.74
p = 0.003
358.86 ± 37.70
p < 0.001
C.
Silver Staining
D.
Microglia (Mac-1)
E.
Astrocytes (GFAP)

FIGURE 3: Neuropathological Assessment of Sandhoff disease in the brainstem. A) Representative images showing GM2 accumulation (green) in SD mice compared to WT. Slight increase in the levels of GM2 aggregation begins at 1.5 months, reach significant levels by 2 months, and stay consistent at 3 months ($F_{4,14} = 8.711$; $p = 0.003$) B) TSPO levels in the brainstem, as determined by [^{3}H]-DPA autoradiography, is significant compared to WT mice at 2 months, and increases to higher levels at 3 months of age (B; $F_{4,53} = 13.002$; $p < 0.001$). C) At both 2 and 3 months, silver staining shows ongoing neurodegeneration. The top row represents low magnification images with the boxes indicating the area of which the high magnification images of the bottom row were generated. D) WT mice exhibit morphologically normal microglia and astrocytes. Microglia activation, as indicated by Mac-1 labeling, is seen at low levels in the brainstem at 1.5 months. SD mice demonstrate a progressive increase over time in Mac-1 labeling compared to WT mice. E) Activated astrocytes are observed beginning as early as 1 month of age in SD mice, and activation becomes more pronounced with age and disease progression in SD mice.

FIGURE 4

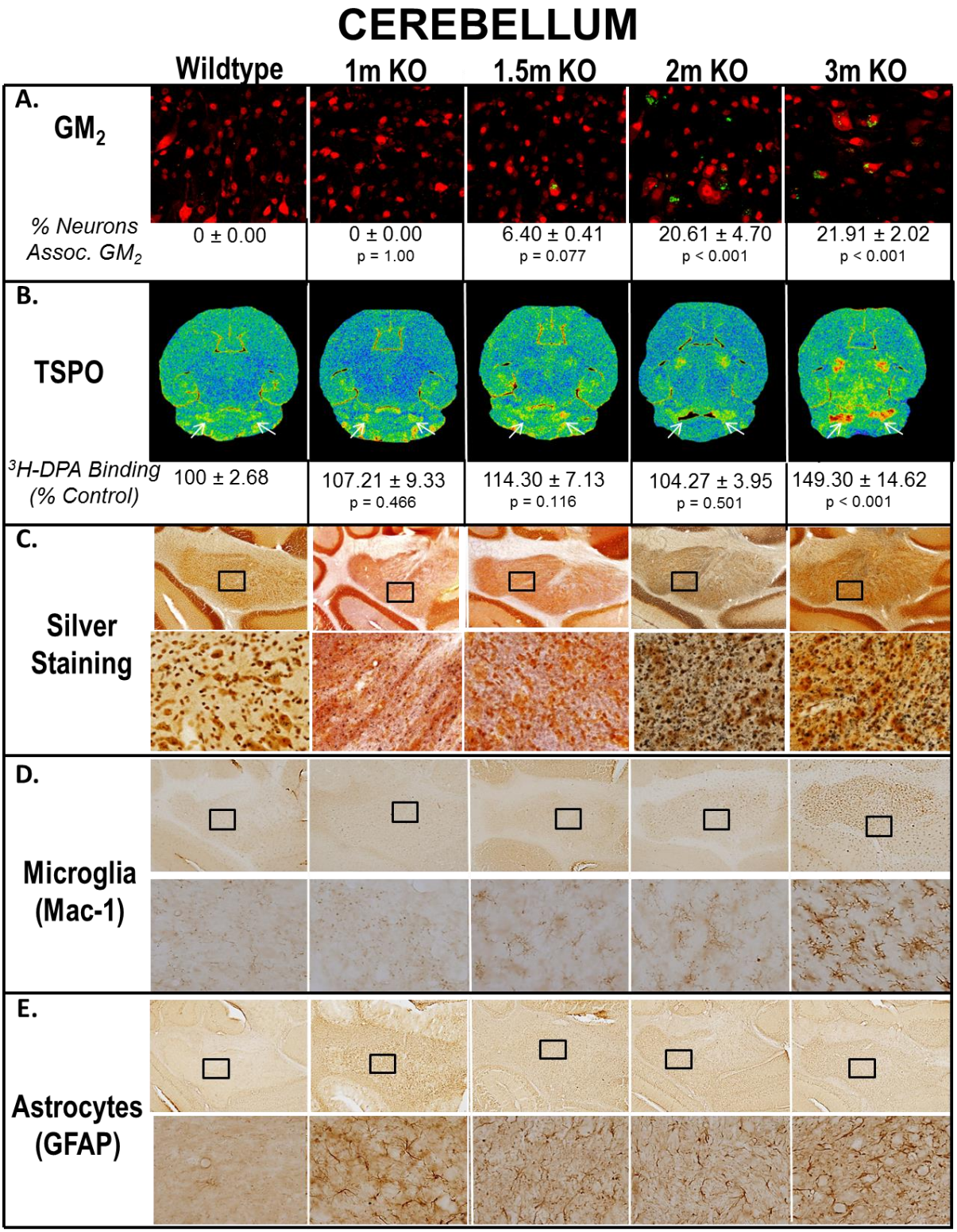
CEREBELLUM
Wildtype
1m KO
1.5m KO
2m KO
3m KO
A.
GM2
% Neurons Assoc. GM2
0 ± 0.00
0 ± 0.00
p = 1.00
6.40 ± 0.41
p = 0.077
20.61 ± 4.70
p < 0.001
21.91 ± 2.02
p < 0.001
B.
TSPO
3H-DPA Binding (% Control)
100 ± 2.68
107.21 ± 9.33
p = 0.466
114.30 ± 7.13
p = 0.116
104.27 ± 3.95
p = 0.501
149.30 ± 14.62
p < 0.001
C.
Silver Staining
D.
Microglia (Mac-1)
E.
Astrocytes (GFAP)

FIGURE 4: Neuropathological Assessment of Sandhoff disease in the cerebellum. A) Representative images of GM2 accumulation in SD mice compared to WT. Low levels of GM2 aggregation (green) begin at 1.5 months, reach significant levels by 2 months, and stay consistent at 3 months of age ($F_{4,14} = 22.150$; $p < 0.001$). B) TSPO levels in the cerebellum, as determined by [^{3}H]-DPA autoradiography, become significantly increased compared to WT mice at 3 months of age ($F_{4, 59} = 6.692$; $p < 0.001$). C) At both 2 and 3 months, representative horizontal brain photomicrographs reveal robust diffuse neurodegeneration as detected through silver staining. The top row represents low magnification images with the boxes indicating the area of which the high magnification images of the bottom row were generated. D) WT mice exhibit morphologically normal microglia and astrocytes. Microglia activation, as indicated by Mac-1 labeling, is observed at 1.5 months and progressively increasing as animals age and the disease progresses. E) Activated astrocytes are observed beginning as early as 1 month of age in SD mice, and activation becomes more pronounced with age and disease progression in SD mice.

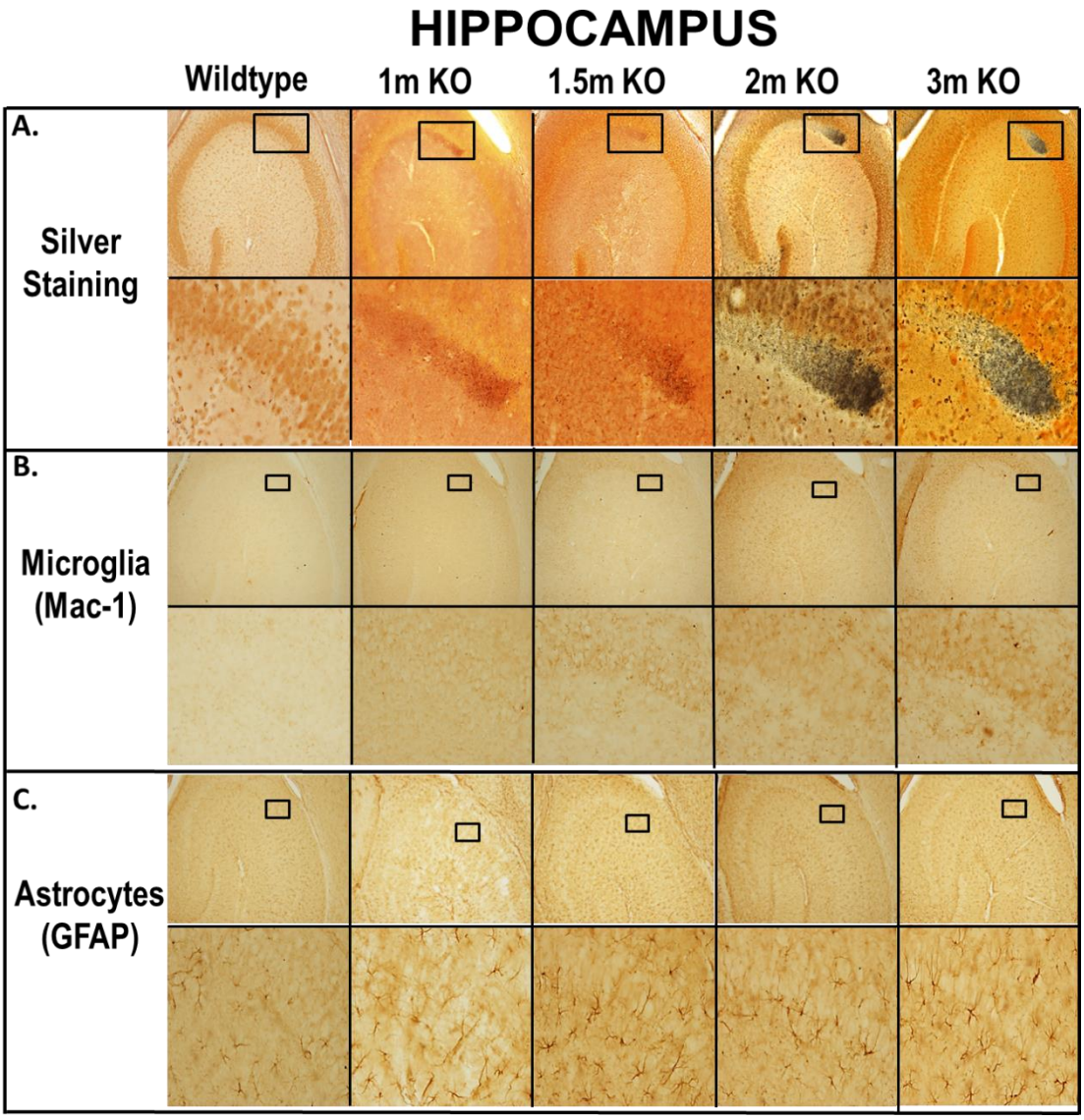

FIGURE 5. Neuropathological Assessment of Sandhoff disease in hippocampus. A) Representative horizontal brain photomicrographs reveal neurodegeneration in the CA2 region of the hippocampus beginning at 1.5 months and continuing as the diseases progresses. The top row represents low magnification images with the boxes indicating the area of which the high magnification images of the bottom row were generated. B) WT and SD mice exhibit morphologically normal microglia. Microglia activation, as indicated by Mac-1 labeling, does not appear to occur as animals age or the disease progresses in this brain region. C) Activated astrocytes are observed at all ages in SD mice at comparable levels to those seen in WT mice.

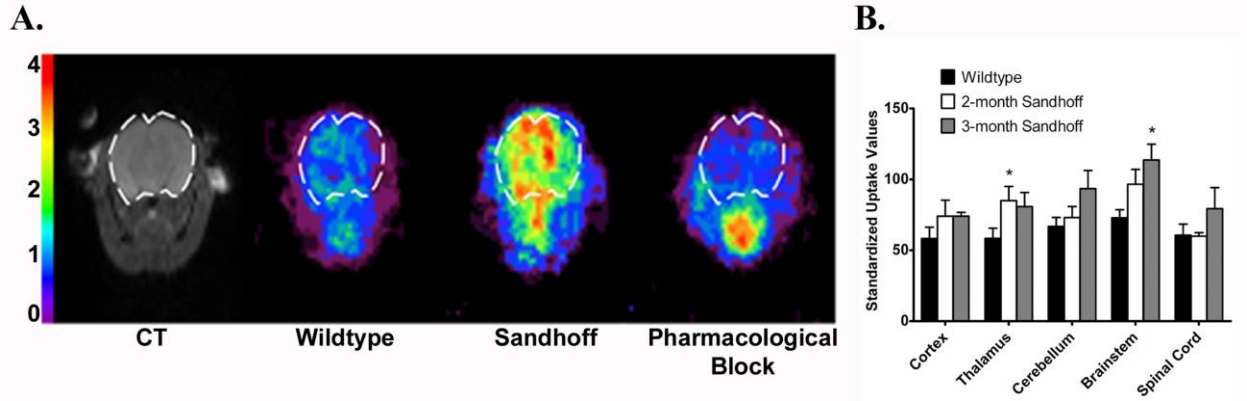

FIGURE 6. In vivo TSPO imaging using [125I]-IodoDPA713 SPECT in the Sandhoff disease mouse brain. A) Representative brain uptake of [125I]IodoDPA-713 in wildtype (WT), 3-month SD mouse, and 3-month SD mouse with pharmacological block using non-radioactive IodoDPA-713. The CT, for orientation purposes, indicates that slices are at the level of the thalamus. Tracer uptake is higher in the brain of the SD mouse, and the uptake was blocked by co-injection of 20 μM non-radiolabeled IodoDPA-713. B) Analysis of [125I]-IodoDPA713 uptake in SD mouse brain. At 2-months of age SD mice exhibited a significant increase in [125I]-IodoDPA713 uptake in the thalamus ($t4=2.81$, $p=0.0484$). At 3-months of age, SD mice expressed a significant increase in [125I]-IodoDPA713 uptake in the brainstem ($t6 = 3.263$, $p = 0.0172$). Images are expressed in units of Standardized Unit Value (SUV) and are normalized for weight and injected dose. Data is expressed as the mean of SUV ± SEM. n = 3–4 mice per group. * p b 0.05 compared to WT.

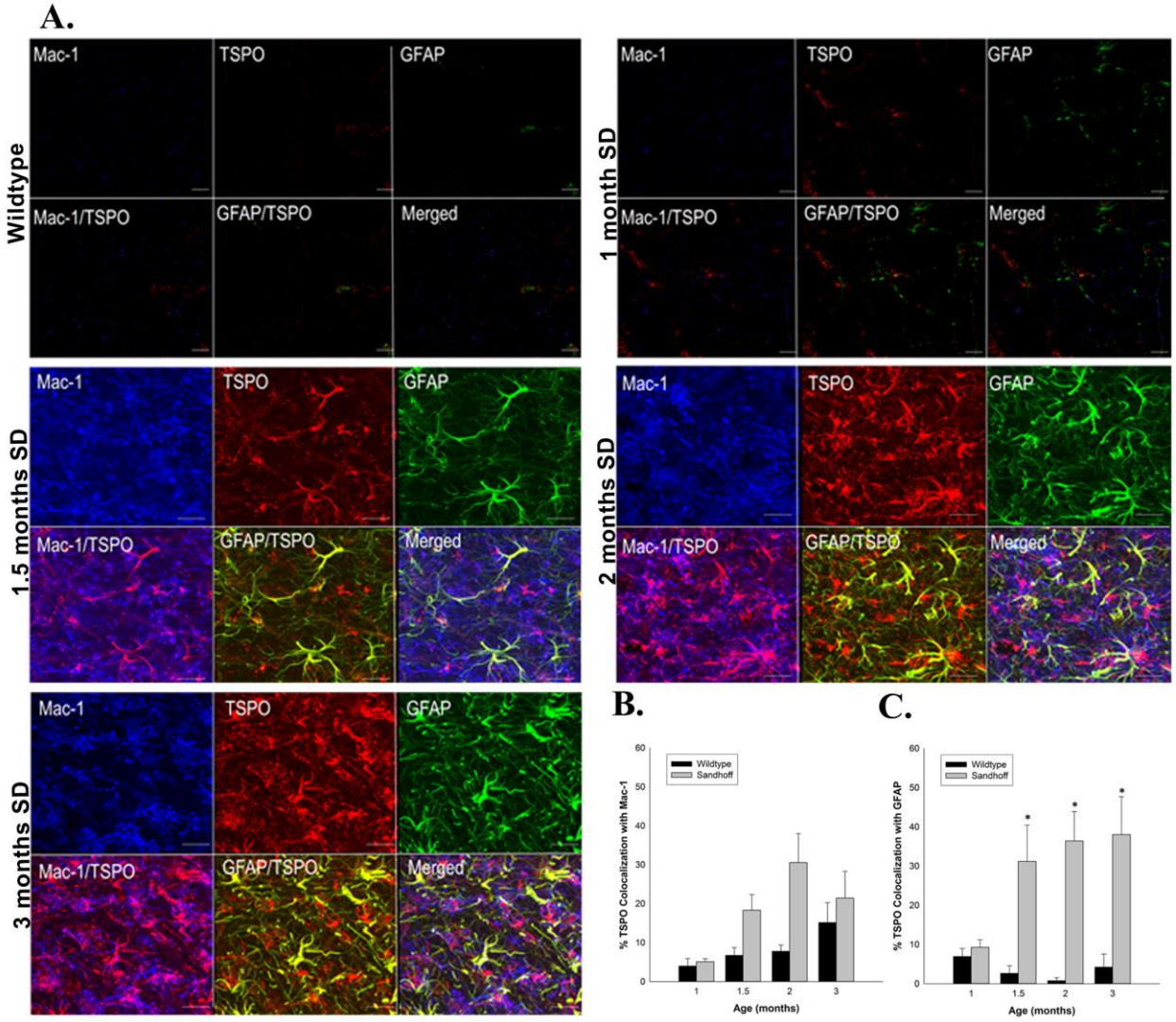

FIGURE 7. Temporal colocalization of TSPO with glial markers in wildtype (WT) and Sandhoff disease (SD) mice in the thalamus. A) Representative triple labeled immunofluorescent confocal images in the thalamus of WT and SD mice at the four different ages. Triple labeled immunofluorescent confocal imaging confirmed that TSPO colocalized with the microglial markerMac-1 as indicated by the purple and magenta colors and astrocyte marker GFAP as indicated by the yellow color. B) In the thalamus, the percent colocalization of TSPO with Mac-1 follows a similar pattern in both the WT and SD mice, with a more pronounced effect in the SD mice. The percent colocalization between TSPO and Mac-1 increases with age in both WT and SD mice and peaks at the 2 months of age. C) The percent colocalization between TSPO and GFAP also differs significantly between WT and SD mice, due to the low signal of both in the WT mice. In the SD mice, we observed a high degree of colocalization beginning at 1.5 months and remaining at 3 months of age. Each value represents the mean ± SEM. n=3–4 animals and experiments.

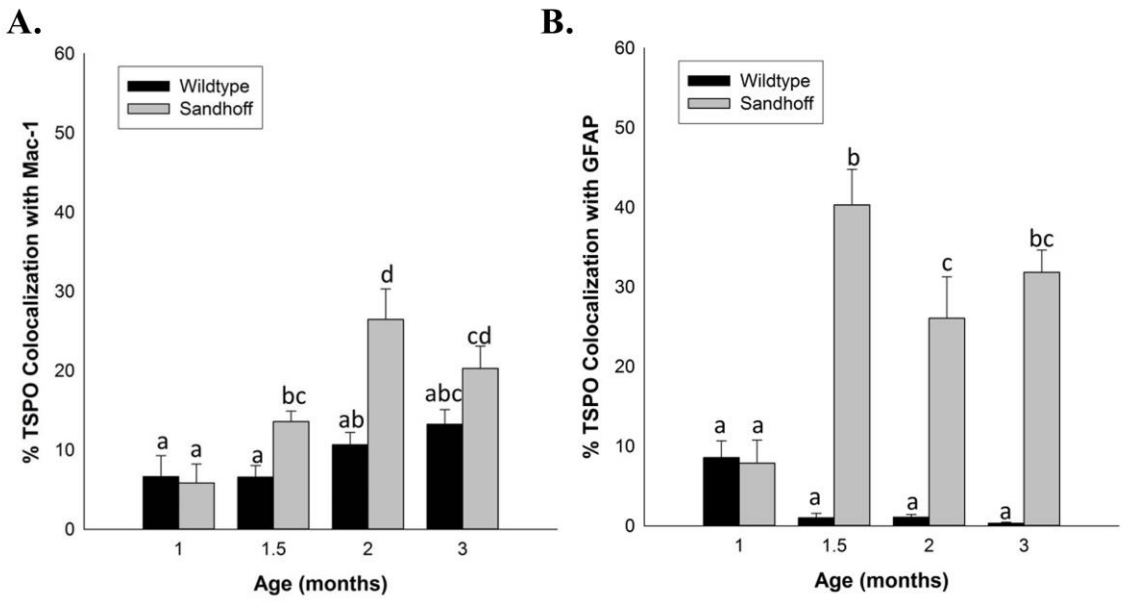

FIGURE 8. Temporal colocalization of TSPO expression with glial markers in wildtype (WT) and Sandhoff disease (SD) mice in the brainstem. A) In the brainstem, the percent colocalization between TSPO and Mac-1 increases with age and follows a similar pattern in both the WT and SD mice, with a more pronounced effect in the SD mice (2 way ANOVA: Age: $F_{3,29} = 11.843$; $p < 0.001$. Genotype: $F_{1,29} = 18.117$. $p < 0.001$. Age x Genotype: $F_{3,29} = 4.089$; $p = 0.019$. 1 way ANOVA: $F_{7,29} = 9.470$; $p < 0.001$. Each value represents the mean ± SEM. n = 3 – 4) B) The percent colocalization between TSPO and GFAP differs significantly between WT and SD mice. In the SD mice, we observed high levels of colocalization beginning at 1.5 months and this amount of colocalization remained elevated up until 3 months of age (2 way ANOVA: Age: $F_{3,28} = 6.457$; $p = 0.003$. Genotype: $F_{1,28} = 130.46$. $p < 0.001$. Age x Genotype: $F_{3,28} = 18.319$; $p < 0.0001$. 1 way ANOVA: $F_{7,28} = 26.807$; $p < 0.001$. Each value represents the mean ± SEM. n = 3– 4). Within a group, bars with different letters are significantly different at $p < 0.05$.

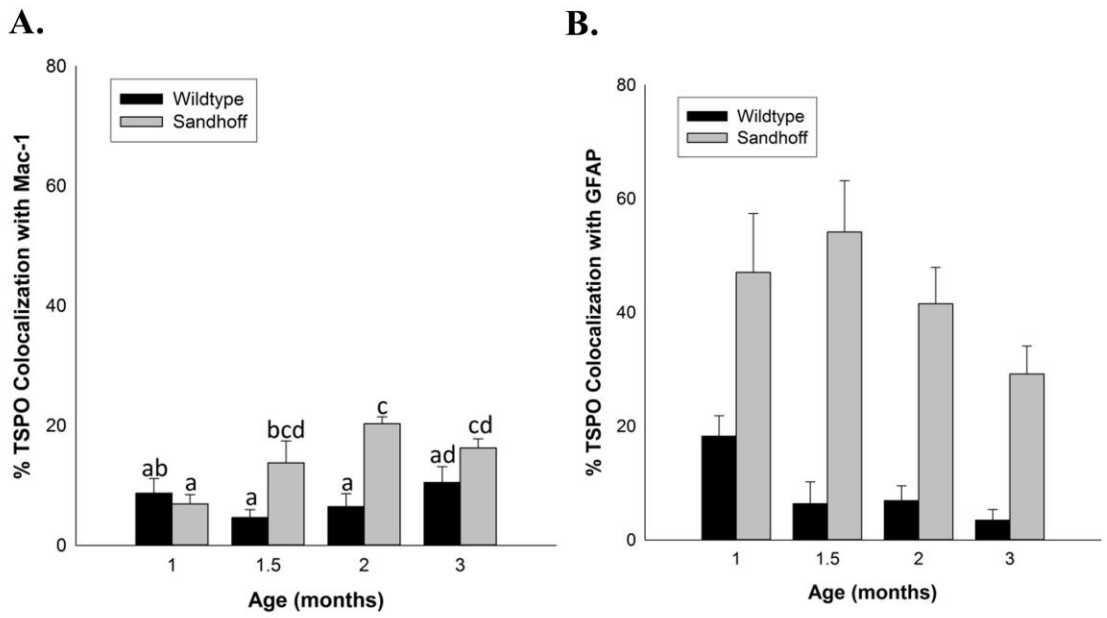

FIGURE 9. Temporal colocalization of TSPO expression with glial markers in wildtype (WT) and Sandhoff disease (SD) mice in the cerebellum. A) In the cerebellum, the percent colocalization between TSPO and Mac-1 increases with age and follows a similar pattern in both the WT and SD mice, with a more pronounced effect in the SD mice (2 way ANOVA: Age: $F_{3,26} = 2.8953$; $p = 0.062$. Genotype: $F_{1,26} = 16.433$. $p < 0.001$. Age x Genotype: $F_{3,26} = 3.778$; $p = 0.028$. 1 way ANOVA: $F_{7,26} = 5.315$; $p = 0.002$. Each value represents the mean ± SEM. n = 3 – 4) B) The percent colocalization between TSPO and GFAP differs significantly between WT and SD mice. In the SD mice, we observed high levels of colocalization beginning at 1 month and these levels of colocalization remained elevated up until 3 months of age (2 way ANOVA: Age: $F_{3,27} = 2.560$; $p = 0.084$. Genotype: $F_{1,27} = 61.830$. $p < 0.001$. Age x Genotype: $F_{3,27} = 1.315$; $p = 0.297$. Each value represents the mean ± SEM. n = 3 – 4). Within a group, bars with different letters are significantly different at $p < 0.05$.

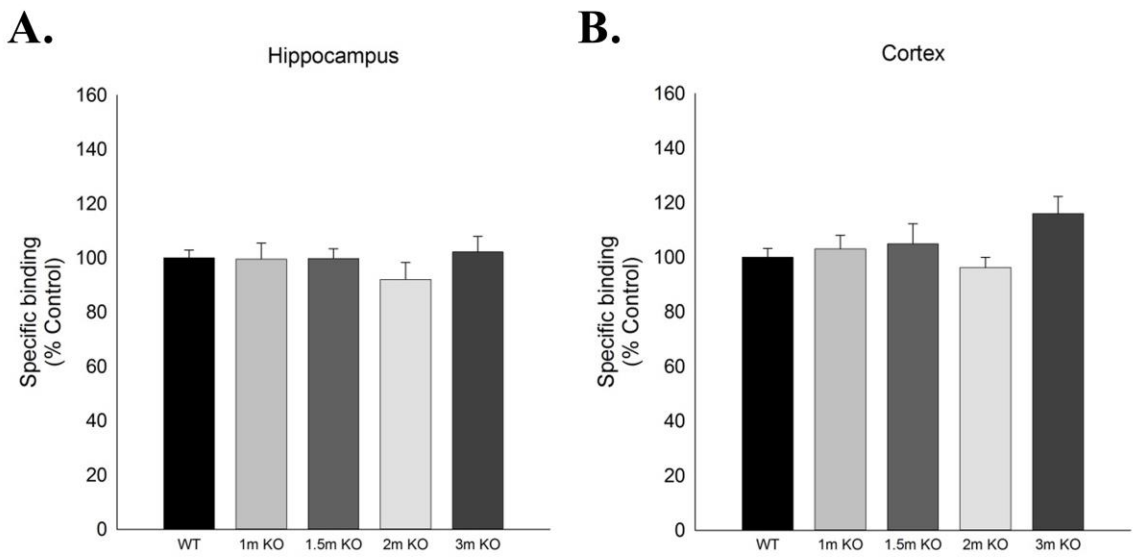

SUPPLEMENTARY FIGURE 1: TSPO levels in the hippocampus and cerebral cortex of Sandhoff disease (SD) mice using [^{3}H]-DPA-713 quantitative autoradiography. TSPO binding did not increase in the hippocampus (A; $F_{4, 62} = 0.559$, $p = 0.693$) or cortex (B; $F_{4, 60} = 1.191$, $p = 0.324$). Each value represents the mean ± SEM.

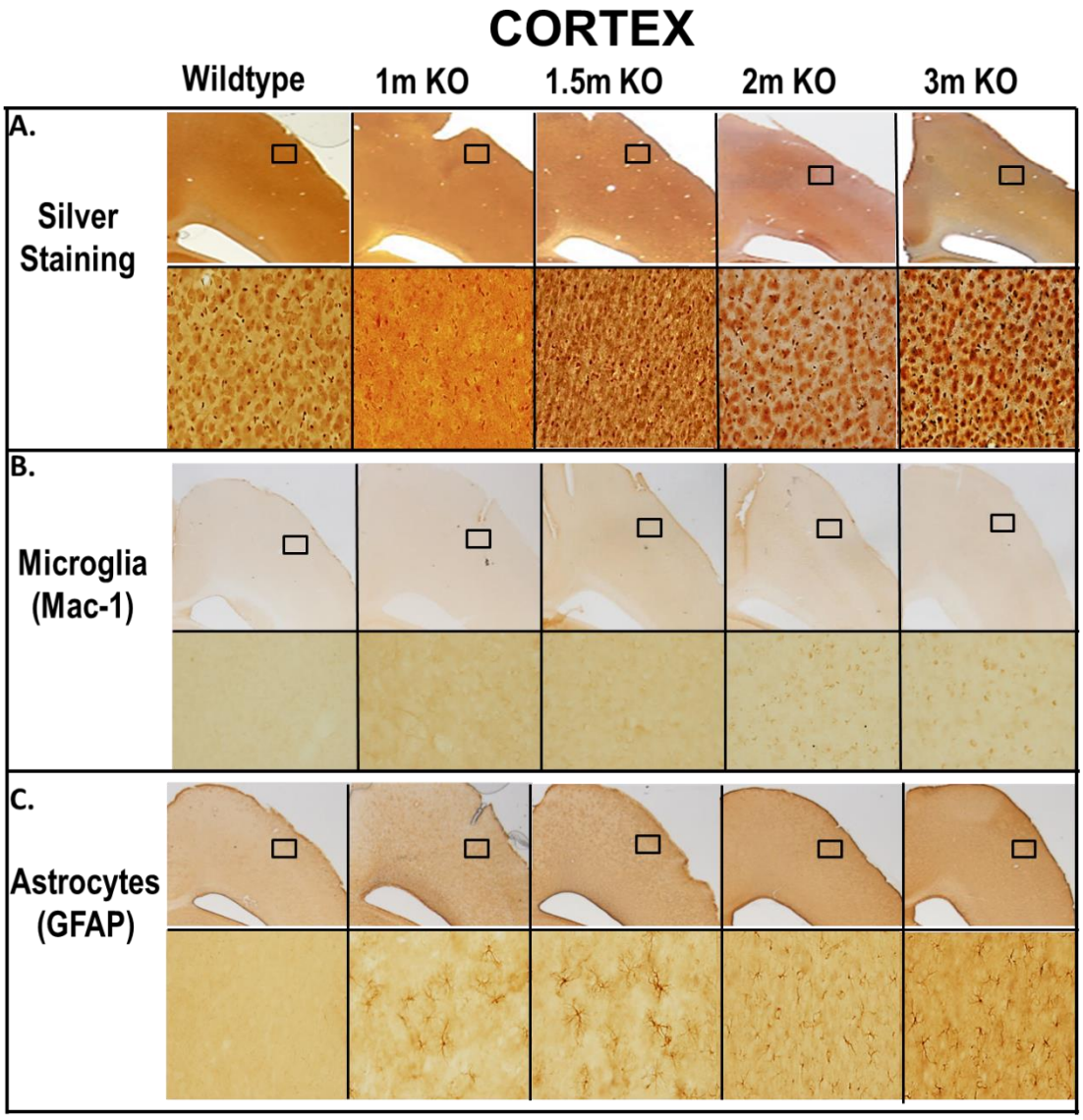

SUPPLEMENTARY FIGURE 2. Neuropathological Assessment of Sandhoff disease in the cerebral cortex. A) Representative horizontal photomicrographs of silver staining reveal slight neurodegeneration at 3 months. The top row represents low magnification images with the boxes indicating the area of which the high magnification images of the bottom row were generated. B) WT and SD mice exhibit morphologically normal microglia. Microglia activation, as indicated by Mac-1 labeling, does not appear to occur as animals age or the disease progresses. C) Activated astrocytes are observed beginning as early as 1 month of age in SD mice, and activation remains at similar levels at all ages.

REFERENCES

Boutin H, Chauveau F, Thominiaux C, Gregoire M-C, James ML, Trebossen R, Hantraye P, Dolle F, Tavitian B, Kassiou M. 2007. ^{11}C-DPA-713: A novel peripheral benzodiazepine receptor PET ligand for *in vivo* imaging of neuroinflammation. J Nucl Med 48(4):573-581.

Chen M-K, Baidoo K, Verina T, Guilarte TR. 2004. Peripheral benzodiazepine receptor imaging in CNS demyelination: functional implications of anatomical and cellular localization. Brain 127(6): 1379-1392.

Chen M-K, Guilarte TR. 2006. Imaging the Peripheral Benzodiazepine Receptor Response in Central Nervous System Demyelination and Remyelination. Toxicol Sci 91(2): 532-539.

Chen M-K, Guilarte TR. 2008. Translocator protein 18 kDa (TSPO): Molecular sensor of brain injury and repair. Pharmacol Ther 118(1):1-17.

Cosenza-Nashat M, Zhao ML, Suh HS, Morgan J, Natividad R, Morgello S, Lee SC. 2009. Expression of the translocator protein of 18-kDa by microglia, macrophages and astrocytes based on immunohistochemical localization in abnormal human brain. Neuropathol Applied Neurobiol 35(3):306-328.

Doorduin J, Klein H, Dierckx R, James M, Kassiou M, de Vries E. 2009. [^{11}C]-DPA-713 and [^{18}F]-DPA-714 as new PET tracers for TSPO: A comparison with [^{11}C]-(R)-PK11195 in a rat model of herpes encephalitis. Mol Imag Biol 11(6):386-398.

Endres CJ, Pomper MG, James M, Uzuner O, Hammoud DA, Watkins CC, Reynolds A, Hilton J, Dannals RF, Kassiou M. 2009. Initial evaluation of ^{11}C-DPA-713, a novel TSPO PET ligand, in humans. J Nucl Med 50(8):1276-1282.

Huang JQ, Trasler JM, Igdoura S, Michaud J, Hanal N, Gravel RA. 1997. Apoptotic cell death in mouse models of G_{M2} gangliosidosis and observations on human Tay-Sachs and Sandhoff diseases. Hum Mol Genet 6(11):1879-1885.

Jeyakumar M, Butters TD, Dwek RA, Platt FM. 2002. Glycosphingolipid lysosomal storage diseases: therapy and pathogenesis. Neuropathol Applied Neurobiol 28(5):343-357.

Kawashima N, Tsuji D, Okuda T, Itoh K, Nakayama K. 2009. Mechanism of abnormal growth in astrocytes derived from a mouse model of GM2 gangliosiodosis. J. Neurochem 111: 1031-1041.

Kipp M, Norkute A, Johann S, Lorenz L, Braun A, Hieble A, Gingele S, Pott F, Richter J, Beyer C. 2008. Brain-Region-Specific Astroglial Responses In Vitro After LPS Exposure. J Mol Neurosci 35:235-243.

Kuhlmann AC, Guilarte TR. 2000. Cellular and subcellular localization of peripheral benzodiazepine receptors after trimethyltin neurotoxicity. J Neurochem 74(4):1694-1704.

Kumar D, Ramanathan S, Khanna M, Palaniappan Y. Bithalamic T2 hypointensity: A diagnostic clue for Sandhoff's disease. Neurol India 2014;62:475-6.

Kyrkanides S, Miller JH, Brouxhon SM, Olschowka JA, Federoff HJ. 2005. B-heoxaminidase lentiviral vectors: transfer into the CNS via systemic administration. Mol Brain Res 133:286-298.

Kyrkanides S, Miller JH, Tallents RH, Brouxho SM, Centola G, Olschowka JA 2007. Intraperitoneal inoculation of Sandhoff mouse neonates with an HIV-1 based lentiviral vector exacerbates the attendant neuroinflammation and disease phenotype. J Neuroinflamm 188:39-47.

Kyrkanides S, Brouxhon SM, Tallents RH, Miller JH, Olschowka JA, O'Banion MK. 2012. Conditional expression of human β-hexosaminidase in the neurons of Sandhoff disease rescues mice from neurodegeneration but not neuroinflammation. J Neuroinflam 9:186.

Maeda J, Higuchi M, Inaji M, Ji B, Haneda E, Okauchi T, Zhang M-R, Suzuki K, Suhara T. 2007. Phase-dependent roles of reactive microglia and astrocytes in nervous system injury as delineated by imaging of peripheral benzodiazepine receptor. Brain Res 1157:100-111.

Maegawa GHB, Stockley T, Tropak M, Banwell B, Blaser S, Kok F, Giugliani R, Mahuran D, Clarke JTR. 2006. The natural history of juvenile or subacute G_{M2} gangliosidosis: 21 new cases and literature review of 134 previously reported. Pediatrics 118(5):e1550-1562.

Mahuran DF. 1999. Biochemical consequences of mutations causing the GM2 gangliosidoses. Biochim Biophys Acta 1455: 105-138.

Myerowitz R, Lawson D, Mizukami H, Mi Y, Tifft CJ, Proia RL. 2002. Molecular pathophysiology in Tay-Sachs and Sandhoff diseases as revealed by gene expression profiling. Hum Mol Genet, 11:1343-1350.

Ordonez A, Pokkali S, DeMarco VP, Klunk M, Mease RC, Foss CA, Pomper MG, Jain SK. 2015. Radioiodinated DPA-713 imaging correlates with bactericidal activity of tuberculosis treatments in mice. Antimicrob Agents Chemother.59(1):642-9.

Raghavendra Rao VL, Dogan A, Bowen KK, Dempsey RJ. 2000. Traumatic brain injury leads to increased expression of peripheral-type benzodiazepine receptors, neuronal death, and activation of astrocytes and microglia in rat thalamus. Exp Neurol 161(1):102-114.

Sango K, Yamanaka S, Hoffmann A, Okuda Y, Grinberg A, Westphal H, McDonald MP, Crawley JN, Sandhoff K, Suzuki K and others. 1995. Mouse models of Tay−Sachs and Sandhoff diseases differ in neurologic phenotype and ganglioside metabolism. Nature Genetics 11(2):170-6.

Saouab R, Mahi M, Abilkacem R, Boumdin H, Chaouir S, Agader O, Amil T, Hanine A. 2011. A Case Report of Sandhoff Disease. Clin Neuroradiol 21:83-85.

Tifft CJ, Proia RL. 1997. The β-hexosaminidase deficiency disorders: Development of a clinical paradigm in the mouse. Annals of Medicine 29(6):557-561.

Venneti S, Lopresti BJ, Wang G, Bissel SJ, Mathis CA, Meltzer CC, Boada F, Capuano S, Kress GJ, Davis DK, Murphey-Corb M, Trichel AM, Wisniewski SR, Wiley CA. 2004. PET imaging of brain macrophages using the peripheral benzodiazepine receptor in a macaque model of neuroAIDS. J Clin Invest 113(7):981-989.

Visigalli I, Moresco RM, Belloli S, Politi LS, Gritti A, Ungaro D, Matarrese M, Turolla E, Falini A, Scotti G, Naldini L, Fazio F, Biffi A. 2009. Monitoring disease evolution and treatment response in lysosomal disorders by the peripheral benzodiazepine receptor ligand PK11195. Neurobiol Dis 34(1):51-62.

Vowinckel E, Reutens D, Becher B, Verge G, Evans A, Owens T, Antel JP. 1997. PK11195 binding to the peripheral benzodiazepine receptor as a marker of microglia activation in multiple sclerosis and experimental autoimmune encephalomyelitis. J Neurosci Res 50(2):345-353.

Wada R, Tifft CJ, Proia RL. 2000. Microglial activation precedes acute neurodegeneration in Sandhoff disease and is suppressed by bone marrow transplantation. Proc Natl Acad Sci USA 97(20):10954-10959.

Wang H, Pullambhatla M, Guilarte TR, Mease RC, Pomper MG. 2009. Synthesis of [125I]iodoDPA-713: A new probe for imaging inflammation. Biochem Biophy Res Comm 389(1):80-83.

Wu T, Li X, Wang Q, Liu Y, Ding Y, Song J, Zhang Y, Yang Y. 2013. HEXB gene study and prenatal diagnosis for a family affected by infantile Sandhoff disease. Zehijan Da Xue Xue Bao Yi Xue Ban.42(4): 403-10.

Yamanaka S, Johnson ON, Norflus F, Boles DJ, Proia RL. 1994. Structure and expression of the mouse β-hexosaminidase genes, Hexa and Hexb. Genomics 21(3):588-596.

Yun Y, Lee S. 2005. A Case Report of Sandhoff Disease. Korean J Ophthalmol 19:68-72.

Chapter 3: TSPO-ligand induced ROS production in primary microglia: experimental evidence supporting NADPH oxidase

ABSTRACT

Translocator protein 18 kDa (TSPO) is a biomarker of brain inflammation and injury that is used in preclinical and clinical studies. However, there is a lack of knowledge on TSPO function in glial cells, the brain cells that express and upregulate TSPO as a result of injury. We previously demonstrated that TSPO ligands (TSPO-L) (1-100 nM) induced intracellular ROS production which was abrogated by NADPH oxidase (NOX2) inhibitors, thereby indicating an association between TSPO and NOX2.

In the present study, we aimed to further investigate the cellular source of ROS production from TSPO-ligand exposure in microglia. TSPO-L exposure (1-100 nM) increased extracellular superoxide production that was abrogated by an NADPH oxidase inhibitor. Furthermore, co-exposure of primary microglia to an activator of NADPH oxidase (PMA) with TSPO-L enhanced extracellular superoxide production compared to vehicle-treated and PMA treated microglia, thereby indicating a positive (additive) relationship between TSPO and NOX2. Neither intracellular nor extracellular TSPO-L induced ROS production was inhibited by the mitochondrial permeability transition pore inhibitor cyclosporine A suggesting that the source of ROS production was not from mitochondria. These findings were further confirmed using MitoSOX, a mitochondrial superoxide specific assay. Finally, we examined the effect of TSPO-L exposure on the redox sensitive transcription factor, nuclear factor erythroid 2 related factor (Nrf2). We discovered that TSPO-L exposure induced Nrf2 translocation from the cytosol into the nucleus, providing supporting evidence for the activation of Nrf2 and for the induction of cytoprotective genes that help maintain microglia redox homeostasis.

1. INTRODUCTION

Translocator protein 18 kDa (TSPO) has a several decade history as a biomarker of brain inflammation and injury (Chen & Guilarte 2008; Papadopoulos et al 2006; Liu et al 2014). However, the function of TSPO is currently under debate as recent studies using TSPO knockout mice have raised significant questions about TSPO's traditionally ascribed function of translocating cholesterol into the mitochondria as the first step in steroidogenesis (Tu et al 2014; Morohaku et al 2014; Banati et al 2014; Fan et al 2015; Papodopoulos et al 1997). Here, we focus on the function of TSPO in microglia, one of the brain cell types that expresses and upregulates TSPO as a result of brain injury.

Microglia, the resident central nervous system (CNS) macrophages, perform several physiological functions including surveilling the brain to maintain brain homeostasis (Haslund-Vinding et al 2016; Vildhardt et al 2017). With brain injury, microglia assume an activated phenotype which can vary depending on the nature and timing of the insult. These activated phenotypes range across a continuum of morphological and molecular changes (Town et al 2005; Vilhardt et al 2017). As phagocytic cells, microglia express high levels of NADPH oxidase which serve to produce a superoxide burst. The function of this superoxide burst is two-fold. First, the superoxide can destroy phagocytized matter and enable microglia's role in host defense and anti-microbial functions. Secondly, this superoxide burst can be used by redox signaling circuits that contribute to the activation of microglia and the maintenance of brain redox homeostasis (Finkel et al 2011; Brieger et al 2012; Holmstrom and Finkel 2014; Haslund-Vindig et al 2016; Vilhardt et al 2017).

Our laboratory has previously demonstrated that physiologically relevant concentrations of TSPO-ligands (TSPO-L) induce microglia functions consistent with an activated state (Choi et

al., 2011). This includes increased phagocytosis, ROS production, and cytokine release. In particular, the increase of intracellular ROS was abrogated with two different NOX inhibitors, apocynin and DPI, indicating an association between TSPO and NADPH oxidase. As TSPO has previously been associated at the outer mitochondrial membrane with VDAC (McEnery et al 1992; Gatliff et al 2014), we wanted to confirm the cellular source of ROS production. There are various potential sources of ROS within the cell including mitochondria, peroxisomes, and several enzymes such as xanthine oxidase, nitric oxide synthetase, p450 cytochromes, and NADPH oxidase. (Brieger et al 2012). Previous studies have suggested a role of TSPO in ROS production in several types of cells (Zeno et al 2009; Veenman et al 2008, Gatliff et al 2014; Gatliff et al 2017; Joo et al 2012; Banfi et al 2004). Here we provide additional support to the initial observation that ROS production induced by exposure to TSPO ligands in microglia is a result of activation of NADPH oxidase. Further, ROS production and activation of NADPH oxidase through exposure to TSPO ligands will also activate cellular processes involved in maintaining redox homeostasis, such as nuclear factor erythroid 2 related factor (Nrf2), a transcription factor that maintains redox homeostasis by translocating to the nucleus to bind to the antioxidant response element and induce the transcription of a battery of antioxidative and cytoprotective genes.

2. MATERIALS & METHODS

2.1 Primary rat microglia cell culture. Primary mixed glial cell cultures were prepared using a modified version of the glial culture technique as previously described (Giulian and Baker, 1986 and Choi et al 2011). Brains from PN1-3 Sprague Dawley rat pups (Harlan, Indianapolis, IN) were dissected, meninges removed and cortices isolated. Tissue was dissociated by trypsination (2.5% trypsin at 37°C for 30 minutes), trituration, and filtration through 40 μm cell strainers. Cells were centrifuged at 400 xg for 10 minutes, resuspended, and plated onto 75 cm2 poly-L-lysine coated

culture flasks in Dulbecco's modified Eagle's medium (DMEM)/F12 (Invitrogen, Carlsbad, CA) containing 10% heat-inactivated fetal bovine serum (FBS) (Hyclone, Logan, UT), 100 U of penicillin, and 100 μg of streptomycin (Invitrogen). Cultures were maintained at 37°C in a humidified chamber of 95% air/5% CO2 for 12-14 days when the glial cultures reached confluency. Microglia were extracted from the glial cultures by shaking the flasks for 3 hours at 200 r.p.m. at 37°C and were collected as floating cells in the media. After centrifugation (400 xg for 10 minutes), cell viability was determined by trypan blue exclusion, and cells were plated according to the assay being tested. Non-adherent cells were removed 20 minutes after plating by changing the culture medium to DMEM:F12 containing 2% FBS. Adherent cells were incubated overnight before being used for experiments. More than 95% of the adherent cells were positive for microglia-specific marker Mac-1 (Chemicon, Billerica, MA) as determined by immunostaining. The animals used for this study had been treated humanely as all the animal studies were reviewed and approved by the Columbia University Medical Center Animal Care and Use Committee.

2.2 J774 Macrophages. Mouse macrophage J774 cells lines were maintained in RPMI media with 10% FBS and 1% (vol/vol) penicillin-streptomycin.

2.3 Treatments. (R)-PK11195 (Advanced Biochemical Compounds, Radeberg, Germany), Ro5-4864 (Sigma-Aldrich, St. Louis, MO), and cyclosporine A (Sigma-Aldrich, St. Louis, MO) were dissolved in 100% ethanol. Stock solutions were diluted in ethanol appropriately such that equal amount of ethanol was added to each treatment containing DMEM:F12 medium containing 2% FBS. Equal amount of ethanol was added to vehicle as control. The percent of ethanol used for treating the cells was less than 0.1%.

Phorbol-12-myristate 13-acetate (PMA), apocynin, rotenone (Rot), and sulforaphane (SF) were dissolved in dimethyl sulfoxide (DMSO), all from Sigma-Aldrich, St. Louis, MO. All stocks were then diluted in DMSO so that an equal amount of DMSO was added to each treatment containing 2% FBS. Equal amount of DMSO was added to vehicle as control. The percent used for treating cells was less than 0.05%. Bacterial lipopolysaccahride (LPS), was dissolved in phenol red free media. Microglia were exposed to 10 nM of PK or Ro; 500 nM of rotenone; 1 mM of sulforaphane; 100 ng/mL of LPS; 100 ng/mL of PMA; and 1mM of apocynin for time of exposure indicated before testing for various assays.

2.4 Immunocytochemistry. 300Kmicroglia were plated onto glass coverslips in a 6 well plate (Corning, Corning, NY). Cells were treated as specified above. Immunocytochemistry was performed via conventional techniques before being incubated in primary antibody rabbit-anti Nrf2 (Santa Cruz 1:200) overnight at 4°C. Briefly, cells were fixed with 4% paraformaldehyde for 20 minutes; washed with 1X phosphate buffered saline (PBS); permeabilized with 0.2% Triton for 10 minutes; washed; and blocked for 1 hour with 10% normal goat serum (Vector Laboratories, Burlingame, CA). After primary antibody incubation and three 5 minute washes, cells were incubated with appropriate Alexa Fluor secondary antibodies (Invitrogen; 1:500) for 1 hour. Cells were mounted with Prolong with DAPI (Invitrogen) to counterstain for cell nuclei.

2.5 Measurement of Reactive Oxygen Species (ROS).

2.5.1 Extracellular ROS was determined by measuring the super oxide dismutase (SOD) inhibitable reduction of cytochrome C. Cytochrome c (Sigma-Aldrich, St. Louis, MO) that was added exogenously. Due to its size, cytochrome c cannot pass through the cell membrane. The exogenous cytochrome c is then reduced by any extracellular superoxide. This produces

ferrocytochrome c, whose absorbance is detected at 550 nm and measured via a plate reader. Cells were incubated for 1 or 24 hours at 37°C in HBSS containing 100 μM cytochrome c in the presence or absence of SOD (600 U/mL) (Sigma-Aldrich, St. Louis, MO). The level of extracellular ROS produced was calculated as the difference in the absorbance observed between the absence and presence of SOD in each treatment, and the results were expressed as the percentage of the vehicle-treated control.

2.5.2 Intracellular ROS was measured using the dichlorofluorescein diacetate (DCF-DA) assay (Molecular Probes, Eugene, OR). DCF-DA readily crosses the cell membranes and is hydrolyzed by intracellular esterases to a non-fluorescent DCF. After oxidation by ROS, DCF-DA is converted to the highly fluorescent dichlorofluorescein, which is detectable using a fluorescent plate reader. 50,000 microglia/well were plated onto a 96-well plate. Cells were incubated for 30 minutes at 37°C in HBSS containing 10 μM DCF-DA. The fluorescence was measured at 485 nm excitation and 530 nm emission with background values subtracted.

2.5.3 Mitochondrial superoxide was measured using MitoSOX Red (Molecular Probes). MitoSOX crosses cell membranes and is targeted to actively respiring mitochondria due to its cationic tryphenylphosphonium substituent. Oxidation of MitoSOX by superoxide results in 2-hydroxyethidum whose fluorescence is measured by a plate reader. 50,000 microglia/well were plated onto a 96-well plate. Cells were incubated for 10 minutes at 37°C in HBSS containing 1 μM MitoSOX Red. The fluorescence was measured at 396nm excitation and 580 nm emission with background values subtracted.

2.6 Immunofluorescence Imaging and Analysis. All coverslips were imaged at 40x magnification with a single point laser scanning confocal microscope (Zeiss LSM 510-Meta) using LSM software at CUMC Microscope Facility. All images within an experiment were taken the same day, using

the same scanning parameters with at least 120 cells counted per condition per experiment. Confocal stacks were then projected into single images. All analyses after image acquisition were performed using Metamorph Offline (Molecular Devices) and integrated intensity was measured.

2.7 Western Blot. J774 macrophages were lysed in radioimmunoprecipitation assay buffer (15 mM NaCl; 50 mM Tris; 5 mM EGTA; 1% Triton; 5% deoxycholate; and 20% SDS. Polyvinylidene fluoride (PVDF) membranes were incubated with the following primary antibodies: 1:1000 TSPO (Abcam ab109497) and 1:10,000 actin (Santa Cruz, sc-1616) in LICOR blocking solution overnight at 4 C. After incubation with corresponding IRDye dye-labeled secondary antibodies (LI-COR) and appropriate washing, membranes were visualized with the Odyssey Infrared Imaging system. Integrated intensity of the protein of interest was normalized to actin levels from the same blot and sample.

2.8 Statistical analysis. Values are expressed as mean ± standard error of the mean (SEM). Each group consisted of three to four independent trials (experiments) for each concentration studied. A one-way ANOVA was used to determine treatment effect followed by Tukey's post-hoc analysis unless otherwise stated.

3. RESULTS

3.1 Extracellular Superoxide Production

3.1.1 With a NADPH oxidase inhibitor

To further explore the relationship between TSPO-ligand exposure and ROS production in microglia, we measured extracellular TSPO-L-induced superoxide production. Consistent with our previous finding (Choi et al.2011), we found that exposure to 10 nM (R)PK-11195 or 10 nM Ro5-4864 resulted in increased extracellular superoxide production, that could be abrogated with the

NADPH oxidase inhibitor apocynin (1mM) (Figure 1A, LPS: t=2.625; p=0.0342. PK: $F_{(2,12)}$=6.543, p=0.015. Ro: $F_{(2,13)}$=5.475; p=0.019. n=3-6 independent experiments). These results provide further supporting evidence that the source of TSPO-L induced ROS production in microglia is from NADPH oxidase, a finding that is consistent across both rat microglia and mouse macrophages (See Results, Section 3.5).

3.1.2 With a NADPH oxidase activator

In addition to blocking NADPH oxidase (NOX2), we activated NADPH oxidase using phorbol 12-myristate 13-acetate (PMA). PMA activates NOX2 through stimulation of Protein kinase C (PKC) and induces a respiratory ROS burst (Cox et al 1985). Exposure to 100 ng/mL of PMA for 1 hour produced a robust increase in extracellular superoxide production, and co-exposure with PMA and either 10 nM of (R)PK-11195 or 10 nM Ro5-4864 enhanced extracellular superoxide production compared to vehicle treated and PMA treated microglia (Figure 1B, PK: $F_{(2,6)}$=122.3, p<0.001. Ro: $F_{(2,6)}$=175.0; p<0.001). This data also suggests a relationship between NADPH oxidase and TSPO-L induced ROS production. That is, upregulation of NOX2 enhances TSPO-L extracellular superoxide production and inhibiting NOX2 blocks TSPO-L extracellular superoxide production.

3.2 Mitochondrial Superoxide production

3.2.1 Cyclosporine A

Previous studies indicate that TSPO is localized at the outer mitochondrial membrane, and has been shown to be associated with VDAC, another outer mitochondrial membrane protein (McEnery et al 1992; Gatliff et al 2014). Therefore, we needed to assess if ROS were originating from the mitochondria, particularly given that the mitochondria are a well-documented source of ROS (Brieger et al 2012; Holmstrom and Finkel 2014) and given the question as to the role of

TSPO in the mitochondrial permeability transition pore (mPTP) (Sileikyte et al 2010, 2011, and 2014; Gatliffe et al 2012). To begin to address the involvement TSPO-L induced ROS in mPTP, we used a mitochondrial permeability transition pore inhibitor, cyclosporine A. Co-exposure of TSPO-ligands with cyclosporine A for 24 hours did not inhibit extracellular superoxide production (Figure 2A, PK: $F_{(2,6)}$=10.73. p=0.010. Ro: $F_{(2,8)}$=6.12; p=0.024) or intracellular ROS production (Figure 2B, PK: $F_{(2,6)}$=13.86. p=0.006. Ro: $F_{(2,6)}$=9.95; p=0.012). Taken together, these data indicate that the mitochondria are not the source of TSPO-L induced ROS at 24 hours.

3.2.2 MitoSOX

We next measured mitochondrial superoxide production using MitoSox in a time course study to rule out the possibility that we may not have been capturing the appropriate time point of a mitochondrial superoxide increase. We used the MitoSOX assay to measure mitochondrial superoxide production at 2, 4, 8, 18, and 24 hours of 10 nM of TSPO-L, (R)PK-11195 and Ro5-4864. We also used antimycin A (complex III inhibitor, 2uM) and rotenone (complex I inhibitor, 500 nM) as positive controls for mitochondrial superoxide production. At all time-points examined, TSPO-L did not induce a significant increase in mitochondrial superoxide, whereas the electron transport chain inhibitors antimycin A and rotenone increased mitochondrial superoxide levels at all time points examined compared to vehicle treated cells (2hrs: $F_{(4,13)}$=6.164; p=0.005. 4hrs: $F_{(4,15)}$=8.940; p=0.001. 8hrs: $F_{(4,11)}$=3.430; p=0.047. 18hrs: $F_{(4,10)}$=4.929; p=0.019. 24hrs: $F_{(4,23)}$=4.561; p=0.007. n = 3-6 independent experiments per time point). This data further supports our hypothesis that TSPO-L induced ROS do not originate from the mitochondria.

3.4 Nrf2 translocation from cytosol to nucleus as a measure of Nrf2 activation

Microglia are one of several cell types that use ROS as signaling molecules (Vilhardt et al 2017). In order to maintain redox homeostasis, cells use ROS to initiate feedback loop mechanisms in order to induce various antioxidant responses (Holmstrom and Finkel et al 2014; Brieger et al 2012; Rastogi et al 2017; Hoffmann and Griffiths 2018). One such antioxidant response regulator is nuclear factor erythroid 2 related factor 2 (Nrf2). Nrf2 is a transcription factor that is found in the cytosol under basal conditions. In the cytosol, Nrf2 is bound to Keap1 to regulate its activity. Under conditions of oxidative stress, the cysteine residues are modified so that Keap1 releases Nrf2 (Dinkova-Kostova et al 2002; Niture et al 2009; Niture et al 2014; Levonen et al 2004; Ma et al 2013), exposing Nrf's nuclear localization signal (NLS), and translocates to the nucleus to bind the antioxidant response element (ARE) in a battery of Nrf2-responsive antioxidant genes. Previous studies have shown that NOX2 activity is an upstream and essential regulator in Nrf2/Keap1 signaling (Sekhar et al 2003). Therefore, we hypothesized that given TSPO-L may induce the translocation of Nrf2 to the nucleus as a cellular response to counter the increase in ROS production. Primary microglia exposed to physiologically relevant concentrations of (R)PK-11195 or Ro5-4864 (1, 10, 100 nM) resulted in a statistically significant increase in the percentage of Nrf2 in the nucleus relative to vehicle treated cells ($F_{(8,1602)}=19.774$; $p<0.0001$). Interestingly, Ro5-4864 induced higher levels of nuclear Nrf2 translocation as compared to (R)PK-11195 at all doses examined, indicating differential potency of these ligands. We used sulforaphane as our positive control as it is a known Nrf2 activator (Zhao et al 2007) in microglia (Dang et al 2012; Brandenburg et al 2010). Our results suggests that the binding of TSPO-L to TSPO may be a signal for the production of NOX2-dependent ROS production that can then induce Nrf2 translocation and activate ARE target genes to mount a response to increased oxidative stress.

3.5 ROS levels and TSPO protein expression

To explore the relationship between ROS production and TSPO protein expression and the time course of an increase in ROS compared to an increase TSPO protein, we used the mouse macrophage cell line J774. Both macrophages and microglia are myeloid in origin (Salter and Begg, 2014; Butovsky et al 2014; Hickman et al 2013), respond to inflammatory insults, and are capable of chemotaxis and pathogen engulfment (Lam et al 2009). Additionally this macrophage cell line is a well-established model system in cell biology and immunology (Ralph et al 1975; Ralph et al 1977; Unkeless et al 1979; Kant et al 2002) due to the fact that these macrophages can be easily maintained and genetically manipulated (Lam et al 2009).

Importantly, the TSPO antibody (Abcam ab109497) our lab has validated through multiple methods (siRNA knockdown in HEK293T cells; shRNA knockdown in J7774 cells; brain tissue from TSPO wildtype, heterozygous, and knockout animals; and primary mouse microglia and primary rat microglia) only reacts with human and mouse TSPO, and not rat TSPO (data not shown). Therefore, we used a mouse macrophage cell line instead of primary rat microglia for these preliminary studies as J774 cells are cells known to express and upregulate TSPO (Pomper et al 2016, patent # US 9,498,546 B2). Similar to our findings in microglia, exposure to TSPO-L or LPS for 24 hours increased both extracellular and intracellular ROS production (S. Figure 1B and 1D). We also examined a 3-hour time point, and we observed an increase in extracellular ROS production at all TSPO-L exposures examined (S. Figure 1A), and an increase in intracellular ROS production with 100 nM (R)-PK, 10 nM Ro, and 100 nM Ro (S. Figure 1C). LPS exposure also increased both extracelullar and intracellular ROS levels at 3 hours.

We next examined TSPO protein levels at 3 and 24 hours in both control and LPS treated macrophages. At 3 hours, TSPO/actin ratios were comparable in Western blot (S. Figure 2). This

was in contrast to the increase in extracellular and intracellular ROS seen at 3 hours. At 24 hours, TSPO/actin ratio was increased 60% in LPS treated macrophages as compared to control macrophages (S. Figure 2), a time when ROS levels are also elevated both intracellularly and extracellularly

4. DICUSSION

In this study, we used two prototypical and specific TSPO ligands, (R)-PK11195 (PK) and Ro5-4864 (Ro) to examine their effect on ROS production in primary microglia. Consistent with our previous study (Choi et al 2011), both PK and Ro increased extracellular ROS production (Figure 1A) at concentrations consistent with their affinity for TSPO (in the nM range). Additionally, co-exposure of microglia to a NADPH oxidase inhibitor, apocynin, abrogated the TSPO-L induce increase in ROS production. Apocynin is a NOX2 inhibitor which acts by preventing the migration of the $p47^{phox}$ subunit to the membrane bound subunits of NOX2, thereby preventing assembly of the active NOX2 complex (Rastogi et al 2017; Stolk et al 1994). It has been noted that apocynin is not specific to NOX2, and that other isoforms of NOX which include the $p47^{phox}$ subunit in the NOX complex will also be affected, notably, the structurally homologous subunit NOXO1 in NOX1 (Rastogi et al 2017). However, the presence of NOX1 in microglia is mixed across the literature with some studies detecting NOX1 gene or protein expression (Savchenko et al 2013), and other studies stating that microglia do not have NOX1 in murine cortical microglia (Vilhardt et al 2017). However, regardless of the isoform of NOX affected, TSPO-L still increase ROS production that is most likely derived from an isoform of NOX, as it can be abrogated by a NOX inhibitor. Additional studies confirming NOX activity induced by TSPO-L exposure will be critical in both wildtype and $gp91^{phox}$ knockout mice.

It has been previously suggested that increased production of ROS by these two TSPO-specific ligands may not only be from NADPH oxidase but also from mitochondria (Choi et al 2011). More specifically some studies have suggested that activation of TSPO can lead to increased ROS production by mitochondria via modulation of the proton pump provided by the FO unit of ATP(synth)ase (Veenman et al., 2008, 2010; Zeno et al., 2009). Still, our results are consistent with a growing body of literature that TSPO ligands increase ROS production in microglia and other cell types (Jayakumar et al., 2002). Additionally, we provide evidence that in microglia the source of ROS is not mitochondrial as indicated by the cyclosporin A and MitoSOX studies. This contributes to the growing number of studies which have challenge the involvement of TSPO in the mitochondrial permeability transition pore-associated process (Sileikyte et al 2014; Kokoszka et al 2004; Krauskopf et al 2006; Baines et al 2007 and 2018; Bernardi et al 2013;)

It is currently unknown exactly how TSPO-L induce functions consistent with an activated state in microglia, and therefore, also unclear how TSPO-L exposure results in an increase in ROS production. Previously, we have suggested that the TSPO-NOX2 interaction produces ROS which in turn causes an activation of Nrf2 to activated downstream antioxidative gene to maintain redox homeostasis. Here we confirm that 24-hour TSPO-L exposure induces Nrf2 nuclear translocation, though it remains to be confirmed which anti-oxidant genes are upregulated in microglia. Preliminary data from our lab suggests that in primary rat microglia, 24-hour exposure to Ro, but not PK, induce heme oxygenase 1 (HO-1) expression, one of several Nrf2-dependent antioxidant genes that functions to degrade heme. This would again indicate differential molecular signaling pathways of how Ro and PK exert varying effects on not only pro-inflammatory genes and cytokine release (Choi et al 2011), but also in cytoprotective genes such as HO-1. Here, the

induction of Nrf2 translocation was consistent across both ligands, although Ro induced greater levels of Nrf2 translocation into the nucleus as compared to PK.

Additionally, our data obtained in the J7774 macrophage cell line indicates that the LPS induced increase in ROS production, seen at 3 hours, precedes the increase in TSPO protein expression, seen by 24 hours (S. Figure 1 and 2). It is possible the increase in ROS seen at 3 hours, activates Nrf2 (Figure 4) whose translocation is observed by 24 hours. Nrf2 may initially induce expression of anti-oxidant genes. However, after sustained exposure to LPS or TSPO-L, and therefore prolonged exposure to ROS levels (elevated ROS levels are still seen at 24 hours), other transcription factors may also be activated in addition to Nrf2. For example, Novo and Parola (2008), propose a model in which at low levels of ROS exposure Nrf2 is translocated into the nucleus to induce an antioxidant response; at intermediate levels of ROS, either NF-kB can be translocated into the nucleus for a pro-inflammatory and adaptive response or AP-1 can be activated for an anti-apoptotic and survival response; and at high levels of ROS, the cell can die either through induction of apoptosis or irreversible cell injury that results in death. It is possible that after 24 hours of exposure to LPS, the macrophages are beginning to or have already transitioned to the recruitment of other transcription factors such as NF-kB and AP-1. Multiple studies have shown that LPS exposure in microglia increases NF-kB and AP-1 protein expression at time points earlier than 24 hours (Zhao et al 2011; Kang et al 2004; Chen et al 2005). Thus, in cases where TSPO becomes upregulated in pathological conditions, the ROS levels have overwhelmed the anti-oxidant response system and this is why we see activation of additional transcription factors such as NF-kB and AP-1, and ultimately upregulation of TSPO protein levels in response to inflammatory agents such as LPS. Using TSPO-L concentrations consistent with their affinity is more reflective of what is happening in physiological, non-activated conditions.

Further studies examining the time course of the activation of various transcription factors will be useful in further characterizing the activation of microglia by TSPO-L. Additionally, studies examining ROS levels and TSPO levels within the same cell as can be done via flow cytometry will help further elucidate the relationship between TSPO and NADPH oxidase derived ROS in microglia.

Taken together, our findings suggest that the binding of PK or Ro to TSPO in microglia induces ROS production that is NADPH oxidase dependent as ROS levels can be abrogated with NADPH oxidase inhibitors and upregulated through co-exposure of NADPH oxidase activators and TSPO-L. The source of ROS appears to be from NADPH oxidase and not from the mitochondria indicating a relationship between TSPO and NADPH oxidase in microglia. We provide supporting evidence for TSPO-L's induction of Nrf2 translocation and may play a role in initiating cellular mechanisms to help maintain redox homeostasis.

A. **B.**

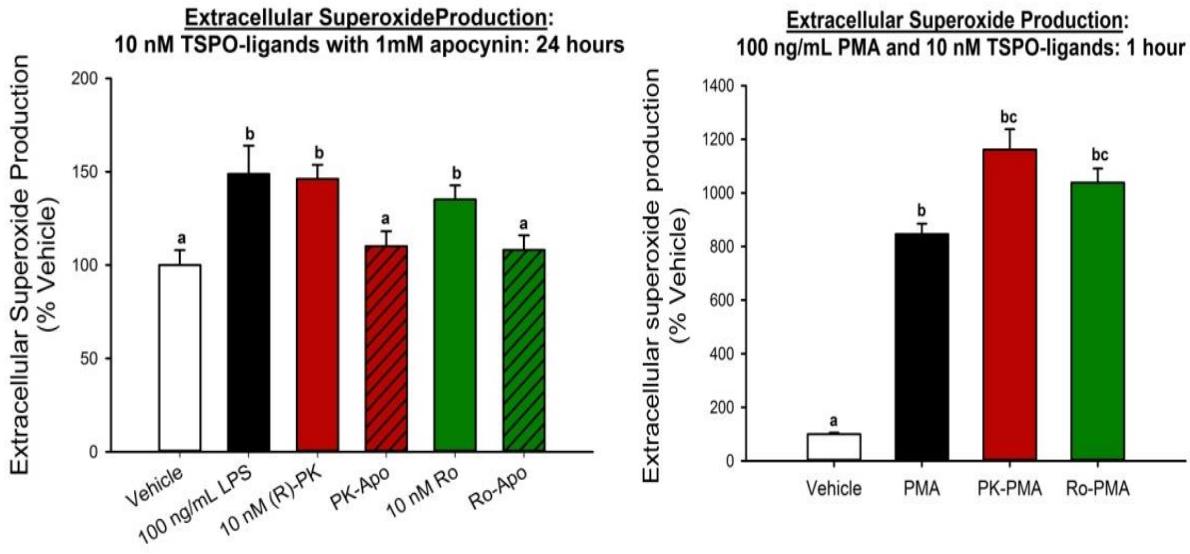

FIGURE 1: TSPO ligands & extracellular ROS production.

A) TSPO-L induced NADPH oxidase-dependent extracellular ROS production. Primary microglia were exposed to (R)-PK11195 (10 nM), Ro-5-4864 (10 nM) or LPS (100 ng/mL) for 24 hrs with or without the NADPH oxidase inhibitor apocynin (1mM). The level of extracellular ROS production was compared to vehicle-treated microglia. Exposure to TSPO-L increased the level of extracellular ROS production, and this effect was mitigated by the NADPH oxidase inhibitor, apocynin (1 mM) (LPS: $t=2.625$; $p=0.0342$. PK: $F_{(2,12)}=6.543$, $p=0.015$. Ro: $F_{(2,13)}=5.475$; $p=0.019$). Data are normalized to vehicle and expressed as mean ± s.e.m. n = 3-6 independent experiments. Bars with different letters are significantly different at $p < 0.05$.

B) Co-exposure of TSPO-L and phorbol 12-myristate 13-acetate (PMA) produced increased levels of extracellular ROS production in primary microglia. Co-exposure of 10 nM TSPO-L with PMA (100 ng/mL for 1 hour), a NADPH oxidase activator, enhanced extracellular ROS production compared to vehicle-treated and PMA-treated microglia (n=3; PK: $F_{(2,6)}=122.3$; $p<0.0001$; Ro: $F_{(2,6)}=175.0$; $p<0.0001$). TSPO-L enhance the effects of NADPH oxidase activation supporting a relationship between TSPO and NADPH oxidase. Data are normalized to vehicle and expressed as mean ± s.e.m. n = 3 sets of independent experiments. Bars with different letters are significantly different at $p < 0.05$.

N.B. Experiments in this figure completed by Dr. Judy Choi

A. **B.**

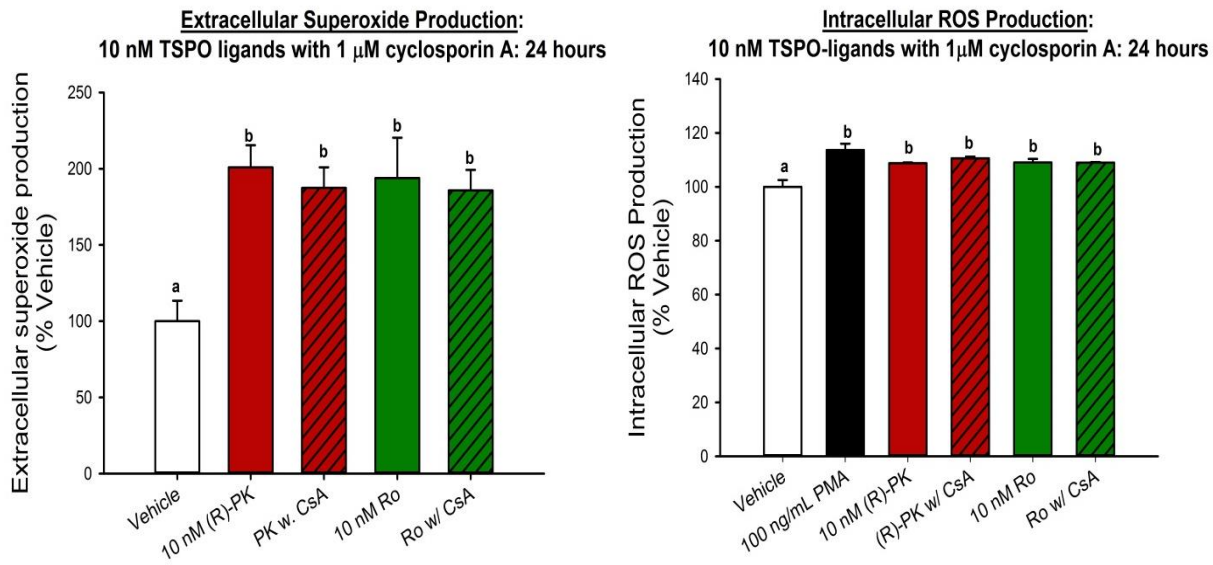

<u>FIGURE 2</u>: TSPO ligands induce extracellular and intracellular ROS production that cannot be inhibited by the mitochondrial permeability transition pore inhibitor, cyclosporin A. TSPO-L induced ROS production was not inhibited by cyclosporine A (1 μM for 24 hours), neither extracellularly (A, n=3-4; <u>PK</u>: $F_{(2,6)}$=10.73; p=0.0104; <u>Ro</u>: $F_{(2,8)}$=6.12; p=0.0244) nor intracellularly (B), n=3; <u>PK</u>: $F_{(2,6)}$=13.86; p=0.0056; <u>Ro</u>: $F_{(2,6)}$=9.945; p=0.0124), indicating that the source of ROS is not from the mitochondria. Data are normalized to vehicle and expressed as mean ± s.e.m. n = 3-6 sets of independent experiments. Bars with different letters are significantly different at $p < 0.05$.

N.B. Experiments in this figure completed by Dr. Judy Choi

A. **B.**

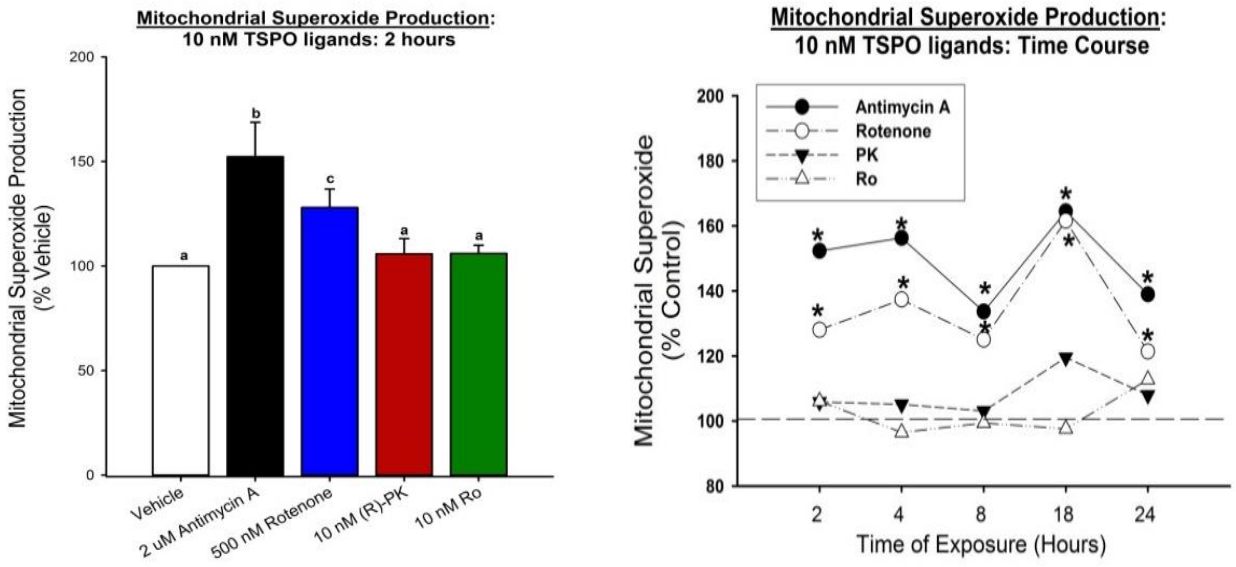

FIGURE 3: TSPO ligands do not increase mitochondria-dependent superoxide production. A) Exposure (2 hrs) of microglia to physiologically relevant (10 nM) concentrations of TSPO-L did not produce an increase in mitochondrial superoxide, whereas mitochondrial electron transport chain inhibitors antimycin A (2 μM) (AA) and rotenone (500 nM) (Rot) produced an enhanced mitochondrial-ROS response. Bars with different letters are significantly different from each other at $p < 0.05$. Data are expressed as the mean ± SEM of 3-4 independent experiments.
B) Time-course of mitochondria-dependent ROS production in primary microglia. TSPO-L did not produce an increase in mitochondrial superoxide at any of the time points examined (2, 4, 8, 18, or 24 hours), whereas mitochondrial electron transport chain inhibitors antimycin A and rotenone produced statistically significant increases in mitochondrial superoxide at all time points examined. (2hrs: $F_{(4,13)}=6.164$; $p=0.005$. 4hrs: $F_{(4,15)}=8.940$; $p=0.001$. 8hrs: $F_{(4,11)}=3.430$; $p=0.047$. 18hrs: $F_{(4,10)}=4.929$; $p=0.019$. 24hrs: $F_{(4,23)}=4.561$; $p=0.007$. n = 3-6 independent experiments per time point) *$p<0.05$ compared to vehicle-treated microglia which is represented by the dashed lines. Data are expressed as the mean ± SEM of 3-6 independent experiments.

FIGURE 4

A.

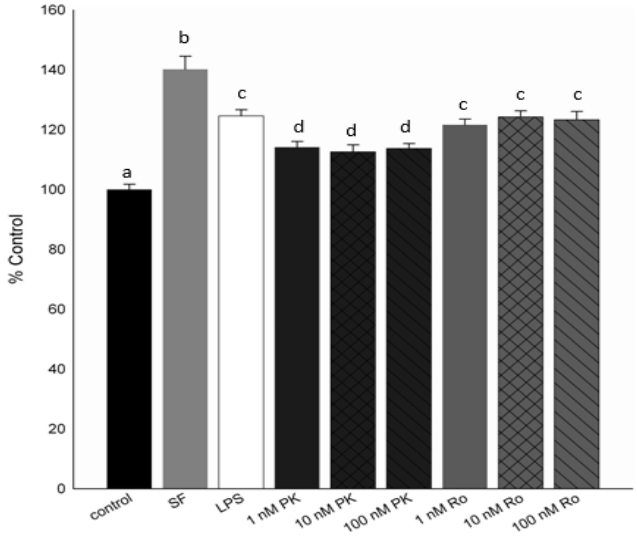
% Control
160
140
120
100
80
60
40
20
0
a
b
c
d
d
d
c
c
c
control
SF
LPS
1 nM PK
10 nM PK
100 nM PK
1 nM Ro
10 nM Ro
100 nM Ro

B.

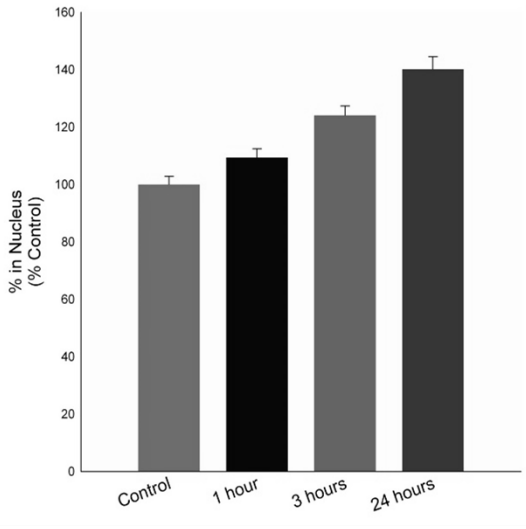
% in Nucleus
(% Control)
160
140
120
100
80
60
40
20
0
Control
1 hour
3 hours
24 hours

C.

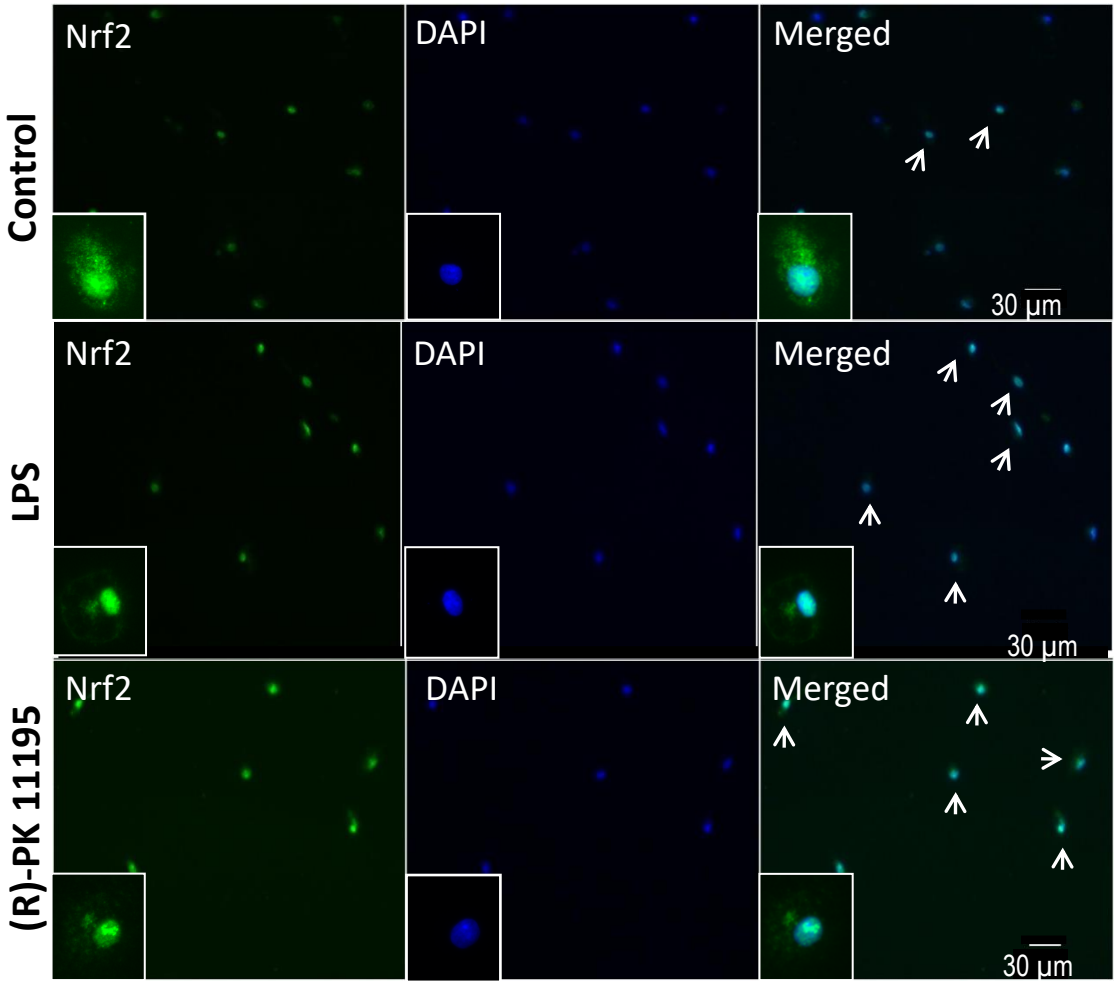
Control
LPS
(R)-PK 11195
Nrf2
DAPI
Merged
30 µm

FIGURE 4. TSPO-ligands induce the translocation of the anti-oxidant transcription factor, Nrf2, to the nucleus.

A) Microglia exposed to physiologically relevant concentrations of TSPO ligands (1, 10, or 100 nM of (R) PK-11195 or Ro5-4864 for 24 hours demonstrated increased Nrf2 levels in the nucleus as compared to the cytosol relative to vehicle treated cells ($F_{(8,1602)}$=19.774, $p<0.0001$)
B) Sulforaphane, a potent Nrf2 activator, was used as a positive control and to assess the time course of Nrf2 translocation in microglia.
C) Selected images of microglia demonstrating increased Nrf2 labeling in the nucleus of LPS and TSPO-L treated cells as compared to control (20x and 63x inset). Under oxidative stress, Keap-1 releases Nrf2, which exposes Nrf2's nuclear localization signal. In the nucleus, Nrf2 binds to the antioxidant response element (ARE), which induces the transcription of various cytoprotective genes involved in maintaining redox homeostasis.

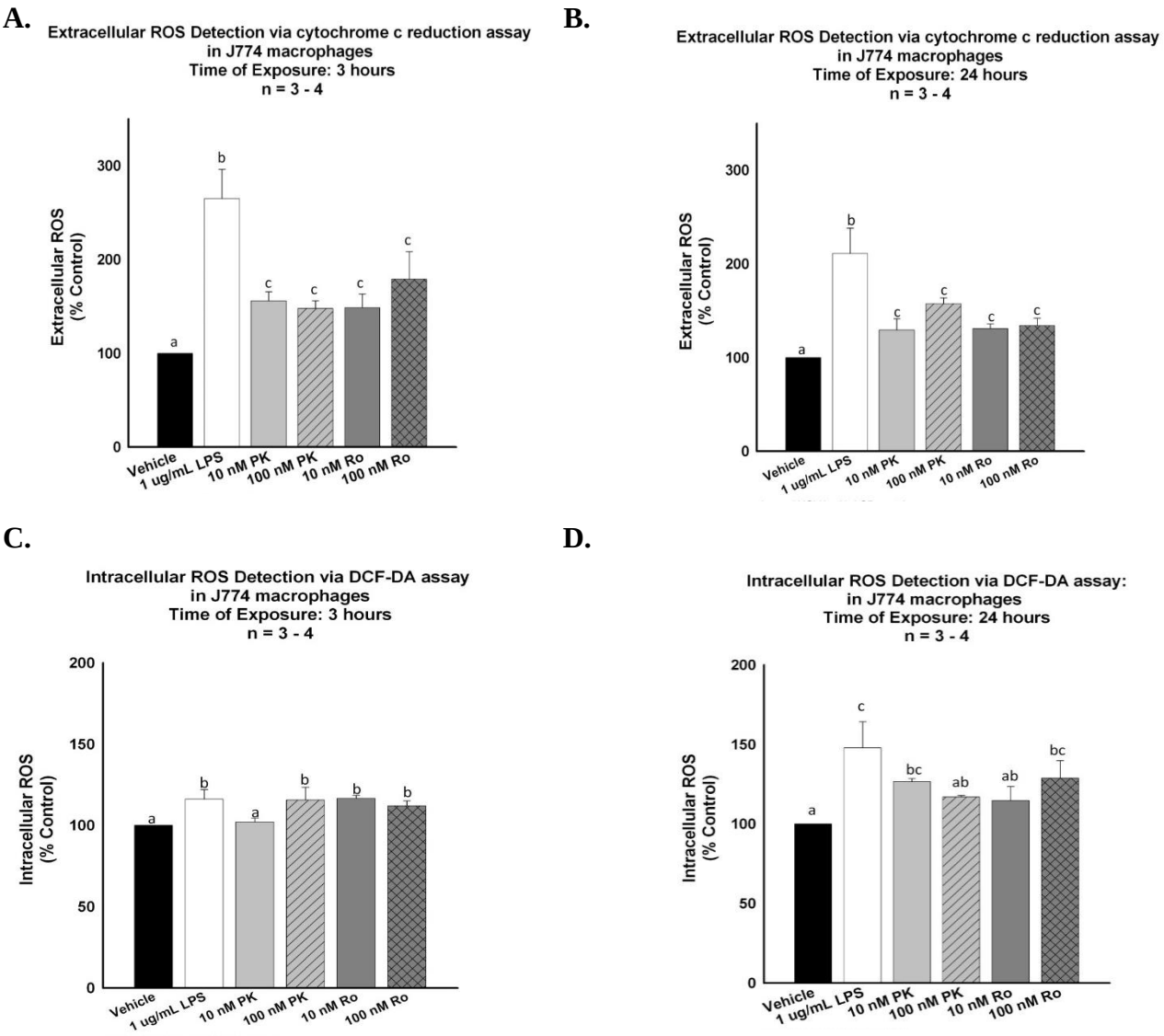

<u>Supplementary FIGURE 1</u>. TSPO-ligands induce intracellular and extracellular ROS production in a macrophage cell line. To assess whether our finding of TSPO-L induced ROS production was specific to microglia, we examined ROS production in a macrophage cell line J774. These cells are known to express and upregulate TSPO. At both 3 hours ($F_{(5,18)}$=11.219; p<0.001) and 24 hours (($F_{(5,19)}$=10.400; p<0.001), TSPO-L induced an increase in extracellular ROS production (A and B). Intracellular ROS production also increased at both 3 hours ($F_{(5,19)}$=3.792; p=0.022) and 24 hours ($F_{(5, 20)}$=3.750; p=0.021), but had a slightly different trend based on ligand dose and time point examined (C and D).

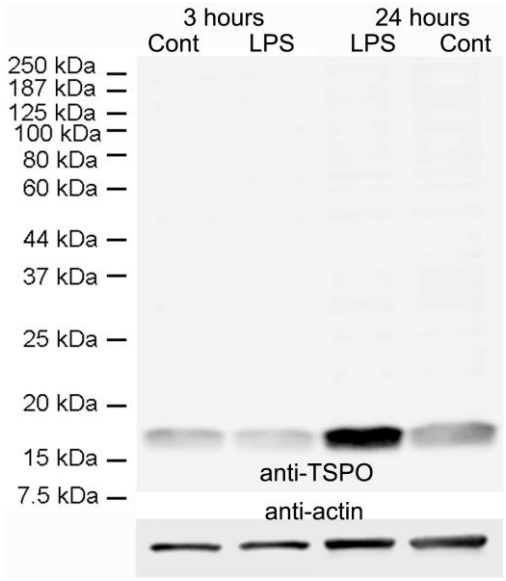

<u>Supplementary FIGURE 2</u>. TSPO protein expression in J774 macrophages at 3 & 24 hours.

TSPO protein levels increased with 24 hour LPS exposure compared to 24 hour control cells. TSPO protein levels did not differ between 3 hour control and LPS treated cells. This data indicates that increases in ROS production precede increases in TSPO protein levels (3 hour time point), and that ROS levels remain elevated at a time when TSPO protein levels have been increased (24 hour time point). A more thorough time course will be required to elucidate the exact nature of the relationship between ROS levels and TSPO protein levels.

N.B. Transfection and Western blot completed by and courtesy of Dr. Chun Zhou.

REFERENCES

Baines, C. P. (2009). The molecular composition of the mitochondrial permeability transition pore. *J Mol Cell Cardiol, 46*(6), 850-857. doi:10.1016/j.yjmcc.2009.02.007

Baines, C. P., & Gutierrez-Aguilar, M. (2018). The still uncertain identity of the channel-forming unit(s) of the mitochondrial permeability transition pore. *Cell Calcium, 73*, 121-130. doi:10.1016/j.ceca.2018.05.003

Baines, C. P., Kaiser, R. A., Sheiko, T., Craigen, W. J., & Molkentin, J. D. (2007). Voltage-dependent anion channels are dispensable for mitochondrial-dependent cell death. *Nat Cell Biol, 9*(5), 550-555. doi:10.1038/ncb1575

Banati, R. B., Middleton, R. J., Chan, R., Hatty, C. R., Kam, W. W., Quin, C., . . . Liu, G. J. (2014). Positron emission tomography and functional characterization of a complete PBR/TSPO knockout. *Nat Commun, 5*, 5452. doi:10.1038/ncomms6452

Banfi, B., Tirone, F., Durussel, I., Knisz, J., Moskwa, P., Molnar, G. Z., . . . Cox, J. A. (2004). Mechanism of Ca2+ activation of the NADPH oxidase 5 (NOX5). *J Biol Chem, 279*(18), 18583-18591. doi:10.1074/jbc.M310268200

Bernardi, P. (2013). The mitochondrial permeability transition pore: a mystery solved? *Front Physiol, 4*, 95. doi:10.3389/fphys.2013.00095

Brandenburg, L. O., Kipp, M., Lucius, R., Pufe, T., & Wruck, C. J. (2010). Sulforaphane suppresses LPS-induced inflammation in primary rat microglia. *Inflamm Res, 59*(6), 443-450. doi:10.1007/s00011-009-0116-5

Brieger, K., Schiavone, S., Miller, F. J., Jr., & Krause, K. H. (2012). Reactive oxygen species: from health to disease. *Swiss Med Wkly, 142*, w13659. doi:10.4414/smw.2012.13659

Butovsky, O., Jedrychowski, M. P., Moore, C. S., Cialic, R., Lanser, A. J., Gabriely, G., . . . Weiner, H. L. (2014). Identification of a unique TGF-beta-dependent molecular and functional signature in microglia. *Nat Neurosci, 17*(1), 131-143. doi:10.1038/nn.3599

Chen, J. C., Ho, F. M., Pei-Dawn Lee, C., Chen, C. P., Jeng, K. C., Hsu, H. B., . . . Lin, W. W. (2005). Inhibition of iNOS gene expression by quercetin is mediated by the inhibition of IkappaB kinase, nuclear factor-kappa B and STAT1, and depends on heme oxygenase-1 induction in mouse BV-2 microglia. *Eur J Pharmacol, 521*(1-3), 9-20. doi:10.1016/j.ejphar.2005.08.005

Chen, M. K., & Guilarte, T. R. (2008). Translocator protein 18 kDa (TSPO): molecular sensor of brain injury and repair. *Pharmacol Ther, 118*(1), 1-17. doi:10.1016/j.pharmthera.2007.12.004

Choi, J., Ifuku, M., Noda, M., & Guilarte, T. R. (2011). Translocator protein (18 kDa)/peripheral benzodiazepine receptor specific ligands induce microglia functions consistent with an activated state. *Glia, 59*(2), 219-230. doi:10.1002/glia.21091

Cox, J. A., Jeng, A. Y., Sharkey, N. A., Blumberg, P. M., & Tauber, A. I. (1985). Activation of the human neutrophil nicotinamide adenine dinucleotide phosphate (NADPH)-oxidase by protein kinase C. *J Clin Invest, 76*(5), 1932-1938. doi:10.1172/JCI112190

Dang, J., Brandenburg, L. O., Rosen, C., Fragoulis, A., Kipp, M., Pufe, T., . . . Wruck, C. J. (2012). Nrf2 expression by neurons, astroglia, and microglia in the cerebral cortical penumbra of ischemic rats. *J Mol Neurosci, 46*(3), 578-584. doi:10.1007/s12031-011-9645-9

Dinkova-Kostova, A. T., Holtzclaw, W. D., Cole, R. N., Itoh, K., Wakabayashi, N., Katoh, Y., . . . Talalay, P. (2002). Direct evidence that sulfhydryl groups of Keap1 are the sensors regulating induction of phase 2 enzymes that protect against carcinogens and oxidants. *Proc Natl Acad Sci U S A, 99*(18), 11908-11913. doi:10.1073/pnas.172398899

Fan, J., Campioli, E., Midzak, A., Culty, M., & Papadopoulos, V. (2015). Conditional steroidogenic cell-targeted deletion of TSPO unveils a crucial role in viability and hormone-dependent steroid formation. *Proc Natl Acad Sci U S A, 112*(23), 7261-7266. doi:10.1073/pnas.1502670112

Finkel, T. (2011). Signal transduction by reactive oxygen species. *J Cell Biol, 194*(1), 7-15. doi:10.1083/jcb.201102095

Gatliff, J., & Campanella, M. (2012). The 18 kDa translocator protein (TSPO): a new perspective in mitochondrial biology. *Curr Mol Med, 12*(4), 356-368.

Gatliff, J., East, D., Crosby, J., Abeti, R., Harvey, R., Craigen, W., . . . Campanella, M. (2014). TSPO interacts with VDAC1 and triggers a ROS-mediated inhibition of mitochondrial quality control. *Autophagy, 10*(12), 2279-2296. doi:10.4161/15548627.2014.991665

Gatliff, J., East, D. A., Singh, A., Alvarez, M. S., Frison, M., Matic, I., . . . Campanella, M. (2017). A role for TSPO in mitochondrial Ca(2+) homeostasis and redox stress signaling. *Cell Death Dis, 8*(6), e2896. doi:10.1038/cddis.2017.186

Giulian, D., & Baker, T. J. (1986). Characterization of ameboid microglia isolated from developing mammalian brain. *J Neurosci, 6*(8), 2163-2178.

Guilarte, T. R., Loth, M. K., & Guariglia, S. R. (2016). TSPO Finds NOX2 in Microglia for Redox Homeostasis. *Trends Pharmacol Sci, 37*(5), 334-343. doi:10.1016/j.tips.2016.02.008

Haslund-Vinding, J., McBean, G., Jaquet, V., & Vilhardt, F. (2017). NADPH oxidases in oxidant production by microglia: activating receptors, pharmacology and association with disease. *Br J Pharmacol, 174*(12), 1733-1749. doi:10.1111/bph.13425

Hickman, S. E., Kingery, N. D., Ohsumi, T. K., Borowsky, M. L., Wang, L. C., Means, T. K., & El Khoury, J. (2013). The microglial sensome revealed by direct RNA sequencing. *Nat Neurosci, 16*(12), 1896-1905. doi:10.1038/nn.3554

Hoffmann, M. H., & Griffiths, H. R. (2018). The dual role of ROS in autoimmune and inflammatory diseases: Evidence from preclinical models. *Free Radic Biol Med*. doi:10.1016/j.freeradbiomed.2018.03.016

Holmstrom, K. M., & Finkel, T. (2014). Cellular mechanisms and physiological consequences of redox-dependent signalling. *Nat Rev Mol Cell Biol, 15*(6), 411-421. doi:10.1038/nrm3801

Jayakumar, A. R., Panickar, K. S., & Norenberg, M. D. (2002). Effects on free radical generation by ligands of the peripheral benzodiazepine receptor in cultured neural cells. *J Neurochem, 83*(5), 1226-1234.

Joo, H. K., Lee, Y. R., Lim, S. Y., Lee, E. J., Choi, S., Cho, E. J., . . . Jeon, B. H. (2012). Peripheral benzodiazepine receptor regulates vascular endothelial activations via suppression of the voltage-dependent anion channel-1. *FEBS Lett, 586*(9), 1349-1355. doi:10.1016/j.febslet.2012.03.049

Kang, G., Kong, P. J., Yuh, Y. J., Lim, S. Y., Yim, S. V., Chun, W., & Kim, S. S. (2004). Curcumin suppresses lipopolysaccharide-induced cyclooxygenase-2 expression by inhibiting activator protein 1 and nuclear factor kappab bindings in BV2 microglial cells. *J Pharmacol Sci, 94*(3), 325-328.

Kant, A. M., De, P., Peng, X., Yi, T., Rawlings, D. J., Kim, J. S., & Durden, D. L. (2002). SHP-1 regulates Fcgamma receptor-mediated phagocytosis and the activation of RAC. *Blood, 100*(5), 1852-1859.

Kaspar, J. W., Niture, S. K., & Jaiswal, A. K. (2009). Nrf2:INrf2 (Keap1) signaling in oxidative stress. *Free Radic Biol Med, 47*(9), 1304-1309. doi:10.1016/j.freeradbiomed.2009.07.035

Kokoszka, J. E., Waymire, K. G., Levy, S. E., Sligh, J. E., Cai, J., Jones, D. P., . . . Wallace, D. C. (2004). The ADP/ATP translocator is not essential for the mitochondrial permeability transition pore. *Nature, 427*(6973), 461-465. doi:10.1038/nature02229

Krauskopf, A., Eriksson, O., Craigen, W. J., Forte, M. A., & Bernardi, P. (2006). Properties of the permeability transition in VDAC1(-/-) mitochondria. *Biochim Biophys Acta, 1757*(5-6), 590-595. doi:10.1016/j.bbabio.2006.02.007

Lam, J., Herant, M., Dembo, M., & Heinrich, V. (2009). Baseline mechanical characterization of J774 macrophages. *Biophys J, 96*(1), 248-254. doi:10.1529/biophysj.108.139154

Levonen, A. L. (2014). Activation of stress signaling pathways by oxidized and nitrated lipids. *Free Radic Biol Med, 75 Suppl 1*, S8. doi:10.1016/j.freeradbiomed.2014.10.846

Levonen, A. L., Hill, B. G., Kansanen, E., Zhang, J., & Darley-Usmar, V. M. (2014). Redox regulation of antioxidants, autophagy, and the response to stress: implications for electrophile therapeutics. *Free Radic Biol Med, 71*, 196-207. doi:10.1016/j.freeradbiomed.2014.03.025

Liu, G. J., Middleton, R. J., Hatty, C. R., Kam, W. W., Chan, R., Pham, T., . . . Banati, R. B. (2014). The 18 kDa translocator protein, microglia and neuroinflammation. *Brain Pathol, 24*(6), 631-653. doi:10.1111/bpa.12196

McEnery, M. W. (1992). The mitochondrial benzodiazepine receptor: evidence for association with the voltage-dependent anion channel (VDAC). *J Bioenerg Biomembr, 24*(1), 63-69.

Morohaku, K., Pelton, S. H., Daugherty, D. J., Butler, W. R., Deng, W., & Selvaraj, V. (2014). Translocator protein/peripheral benzodiazepine receptor is not required for steroid hormone biosynthesis. *Endocrinology, 155*(1), 89-97. doi:10.1210/en.2013-1556

Niture, S. K., Jain, A. K., & Jaiswal, A. K. (2009). Antioxidant-induced modification of INrf2 cysteine 151 and PKC-delta-mediated phosphorylation of Nrf2 serine 40 are both required for stabilization and nuclear translocation of Nrf2 and increased drug resistance. *J Cell Sci, 122*(Pt 24), 4452-4464. doi:10.1242/jcs.058537

Niture, S. K., Jain, A. K., & Jaiswal, A. K. (2009). Antioxidant-induced modification of INrf2 cysteine 151 and PKC-delta-mediated phosphorylation of Nrf2 serine 40 are both required for stabilization and nuclear translocation of Nrf2 and increased drug resistance. *J Cell Sci, 122*(Pt 24), 4452-4464. doi:10.1242/jcs.058537

Niture, S. K., Kaspar, J. W., Shen, J., & Jaiswal, A. K. (2010). Nrf2 signaling and cell survival. *Toxicol Appl Pharmacol, 244*(1), 37-42. doi:10.1016/j.taap.2009.06.009

Niture, S. K., Khatri, R., & Jaiswal, A. K. (2014). Regulation of Nrf2-an update. *Free Radic Biol Med, 66*, 36-44. doi:10.1016/j.freeradbiomed.2013.02.008

Novo, E., & Parola, M. (2008). Redox mechanisms in hepatic chronic wound healing and fibrogenesis. *Fibrogenesis Tissue Repair, 1*(1), 5. doi:10.1186/1755-1536-1-5

Papadopoulos, V., Amri, H., Boujrad, N., Cascio, C., Culty, M., Garnier, M., . . . Drieu, K. (1997). Peripheral benzodiazepine receptor in cholesterol transport and steroidogenesis. *Steroids, 62*(1), 21-28.

Papadopoulos, V., Baraldi, M., Guilarte, T. R., Knudsen, T. B., Lacapere, J. J., Lindemann, P., . . . Gavish, M. (2006). Translocator protein (18kDa): new nomenclature for the peripheral-type benzodiazepine receptor based on its structure and molecular function. *Trends Pharmacol Sci, 27*(8), 402-409. doi:10.1016/j.tips.2006.06.005

Ralph, P., & Nakoinz, I. (1975). Phagocytosis and cytolysis by a macrophage tumour and its cloned cell line. *Nature, 257*(5525), 393-394.

Ralph, P., & Nakoinz, I. (1977). Antibody-dependent killing of erythrocyte and tumor targets by macrophage-related cell lines: enhancement by PPD and LPS. *J Immunol, 119*(3), 950-954.

Rastogi, R., Geng, X., Li, F., & Ding, Y. (2016). NOX Activation by Subunit Interaction and Underlying Mechanisms in Disease. *Front Cell Neurosci, 10*, 301. doi:10.3389/fncel.2016.00301

Salter, M. W., & Beggs, S. (2014). Sublime microglia: expanding roles for the guardians of the CNS. *Cell, 158*(1), 15-24. doi:10.1016/j.cell.2014.06.008

Savchenko, V. L. (2013). Regulation of NADPH oxidase gene expression with PKA and cytokine IL-4 in neurons and microglia. *Neurotox Res, 23*(3), 201-213. doi:10.1007/s12640-012-9327-6

Sekhar, K. R., Crooks, P. A., Sonar, V. N., Friedman, D. B., Chan, J. Y., Meredith, M. J., . . . Freeman, M. L. (2003). NADPH oxidase activity is essential for Keap1/Nrf2-mediated induction of GCLC in response to 2-indol-3-yl-methylenequinuclidin-3-ols. *Cancer Res, 63*(17), 5636-5645.

Sileikyte, J., Blachly-Dyson, E., Sewell, R., Carpi, A., Menabo, R., Di Lisa, F., . . . Forte, M. (2014). Regulation of the mitochondrial permeability transition pore by the outer membrane does not involve the peripheral benzodiazepine receptor (Translocator Protein of 18 kDa (TSPO)). *J Biol Chem, 289*(20), 13769-13781. doi:10.1074/jbc.M114.549634

Sileikyte, J., Petronilli, V., Zulian, A., Dabbeni-Sala, F., Tognon, G., Nikolov, P., . . . Ricchelli, F. (2011). Regulation of the inner membrane mitochondrial permeability transition by the outer membrane translocator protein (peripheral benzodiazepine receptor). *J Biol Chem, 286*(2), 1046-1053. doi:10.1074/jbc.M110.172486

Sileikyte, J., Roy, S., Porubsky, P., Neuenswander, B., Wang, J., Hedrick, M., . . . Bernardi, P. (2010). Small Molecules Targeting the Mitochondrial Permeability Transition. In *Probe Reports from the NIH Molecular Libraries Program*. Bethesda (MD).

Stolk, J., Hiltermann, T. J., Dijkman, J. H., & Verhoeven, A. J. (1994). Characteristics of the inhibition of NADPH oxidase activation in neutrophils by apocynin, a methoxy-substituted catechol. *Am J Respir Cell Mol Biol, 11*(1), 95-102. doi:10.1165/ajrcmb.11.1.8018341

Town, T., Nikolic, V., & Tan, J. (2005). The microglial "activation" continuum: from innate to adaptive responses. *J Neuroinflammation, 2*, 24. doi:10.1186/1742-2094-2-24

Tu, L. N., Zhao, A. H., Stocco, D. M., & Selvaraj, V. (2015). PK11195 effect on steroidogenesis is not mediated through the translocator protein (TSPO). *Endocrinology, 156*(3), 1033-1039. doi:10.1210/en.2014-1707

Unkeless, J. C., Kaplan, G., Plutner, H., & Cohn, Z. A. (1979). Fc-receptor variants of a mouse macrophage cell line. *Proc Natl Acad Sci U S A, 76*(3), 1400-1404.

Veenman, L., Shandalov, Y., & Gavish, M. (2008). VDAC activation by the 18 kDa translocator protein (TSPO), implications for apoptosis. *J Bioenerg Biomembr, 40*(3), 199-205. doi:10.1007/s10863-008-9142-1

Vilhardt, F., Haslund-Vinding, J., Jaquet, V., & McBean, G. (2017). Microglia antioxidant systems and redox signalling. *Br J Pharmacol, 174*(12), 1719-1732. doi:10.1111/bph.13426

Zeno, S., Zaaroor, M., Leschiner, S., Veenman, L., & Gavish, M. (2009). CoCl(2) induces apoptosis via the 18 kDa translocator protein in U118MG human glioblastoma cells. *Biochemistry, 48*(21), 4652-4661. doi:10.1021/bi900064t

Zhao, X., Sun, G., Zhang, J., Strong, R., Dash, P. K., Kan, Y. W., . . . Aronowski, J. (2007). Transcription factor Nrf2 protects the brain from damage produced by intracerebral hemorrhage. *Stroke, 38*(12), 3280-3286. doi:10.1161/STROKEAHA.107.486506

Zhao, Y. Y., Yu, J. Z., Li, Q. Y., Ma, C. G., Lu, C. Z., & Xiao, B. G. (2011). TSPO-specific ligand vinpocetine exerts a neuroprotective effect by suppressing microglial inflammation. *Neuron Glia Biol, 7*(2-4), 187-197. doi:10.1017/S1740925X12000129

Chapter 4: A Novel Molecular Interaction of TSPO with NADPH oxidase in Microglia

ABSTRACT

Translocator Protein 18 kDa (TSPO) is a glial stress response protein that is widely used as a biomarker of brain injury and neuroinflammation in preclinical and clinical neuroimaging. TSPO ligands have been shown to impart beneficial therapeutic effects in animal models of neurological disease. However, there is a paucity of knowledge on the function(s) of TSPO in glial cells, the cells that upregulate TSPO levels in diverse pathologies. Recent studies using conditional and global TSPO knockout mice have questioned the role of TSPO in translocating cholesterol across the outer mitochondrial membrane as the first step in steroidogenesis. Here, we report a novel interaction of TSPO with NADPH oxidase in microglia that implicates the production of reactive oxygen species for modulation of redox homeostasis**.**

1. INTRODUCTION

Translocator Protein 18 kDa (TSPO) is a clinical neuroimaging biomarker of brain injury and neuroinflammation that is able to detect diverse brain pathologies (Chen & Guilarte 2008; Papdopoulos et al 2006; Liu et al 2014). TSPO levels are low, nearly undetectable in the normal brain neuropil, but they increase markedly and selectively at primary and secondary sites of brain injury and neuroinflammation (Chen & Guilarte 2008). In this way, TSPO can be used to evaluate the neurotoxicity of various environmental compounds and to track neuroinflammation in a multitude of neurological diseases that include an inflammatory component such as Alzheimer's disease, Parkinson's disease, amyotrophic lateral sclerosis (ALS), traumatic brain injury, multiple sclerosis, and Zika virus infections, amongst many others (Zimmer et al 2014; Gerard et al 2006; Zurcher et al 2014; Couglin et al 2015 & 2017; Politis et al 2012; Kuszpit et al 2017).

The cellular framework for TSPO as a biomarker is based on the activation of microglia and astrocytes, the glial cell types that express and upregulate TSPO levels following nervous system insults (Chen & Guilarte 2008; Kuhlmann & Guilarte 1999; Maeda et al 2007). During the last several decades, a number of diverse functions have been attributed to TSPO, including the transport of cholesterol into mitochondria as the rate limiting step in steroidogenesis; regulation of the mitochondrial permeability transition pore (MitoPTP); reactive oxygen species (ROS) production; and porphyrin/heme transport, amongst various other functions (Papadopoulos et al 1997; Chen & Guilarte 2008; Veenman et al 2008; Sileikyte et al 2010; Batako et al 2015). Further, an early report claimed that knocking out *Tspo* in mice was embryonic lethal (Papadopoulos et al 1997). However, new evidence has emerged that has questioned the dogma that deleting *Tspo* is embryonic lethal and whether TSPO plays an essential role in steroidogenesis or regulates the MitoPTP. Several studies have now shown that TSPO knockout (KO) mice are viable, and that

TSPO is not required for steroidogenesis (Banati et al 2014; Morohaku et al 2014; Tu et al 2014;) and does not participate in the regulation of the MitoPTP (Sileikyte et al 2014). Structural biology data also shows that oligomerization of TSPO is unlikely to form a pore for cholesterol transport, as previously proposed (Li et al 2013). Thus, different lines of investigation provide evidence to support the notion that TSPO may not be directly involved in steroidogenesis. Understanding the functional significance of TSPO upregulation in glial cells under conditions of diverse neuropathologies is important in order to advance our understanding of glial cell biology. Further, insight into TSPO function may provide new avenues for devising therapeutic strategies for mitigating or modulating neuroinflammation, a common pathology in many neurodegenerative disorders.

Microglia are the resident immune cells of the brain with an ability to sense and respond to cellular signals resulting from disruption of brain homeostasis (Hanisch et al 2007; Salter & Beggs 2014; Liu et al 2014). Microglia have a hallmark morphological response and markedly increase TSPO levels shortly after brain injury with a time course that is dependent on the type and degree of injury (Chen & Guilarte 2008; Maeda et al 2007). Although TSPO appears to play a role in the neuroinflammatory response (Beckers et al 2018; Lavisse et al 2012), there is a lack of knowledge on the precise molecular mechanism(s) and function(s) of TSPO in the inflammatory response of microglia. Consistent with the notion of a role of TSPO in immune activation, recent studies in Tspo-/- mice (versus Tspofl/fl) indicate that the majority of the differentially expressed genes were related to the immune response (Jamin et al 2005; Rone et al 2009; Tu et al 2014; Fan et al 2015; Taylor et al 2014; Gatliffe & Campenella 2016) providing additional support to a functional connection with inflammation. Further, examination into the microglial phenotype that is involved in TSPO upregulation indicates that in M1 proinflammatory microglia, TSPO

expression increases, whereas in M2 anti-inflammatory microglia, TSPO expression remains constant (Beckers et al 2018). While there is some evidence that overexpression of TSPO increased expression of alternatively activated M2 stage related genes, these studies were done in the transformed cell line of BV-2 microglia, and therefore may not be as biologically representative as studies done in primary microglia (Bae et al 2014).

Microglia exposed to physiologically relevant concentrations (nM) of TSPO-specific ligands increase ROS production that is abrogated by different types of NADPH oxidase (NOX2) inhibitors (Choi et al 2011). These experiments provided the first evidence of a potential relationship between TSPO and NOX2 in microglia. NOX2 is a major source of ROS production in the central nervous system, and similar to TSPO, NOX2 is highly enriched in microglia. (Nayernia et al 2015; Papadopoulos et al 2006). NOX2 is a multi-subunit enzyme composed of the cytosolic subunits $p40^{phox}$, $p47^{phox}$, $p67^{phox}$, the small G-protein Rac1, and the plasma membrane subunits $p22^{phox}$ and $gp91^{phox}$. The plasma membrane subunit $gp91^{phox}$ is processed and matured in the endoplasmic reticulum (ER) via the incorporation of two heme molecules into its precursor gp65, followed by glycosylation to form the mature form of $gp91^{phox}$ (Yu et al 1997, 1998, and 1999; DeLeo et al 2000). In the ER, the mature $gp91^{phox}$ is then able to dimerize with $p22^{phox}$ to form flavocytochrome b558 ($Cytb_{558}$), the main subunit of NOX2 (DeLeo et al 2000; Yu et al 1997, 1998, and 1999). This heterodimer traffics to relevant locations within the secretory pathway to membrane compartments and lipid rafts. In phagocytes such as neutrophils and macrophages, activation of NOX2 occurs when a stimulus promotes the phosphorylation of $p47^{phox}$. The cytosolic subunits subsequently translocate to the membrane where they assemble with $Cytb_{558}$ to form a membrane-bound complex to generate superoxide (Yu et al 1998). Studies have shown that cholesterol is also needed for the NOX2 cytosolic subunits to translocate to the

plasma membrane or lipid rafts in order to form an active NOX2 complex (Vilhardt et al 2004; Shao et al 2003). Therefore, a potential interaction of TSPO with NOX2 may be based on the ability of TSPO to bind cholesterol (Li et al 1998) and heme (Taketani et al 1995; Vanhee et al 2011) both of which are required to form an active NOX2 complex. In this study, we provide new evidence of a direct molecular interaction between TSPO and NOX2 in microglia that may form the basis for the regulation of NOX2-dependent reactive oxygen species (ROS) production for redox homeostasis.

2. MATERIALS & METHODS

2.1 Primary microglia cell culture: Primary mixed glial cell cultures were prepared using a modified version of the glial culture technique as previously described with PN 1-3 C57/Bl6 mouse pups (Gordon et al 2011; Giulian & Baker 1986). At 12-14 days, microglia were separated from the glial cultures by shaking the flasks for 3 hours at 120 r.p.m. and collected as floating cells in the media. After centrifugation for 10 minutes at 400 x g, cell viability was determined by trypan blue exclusion, and cells were plated at various densities according to the assay being tested. Around 94% of the adherent cells were positive for microglia-specific marker Mac-1 as determined by immunostaining. Cells rested overnight (16-20 hours) before any dosing or assays were performed. The animals used for this study had been treated humanely as all the animal studies were reviewed and approved by each institutions Animal Care & Use Committee.

2.2 Treatments: Bacterial lipopolysaccahride (LPS) was dissolved in phenol red free media to create a stock solution of 1 mg/mL. A solution of 100 ng/mL of LPS was made fresh for each experimental exposure. Microglia were exposed to 100 ng/mL of LPS for time of exposure indicated.

2.3 Antibody Validation via gene silencing by spinoculation using shRNA lentiviral particles: Validation of TSPO, gp91, and p22 antibodies was performed using shRNA transduction in J7774 cells a gift from Dr. Martin Pomper's laboratory. All shRNAs and empty vectors (EV) used in this study were from Sigma MISSION. (St. Louis, MO). Clones tested included TSPO: TRCN00000102106 (#102106); TRCN00000102107 (#102107); TRCN00000102109 (#102109). gp91 (Cybb): TRCN00000435339 (#435339); TRCN00000422819 (#422819); TRCN00000240564 (#240564). p22 (Cyba): TRCN00000240562 (#240562); TRCN00000240565 (#240565); TRCN00000011889 (#011889). Clones #102106 (TSPO), #435339 (gp91), and #240565 (p22) results are pictured in Figure 1A. A suspension of 100,000 cells/ml was treated with 8 μg/ml of hexadimethrine bromide (107689, Sigma, St. Louis, MO), exposed to lentiviral particles at a multiplicity of infection (MOI) of 15, centrifuged at 800xg for 30 min at room temperature. Cells were then resuspended and plated at a density of 20,000 cells/well. After 48 hr, cells were selected by 1 μg/ml puromycin (A11138, Invitrogen, Carlsbad, CA) for 4.5 days to select for cells which had been transduced. After puromycin selection, cells were put in fresh media for 7 days before being harvested for Western blot.

2.4 Transgenic mice: The animal procedures described in this study were approved by Florida International University Institution Animal Care & Use Committee. Mice heterozygous for translocator protein kDa (TSPO) were obtained from Helmholtz Zentrum Munich (GMC) as part of the International Mouse Phenotyping Consortium (IMPC) and INFRAFRONTIER/European Mouse Mutant Archive (EMMA). TSPO tm1b mice were produced on a C57BL/6NTac background and mice were produced by treating 2-cell embryos with Cre enzyme as described previously (Ryder et al., 2014). Tm1b allele embryos have a reporter-tagged deletion allele (post-

Cre). Critical exons, in this case exons 2 and 3 of *Tspo*, are deleted by creating a frame shift using the Cre method.

2.5 Immunoprecipitation & Western Blots: Cells were plated onto 60-mm dishes at a density of 500,000 cells per dish. Cells were harvested in a mild lysis buffer containing 0.2 mM sodium orthovanadate, 5 mM sodium fluoride, 0.5% NP-40, 2.5 mM EDTA, 150 mM potassium chloride, and 10mM Tris, pH 7.4 (adapted from (Miao & Degterev, 2009). Multiple microglia extractions were combined in order to load 415 ug protein per treatment condition for each immunoprecipitation experiment. Cells were harvested for whole cell protein levels using the same method of Brewer et al 2007. Protein concentration was determined using the Lowry assay.

For each immunoprecipitation experiment, cell lysates were pre-cleared by incubating the lysate with IgG beads for 2 hours to eliminate any nonspecific binding to beads. Samples were then incubated with the anti-TSPO antibody (Abcam, ab109497, 1:10) overnight at 4˚C. Next, lysate was incubated for 2 hours with 200 uL of Protein G Dynabeads to allow the Fc region of the antibody to bind to the IgG coated beads. All immunoprecipitation-related incubations were performed at 4˚C. A sample of the initial lysate was retained for analysis of total protein and is referred to as the "input" fraction. Proteins were separated on 4-15% TGX Precast Gels, (Biorad, Hercules, CA.) and transferred to polyvinylidene difluoride (PVDF) membranes. For non-immunoprecipitation samples (i.e. the Input fraction), 25 ug of protein were loaded per condition per lane. Immobilon-FL PVDF Western blot membranes (EMD Millipore IPFL00010) were incubated with corresponding primary antibodies: goat anti-TSPO (Abcam, ab118913, 1:1000); rabbit anti-TSPO (Abcam, 109497, 1:1000); mouse anti-gp91^{phox} (BD Transduction Laboratories, 611415, 1:200); mouse anti-p22^{phox} (Santa Cruz, sc-130551, 1:100); rabbit anti-mouse VDAC (Abcam, ab15895, 1:500). Quick Western Kit-IRDye 680RD was also used as it does not bind to

denatured mouse or rabbit monoclonal antibodies. Standard Western blot LICOR secondary antibodies (IRDye 800 CW Donkey anti-Mouse and IRDye 680LT donkey anti-rabbit, 1:10,000) were also used to confirm specificity of Quick Western Kit IRDye 680RD.

2.6 Gene Expression & RT-PCR: Gene expression for *Tspo, Cybb, Cyba,, VDAC1,* and *GAPDH*. RNA was isolated from primary mouse microglia cells treated with vehicle or 100ng/mL of LPS for 18 hours by using RNAqueous Micro Kit (AM1931, Invitrogen, Carlsbad, CA). RNA content was measured using NanoDrop spectrophotometer (Thermo Scientific, United States). Reverse transcription of RNA was performed with High-Capacity RNA-to-cDNA kit (Applied Biosystems, Invitrogen, Carslbad, CA). qRT-PCR was performed using 1ul of cDNA diluted to 20ng/ul, TaqMan multiplex master mix (Applied Biosystems, Invitrogen, Carslbad, CA) and TaqMan mouse primers into a final reaction of volume of 10ul. Primers used included: TSPO (Mm00437828_m1-FAM-MGB); Cybb (Mm01287743_m1-FAM-MGB); Cyba (Mm00514478_m1-FAM-MGB); Vdac1 (Mm00834272_m1-FAM-MGB); and GAPDH (Mm999999915_g1-VIC-MGB). The results were evaluated using QuantStudio Real-Time PCR Software v1.3. Amplification specificity was confirmed by melting curve analysis and the quantification was carried out using the ΔΔCt method (Schmittgen & Livak, 2008). All samples were normalized to GAPDH. Data is 6 independent experiments run on the same plate for each gene. All samples were run in triplicate.

2.7 Immunocytochemistry: 100,000 microglia were plated onto PLL glass coverslips (Fisher Scientific, 08-774-383) in 12 well plates. Cells were treated for 18 hours with vehicle (media) or 100 ng/mL lipopolysaccharide (LPS) in media supplemented with 2% FBS. Immunocytochemistry was performed via conventional techniques: fixing cells with 4% paraformaldehyde; permeabilizing cells with 0.2% Triton; blocking with 10% normal donkey serum (Jackson

Laboratories, Bar Harbor, ME) for 3 hrs before being incubated with primary antibodies: goat anti-TSPO (Abcam, ab118913, 1:500); mouse anti-gp91^{phox} (BD Transduction Laboratories, 611415, 1:100); mouse anti-p22^{phox} (Santa Cruz, sc-130551, 1:100); rabbit anti-mouse VDAC (Abcam, ab15895, 1:500). After washing, cells were incubated with appropriate Alexa Fluor secondary antibodies for 1 hr (Life Technologies; AF 488, 594, and 647, 1:500). Cells were mounted with Prolong with DAPI (Life Technologies) to counterstain for nuclei.

2.8 Immunohistochemistry. Free-floating brain sections from PFA-perfused mice were sectioned using a freezing microtome (Leica Microsystems Inc., Bannockburn, IL). For immunofluorescence triple labeling of Mac-1, TSPO, and gp91^{phox}, free-floating brain sections were blocked with 5% normal donkey serum containing 0.2% Triton X-100 for 1 hour followed by primary antibody incubation: rat-anti-Mac-1 (BD Pharmigen; 1:250), rabbit-anti-TSPO (Abcam; ab109497, 1:500), and goat-anti-gp91^{phox} (Santa Cruz, (sc-5827) 1:150) at 4°C overnight. Sections were incubated with appropriate Alexa Fluor secondary antibodies (Life Technologies; 1:500).

2.9 Immunofluorescence Imaging and Analysis. Immunofluorescence-labeled cells were imaged at 60x magnification with a 1.6x zoom using a laser scanning confocal microscope (Fluoview FV10i, Olympus, Center Valley, PA), utilizing the FV10 image software. All coverslips stained under the same conditions were imaged using the same scanning parameters on the same day. Five to six confocal stacks were obtained for each experimental condition with at least 25 cells counted per condition. Confocal stacks were projected into single images using the maximum fluorescence. All images were analyzed using Metamorph Offline (Molecular Devices, Downington, PA). The threshold level was kept at the same level for analysis in images obtained from the same experiment for each channel. For colocalization analyses, gray scale images of each

wavelength (each protein) were used to examine the area of colocalized pixels of both wavelengths to calculate the percent colocalization of their signals. Percent colocalization was calculated as previously described by Stansfield et al 2012. Briefly, Colocalization of Protein A with Protein B = Area (A with B) / Total Area (A) where A and B are individual wavelengths for the same image. To assess colocalization of 3 proteins (Proteins A, B, and C), a binary image was created where when A and B colocalized, a pixel was generated. This was done for the entire image to create image AB' representing pixels where A and B colocalized. The colocalization of proteins (A+B) with C was then quantified using images AB' and C.

2.10 Duolink Proximity Libation Assay. Duolink experiments were performed according to manufacturer's instructions with minor modifications (Sigma, Duolink In Situ Detection Reagents Red, DUO92008). After vehicle or LPS treatment, cells were fixed with 4% paraformaldehyde. Cells were permeabilized with 0.2% Triton for 25 minutes and blocked with 10% normal donkey serum before being incubated for corresponding primary antibodies for 72 hours at 4˚C: goat anti-TSPO (Abcam, ab118913, 1:500); mouse anti-gp91^{phox} (BD Transduction Laboratories, 611415, 1:200); mouse anti-p22^{phox} (Santa Cruz, sc-130551, 1:100); rabbit anti-mouse VDAC (Abcam, ab15895, 1:500). After washing, cells underwent exposure to PLA Probes (Goat PLUS and Mouse MINUS; or Goat PLUS and Rabbit MINUS); ligation solution, and amplification solution as per manufacturer's instructions.

2.11 Immuno-Electron Microscopy for TSPO labeling of microglia:

Microglia were plated at a density of 500,000 in a 6 cm plate. Cells were treated with either vehicle or LPS (100 ng/mL) for 18 hrs. Following exposure, media was removed and cells were fixed with 0.1% glutaraldehyde (GRA) + 4% paraformaldehyde (PFA) in 0.1 M phosphate buffer (PB) for 60 m. Cells were rinsed, cryoprotected and placed in a -80 C freezer for 30 m. Cells were allowed

to thaw in chilled cryoprotectant, which was removed by using subsequent changes of increasingly diluted cryoprotectant. Cells were blocked in 10% Normal Goat Serum with 0.1% Bovine Serum Albumin in PB for 1 h. Cells were then incubated in rabbit anti-TSPO (Abcam, MA, USA) at a 1:100 dilution for 24 hr at RT followed by an incubation at 4 C for 48 h. Cells were washed then incubated in a 1:100 dilution of goat-anit-rabbit 1.4 nm gold particle conjugated secondary antibody (Nanoprobes, NY, USA) for 2 h at RT. Secondary antibody was rinsed and gold particles were enhanced using HQ silver enhancement (Nanoprobes, NY, USA) for 2 m. Silver enhancement was removed, and cells were fixed in 2.5% GTA for 30 m. GTA was rinsed off and cells were post-fixed in 1% osmium tetroxide for 20 m. Osmium was rinsed and cells were dehydrated using successively increasing concentrations of ethanol, including a 70% mixture of ethanol with uranyl acetate to increase membrane contrast. After cells reached 100% ethanol, they were gently scraped from the dish and spun down at 800 g for 10 m. Cells were placed in the transition solvent propylene oxide and left overnight in a 1:1 mixture of propylene oxide and Spurr's low viscosity resin (Electron Miscroscopy Sciences, PA, USA). Cells were transferred to pure SPurr Resin for 24 h then allowed to polymerize in fresh resin for 8 h at 70 C. Resin blocks were cut from microfuge tubes and sectioned to a thickness of ~60 nm. Floating sections were picked up on a 200 mesh copper grids, counterstained with lead citrate for 5 m and examined under a FEI Ecnai Spirit Transmission Electron Microscope (FEI, OR, USA) operated at 60 kV.

2.12 Data analysis: Values are expressed as mean ± standard error of the mean (SEM). Student's paired t-tests were performed for Western Blot analyses and colocalization analyses. A two-way measure of analysis of variance was performed for colocalization analysis between wildtype and Sandhoff mice at 4 different ages. For all tests, significance level was set at $p < 0.05$. Outliers

determined to be greater than or less than two standard deviations above or below the mean were excluded. For percent vehicle values, statistics were run on log-transformed values.

3. RESULTS

3.1 Co-immunoprecipitation of TSPO, gp91^{phox}, p22^{phox}, and VDAC: To explore the relationship between TSPO and the NOX2 subunits gp91^{phox} and p22^{phox}, we performed TSPO immunoprecipitation experiments in primary mouse microglia using antibodies independently validated in our lab (Figure 1) under both LPS activated and non-activated conditions. Our primary murine microglia cultures are approximately 94% pure as determined by Mac-1 immunostaining (Figure 2), and LPS concentration and duration of exposure were determined to be non-cytotoxic to microglia (Figure 3). We used voltage-dependent anion channel (VDAC) as a positive control for the TSPO immunoprecipitation studies because TSPO and VDAC have been shown to colocalize and co-immunoprecipitate (McEnery et al 1992; Gatliffe et al 2014). Figure 4, panels A and B show that TSPO, gp91^{phox}, and p22^{phox} protein levels in the input fraction (whole cell lysate) increase significantly following LPS activation (100 ng/mLfor 18 hr) of microglia relative to non-activated conditions. VDAC protein levels did not change with microglia activation. This pattern of protein expression with activated microglia is consistent with gene expression changes determined by quantitative real-time PCR (Figure 4, panel C). Panels D and E in Figure 4 depict TSPO immunoprecipitation results probing for the presence of TSPO, gp91^{phox}, p22^{phox}, and VDAC protein. Western blot of the TSPO-immunoprecipitated fraction shows that gp91^{phox}, p22^{phox}, and VDAC co-immunoprecipitate with TSPO providing the first direct evidence of protein-protein interactions with NOX2 subunits. When we compared the level of these proteins in LPS activated vs non-activated microglia, we found a significant decrease in gp91^{phox} and

p22^{phox} protein levels that co-immunoprecipitated with TSPO, with no change in VDAC protein levels (Figure 4, panel E). Overall, these findings indicate that gp91^{phox} and p22^{phox} are associated with TSPO, and that this interaction is partially disrupted by LPS activation.

3.2 Immunofluorescence confocal imaging studies: To further confirm the TSPO-NOX2 subunit interaction, we performed triple-labeled immunofluorescent confocal imaging studies of TSPO, gp91^{phox}, p22^{phox}, and VDAC in non-activated and LPS activated microglia. Figure 5 shows TSPO's colocalization with gp91^{phox}, p22^{phox}, or VDAC, in Mac-1 labeled microglia at both high and low magnification. These images show extensive colocalization of TSPO with gp91^{phox}, p22^{phox}, and VDAC. Figure 8 depicts a summary view of the quantification of the colocalization of TSPO with gp91^{phox}, p22^{phox}, VDAC, and LAMP-2 confocal imaging (representative images used for colocalization quantification are in Figure 6 and Figure 7). The percent colocalization of TSPO with gp91^{phox}, p22^{phox}, and VDAC ranged from approximately 60-80%, whereas TSPO's colocalization with the lysosomal marker, LAMP-2 was approximately 20% (Figure 8, Panel A). When we compared the colocalization of TSPO with the NOX2 subunits and VDAC in LPS activated versus non-activated primary microglia, we again observed an effect of microglia activation on these protein-protein interactions similar to the co-immunoprecipitation studies. The percent of gp91^{phox} or p22^{phox} that colocalized with TSPO decreased significantly from approximately 60% to 40% in activated versus non-activated microglia (Figure 8, Panel B). A similar effect was observed with VDAC suggesting that a putative TSPO-gp91^{phox}-p22^{phox}-VDAC complex is disrupted when microglia are activated with LPS (Figure 8, panel B). Moreover, when we analyzed the fraction of the TSPO-p22^{phox}, or TSPO-gp91^{phox} colocalization that also colocalizes with VDAC, we observed the same decrease with LPS activation (Figure 8, panel C).

(Additional colocalization analyses are depicted in Figure 9). These findings suggest that under non-activated conditions, there is a TSPO complex with $gp91^{phox}$ and $p22^{phox}$ that is associated with VDAC. However, when microglia become activated, a significant fraction of $gp91^{phox}$ and $p22^{phox}$ appears to dissociate from TSPO. This dissociation may reflect the movement of $gp91^{phox}$ and $p22^{phox}$ (possibly as a $Cytb_{558}$ complex) to other subcellular compartments, such as lipid rafts or the plasma membrane, to form an active NOX2 complex with the cytosolic subunits.

3.3 Proximity Ligation Assay supports a TSPO-NOX2-VDAC interaction in microglia: To provide further validation and scientific rigor and of a TSPO-$gp91^{phox}$-$p22^{phox}$-VDAC complex in microglia, we used a proximity ligation assay (PLA) approach. This is a powerful and sensitive method that can detect protein-protein interaction(s) in the native state of cells when proteins are in close proximity to each other, in this case about 40 nm apart (Bagchi et al 2015; Fredriksson et al 2002; Gullberg et al 2004). Briefly, samples are incubated with primary antibodies to bind to the two proteins of interest. Secondary antibodies conjugated with positive and negative oligonucleotides (PLA probes) are then incubated with the samples. Next, ligase and two additional oligonucleotides are introduced. These oligonucleotides will hybridize to the PLA probes, and if in close enough proximity (~40 nm), form a closed circle. In the DNA circle, one of the antibody conjugated DNA probes serves as a primer for rolling circle amplification (RCA) and a repeated sequence (concatemeric) product is generated when DNA polymerase and nucleotides are added. Fluorescently labeled oligonucleotides proceed to bind to the RCA product and ultimately allow visualization of the protein-protein interaction via fluorescence microscopy. Figure 10, Panels A-C depict confocal images of TSPO-$gp91^{phox}$, TSPO-$p22^{phox}$ and TSPO-VDAC interactions respectively using PLA in overlay with phase imaging of microglia. The different

protein-protein interactions are clearly visible throughout the cell providing further support of direct interactions of TSPO with $gp91^{phox}$, $p22^{phox}$, and VDAC. Figure 10, Panels D-F depict the PLA quantitative results. Notably, it appears that the rank order of the degree of the colocalization of TSPO with $gp91^{phox}$ followed by $p22^{phox}$ and VDAC are similar in both the immunocytochemistry results (see Figure 8, panel A) and the proximity ligation assay results (see Figure 10, panels D-F). Unlike the co-immunoprecipitation and immunofluorescence confocal imaging studies, we did not observe an effect of LPS activation in decreasing the number of TSPO-NOX2 interactions. The lack of the difference between vehicle and LPS activated cells in the degree of protein-protein interactions in the PLA assay could be due to several reasons. First, the primary antibody concentration is specifically optimized to detect a portion of the interactions occurring within the cell, but not all of the interactions occurring in the cell. The purpose of not detecting all interactions is so that we can detect positive PLA signals, without the fluorescent signals coalescing, which would prevent quantification of the signal and full resolution of the subcellular localization of where the interaction is occurring. Since PLA is a highly sensitive method of protein-protein interaction detection, we still detect the interactions that are present, but are no longer detecting the difference in the degree of the interaction between the two treatments. This is in contrast to the co-immunoprecipitation and whole cell confocal imaging data that detect these proteins in the entire cell versus the PLA only detecting a fraction on the total protein-protein interactions. Additionally, Jalili et al 2017 published a paper examining how the kinetic properties of antibodies can affect PLA performance. More specifically, the Kc of an antibody affected the limit of detection in that low-affinity antibodies had higher limits of detection and high affinity antibodies had lower limits of detection. Therefore, if one of the antibodies we are using has a different Kc than another, it is not appropriate to compare the degree of interactions across the

three sets of experiments of gp91^{phox}, p22^{phox}, and VDAC given that the affinity of the antibodies could affect PLA performance. Nevertheless, the PLA method also confirmed that TSPO interacts with the NOX2 subunits and VDAC.

3.4 What are the subcellular localization(s) of a TSPO-NOX2 subunit interaction in microglia? It is known that TSPO and VDAC are present at the outer mitochondrial membrane and that gp91^{phox} and p22^{phox} mature and form the Cytb$_{558}$ heterodimer in the ER. We have proposed that these proteins are interacting at the mitochondria-associated endoplasmic reticulum (ER) membrane or MAM (Guilarte et al 2016). To examine whether TSPO is found at the MAM, we performed immuno-electron microscopy of TSPO in LPS-activated and non-activated primary microglia. Figure 11 depicts images of microglia under normal culture conditions in Panel A, and after LPS exposure in Panel B. Overall, there is an increase in TSPO labeling in the mitochondria (see yellow stars) as well as in other subcellular compartments such as the plasma membrane (arrows in panel B) in LPS-activated microglia. Panels C and D are higher magnification images of non-activated microglia indicating high TSPO levels in the outer mitochondria membrane and at the MAM (see arrows in panel C) as well as in the ER (yellow arrow heads in panel D) and at or just below the plasma membrane (arrows in panel D). This figure demonstrates that while TSPO is highly expressed in the outer mitochondria membrane, it is also expressed in other cellular compartments including the MAM (large, thick arrows in Figure 11, panel C).

3.5 The TSPO-NOX2 interaction also occurs in murine brain tissue: The studies presented so far have been performed in primary microglia cultures. To show that the TSPO-NOX2 interaction is not merely an epiphenomenon of culturing primary microglia, we performed studies in the intact

mouse brain i*n situ*. For this aim, we performed triple-label immunofluorescence confocal imaging in Sandhoff disease transgenic mice, a model in which we have previously shown substantial neurodegeneration and increased TSPO levels in the thalamus, cerebellum and brainstem (Loth et al 2016). Figure 12 shows that TSPO and $gp91^{phox}$ do colocalize in microglia in situ. Thus, the TSPO-NOX2 interaction not only occurs in primary microglia in culture, but also *in situ* in the intact brain. Furthermore, the TSPO-NOX2 interaction in the brain of Sandhoff disease mice increases as a function of age and progression of neurological disease expression (Figure 12, panels B-D).

4. DISCUSSION

The main finding of the present study is the demonstration, using multiple experimental approaches, of a direct molecular interaction of TSPO with two subunits of NOX2 in microglia. We also provide new evidence that the TSPO-NOX2 interaction is associated with VDAC as a putative complex at the MAM. Moreover, the TSPO-NOX2-VDAC complex is disrupted by LPS-mediated microglia activation.

A functional association between TSPO and the NOX2 subunits $gp91^{phox}$ and $p22^{phox}$ and VDAC is possible for 3 primary reasons: **1)** TSPO can bind both cholesterol (Li et al 1998) and heme (Taketani et al 1995; Veenman et al 2011), **2)** TSPO is found at the MAM, a point of communication between the mitochondria and the ER and **3)** the MAM is a subcellular site where heme transport to heme acceptor proteins is known to occur (Asagami et al 1994) and where there are high concentrations of cholesterol found due to lipid raft microdomains, that can serve as a platform for the binding of cholesterol to TSPO (Fujimoto et al 2011). We propose a working model in microglia in which heme is bound to the TSPO dimer. When microglia are activated,

cholesterol is mobilized, binds to TSPO at the CRAC (cholesterol recognition/interaction amino acid consensus) domain, and promotes the dissociation of TSPO from VDAC as well as the dissociation of TSPO dimers, thereby reducing the affinity of TSPO for heme; this reduction in heme affinity, promotes heme efflux from mitochondria through the MAM for transfer to the gp65 precursor of $gp91^{phox}$ at the ER (Figure 13). We propose that this molecular mechanism allows TSPO modulation of $gp91^{phox}$ formation and maturation, and through this mechanism, TSPO is able to regulate NOX2 activity and redox homeostasis in microglia.

This model is consistent with several independent lines of evidence: **1)** the TSPO homolog in the Gram-negative bacterium *Rhodobacter sphaeroides* TspO is able to control efflux of tetrapyrole intermediates of the heme/bacteriochlorophyll biosynthetic pathway (Yeliseev et al 1999), **2)** structural biology studies demonstrate that cholesterol and porphyrin/heme are bound at two distinct sites of *RsTSPO*, and that both cholesterol and porphyrin/heme inversely and allosterically influence the binding of one another (Li et al 2013), **3)** porphyrins/heme can induce the dimerization of RsTSPO (Yeliseev et al 2000), **4)** porphyrin/heme binding to TSPO initially inhibits VDAC conductance of Ca2+ in a dose-dependent manner that is not altered by mPTP inhibitors (Tamse et al 2008), **5)** cholesterol binding at the CRAC domain promotes the dissociation of TSPO dimers in reconstituted mammalian TSPO in liposomes (Jaipuria et al 2017) and **6)** TSPO can affect subcellular localization of proteins, as has been demonstrated in *A. thaliana* where TSPO binds to PIP2;7 to prevent PIP2;7's translocation to the plasma membrane in response to abiotic stress (Hachez et al 2014). We will elaborate on these 6 supporting points below.

rsTSPO has been shown to function as a membrane-bound protein for the transfer of heme/ porphyrins to control the efflux of tetrapyrole intermediates of the heme/bacteriochlorophyll biosynthetic pathway (Yeliseev and Kaplan 1999). This is relevant to the function of the

mammalian TSPO because the ability of *RsTSPO* to efflux tetrapyrroles can be replaced by the mammalian TSPO, indicating a highly conserved function (Yeliseev, Kruegar, & Kaplan, 1997). A heme transfer function for TSPO also arises from the highly-conserved tryptophan residues in the first periplasmic loop between the first and second membrane-spanning domains (Yesileev & Kaplan 2000; Li et al 2013). These tryptophan residues are similar to WWD heme-binding motifs found in proteins involved in transmembrane heme delivery (Goldman et al 1998; Richard-Fogal and Kranz 2010). The WWD domain binds heme to present it to an acceptor protein such that the heme vinyl group attaches to the reduced cysteinyl residues in the acceptor hemoprotein (Goldman et al 1998; Richard-Fogal and Kranz 2010). This process prevents heme oxidation at the site of the transmembrane heme transfer.

Consistent with this hypothesis, the MAM is a subcellular site where heme transport occurs from the mitochondria to the ER (Asagami et al 1994). Studies have shown that the MAM is a preferential site for heme transport to heme acceptor proteins such as cytochrome P450 (Asagami et al 1994). Our TSPO-IEM results indicate that TSPO is at the appropriate subcellular location for the transfer of mitochondrial-synthesized heme to heme-accepting proteins in the ER, such as gp65, the precursor of $gp91^{phox}$. As noted previously, $gp91^{phox}$ is processed and matured in the ER via the incorporation of two heme molecules into its precursor gp65, followed by glycosylation to form the mature $gp91^{phox}$. In the ER, the mature $gp91^{phox}$ is then able to dimerize with $p22^{phox}$ to form $Cytb_{558}$. This heterodimer then traffics to relevant locations within the secretory pathway to membrane compartments such as lipid rafts (Shao et al 2003; Vilhardt et al 2004; DeLeo et al 2000; Yu et al 1997, 1998, and 1999).

Additionally, there are high concentrations of cholesterol in MAM lipid raft microdomains that may serve as a platform for both the binding of cholesterol to TSPO and for the efflux of heme

out of mitochondria (Fujimoto et al 2011). Therefore, the MAM may be a subcellular site where TSPO, cholesterol, and heme are found in lipid rafts that serve as a platform for the formation of a TSPO-gp91^{phox}-p22^{phox}-VDAC complex.

Therefore, it is possible that under physiological conditions, heme is bound to TSPO and microglia activation mobilizes cholesterol to promote TSPO dimer dissociation and transfer of heme from mitochondria to the MAM. Consistent with this hypothesis, a study using high resolution solid-state NMR of reconstituted mammalian TSPO in liposomes shows that cholesterol binding at the CRAC domain promotes the dissociation of TSPO from a homodimer to monomers through an allosteric mechanism that connects the cholesterol binding motif (the CRAC domain) at the cytosolic end of TSPO with a GxxxG oligomerization motif on the opposite end of the TSPO structure (Jaipuria et al 2017). Notably, VDAC, is a protein that also contains GxxxG domains (Thinnes et al 2012) and cholesterol binding may not only influence the TSPO-NOX2 interaction, but also the TSPO-VDAC interaction by conformational changes in which this TSPO-VDAC association can be disrupted by microglia activation as noted in our immunofluorescence confocal imaging studies. Relatedly, Tamse and colleagues demonstrated that increased porphyrin limits the conductance of VDAC in rat cardiac mitochondria by decreasing Ca2+ influx and inducing VDAC closure. The authors hypothesize that due to the nanomolar affinity of porphyrin to TSPO and given TSPO's interaction with VDAC, porphyrin modulates VDAC conductance through its binding to TSPO (Tamse et al 2008). When porphyrin is no longer bound to TSPO, VDAC can flux as needed. These data indicate another way in which TSPO's interaction with porprhyrin/heme can affect its association with other proteins and in this case VDAC.

Collectively, our findings suggest that TSPO may be able to regulate the synthesis of the principal NOX2 subunit (i.e., gp91^{phox}), and thus be able to modulate NOX2 activity in microglia.

This finding is consistent with a known function of TSPO in the plant *Arabidopsis thaliana* in which the homologous TspO responds to abiotic stress (Vanhee et al 2011). Abiotic stress in A. thaliana increases TSPO levels, and TSPO regulates the cell surface expression of the aquaporin PIP2;7 by interacting with PIP2;7 at the ER and Golgi membranes (Hachez et al 2014). The interaction of TSPO with PIP2;7 provides a mechanism by which TSPO can modulate the expression of plasma membrane proteins. Similarly, TSPO may be able to modulate the expression of $gp91^{phox}$ at the plasma membrane by regulating the synthesis of its heme-containing subunit.

One question that arises is whether the interaction of TSPO with the NOX2 subunits is specific to microglia. Microglia are cells that have high levels of NOX2 relative to other cell types, given their function as the "macrophages of the brain" and use of ROS as a signaling molecule (Harisch et al 2009). Microglia are also one of the two cell types in the brain that express TSPO, the other being astrocytes. However, microglia and astrocytes exhibit different temporal responses in their inflammatory response and specifically in their TSPO up and down regulation (Chen and Guilarte 2008; Loth el al 2016). Therefore, TSPO may be serving a different function in astrocytes that is not associated with NOX2.

One potential explanation is that TSPO could still be binding heme, but given that astrocytes have a different proteomic profile than microglia, the proteins which would require and receive heme in astrocytes would be different. One such candidate would be heme oxygenase 1 (HO-1), an antioxidant enzyme which not only requires heme in its structure, but also degrades cellular heme into carbon monoxide and biliverdin. Previous studies have shown that HO-1 is upregulated in multiple cell types that involve oxidative stress, and that the time course of upregulation of HO-1 is dependent on cell type. For example, HO-1 in cultured astrocytes is upregulated earlier in time as compared to neurons in response to neurotoxic models of Parkinson's

disease (MPP+ or α-synuclein) (Yu et al 2016). This implies differential mechanisms for HO-1 induction in astrocytes and neurons. We know that TSPO upregulation can occur in both microglia and astrocytes, and currently, there is limited evidence that TSPO is found in neurons. Perhaps part of TSPO's ability to transfer heme to relevant enzymes involved in ROS production and antioxidant responses is related to microglia and astrocytes being more resistant to oxidative damage than neurons (Yu et al 2016).

In addition to different functions in different cell types, the interaction of TSPO and NOX to microglia will undoubtedly vary over time, as ROS levels change, as the cytokine milieu shifts, and as TSPO is upregulated and downregulated. There is preliminary evidence in Leydig cells that as ROS levels increase due to photoirradiation, an increase in TSPO oligomers is seen with molecular weights observed at multiple values: approximately 36, 72, 90 kDa depending on the length of exposure and presence of progesterone (Delavoie et al 2003). Thus, we could be capturing the time point where TSPO is being upregulated (as per input fraction and gene expression levels in Figure 4) in order to create oligomers, potentially larger than dimers. Teboul et al 2012 identified tetramers in mouse histidine tagged reconstituted recombinant TSPO in a lipid environment and dimers in the bacterial equivalent. The oligomeric status of TSPO in microglia remains to be determined in either physiological or pathological conditions. Whether or not a tetramer of TSPO can bind heme is also unknown. Furthermore, depending on how the microglia are activated whether via LPS, photoirradiation, ATP, could vary how TSPO responds. Choi et al 2011 saw differential responses when activing microglia with ATP vs LPS. Similarly, Veenman et al 2016, observed that short durations and low concentrations of TSPO ligands generally enhances ROS production, whereas long durations and/or high concentrations of TSPO ligands generally reduces ROS production. However, based on the conflicting literature, the response of

TSPO appears to be extremely context dependent which may in fact be a reflection of TSPO's function to maintain homeostasis, and therefore help preserve its ability to respond differently in different situations.

Taken together, our findings provide confirmation of the protein-protein interactions among TSPO-gp91-p22-VDAC at the MAM in primary mouse microglia. These protein-protein interactions appear to vary in strength depending on whether microglia are activated or non-activated, or in other words in physiological vs pathological conditions. We provide supporting evidence for a model in which the TSPO-NOX2-VDAC interaction modulates the subcellular localization of $gp91^{phox}$ and $p22^{phox}$ proteins through the supply of heme, in order to ultimately alter NOX2 activity, to help maintain redox homeostasis.

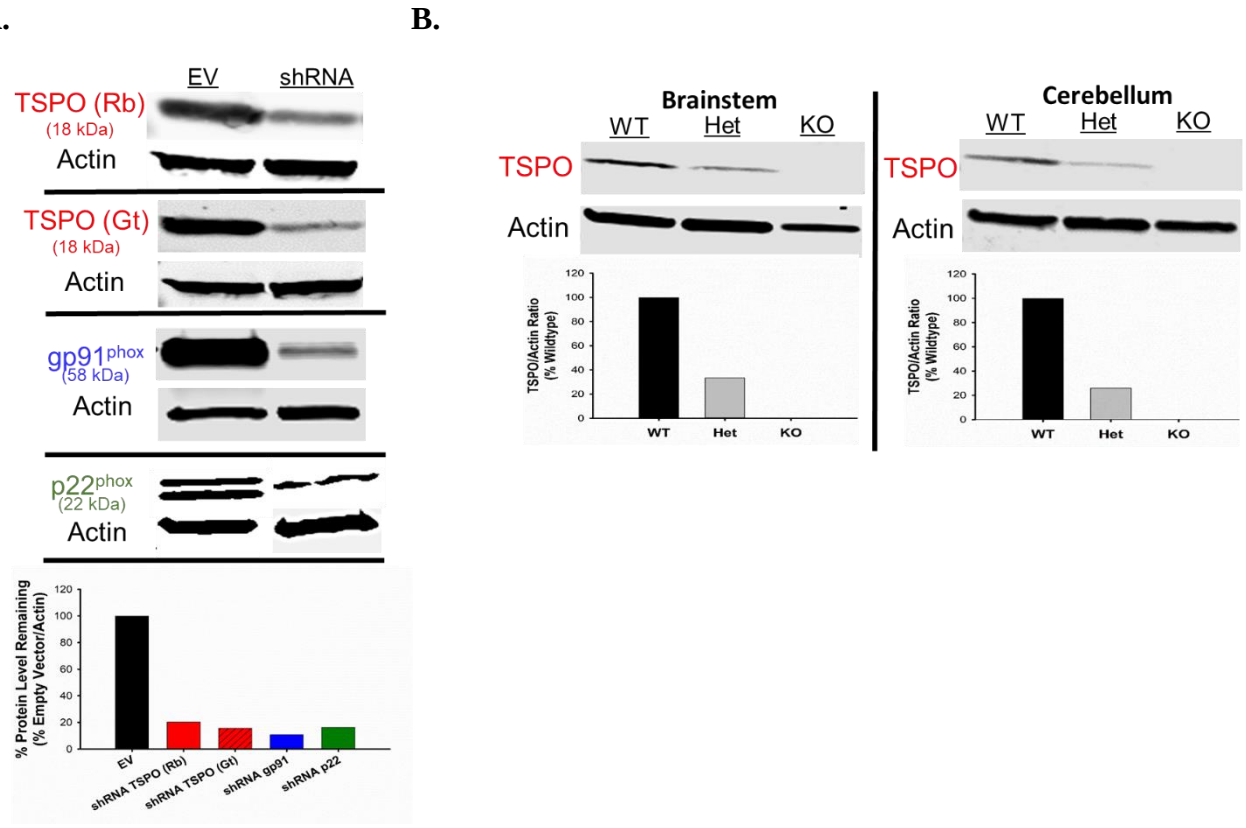

FIGURE 1: Antibody validation: We confirmed the specificity of each antibody used for the immunoprecipitation, colocalization, and proximity ligation assay experiments using shRNA knockdown in the J774 murine macrophage cell line (A) and with TSPO wildtype (WT), heterozygous (Het), and knockout (KO) mice (B). shRNA experiments were done via lentiviral transduction and used an empty vector as control. Multiple shRNA's were tested for each protein of interest with one specific shRNA shown here (#102106 (TSPO), #435339 (gp91), and #240565 (p22)). Brains were dissected from TSPO mice, and protein acquired from the brainstem and cerebellum is shown here. Actin was used as a loading control. N.B. shRNA transduction experiments performed in conjunction with Dr. Diane B. Re

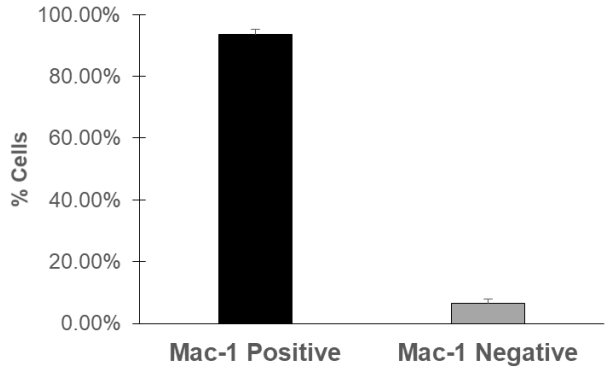

FIGURE. 2: Purity of Microglia Cultures. Purity of cultures was assessed via microglia Mac-1 immunostaining. Of the cells extracted from mixed glial cultures via the shaking method, 93.6% of cells were positive for Mac-1, with 6.4% of cells being positive for DAPI only (n=6, mean ± s.e.m.).

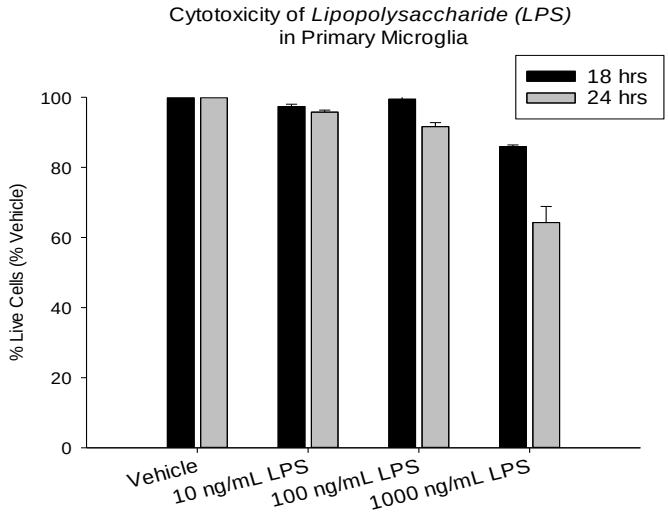

FIGURE 3. Cytotoxicity of *lipopolysaccharide (LPS)*. Primary murine microglia were dosed with specified doses of LPS for 18 or 24 hours and the percentage of live and dead cells were counted via the Live/Dead assay. Increased toxicity was seen with 1 ug/mL of LPS at both 18 and 24 hours. With 100 ng/mL of LPS, about 10-15% of cells were dead at 24 hours, as compared to less than 3% at 18 hours. n = 3 independent experiments for each time point.

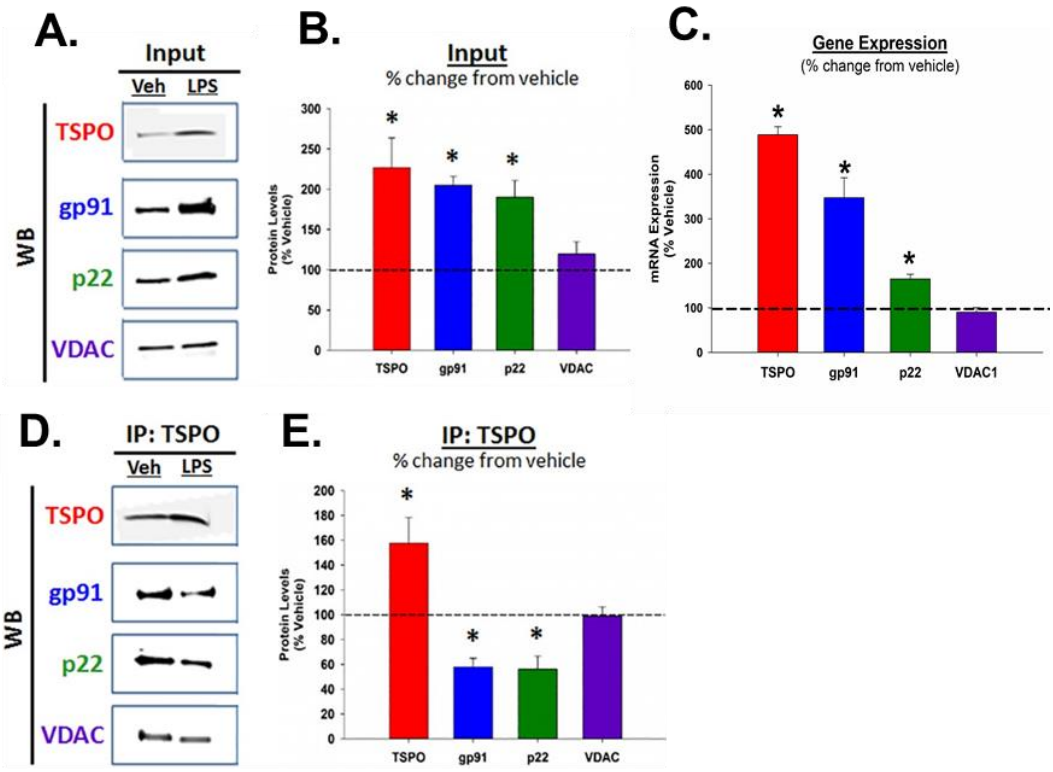

FIGURE 4: Effect of lipopolysaccharide (LPS) activation of primary microglia on TSPO, gp91^{phox}, p22^{phox}, and VDAC protein and gene expression levels. Western blot of primary microglia whole cell extracts (input) after 18 hour exposure to vehicle (media) or 100 ng/mL LPS-activated conditions (A). TSPO, gp91^{phox}, and p22^{phox} protein levels were increased as a result of LPS stimulation, while VDAC levels did not change. Quantification of protein levels (B) and gene expression levels (C). Data are normalized to vehicle and expressed as mean ± s.e.m. n = 8 independent experiments. *p<0.05 compared to vehicle-treated microglia. Student's paired t-test: TSPO: p = 0.001; gp91: p < 0.001; p22: p < 0.001; VDAC: p = 0.346.C: Quantification of gene expression levels. Data are normalized to vehicle and expressed as mean ± s.e.m. n = 6 independent experiments. *p<0.05 compared to vehicle-treated microglia. Student's paired t-test: TSPO: p < 0.001; gp91: p = 0.002; p22: p < 0.001; VDAC: p = 0.382.

Co-immunoprecipitation of TSPO, gp91^{phox}, p22^{phox}, and VDAC. Western blot of TSPO pull-down (IP) after 18 hour exposure to vehicle or 100 ng/mL LPS-stimulated conditions (D). gp91^{phox}, p22^{phox}, and VDAC proteins co-immunoprecipitate with TSPO. LPS stimulation increased the amount of TSPO protein compared to the vehicle condition. Interestingly, the amount of gp91^{phox} and p22^{phox} protein levels decreased in the LPS condition relative to vehicle treated cells, suggesting that the TSPO-NOX2 subunit interaction weakens under LPS-stimulated conditions. No effect was found with VDAC (E). Data are normalized to vehicle and expressed as mean ± s.e.m. n = 4-6 independent experiments. *p<0.05 compared to vehicle-treated microglia. Student's paired t-test: TSPO: p = 0.036; gp91: p = 0.005; p22: p < 0.045; VDAC: p = 0.743.

N.B. Gene expression experiments performed by Dr. Vanessa Nunes de Paiva with assistance from Dr. Diana Azzam.

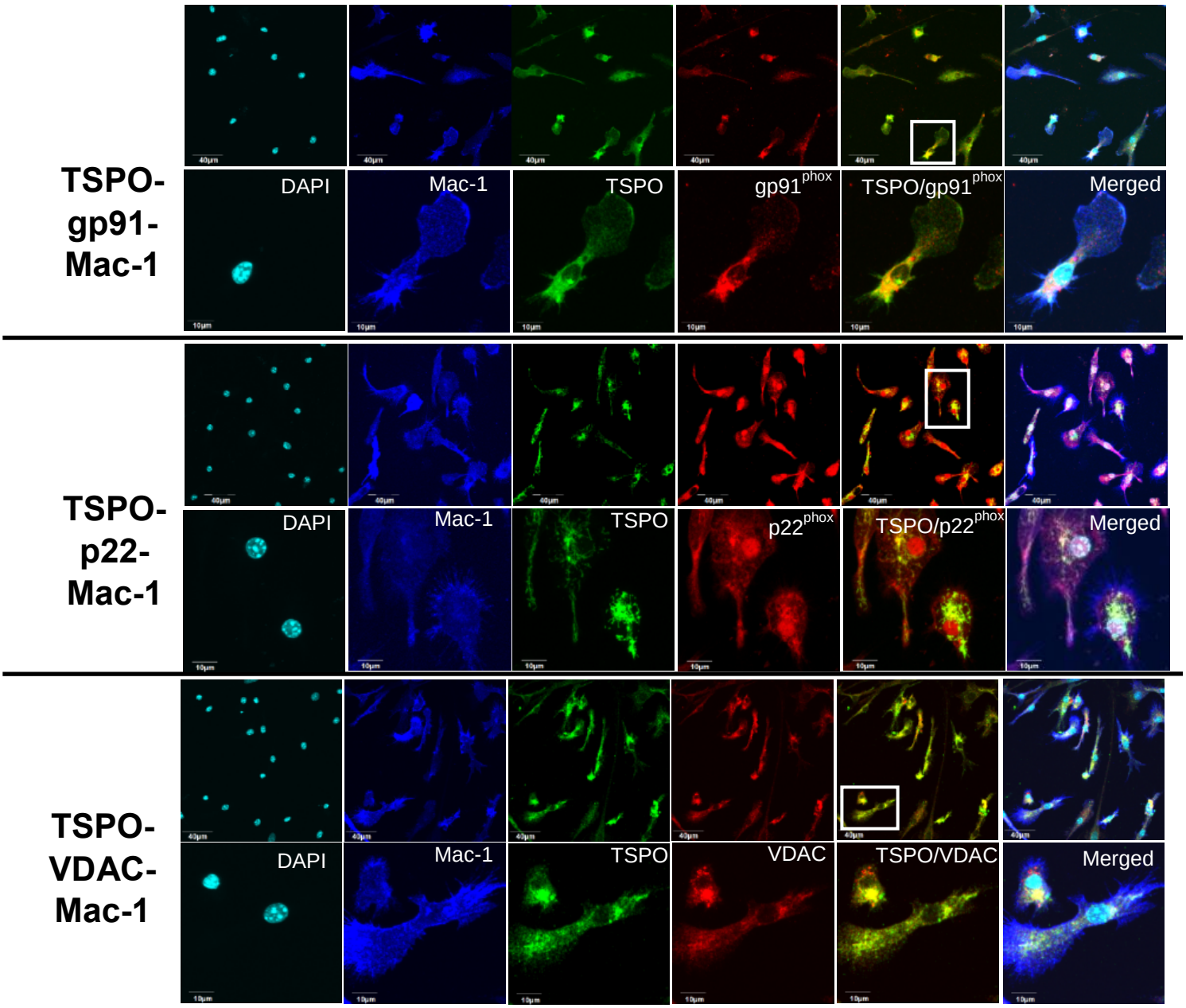

FIGURE 5. TSPO, gp91^{phox}, p22^{phox}, VDAC, and Mac-1 immunolabeling in primary microglia. Triple labeled immunofluorescent confocal images of TSPO and gp91^{phox} in microglia (Mac-1 labeled) cells. Confocal images confirmed that TSPO and gp91^{phox} colocalized as indicated by the yellow color. Confocal images also confirmed that TSPO and VDAC, and TSPO and p22^{phox} colocalized in microglia. Low magnification scale bar = 40 um. High magnification scale bar = 10 um.

A. **B.**

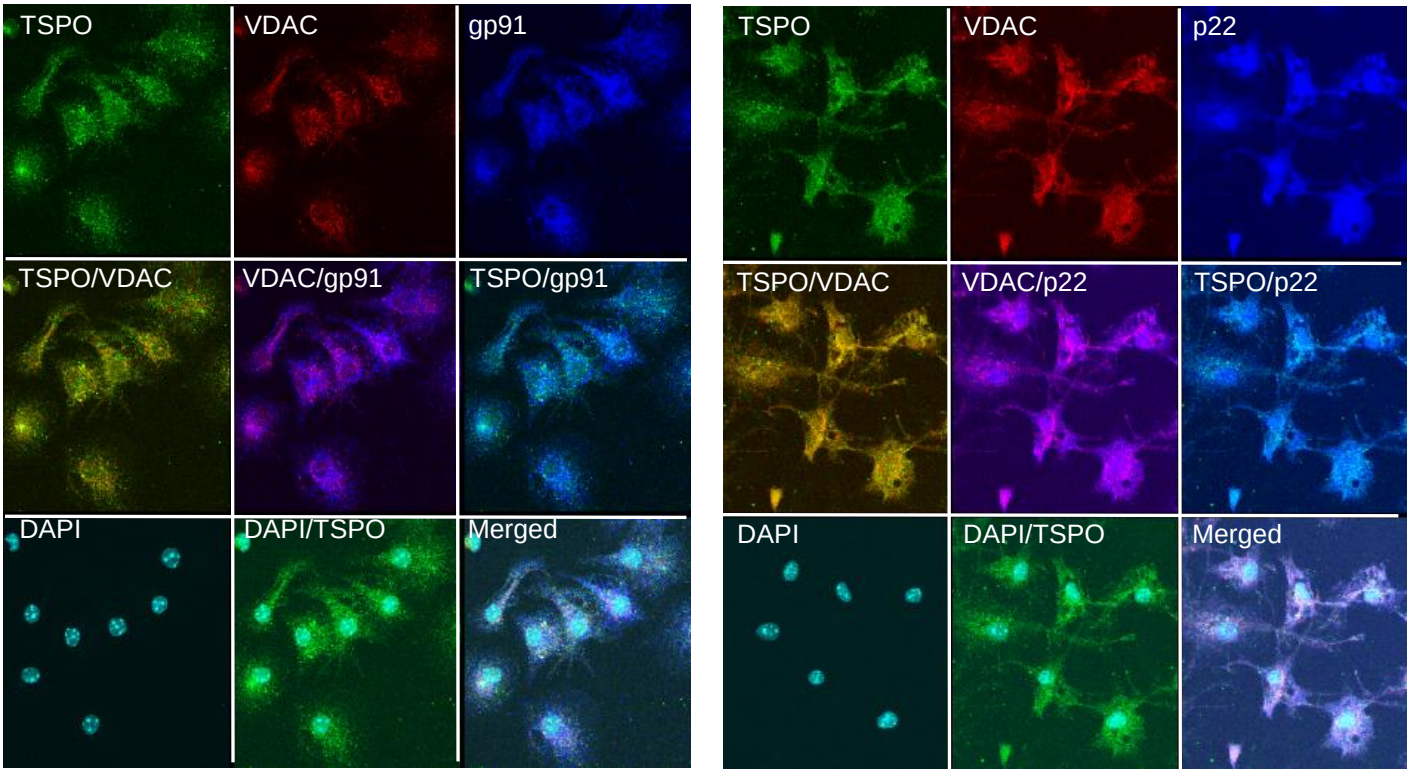

FIGURE 6: TSPO/gp91/VDAC and TSPO/p22/VDAC immunolabeling in primary microglia. Representative triple labeled immunofluorescent confocal images of microglia used for analyses represented in Figure 8. Imaging and analyses confirmed that TSPO colocalized with the mitochondrial protein VDAC, as represented by the yellow color, and that TSPO colocalized with both $gp91^{phox}$ and $p22^{phox}$ as represented by the purple/magenta colors. Images were taken with a 60x objective with a 1.6x zoom.

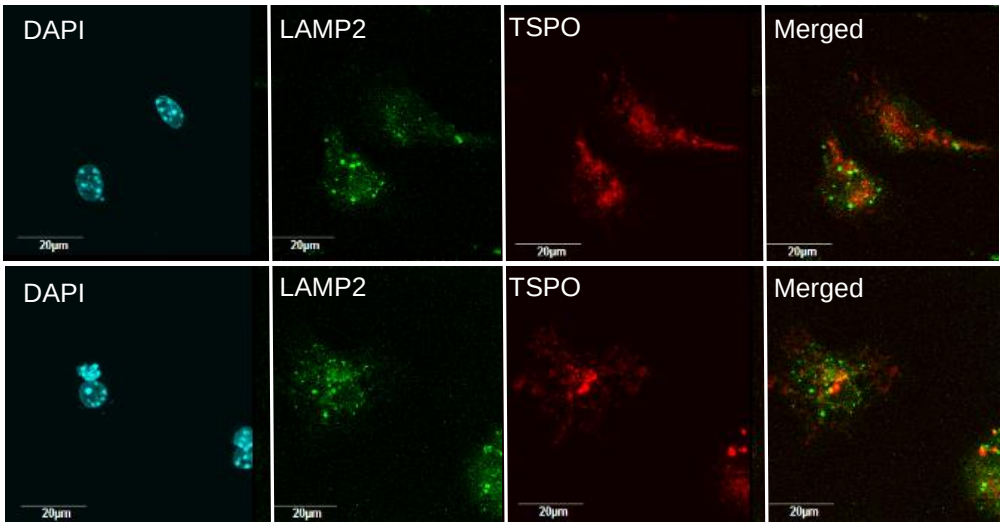

FIGURE 7: TSPO/LAMP2 immunolabeling in primary microglia. Representative double labeled immunofluorescent confocal images of microglia used for analyses represented in Figure 8. Imaging and analyses confirmed that TSPO had low levels of colocalization with the lysosomal marker, LAMP-2 (Vehicle = 20.13% ± 7.25%; LPS = 12.46% ± 5.76%). n = 3 independent experiments for TSPO/LAMP2 labeling with 35+ microglia counted per treatment condition per experiment. Scale bar = 20 um.

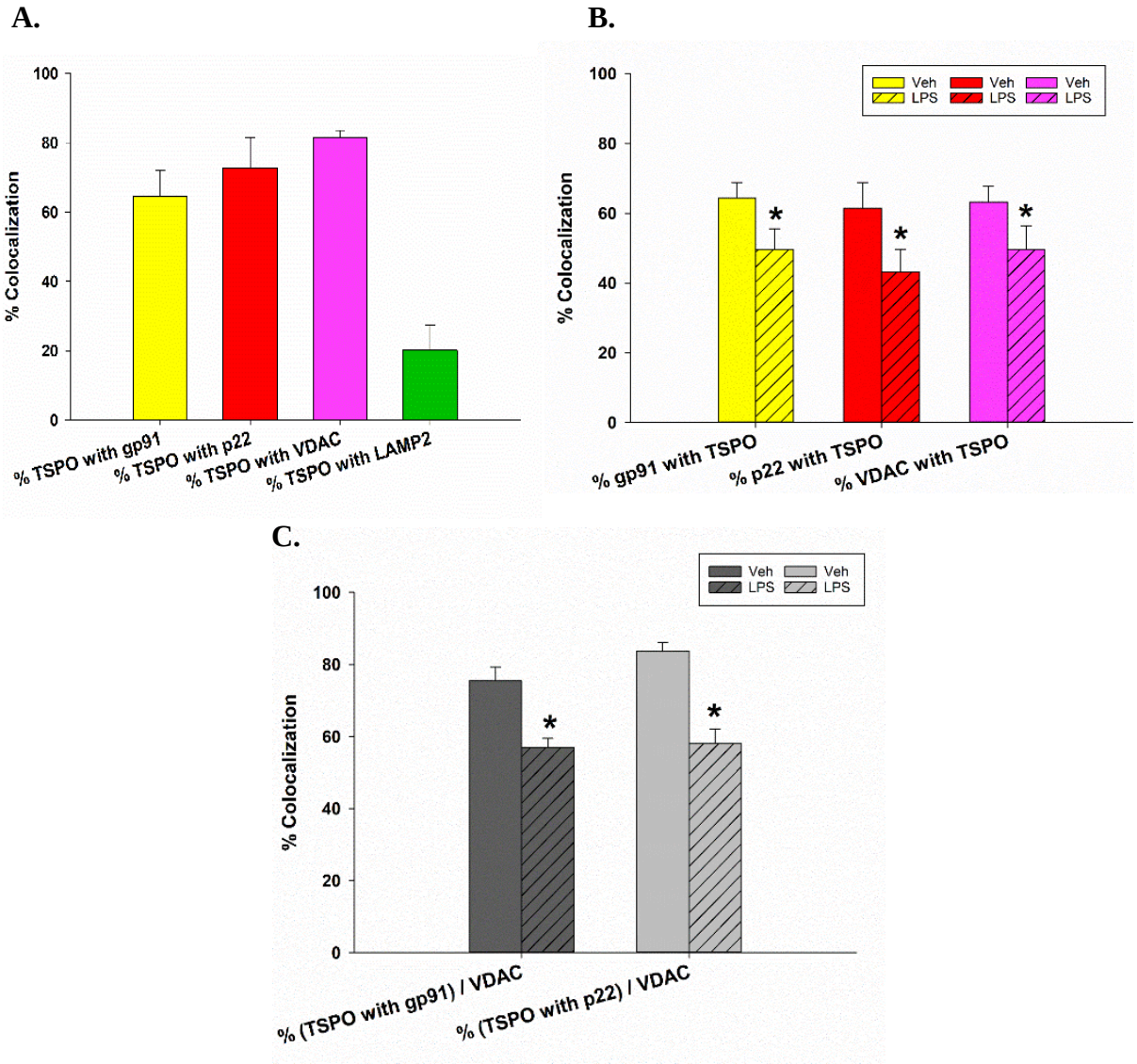

FIGURE 8. TSPO, gp91^{phox}, p22^{phox}, VDAC, and LAMP-2 colocalization quantification summary in primary microglia. Colocalization analyses revealed that TSPO had high levels of colocalization (>60%) with gp91, p22, and VDAC and low levels of colocalization with the lysosomal marker, LAMP-2 in vehicle treated microglia (A). The percentage of gp91^{phox}, p22^{phox}, and VDAC that colocalized with TSPO decreased when microglia were treated with 100 ng/mL of LPS for 18 hours (B) as compared to vehicle conditions (Student's paired t-test: % gp91 with TSPO: $p = 0.004$; %p22 with TSPO: $p = 0.002$; % VDAC with TSPO: $p = 0.003$). Under stimulated conditions, TSPO associated with gp91 and TSPO associated with p22, exhibit significantly decreased colocalization with VDAC suggesting a movement from the mitochondria to other cellular compartments (C) (Student's paired t-test: % (TSPO with gp91)/ VDAC: $p < 0.001$. % (TSPO with p22) / VDAC: $p = 0.004$). Data are expressed as mean ± s.e.m. n = 5-7 independent experiments with 35+ microglia counted per treatment condition per experiment. n = 3 independent experiments for TSPO/LAMP2 labeling with 35+ microglia counted per treatment condition per experiment.

FIGURE 9.

A. **B.** **C.**

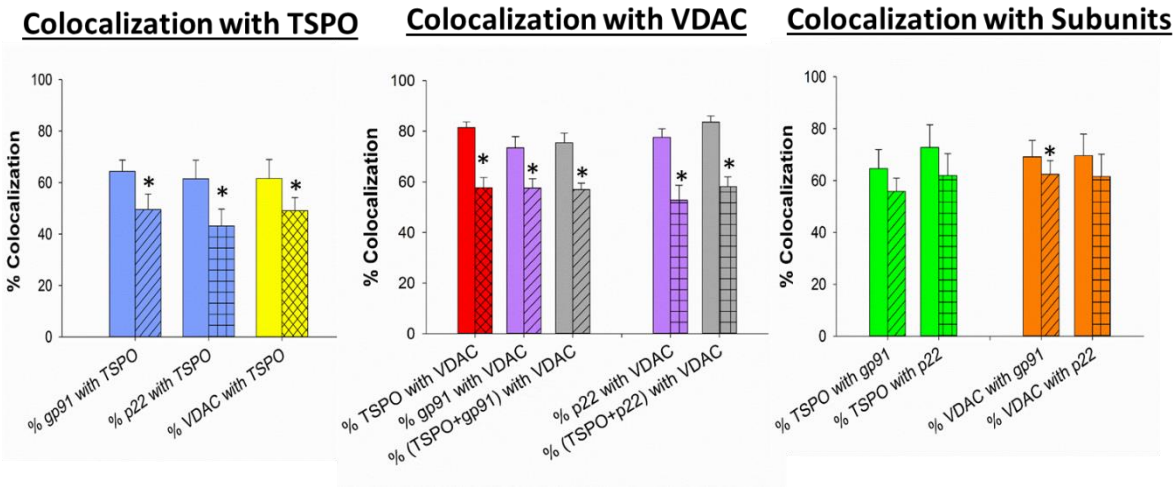

D.

% Colocalization of A with B (Veh. vs. LPS)		B			
		TSPO	gp91	p22	VDAC
A	TSPO		↓	↓	↓*
	gp91	↓*			↓*
	p22	↓*			↓*
	VDAC	↓*	↓*	↓	
	TSPO+gp91				↓*
	TSPO+p22				↓*

FIGURE 9. Colocalization quantification: detailed view. The data demonstrates that LPS stimulation decreased the degree of colocalization of gp91, p22, and VDAC with TSPO (A). Additionally, LPS stimulation also decreased the degree of the colocalization of TSPO with VDAC; gp91 with VDAC; and of TSPO+gp91 with VDAC (B), indicating movement of the TSPO-NOX2 complex away from the mitochondria. The same data pattern was also shown when examining p22 colocalization with TSPO and VDAC (B). TSPO and VDAC both independently colocalized with both subunits, but only the colocalization of VDAC with gp91 exhibited a statistically significant trend of decreased colocalization with LPS stimulation (C). Summary of A, B, and C in Panel D. Vehicle treated cells are solid bars, and LPS treated cells are patterned bars (n = 7 in TSPO/gp91/VDAC experiments. n = 5 in TSPO/p22/VDAC experiments. *$p<0.05$ compared to vehicle treated microglia. 35+ cells counted per condition). Paired t-tests (Vehicle vs. LPS): % gp91 with TSPO: $p = 0.004$. % p22 with TSPO: $p = 0.002$. % VDAC with TSPO: $p = 0.003$. % TSPO with VDAC: $p = 0.005$ % gp91 with VDAC: $p = 0.002$. % (TSPO+gp91) with VDAC: $p < 0.001$. % p22 with VDAC: $p = 0.004$. % (TSPO+p22) with VDAC: $p = 0.004$. % TSPO with gp91: $p = 0.053$. % TSPO with p22: $p = 0.129$. % VDAC with gp91: $p = 0.006$. % VDAC with p22: $p = 0.339$.

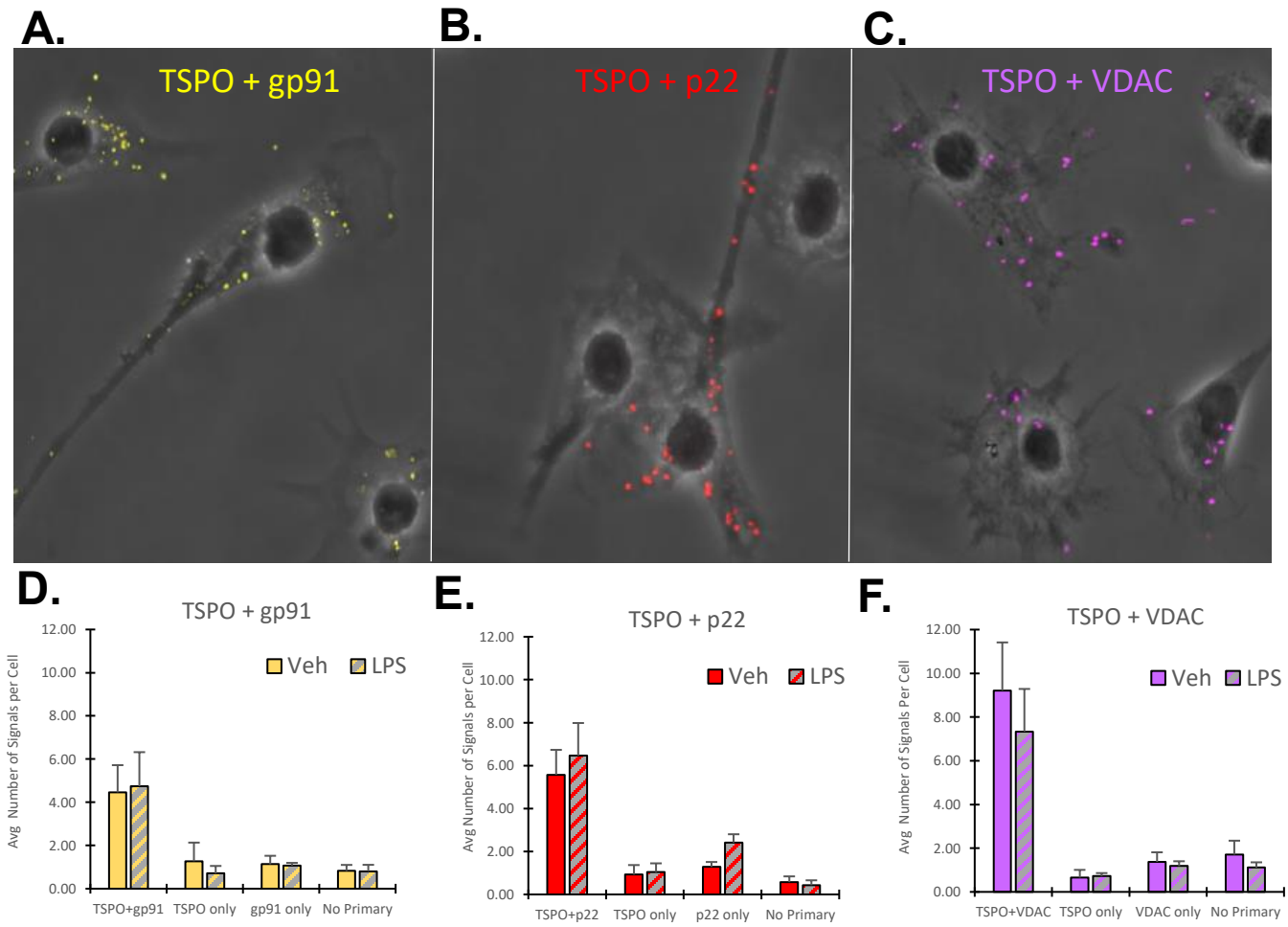

FIGURE 10. TSPO Duolink Proximity Ligation Assay in vehicle and LPS-stimulated primary microglia. Representative Duolink, phase & pseudo-colored confocal images of dual labeling condition: TSPO + gp91 (A); TSPO + p22 (B); TSPO + VDAC (C) with quantification of average number of Duolink signals per microglia in both vehicle and LPS (100 ng/mL) conditions at 18 hours (D, E, F). PLA experiments confirm that TSPO interacts with the NOX2 subunits $gp91^{phox}$ and $p22^{phox}$, as well as the mitochondrial protein, VDAC. Imaging and quantification included negative controls for labeling conditions of single antibody only, as well as no primary antibody, to ensure signal specificity. Data are expressed as mean ± s.e.m. n = 6-7 independent experiments with 30+ cells counted per treatment and per labeling condition.

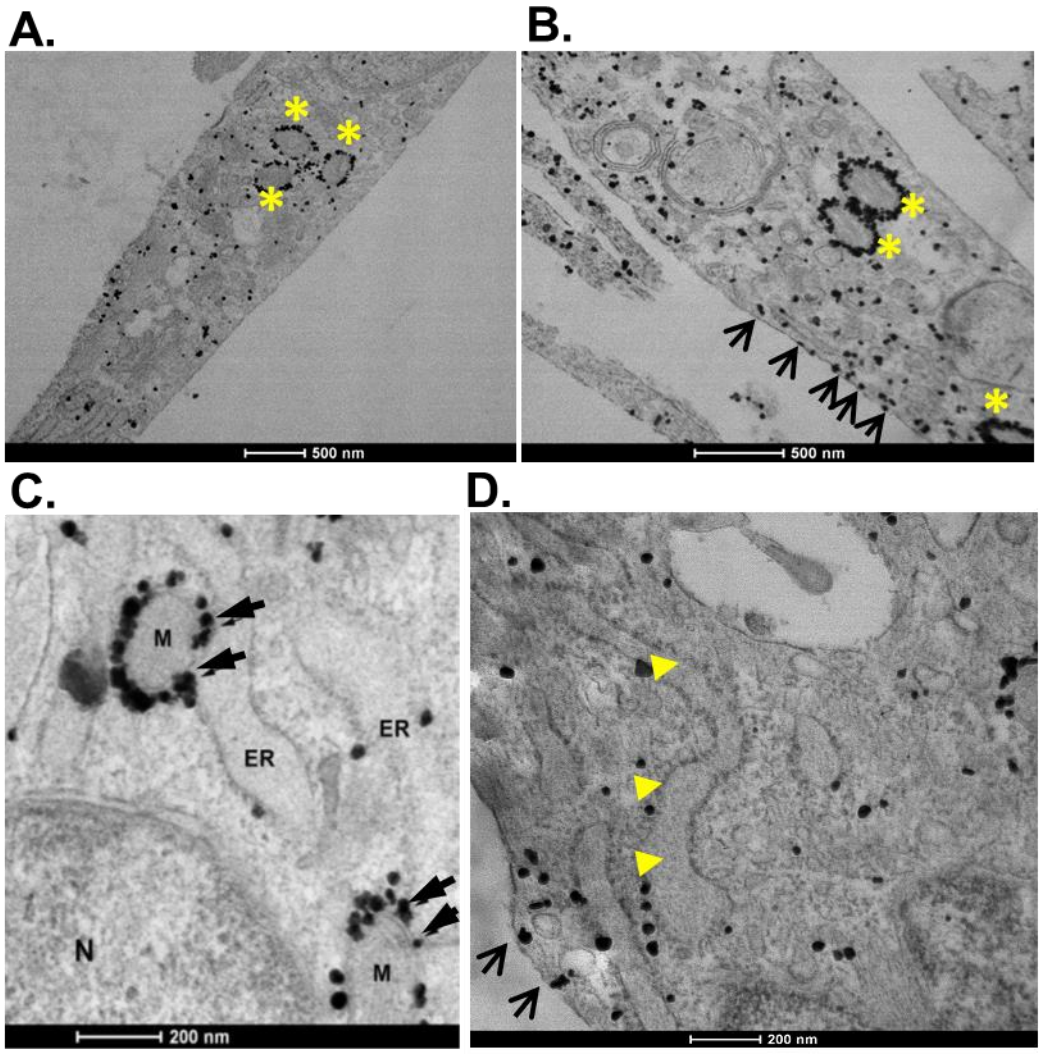

FIGURE 11. Immunogold electron microscopy of TSPO in primary microglia. TSPO labeling in vehicle (A) and LPS treated (B) cells. Yellow stars indicate TSPO labeling at the mitochondria, and black arrows indicate TSPO labeling at the plasma membrane. Higher magnification images (C and D) show TSPO is present at the mitochondria (M), the mitochondrial associated membrane (MAM) arrows)), and in the endoplasmic reticulum (ER) membrane as indicated by the yellow arrow heads. N= nucleus.
N.B. Immunogold electron microscopy completed by and courtesy of Dr. Sara Rose Guariglia.

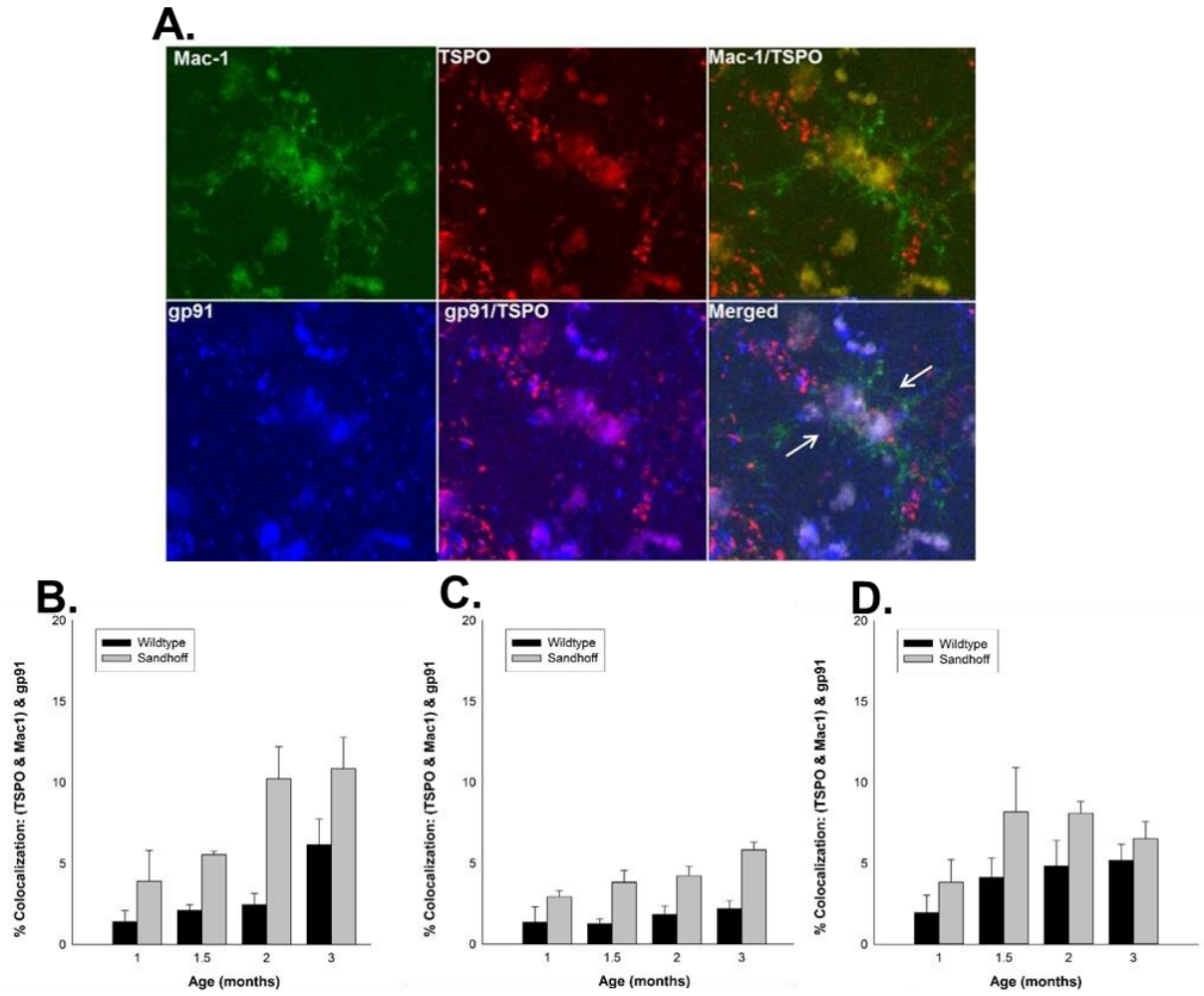

FIGURE 12. TSPO & gp91 in microglia *ex vivo.* TSPO & gp91 in microglia *in situ*

A) Representative triple labeled immunofluorescent confocal images in the thalamus of a 2 month Sandhoff disease mouse. Imaging confirmed that TSPO in Mac-1 labeled microglia colocalized with $gp91^{phox}$. B-D) Quantification of percent colocalization of TSPO in microglia with $gp91^{phox}$ in brain regions that demonstrate TSPO upregulation and neurodegeneration: the thalamus (B), cerebellum (C), and brainstem (D) in wildtype and Sandhoff disease mice. Percent colocalization appears to increase as a function of disease and age. (2-way ANOVA: Thalamus: Age: $F_{3,7}$= 4.257; p=0.017. Genotype: $F_{1,7}$=11.081; p = 0.003; Age x Genotype: $F_{3,7}$=1.548; p=0.232. Cerebellum: Age: $F_{3,7}$= 8528; p=0.001. Genotype: $F_{1,7}$=11.093; p = 0.003; Age x Genotype: $F_{3,7}$=0.896; p=0.460. Brainstem: Age: $F_{3,7}$= 1.827; p=0.170. Genotype: $F_{1,7}$=7.298; p = 0.013; Age x Genotype: $F_{3,7}$=0.399; p=0.755.) Each value represents the mean ± SEM. n = 4 animals and experiments.

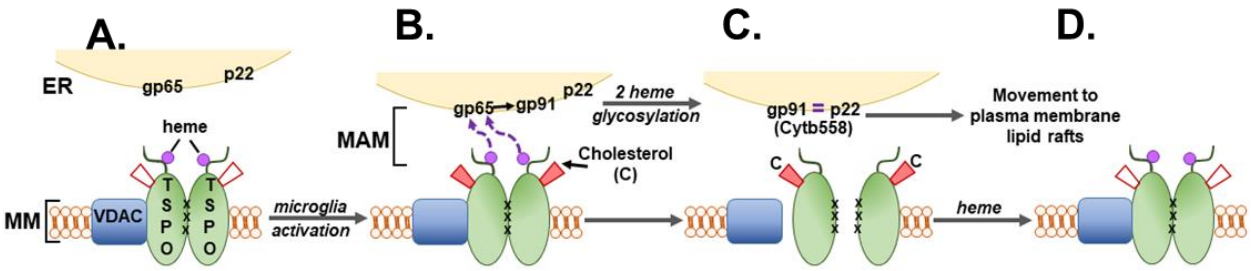

FIGURE 13. Working model of TSPO function in microglia. In a physiological state, TSPO exists as a dimer with 2 heme molecules bound at the outer mitochondrial membrane in conjunction with VDAC (A). When microglia are activated to a pro-inflammatory state (M1) via LPS, cholesterol binds to TSPO, the TSPO dimers dissociate from each other and VDAC at the GxxxG motif, and heme is effluxed from TSPO across the MAM to the ER. In the ER, gp65, the precursor of $gp91^{phox}$, receives the 2 heme molecules and is glycosylated to generate mature gp91phox (B). $gp91^{phox}$ is able to bind to $p22^{phox}$ via the 2 heme molecules, and this heterodimer (Cytb558) is able to traffic to other parts of the cell to form the active NOX2 enzyme complex (C). When microglia return to their physiological state, cholesterol is no longer bound to TSPO, TSPO reforms as a dimer and its association with VDAC, and heme rebinds to TSPO (D). In this way, the TSPO-NOX2-VDAC interaction modulates the subcellular localization of $gp91^{phox}$ and $p22^{phox}$ proteins, in order to ultimately alter NOX2 activity and help maintain redox homeostasis.

N.B. Figure design by Jennifer Dziedzic; Conceptualized by Dr. Tomás Guilarte and Meredith Loth

REFERENCES

Asagami, H., Hino, Y., Kang, D., Minakami, S., & Takeshige, K. (1994). Preferential heme transport through endoplasmic reticulum associated with mitochondria in rat liver. *Biochim Biophys Acta, 1193*(2), 345-352.

Bae, K. R., Shim, H. J., Balu, D., Kim, S. R., & Yu, S. W. (2014). Translocator protein 18 kDa negatively regulates inflammation in microglia. *J Neuroimmune Pharmacol, 9*(3), 424-437. doi:10.1007/s11481-014-9540-6

Bagchi, S., Fredriksson, R., & Wallen-Mackenzie, A. (2015). In Situ Proximity Ligation Assay (PLA). *Methods Mol Biol, 1318*, 149-159. doi:10.1007/978-1-4939-2742-5_15

Banati, R. B., Middleton, R. J., Chan, R., Hatty, C. R., Kam, W. W., Quin, C., . . . Liu, G. J. (2014). Positron emission tomography and functional characterization of a complete PBR/TSPO knockout. *Nat Commun, 5*, 5452. doi:10.1038/ncomms6452

Batoko, H., Veljanovski, V., & Jurkiewicz, P. (2015). Enigmatic Translocator protein (TSPO) and cellular stress regulation. *Trends Biochem Sci, 40*(9), 497-503. doi:10.1016/j.tibs.2015.07.001

Beckers, L., Ory, D., Geric, I., Declercq, L., Koole, M., Kassiou, M., . . . Baes, M. (2018). Increased Expression of Translocator Protein (TSPO) Marks Pro-inflammatory Microglia but Does Not Predict Neurodegeneration. *Mol Imaging Biol, 20*(1), 94-102. doi:10.1007/s11307-017-1099-1

Chen, M. K., & Guilarte, T. R. (2008). Translocator protein 18 kDa (TSPO): molecular sensor of brain injury and repair. *Pharmacol Ther, 118*(1), 1-17. doi:10.1016/j.pharmthera.2007.12.004

Choi, J., Ifuku, M., Noda, M., & Guilarte, T. R. (2011). Translocator protein (18 kDa)/peripheral benzodiazepine receptor specific ligands induce microglia functions consistent with an activated state. *Glia, 59*(2), 219-230. doi:10.1002/glia.21091

Coughlin, J. M., Wang, Y., Minn, I., Bienko, N., Ambinder, E. B., Xu, X., . . . Pomper, M. G. (2017). Imaging of Glial Cell Activation and White Matter Integrity in Brains of Active and Recently Retired National Football League Players. *JAMA Neurol, 74*(1), 67-74. doi:10.1001/jamaneurol.2016.3764

Coughlin, J. M., Wang, Y., Munro, C. A., Ma, S., Yue, C., Chen, S., . . . Pomper, M. G. (2015). Neuroinflammation and brain atrophy in former NFL players: An in vivo multimodal imaging pilot study. *Neurobiol Dis, 74*, 58-65. doi:10.1016/j.nbd.2014.10.019

Delavoie, F., Li, H., Hardwick, M., Robert, J. C., Giatzakis, C., Peranzi, G., . . . Papadopoulos, V. (2003). In vivo and in vitro peripheral-type benzodiazepine receptor polymerization: functional significance in drug ligand and cholesterol binding. *Biochemistry, 42*(15), 4506-4519. doi:10.1021/bi0267487

DeLeo, F. R., Burritt, J. B., Yu, L., Jesaitis, A. J., Dinauer, M. C., & Nauseef, W. M. (2000).

Processing and maturation of flavocytochrome b558 include incorporation of heme as a prerequisite for heterodimer assembly. *J Biol Chem, 275*(18), 13986-13993.

Fan, J., Campioli, E., Midzak, A., Culty, M., & Papadopoulos, V. (2015). Conditional steroidogenic cell-targeted deletion of TSPO unveils a crucial role in viability and hormone-dependent steroid formation. *Proc Natl Acad Sci U S A, 112*(23), 7261-7266. doi:10.1073/pnas.1502670112

Fan, J., Lindemann, P., Feuilloley, M. G., & Papadopoulos, V. (2012). Structural and functional evolution of the translocator protein (18 kDa). *Curr Mol Med, 12*(4), 369-386.

Fredriksson, S., Gullberg, M., Jarvius, J., Olsson, C., Pietras, K., Gustafsdottir, S. M., . . . Landegren, U. (2002). Protein detection using proximity-dependent DNA ligation assays. *Nat Biotechnol, 20*(5), 473-477. doi:10.1038/nbt0502-473

Fujimoto, M., & Hayashi, T. (2011). New insights into the role of mitochondria-associated endoplasmic reticulum membrane. *Int Rev Cell Mol Biol, 292*, 73-117. doi:10.1016/B978-0-12-386033-0.00002-5

Gatliff, J., & Campanella, M. (2016). TSPO: kaleidoscopic 18-kDa amid biochemical pharmacology, control and targeting of mitochondria. *Biochem J, 473*(2), 107-121. doi:10.1042/BJ20150899

Gatliff, J., East, D., Crosby, J., Abeti, R., Harvey, R., Craigen, W., . . . Campanella, M. (2014). TSPO interacts with VDAC1 and triggers a ROS-mediated inhibition of mitochondrial quality control. *Autophagy, 10*(12), 2279-2296. doi:10.4161/15548627.2014.991665

Gerhard, A., Pavese, N., Hotton, G., Turkheimer, F., Es, M., Hammers, A., . . . Brooks, D. J. (2006). In vivo imaging of microglial activation with [11C](R)-PK11195 PET in idiopathic Parkinson's disease. *Neurobiol Dis, 21*(2), 404-412. doi:10.1016/j.nbd.2005.08.002

Giniatullin, A., Petrov, A., & Giniatullin, R. (2015). The involvement of P2Y12 receptors, NADPH oxidase, and lipid rafts in the action of extracellular ATP on synaptic transmission at the frog neuromuscular junction. *Neuroscience, 285*, 324-332. doi:10.1016/j.neuroscience.2014.11.039

Giorgi, C., Missiroli, S., Patergnani, S., Duszynski, J., Wieckowski, M. R., & Pinton, P. (2015). Mitochondria-associated membranes: composition, molecular mechanisms, and physiopathological implications. *Antioxid Redox Signal, 22*(12), 995-1019. doi:10.1089/ars.2014.6223

Giulian, D., & Baker, T. J. (1986). Characterization of ameboid microglia isolated from developing mammalian brain. *J Neurosci, 6*(8), 2163-2178.

Giulian, D., & Baker, T. J. (1986). Characterization of ameboid microglia isolated from developing mammalian brain. *J Neurosci, 6*(8), 2163-2178.

Goldman, B. S., Beck, D. L., Monika, E. M., & Kranz, R. G. (1998). Transmembrane heme

delivery systems. *Proc Natl Acad Sci U S A, 95*(9), 5003-5008.

Gordon, R., Hogan, C. E., Neal, M. L., Anantharam, V., Kanthasamy, A. G., & Kanthasamy, A. (2011). A simple magnetic separation method for high-yield isolation of pure primary microglia. *J Neurosci Methods, 194*(2), 287-296. doi:10.1016/j.jneumeth.2010.11.001

Guilarte, T. R., Loth, M. K., & Guariglia, S. R. (2016). TSPO Finds NOX2 in Microglia for Redox Homeostasis. *Trends Pharmacol Sci, 37*(5), 334-343. doi:10.1016/j.tips.2016.02.008

Gullberg, M., Gustafsdottir, S. M., Schallmeiner, E., Jarvius, J., Bjarnegard, M., Betsholtz, C., . . . Fredriksson, S. (2004). Cytokine detection by antibody-based proximity ligation. *Proc Natl Acad Sci U S A, 101*(22), 8420-8424. doi:10.1073/pnas.0400552101

Hachez, C., Veljanovski, V., Reinhardt, H., Guillaumot, D., Vanhee, C., Chaumont, F., & Batoko, H. (2014). The Arabidopsis abiotic stress-induced TSPO-related protein reduces cell-surface expression of the aquaporin PIP2;7 through protein-protein interactions and autophagic degradation. *Plant Cell, 26*(12), 4974-4990. doi:10.1105/tpc.114.134080

Hanisch, U. K., & Kettenmann, H. (2007). Microglia: active sensor and versatile effector cells in the normal and pathologic brain. *Nat Neurosci, 10*(11), 1387-1394. doi:10.1038/nn1997

Innamorato, N. G., Lastres-Becker, I., & Cuadrado, A. (2009). Role of microglial redox balance in modulation of neuroinflammation. *Curr Opin Neurol, 22*(3), 308-314. doi:10.1097/WCO.0b013e32832a3225

Issop, L., Fan, J., Lee, S., Rone, M. B., Basu, K., Mui, J., & Papadopoulos, V. (2015). Mitochondria-associated membrane formation in hormone-stimulated Leydig cell steroidogenesis: role of ATAD3. *Endocrinology, 156*(1), 334-345. doi:10.1210/en.2014-1503

Jaipuria, G., Leonov, A., Giller, K., Vasa, S. K., Jaremko, L., Jaremko, M., . . . Zweckstetter, M. (2017). Cholesterol-mediated allosteric regulation of the mitochondrial translocator protein structure. *Nat Commun, 8*, 14893. doi:10.1038/ncomms14893

Jalili, R., Horecka, J., Swartz, J. R., Davis, R. W., & Persson, H. H. J. (2018). Streamlined circular proximity ligation assay provides high stringency and compatibility with low-affinity antibodies. *Proc Natl Acad Sci U S A, 115*(5), E925-E933. doi:10.1073/pnas.1718283115

Jamin, N., Neumann, J. M., Ostuni, M. A., Vu, T. K., Yao, Z. X., Murail, S., . . . Lacapere, J. J. (2005). Characterization of the cholesterol recognition amino acid consensus sequence of the peripheral-type benzodiazepine receptor. *Mol Endocrinol, 19*(3), 588-594. doi:10.1210/me.2004-0308

Kim, E. Y., Anderson, M., Wilson, C., Hagmann, H., Benzing, T., & Dryer, S. E. (2013). NOX2 interacts with podocyte TRPC6 channels and contributes to their activation by diacylglycerol: essential role of podocin in formation of this complex. *Am J Physiol Cell Physiol, 305*(9), C960-971. doi:10.1152/ajpcell.00191.2013

Kuszpit, K., Hollidge, B. S., Zeng, X., Stafford, R. G., Daye, S., Zhang, X., . . . Bocan, T. M.

(2018). [(18)F]DPA-714 PET Imaging Reveals Global Neuroinflammation in Zika Virus-Infected Mice. *Mol Imaging Biol, 20*(2), 275-283. doi:10.1007/s11307-017-1118-2

Lavisse, S., Guillermier, M., Herard, A. S., Petit, F., Delahaye, M., Van Camp, N., . . . Escartin, C. (2012). Reactive astrocytes overexpress TSPO and are detected by TSPO positron emission tomography imaging. *J Neurosci, 32*(32), 10809-10818. doi:10.1523/JNEUROSCI.1487-12.2012

Li, F., Xia, Y., Meiler, J., & Ferguson-Miller, S. (2013). Characterization and modeling of the oligomeric state and ligand binding behavior of purified translocator protein 18 kDa from Rhodobacter sphaeroides. *Biochemistry, 52*(34), 5884-5899. doi:10.1021/bi400431t

Liu, G. J., Middleton, R. J., Hatty, C. R., Kam, W. W., Chan, R., Pham, T., . . . Banati, R. B. (2014). The 18 kDa translocator protein, microglia and neuroinflammation. *Brain Pathol, 24*(6), 631-653. doi:10.1111/bpa.12196

Loth, M. K., Choi, J., McGlothan, J. L., Pletnikov, M. V., Pomper, M. G., & Guilarte, T. R. (2016). TSPO in a murine model of Sandhoff disease: presymptomatic marker of neurodegeneration and disease pathophysiology. *Neurobiol Dis, 85*, 174-186. doi:10.1016/j.nbd.2015.11.001

Maeda, J., Higuchi, M., Inaji, M., Ji, B., Haneda, E., Okauchi, T., . . . Suhara, T. (2007). Phase-dependent roles of reactive microglia and astrocytes in nervous system injury as delineated by imaging of peripheral benzodiazepine receptor. *Brain Res, 1157*, 100-111. doi:10.1016/j.brainres.2007.04.054

Marchi, S., Patergnani, S., & Pinton, P. (2014). The endoplasmic reticulum-mitochondria connection: one touch, multiple functions. *Biochim Biophys Acta, 1837*(4), 461-469. doi:10.1016/j.bbabio.2013.10.015

McEnery, M. W., Snowman, A. M., Trifiletti, R. R., & Snyder, S. H. (1992). Isolation of the mitochondrial benzodiazepine receptor: association with the voltage-dependent anion channel and the adenine nucleotide carrier. *Proc Natl Acad Sci U S A, 89*(8), 3170-3174.

Miao, B., & Degterev, A. (2009). Methods to analyze cellular necroptosis. *Methods Mol Biol, 559*, 79-93. doi:10.1007/978-1-60327-017-5_6

Morohaku, K., Pelton, S. H., Daugherty, D. J., Butler, W. R., Deng, W., & Selvaraj, V. (2014). Translocator protein/peripheral benzodiazepine receptor is not required for steroid hormone biosynthesis. *Endocrinology, 155*(1), 89-97. doi:10.1210/en.2013-1556

Nayernia, Z., Jaquet, V., & Krause, K. H. (2014). New insights on NOX enzymes in the central nervous system. *Antioxid Redox Signal, 20*(17), 2815-2837. doi:10.1089/ars.2013.5703

Papadopoulos, V., Baraldi, M., Guilarte, T. R., Knudsen, T. B., Lacapere, J. J., Lindemann, P., . . . Gavish, M. (2006). Translocator protein (18kDa): new nomenclature for the peripheral-type benzodiazepine receptor based on its structure and molecular function. *Trends Pharmacol Sci, 27*(8), 402-409. doi:10.1016/j.tips.2006.06.005

Politis, M., Giannetti, P., Su, P., Turkheimer, F., Keihaninejad, S., Wu, K., . . . Piccini, P. (2012).

Increased PK11195 PET binding in the cortex of patients with MS correlates with disability. *Neurology, 79*(6), 523-530. doi:10.1212/WNL.0b013e3182635645

Richard-Fogal, C., & Kranz, R. G. (2010). The CcmC:heme:CcmE complex in heme trafficking and cytochrome c biosynthesis. *J Mol Biol, 401*(3), 350-362. doi:10.1016/j.jmb.2010.06.041

Rone, M. B., Fan, J., & Papadopoulos, V. (2009). Cholesterol transport in steroid biosynthesis: role of protein-protein interactions and implications in disease states. *Biochim Biophys Acta, 1791*(7), 646-658. doi:10.1016/j.bbalip.2009.03.001

Ryder, E., Doe, B., Gleeson, D., Houghton, R., Dalvi, P., Grau, E., . . . Ramirez-Solis, R. (2014). Rapid conversion of EUCOMM/KOMP-CSD alleles in mouse embryos using a cell-permeable Cre recombinase. *Transgenic Res, 23*(1), 177-185. doi:10.1007/s11248-013-9764-x

Schmittgen, T. D., & Livak, K. J. (2008). Analyzing real-time PCR data by the comparative C(T) method. *Nat Protoc, 3*(6), 1101-1108.

Shao, D., Segal, A. W., & Dekker, L. V. (2003). Lipid rafts determine efficiency of NADPH oxidase activation in neutrophils. *FEBS Lett, 550*(1-3), 101-106.

Sileikyte, J., Petronilli, V., Zulian, A., Dabbeni-Sala, F., Tognon, G., Nikolov, P., . . . Ricchelli, F. (2011). Regulation of the inner membrane mitochondrial permeability transition by the outer membrane translocator protein (peripheral benzodiazepine receptor). *J Biol Chem, 286*(2), 1046-1053. doi:10.1074/jbc.M110.172486

Stansfield, K. H., Pilsner, J. R., Lu, Q., Wright, R. O., & Guilarte, T. R. (2012). Dysregulation of BDNF-TrkB signaling in developing hippocampal neurons by Pb(2+): implications for an environmental basis of neurodevelopmental disorders. *Toxicol Sci, 127*(1), 277-295. doi:10.1093/toxsci/kfs090

Taketani, S., Kohno, H., Furukawa, T., & Tokunaga, R. (1995). Involvement of peripheral-type benzodiazepine receptors in the intracellular transport of heme and porphyrins. *J Biochem, 117*(4), 875-880.

Tamse, C., Lu, X., Mortel, E., Cabrales, E., Feng, W., & Schaefer, S. (2008). The peripheral benzodiazepine receptor modulates Ca2+ transport through the VDAC in rat heart mitochondria. *Journal of Clinical and Basic Cardiology, 11*(1), 24-29.

Taylor, J. M., Allen, A. M., & Graham, A. (2014). Targeting mitochondrial 18 kDa translocator protein (TSPO) regulates macrophage cholesterol efflux and lipid phenotype. *Clin Sci (Lond), 127*(10), 603-613. doi:10.1042/CS20140047

Teboul, D., Beaufils, S., Taveau, J. C., Iatmanen-Harbi, S., Renault, A., Venien-Bryan, C., . . . Lacapere, J. J. (2012). Mouse TSPO in a lipid environment interacting with a functionalized monolayer. *Biochim Biophys Acta, 1818*(11), 2791-2800. doi:10.1016/j.bbamem.2012.06.020

Thinnes, F. P. (2012). On GxxxG in N-terminal stretches of type-1 VDAC/porin: critical in vertebrate apoptosis, missing in plants. *Plant Mol Biol, 79*(1-2), 1-3. doi:10.1007/s11103-012-

9900-7

Tu, L. N., Morohaku, K., Manna, P. R., Pelton, S. H., Butler, W. R., Stocco, D. M., & Selvaraj, V. (2014). Peripheral benzodiazepine receptor/translocator protein global knock-out mice are viable with no effects on steroid hormone biosynthesis. *J Biol Chem, 289*(40), 27444-27454. doi:10.1074/jbc.M114.578286

van Vliet, A. R., Verfaillie, T., & Agostinis, P. (2014). New functions of mitochondria associated membranes in cellular signaling. *Biochim Biophys Acta, 1843*(10), 2253-2262. doi:10.1016/j.bbamcr.2014.03.009

Vanhee, C., Zapotoczny, G., Masquelier, D., Ghislain, M., & Batoko, H. (2011). The Arabidopsis multistress regulator TSPO is a heme binding membrane protein and a potential scavenger of porphyrins via an autophagy-dependent degradation mechanism. *Plant Cell, 23*(2), 785-805. doi:10.1105/tpc.110.081570

Veenman, L., Shandalov, Y., & Gavish, M. (2008). VDAC activation by the 18 kDa translocator protein (TSPO), implications for apoptosis. *J Bioenerg Biomembr, 40*(3), 199-205. doi:10.1007/s10863-008-9142-1

Veenman, L., Vainshtein, A., Yasin, N., Azrad, M., & Gavish, M. (2016). Tetrapyrroles as Endogenous TSPO Ligands in Eukaryotes and Prokaryotes: Comparisons with Synthetic Ligands. *Int J Mol Sci, 17*(6). doi:10.3390/ijms17060880

Verma, A., Nye, J. S., & Snyder, S. H. (1987). Porphyrins are endogenous ligands for the mitochondrial (peripheral-type) benzodiazepine receptor. *Proc Natl Acad Sci U S A, 84*(8), 2256-2260.

Vilhardt, F., & van Deurs, B. (2004). The phagocyte NADPH oxidase depends on cholesterol-enriched membrane microdomains for assembly. *EMBO J, 23*(4), 739-748. doi:10.1038/sj.emboj.7600066

Wang, M., Wang, X., Zhao, L., Ma, W., Rodriguez, I. R., Fariss, R. N., & Wong, W. T. (2014). Macroglia-microglia interactions via TSPO signaling regulates microglial activation in the mouse retina. *J Neurosci, 34*(10), 3793-3806. doi:10.1523/JNEUROSCI.3153-13.2014

Yeliseev, A. A., & Kaplan, S. (1995). A sensory transducer homologous to the mammalian peripheral-type benzodiazepine receptor regulates photosynthetic membrane complex formation in Rhodobacter sphaeroides 2.4.1. *J Biol Chem, 270*(36), 21167-21175.

Yeliseev, A. A., & Kaplan, S. (1999). A novel mechanism for the regulation of photosynthesis gene expression by the TspO outer membrane protein of Rhodobacter sphaeroides 2.4.1. *J Biol Chem, 274*(30), 21234-21243.

Yeliseev, A. A., & Kaplan, S. (2000). TspO of rhodobacter sphaeroides. A structural and functional model for the mammalian peripheral benzodiazepine receptor. *J Biol Chem, 275*(8), 5657-5667.

Yeliseev, A. A., Krueger, K. E., & Kaplan, S. (1997). A mammalian mitochondrial drug receptor functions as a bacterial "oxygen" sensor. *Proc Natl Acad Sci U S A, 94*(10), 5101-5106.

Yu, L., Quinn, M. T., Cross, A. R., & Dinauer, M. C. (1998). Gp91(phox) is the heme binding subunit of the superoxide-generating NADPH oxidase. *Proc Natl Acad Sci U S A, 95*(14), 7993-7998.

Yu, L., Zhen, L., & Dinauer, M. C. (1997). Biosynthesis of the phagocyte NADPH oxidase cytochrome b558. Role of heme incorporation and heterodimer formation in maturation and stability of gp91phox and p22phox subunits. *J Biol Chem, 272*(43), 27288-27294.

Yu, X., Song, N., Guo, X., Jiang, H., Zhang, H., & Xie, J. (2016). Differences in vulnerability of neurons and astrocytes to heme oxygenase-1 modulation: Implications for mitochondrial ferritin. *Sci Rep, 6*, 24200. doi:10.1038/srep24200

Zavala, F., Masson, A., Brys, L., de Baetselier, P., & Descamps-Latscha, B. (1991). A monoclonal antibody against peripheral benzodiazepine receptor activities the human neutrophil NADPH-oxidase. *Biochem Biophys Res Commun, 176*(3), 1577-1583.

Zavala, F., Veber, F., Taupin, V., Nguyen, A. T., & Descamps-Latscha, B. (1990). Reconstitution of peripheral benzodiazepine receptor expression in X-linked chronic granulomatous disease by interferon-gamma. *Lancet, 336*(8717), 758-759.

Zimmer, E. R., Leuzy, A., Benedet, A. L., Breitner, J., Gauthier, S., & Rosa-Neto, P. (2014). Tracking neuroinflammation in Alzheimer's disease: the role of positron emission tomography imaging. *J Neuroinflammation, 11*, 120. doi:10.1186/1742-2094-11-120

Zurcher, N. R., Loggia, M. L., Lawson, R., Chonde, D. B., Izquierdo-Garcia, D., Yasek, J. E., . . . Atassi, N. (2015). Increased in vivo glial activation in patients with amyotrophic lateral sclerosis: assessed with [(11)C]-PBR28. *Neuroimage Clin, 7*, 409-414. doi:10.1016/j.nicl.2015.01.009

Chapter 5: Conclusions & Future Directions

CONCLUSIONS

In summary, this series of studies generated some potential answers and raised several critical questions about TSPO in the brain. First, in specific aim 1, we confirmed the use of TSPO as a biomarker of brain injury in a genetic model of neurodegeneration, Sandhoff disease. Upregulation of TSPO was regionally and temporally specific and appeared prior to detection of neurodegeneration and behavioral manifestations of disease. Additionally, this is one of the first studies to longitudinally track the cellular source of TSPO (microglia or astrocytes) and how the TSPO cellular signal varied across brain region and disease progression. As we come to understand the function of TSPO, it will be critical to understand which cell type the TSPO signal is originating from in the onset and progression of neuroinflammation.

Second, we confirmed the use of a novel TSPO ligand [^{125}I]-IodoDPA-713 for both *in vivo* imaging and *ex vivo* quantitative autoradiography. The use of an iodinated ligand has two major technical advantages. Development of an autoradiogram changes from 6 weeks with the tritiated ligand, to 1 hour for an iodinated ligand. In regards to *in vivo* imaging, the ability to use [^{125}I]-IodoDPA-713 in SPECT studies eliminates the need to have an in-house cyclotron for ligands that are labeled with ^{11}C for PET studies.

Given that we have characterized TSPO so extensively in the CNS, this model would also be useful to examine TSPO in the peripheral blood cells to determine if TSPO levels in the CNS correlate with TSPO levels in the blood. Non-invasive and low cost techniques would be extremely valuable to assessing neuroinflammation given the only way to currently determine TSPO levels in the brain is through PET imaging (high cost) or biopsy (highly invasive).

In conjunction with our TSPO-related discoveries, we also added two novel pathological findings in the Sandhoff disease murine model. We detected neurodegeneration in the CA2 region of the hippocampus, which to our knowledge, has not been previously documented. We also confirmed prior *in vitro* studies indicating that astrocytes cultured from Sandhoff disease mice have increased proliferation (Kawashima et al 2009) and increased number of GFAP-positive astrocytes, even when β-hexosaminidase was conditionally expressed in neurons (Kyrkanides et al 2012). At the whole animal level, we detected an increase in hypertrophic and GFAP-positive astrocytes at 1 month, further supporting increased proliferation and potentially abnormally functioning astrocytes in this Sandhoff disease animal model.

In addition to our TSPO biomarker studies, we have contributed significantly to questions on the function of TSPO, specifically within the context of microglia. In specific aim 2, we have explored the relationship between TSPO and NADPH oxidase (NOX2), both in terms of ROS production, as well as protein-protein interactions. First, we provided multiple lines of evidence supporting that the TSPO-ligand induced increase in ROS production in microglia is derived from NOX2 and not from the mitochondria. Further, we have done preliminary assessment in regards to the antioxidant response being mounted after 24 hours of TSPO-ligand exposure through activation/translocation of Nrf2 to the nucleus and activation of HO-1 by Ro, but perhaps not PK.

To expand on the TSPO and NOX2 relationship, we examined whether TSPO was physically interacting with NOX2. We confirmed that TSPO is interacting with the NOX2 subunits, $gp91^{phox}$ and $p22^{phox,}$ as well as the mitochondrial protein VDAC using three independent experimental methods: 1) colocalization analyses of triple labeled immunofluorescence; 2) TSPO immunoprecipitation that confirms co-immunoprecipitation of gp91, p22, and VDAC; and 3) TSPO Duolink Proximity Ligation Assay that confirms TSPO interacts with $gp91^{phox}$, $p22^{phox}$, and

VDAC. Our immunofluorescence and immuno electron microscopy data suggests that the putative TSPO- gp91^{phox}-p22^{phox}-VDAC complex may occur at the mitochondrial associated ER membrane (MAM). Our data also indicates that TSPO's interaction with both of the NOX2 subunits and VDAC is disrupted by microglia activation.

Collectively, these results are consistent with the model we propose in Figure 13, Chapter 4. As our model rests on TSPO's well-documented ability to bind both heme and cholesterol (Li et al 2014; Jaipuria et al 2017; Yeliseev and Kaplan 1999), several questions relating to heme and cholesterol binding and subcellular localization in microglia arise. Can we detect heme binding to TSPO in microglia, specifically within a TSPO pulldown? Based on our IP results, we would expect to see more heme bound to TSPO in the non-activated condition vs the LPS-activated condition. Does adding cholesterol (or blocking cholesterol synthesis) change the degree of the TSPO-NOX interaction? We would hypothesize that adding cholesterol would increase dissociation of the TSPO homodimers, as presumably the cholesterol would bind to the CRAC domain and shift the equilibrium towards monomers. If cholesterol is bound, then TSPO's affinity for heme is decreased, and hence we would expect to see a decrease in the TSPO-NOX2 subunits interaction since TSPO would not be able to bind heme.

How does LPS treatment affect cholesterol levels? Perhaps part of the reason we are seeing a decreased TSPO-NOX2 subunit interaction is because LPS treatment actually increases cholesterol synthesis, and thereby increases the cholesterol available to bind to TSPO and encourages dissociation of the TSPO homodimers.

What is the monomer:dimer (oligomer?) ratio in activated and non-activated conditions and how does adding cholesterol change this ratio? Is the TSPO-NOX interaction occurring in other compartments in the cell? Is TSPO interacting with other proteins besides NOX and VDAC?

These are just some of the several interesting lines of investigation that arise based on our current findings.

Limitations & Future Directions

In addition to the questions stated above, there are additional lines of evidence that can be pursued in addressing the specific aims. While we have gained a better understanding of how the TSPO-NOX2 interaction changes when stimulated with the M1 proinflammatory activator LPS, it would be beneficial to examine the TSPO-NOX2 interaction with more endogenous activators such as ATP. While both are documented to generate a pro-inflammatory response in microglia, LPS and ATP act through different mechanisms. LPS is derived from the outer membranes of Gram-negative bacteria, and therefore, microglia recognize the material as foreign and non-self. LPS triggers a pro-inflammatory response by binding to toll-like receptor 4 (TLR 4) (Block et al 2007). This subsequently leads to the activation of the IKK complex, degradation of IκB, and activation of the NF-κB pathway (Akira and Takeda, 2004). In contrast, ATP effects are mediated through purinergic receptors (Haynes et al 2006; Skaper et al 2010). ATP is a chemical signal released by injured neurons and can be detected by microglia via P2X and P2Y purinergic receptors (Haynes et al., 2006; Skaper et al., 2010). Neurons can release ATP during neuronal injury, and microglia can rapidly respond to ATP via chemotaxis and binding to purinergic receptors such as $P2X_7$, which results in the opening of channels permeable to Na^+, K^+, and Ca^{2+}. Subsequently, $P2X_7$ receptor activation can lead to activation of phospholipases A_2 and D and MAP kinases, which can influence the transcriptional activities of not only NF-κB but also CREB and AP-1. Thus, particularly in neurodegenerative diseases, ATP may be a particularly relevant activator of microglia and worthy of investigating as a model of activation and mediator of the TSPO-NOX2 interaction.

Additionally, it would be valuable to induce an anti-inflammatory "M2" phenotype (perhaps by using IL-4) in microglia and asses TSPO levels and TSPO's interaction with NOX2. Previously, IL-4 exposure has been shown to have an effect on NOX2 subunit gene expression with gp91(CYBB) and p22(CYBA) being up regulated at 4 hours, and being down regulated at 8 hours and further downregulated at 24 hours in primary rat cortical microglia (Savchenko et al 2013). In regards to TSPO, there is conflicting evidence as to whether TSPO is associated with more of a M1 or M2 phenotype. Bae and colleagues found that TSPO negatively regulates inflammation in microglia and increased TSPO expression is associated with increased M2 stage related genes at 24 hours in BV-2 cells, a transformed microglia cell line (Bae et al 2014). However, Beckers et al 2018 found that TSPO gene expression was increased at 24 hours through M1 phenotype induction (by either LPS or IL-1β/IFNγ) and not through M2 phenotype induction via IL-4 in primary mouse microglia. Taken together, these studies demonstrate how different cell models can generate conflicting data (BV-2 cells vs primary microglia), and also how critical it is to do time course experiments to better perceive and clarify molecular pathways and trajectories (upregulation of CYBB and CYBA at 4 hours and down regulation at 8 and 24 hours).

Further, to gain more insight into how TSPO-ligands are working to activate microglia and why it is that one TSPO ligand is protective and the other is not, it would be interesting to examine whether the TSPO-NOX2 interaction changes when exposing the cells to the TSPO-ligands PK or Ro. For example, we have not yet examined if TSPO ligands change protein levels or activity levels of NOX2. It will be interesting to determine if TSPO-L exposure changes protein expression of NOX2 subunits and if these exposures also have a functional effect in terms of NOX2 activity levels. As previously stated, PK and Ro have different binding sites on TSPO (Figure 1, Chapter 1). Traditionally, PK has been viewed as an antagonist and Ro has been viewed as an agonist.

Thermodynamic analysis has shown that [^{3}H]-Ro5-4864 binding is enthalpy driven while [^{3}H]-PK11195 is entropy driven. Thus, it has been suggested that Ro5-4864 might be a TSPO agonist or partial agonist while PK11195 might be a TSPO antagonist (Le Fur et al 1983). However, this classification is not definitive as reports have indicated that these ligands exert similar or opposite effects under various physiological conditions such as apoptosis (Veenman et al2007). In our model of primary microglia, we have seen similar effects of PK and Ro (increase in ROS production; increase in Nrf2 translocation). However, as documented in Choi et al 2011, there are differential effects of these ligands in primary microglia as well. For example, exposure to Ro in the presence of LPS increased the number of apoptotic microglia, an effect that could be blocked by PK. These differential effects are also seen within various models of disease. In a model of Alzheimer's, Ro ligand administration has been shown to improve both behavioral outcomes and pathology associated with AD, whereas PK only demonstrated modest improvement in reduced levels of soluble β-amyloid (Barron et al 2013). However, in other disease models such as ALS, PK ligand administration has been shown to improve behavioral outcomes in females and decrease motor neuron death *in vitro* whereas other TSPO ligands had no effect (Obis el al 2018, in preparation). Taken together, these data further support that TSPO-ligands may have different mechanisms of action and initiate different molecular signaling cascades, and therefore need to be studied independently.

Species differences

It is important to note that there have been some studies that indicate species differences, particularly within regards to ROS production. Colton and colleagues assessed both ROS and nitric oxide (NO) production in human, hamster, rat, or mouse microglia. After 2 hours stimulation with opsonized zymosan, human and hamster microglia generate similar levels of superoxide, whereas

rat microglia produced significantly less superoxide. When measuring NO, microglia were stimulated with LPS 5ug/mL, rIL-1β (200U/mL), and TNF-α (1000U/mL) for 48 hours. Human and hamster microglia responded similarly, whereas mouse microglia had a much larger response. This study indicates that perhaps hamster microglia may be more representative of human microglia in terms of the magnitude and timing of their response. However, it is important to note that the dose and time point for the NO production assay are particularly high (5 ug/mL LPS) and long (48 hours) respectively, particularly for microglia. Thus, the viability of these cells should be confirmed at these doses and time points in order to confirm that cells are still alive, and a physiological effect is being measured as opposed to an effect in a dying cell.

Related to these species differences reported, a report by Owen et al 2017 documented no change in TSPO gene expression levels in human adult microglia or human fetal microglia when stimulated with IFN-γ/LPS or IL4/IL13 for 48 hours. This was in contrast to murine primary microglia which had a 9 fold increase in TSPO gene expression when stimulated with IFN-γ/LPS for 48 hours. While human microglia were confirmed to be live and responsive to stimulation as assessed by increased TNF-α levels, it would still be beneficial to again examine different time points to assess if human microglia do not actually upregulate TSPO in response to these stimuli, or if it is merely a missed window of detection. Given the drastically different life spans of rodents and humans, it would not be entirely surprising if their molecular temporal responses to various stimuli varied even slightly. It should also be noted that the human adult microglia were isolated from epileptic patients, and thus may not be representative of the physiological response of microglia. Additionally, this data calls into major question, if microglia are not responsible for the upregulation of TSPO, then exactly which cell type *is* upregulating TSPO in the human PET studies?

Cell culture models

All cell culture studies in this dissertation were performed in microglia only cultures, (~94% pure). While this is critical in isolating how TSPO and NOX2 interact in microglia, it is not necessarily indicative of what is happening at the whole brain level and the cross-talk among the various cell types. While we did confirm that TSPO colocalizes with $gp91^{phox}$ in Mac-1 labeled cells in the Sandhoff disease brain, and thus verified that the TSPO-NOX2 association is not merely an epiphenomenon of cell culture conditions, it would be useful to look in a model that is more representative of what is happening in the brain. A potential stepping stone before moving to the whole animal, would be to examine TSPO within a mixed glial culture. In this way, microglia and astrocytes, both of which express and upregulate TSPO, would be able to communicate with each other. The cross-talk between these two cell types is well documented in studies by Liddelow et al 2017 and Rothhammer et al 2018, among several others, and in particular, the ways in which microglia modulate pro-inflammatory and neurotoxic activities in astrocytes. It is possible that without the astrocyte input and trophic support, microglia behave slightly differently in their activation response. For example, experiments in primary mouse microglia only are generally not performed at time points outside of 48 hours due to the fact that more than 50% of the plate pure primary microglia die after 48 hours of incubation under normal culture conditions. This severely limits the types of experiments that can be done with primary microglia. Therefore, doing experiments in a mixed glial culture, as well as microglia only cultures and astrocyte only cultures, would provide insight into the communication between these two cell types and how together they contribute to TSPO biology.

Astrocytes, as previously mentioned, are the other type of cell within the brain that express and upregulate TSPO in response to brain injury. However, astrocytes and microglia have different

temporal responses in their TSPO response (Loth et al 2016; Kuhlman & Guilarte 1999 and 2000; Chen et al 2004; Maeda et al 2007; Lavisse et al 2012). This differential response indicates that TSPO is potentially serving different functions in microglia vs astrocytes. Astrocytes are cells that are more steroidogenic in nature, and thus it is plausible that the function of TSPO in astrocytes is more closely related to steroidogenesis. Preliminary data from out lab indicates that *Cyp11a*, the gene that encodes cytochrome P450scc to convert cholesterol to pregnenolone as the first step in steroidogenesis, is expressed 10 fold higher in rat astrocytes as compared to microglia (Figure 1). Of note, microglia are of myeloid origin whereas astrocytes originate from progenitor cells in the neuroepithelium of the developing CNS (Salter & Beggs 2014).

Sex differences

Additionally, it will be useful to examine if there are sex specific differences in cells cultured from male pups only vs female pups only, in both microglia and astrocytes. Up until recently, only a handful studies have controlled for sex when culturing cells from neonates. Both astrocytes and microglia are known to be sexually dimorphic in number, differentiation, and function (Santos-Galindo et al 2011; Kopec et al 2017; Lenz et al 2013; Prilutsky et al 2017;), even before sexual maturity. There is also evidence that even neonatal exposure to steroids can affect the inflammatory response of astrocytes as cultures generated from males only or females only show different inflammatory response profiles (Kuo et al 2010; Santos-Galindo et al 2011). Additionally, TSPO upregulation has been shown to be sexually dimorphic in some contexts including the heart in a myocarditis model (Fairweather et al 2014), renal tissue in an inescapable shock model (Drugan et al 1991); adrenal, renal, and gonadal tissue in an early handling and environmental stress model (Weizman et al 1999); endocrine and immune tissues in a prenatal diazepam exposure model (Burgi et al 2000); and proximal tubules in renal tissue in a model of

renal ischemia reperfusion model (Robert et al 2011). Only a handful of studies have examined sexual dimorphism and TSPO in the brain (Mirzatoni et al 2010; Santos-Galindo et al 2011; Garcia et al 2008), and two out of three of these studies looked at TSPO at the whole brain or brain region level (cerebellum), with the Santos-Galindo study being the only study to examining TSPO sexual dimorphism on the cellular level (astrocytes).

Related to sexual dimorphism in seen in TSPO, several neurological diseases including multiple sclerosis, Parkinson's disease, schizophrenia, stroke, Alzheimer's disease, ALS, and substance abuse show sex differences in incidence, age of onset, symptomatology or outcome (Clayton and Collins 2014). Of the neurological diseases mentioned above that demonstrate sex differences, several of these are also diseases in which TSPO, a biomarker of brain inflammation and injury, has been shown to be involved. The sex differences seen in cell number, differentiation, and function are thought to underlie some of the differences seen between males and females in the brain's response to pathological insults. Furthermore, studies have shown that astrocytes cultured from male or female postnatal day (PND) 1 mice, demonstrate differential responses to inflammatory challenges, not only in cytokine and chemokine expression, but also in TSPO expression (Santos-Galindo et al 2011). This variance in response appears to be mediated by testosterone, as astrocytes cultured from androgenized PND 1 females exhibited and mounted a similar inflammatory response as astrocytes cultured from PND 1 males (Santos-Galindo et al 2011). These results were in line with other studies demonstrating that cortical astrocytes from female mice are more resistant than male cortical astrocytes to oxygen-glucose deprivation (Liu et al 2007 and 2008). This protection was found to be associated with enhanced aromatase activity: the female cortical astrocytes had higher levels of aromatase expression and activity, and cell death can be prevented in the male astrocytes by either giving them the female astrocyte conditioned

media or by supplementing with estradiol. Additionally, cell death in female astrocytes could be induced by administering an aromatase inhibitor (Liu et al 2007 and 2008). Thus, if the inflammatory response of these two cell types is sexually dimorphic, then this has the potential to affect TSPO biology and thus is a critical avenue of study so that effects are not masked by not controlling for sex when generating cells for cell culture.

TSPO KO mice

The advent of the TSPO knockout mouse, which have no impairments in survival or steroidogenesis, was a major contradiction to the leading central dogma. This knockout mouse has completely redefined the TSPO field and will be a major tool in discovering what the actual function of TSPO is in various cell types in physiological and pathological conditions. In particular, these mice are particularly advantageous for microglia studies as siRNA and shRNA work are extremely challenging given the sensitivity of microglia in culture (i.e. more than 50% of the plated pure primary microglia die after 48 hours of incubation under normal culture condition) and the low yield of microglia per dissection. While other methods exist to increase the number of microglia extracted from a mixed glial culture (CD11b coated beads (Gordon et al 2011), mild trypsinization (Saura et al 2003)), these methods have the potential to increase the degree to which microglia are primed for activation. Our goal is to measure physiological responses of microglia, and not the responses of an already activated microglia. Cell culture conditions already put microglia in a slightly primed state, and thus adding a chemical component of activation, whether that is binding to a CD11b coated bead or through exposure to trypsin, has the potential to skew our results. Thus, we have made the decision to solely work with microglia that have been activated mechanically via shaking for 2-4 hours only (some groups do overnight), and allow the microglia to rest and reacclimate for 16-20 hours before using them for our studies.

We have recently acquired heterozygous TSPO knockout mice from Helmholtz Zentrum Munich (GMC) as part of the International Mouse Phenotyping Consortium (IMPC) and INFRAFRONTIER/European Mouse Mutant Archive (EMMA). TSPO tm1b mice were produced on a C57BL/6NTac background and mice were produced by treating 2-cell embryos with Cre enzyme as described previously (Ryder et al., 2014). Tm1b allele embryos have a reporter-tagged deletion allele (post-Cre). Critical exons, in this case exons 2 and 3 of *Tspo,* are deleted by creating a frame shift using the Cre method. Notably, our TSPO antibodies that we have validated bind to amino acids 161-169 which are located in exon 4 of *Tspo*.

While several lines of experiments are planned with these mice, we have generated some preliminary data to guide our future experiments in regards to examining the TSPO-NOX2 relationship. The rationale behind these preliminary studies is that if TSPO is interacting with these two NOX subunits, what happens to NOX levels when TSPO is no longer present? Our microglia data indicates a protein-protein interaction between TSPO and NOX2. Further, studies from neutrophils in patients with chronic granulomatous disease (CGD), also suggest a functional relationship between TSPO and NOX2. CGD is characterized by a mutation in one of five NOX subunits. X-CGD has a mutation in CYBB, the gene that encodes for $gp91^{phox}$. In patients with X-linked CGD, they have low superoxide activity and thus cannot generate a bactericidal response, presumably due the mutations in the heme binding domain of $gp91^{phox}$ that renders NOX2 non-functional and incapable of producing a superoxide burst. In these patients, Zavola et al 1990a noted that they had decreased levels of TSPO binding in the membrane of polymorphonuclear neutrophils (PMN's). This was in contrast to those patients with the autosomal recessive form of CGD, mutations in one of the other 5 NOX subunits, who do not have impairments in superoxide burst production from neutrophils and also had normal levels of TSPO binding in PMN's. Notably,

one X-CGD patient as noted in Lane 10 of Figure 3 of their paper, still had comparable levels of TSPO binding as compared to control patients. The authors of this paper acknowledge this case and attribute it to the patient being a variant for TSPO expression. However, other studies by Zavola's group have strengthened the direct relationship between TSPO binding and $gp91^{phox}$, in that treating monocytes from X-CGD patients with IFN-γ partially restores Cytb558 expression and phagocyte bactericidal activity, as well as TSPO levels in monocytes (Zavola et al 1990b). The authors suggest that TSPO is another NOX2 molecular component target of IFN-γ in CGD associated with Cytb558 deficiency.

However, most of the above mentioned studies have examined the relationship of TSPO in regards to CGD in neutrophils, with the exception of the IFN-γ studies using monocytes. Whether or not the TSPO-$gp91^{phox}$ relationship remains and/or is the same in other cell types such as microglia, remains to be determined. The relationship could potentially differ in that, at rest, neutrophils already have high levels of TSPO, whereas at rest, microglia have low levels of TSPO. A study by Canat et al 1992 and colleagues measured TSPO ligand binding and mRNA expression in human blood cell populations. The highest levels of TSPO were seen in neutrophils and monocytes, with intermediate levels in lymphocytes, and low levels in platelets and erythrocytes. Canat's study also suggested that in addition to the mitochondria, there must an additional subcellular location for TSPO, in addition to the mitochondria. Erythrocytes extrude their mitochondria before they leave the bone marrow, and neutrophils decrease mitochondrial content along the granulocyte differentiation pathway (Woods & Williams 1996). Both sets of authors suggest that TSPO can also be at the plasma membrane, one reason being that exposing intact PMNs to a TSPO antibody stimulated an oxidative burst (Zavala et al 1990). Similarly, Woods et al 1996 documented TSPO having two different subcellular localizations in two different rat liver

cell types, and Berkovich et al 1993 documented two different DBI binding sites in human leukocytes, presumably mitochondrial and plasma membrane, that demonstrated different affinities for two different endogenous ligands. However, our immunofluorescence studies indicate that in vehicle treated microglia, nearly 80% of TSPO is associated with VDAC, a mitochondrial protein. Therefore, potentially different subcellular localizations of TSPO could contribute to a different function of TSPO and therefore, a different relationship with NOX2.

It is also important to reiterate that the dose used in studies will have a major impact on whether TSPO will enhance an oxidative response. As Woods and Williams mention, benzodiazepines [TSPO] have biphasic effects where they will be stimulatory at low concentrations and inhibitory at high doses. They cite 4 studies: three indicating how picomolar concentrations of Ro induce chemotaxis (Ruff et al 1985) and how nanomolar concentrations of TSPO ligands induce a superoxide burst (Zavala et al 1987 and 1990; Choi et al 2011). In contrast, *in vivo* studies using 1 mg/kg TSPO-L i.p injections decreased the oxidative response in that there was less IL-1, IL-6, and TNF released. Thus, TSPO's relationship with NOX will likely vary based on TSPO ligand, TPSO ligand concentration, basal TSPO levels of that cell type, subcellular localization of TSPO, as well as the oxidative/redox state of the cell type.

In our initial studies with the TSPO KO mice, we have confirmed that TSPO is indeed deleted from knockout animals (Figure 2), both at the gene and the protein level. To begin to explore how a global knockout of TSPO affects NOX levels in brain tissue, we are starting by assessing $gp91^{phox}$ and $p22^{phox}$ protein expression in brain regions dissected from 3 month male and female wildtype (WT), heterozygous (Het), and knockout (KO) mice. We have performed Western blot in 6 brains regions (brainstem, cerebellum, cortex, hippocampus, midbrain, striatum) for 1 female wildtype and 1 female knockout (Figure 4), as well as in the brainstem and cerebellum

of 2 male wildtype, heterozygous, and knockout animals (Figure 3), and are in the process of collecting tissue to have n = 6 for each group. While the n is low (n=3), current data suggests that global TSPO KO mice have increased $gp91^{phox}$ protein levels in certain brain regions as compared to WT mice. We see a 1.5 fold increase in the midbrain in TSPO KO female mouse as compared to the female wildtype. (Notably, the midbrain which contains the substantia nigra, has been documented to have the greatest density of microglia in the brain (Mittelbronn et al 2001)). In TSPO KO males, we see a 2.2 fold increase in brainstem and a 1.6 fold increase in the cerebellum of $gp91^{phox}$ protein levels as compared to the male wildtype. It is important to note we cannot compare across brain regions, as each region contains its own proportion of microglia, astrocytes, neurons, oligodendrocytes, etc and only certain cell types are documented and/or expected to express NOX2 or TSPO. It will be critical to assess protein levels at the cellular level in cells (e.g., microglia) cultured from TSPO WT, Het, and KO brains.

Interestingly, the molecular weight of $gp91^{phox}$ is around 91 kDa in tissue samples, whereas the molecular weight of $gp91^{phox}$ in our microglia cultures was about 58 kDa. This molecular weight in cell culture corresponds with the specified molecular weight on the product sheet, as well as several other groups reporting this molecular weight in cell culture (Yu et al 1998; Zhen et al 1998; Argawal et al 2012; Jacobsen et al 1999). This discrepancy in our data regarding the molecular weight can potentially be attributed to the fact that microglia may depend on signals from other cells within the brain to initiate glycosylation of the precursor of $gp91^{phox}$, gp65. It will be critical to assess NOX2 activity levels both in microglia cultures, mixed glial cultures, and within brain tissue.

We have also generated some preliminary immunocytochemistry data from microglia generated from TSPO WT and KO mice. Triple-labeled immunofluorescence again confirms the

deletion of TSPO. Additionally, in measuring total gray value, gp91 signal was greater in TSPO KO microglia as compared to TSPO WT microglia (Figure 5).

Thus far the preliminary studies have only examined basal levels of proteins. It will be interesting to see how a TSPO KO mouse responds when a biological challenge is presented (i.e. LPS, PMA, etc) at the behavioral and pathological level. Most studies using TSPO KO mice have mainly focused on characterizing the mouse and these studies have found few differences compared to WT mice (Tu et al 2014; Morohaku et al; Banati et al 2014). While Banati and colleagues did determine that in response to a facial lesion axotomy, microglia could still activate without expressing TSPO, it will be vitally important to see how the inflammatory response trajectory is different in the TSPO KO mice.

Thus, given the background of uncertainty regarding the function of TSPO, it has become critical to re-examine the function of TSPO in all contexts, not only including cell type, but also within regards to sex, species, inflammation activation models, time course and TSPO genotype. This increase in knowledge will serve to maximize TSPO's potential not only as a biomarker of brain injury and disease progression, but also its promise as a therapeutic target in neurodegenerative disease and neurotoxicant exposure. Our studies examining TSPO's relationship and interactions with NOX2 and VDAC in particular have the potential to revolutionize and redefine the TSPO field and aid in designing better therapeutic interventions for the multitude of neurological diseases that involve neuroinflammation as assessed by TSPO and excessive/pathological levels of ROS production as assessed by NOX2 activity. However, as alluded to earlier, TSPO modulation of ROS production is bimodal, and the effects are highly dependent on TSPO ligand concentration and duration of exposure, as well as the cell types used.

These differential effects support TSPO's role in maintaining homeostasis and how its role may vary in physiological (healthy) and pathological (diseased). As researchers, we will need to be meticulous in documenting conditions so that we can fully and accurately ascertain when and in which contexts TSPO-ligand administration may be therapeutic and useful in ameliorating neuroinflammation.

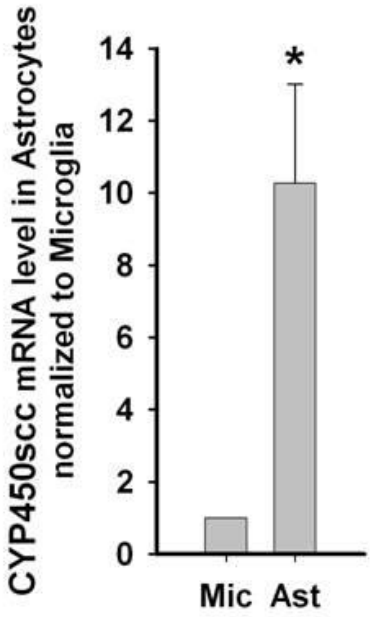

FIGURE 1. CYP450scc mRNA Levels in Rat Microglia & Astrocytes

Measuring the mRNA levels in the first enzyme of the steroidogenesis pathway, CYP450scc which converts cholesterol to pregnenolone, in microglia vs. astrocytes. Astrocytes have about 10 fold greater levels of this enzyme indicating potentially higher levels of steroid synthesis occurring in astrocytes as compared to microglia.

N.B. Experiment and analysis courtesy of and provided by Dr. Chun Zhou.

A.

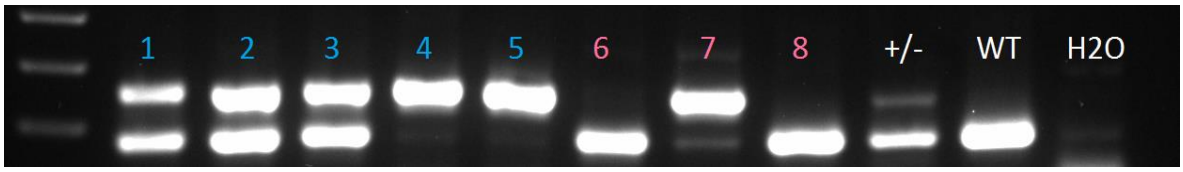

B.

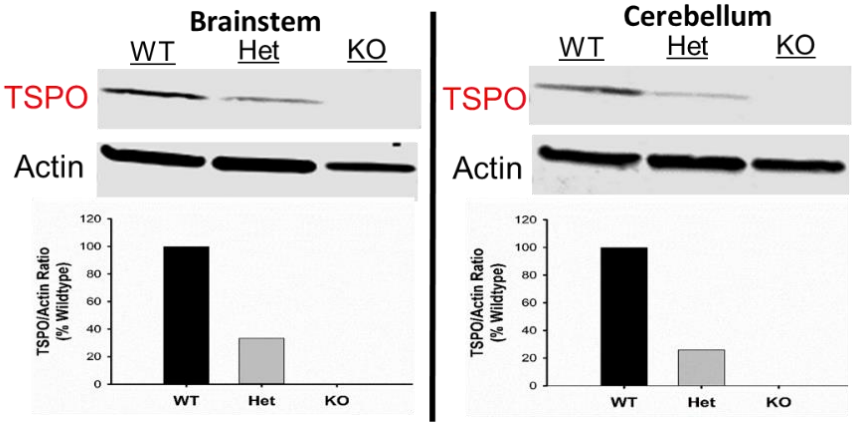

FIGURE 2. Genotype confirmation of TSPO wildtype, heterozygous, and knockout mice.

TSPO endpoint genotyping representing wildtype (WT), heterozygous (Het), and knockout (KO) mice (A). The lower band represents TSPO (188 bp), and the higher band represents LAR3 (244 bp), which is inserted when TSPO is deleted to confirm that the gene is in fact deleted and not merely the absence of detection. Therefore, two bands represent a Het mouse (Lanes 1, 2, 3, and +/- as a positive Het control). One upper band represents a KO (Lanes 4, 5, and 7). One lower band represents a WT (Lanes 6, 8, and WT the positive control). Western blot confirms genotypes of the animals as assessed by TSPO protein levels in the dissected brains regions of the brainstem and cerebellum (B). Based off of the TSPO Het animals, one allele does not appear sufficient to compensate for normal TSPO protein levels.

N.B. Genotyping in Panel A done by and courtesy of Ms. Deborah Brooks

A.

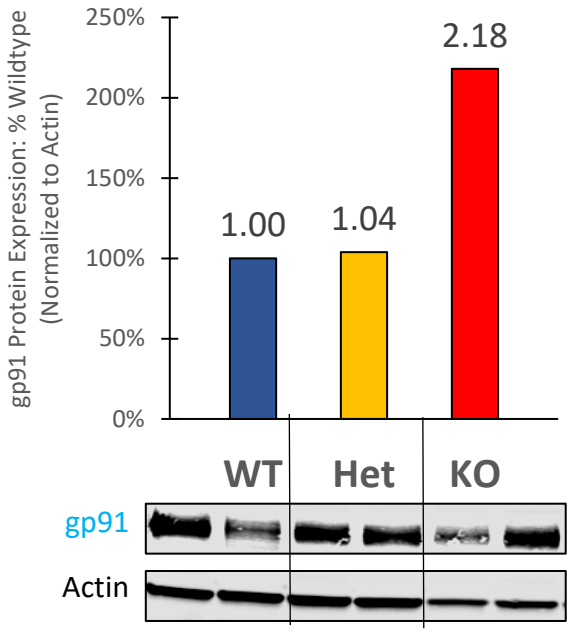

B.

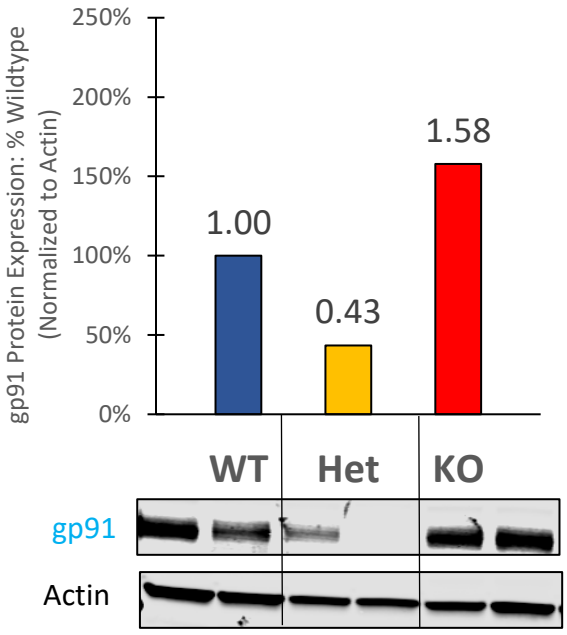

FIGURE 3. gp91^{phox} Protein Levels in Brain Tissue: Males

Preliminary data suggests that in the brainstem (A) and cerebellum (B), gp91/actin ratios are elevated in TSPO male knockout mice as compared to TSPO wildtype mice. n = 2 animals per genotype, with each sample run in duplicate (duplicates not shown).

A.

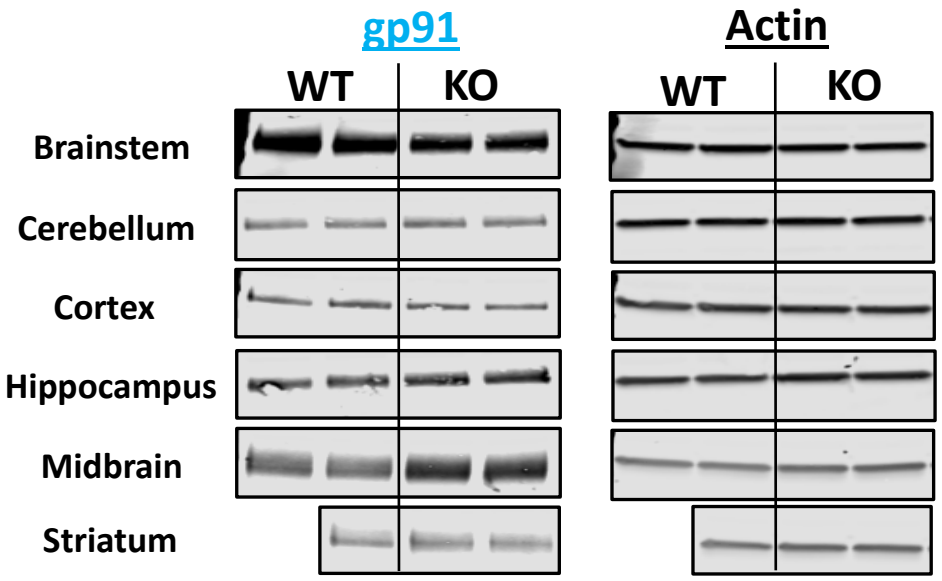

B.

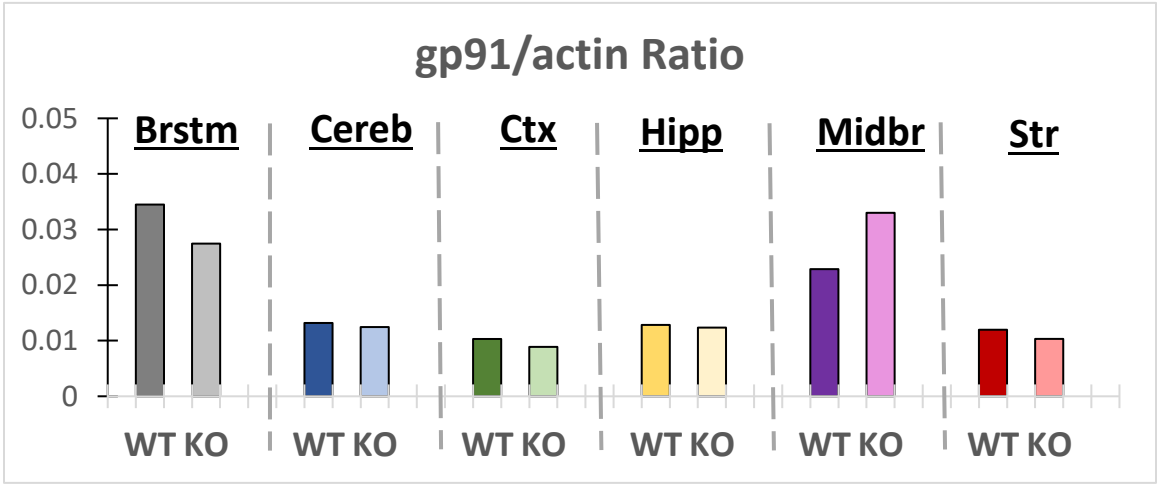

FIGURE 4. gp91 Protein Levels in Brain Tissue: Females

Preliminary data suggests gp91/actin ratios are similar in WT and KO female animals, except for the midbrain, where gp91 levels were 44% higher in the KO as compared to WT. Figure 3 and 4 suggest that there may be sex differences in the TSPO KO mice in regards to gp91 protein levels. n = 1 animal per genotype. Samples were run in duplicate, as shown.

A. **B.**

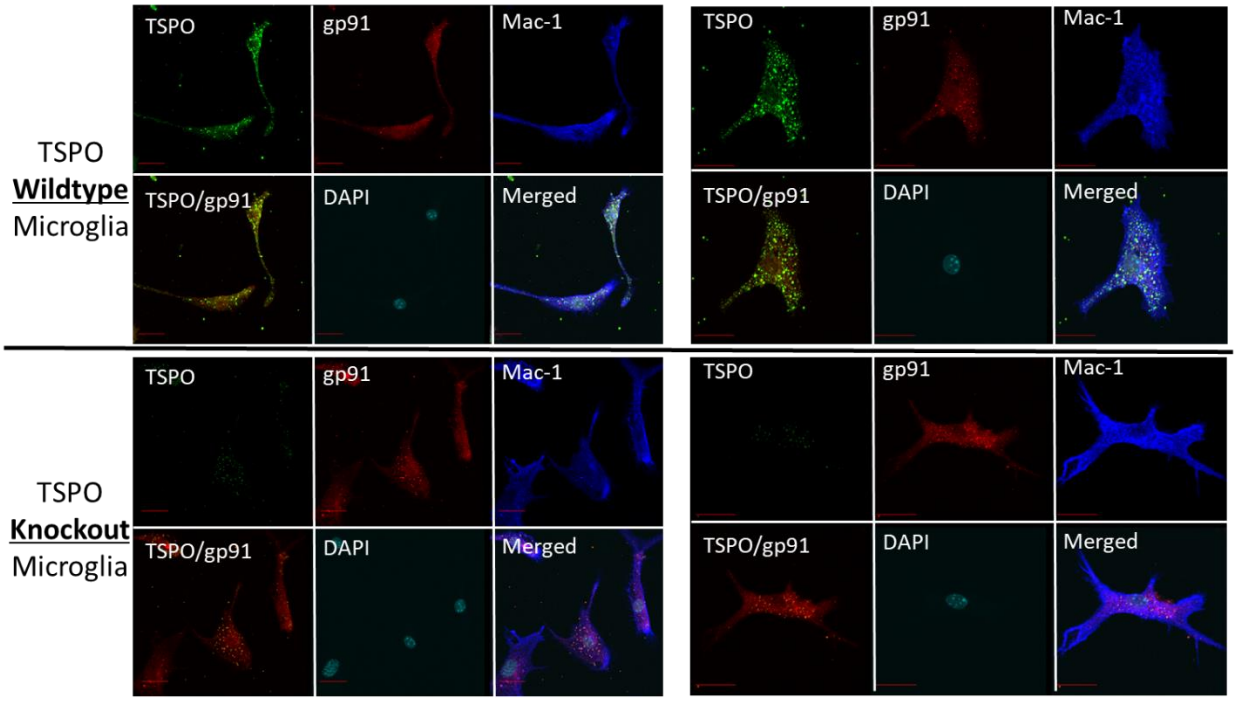

C.

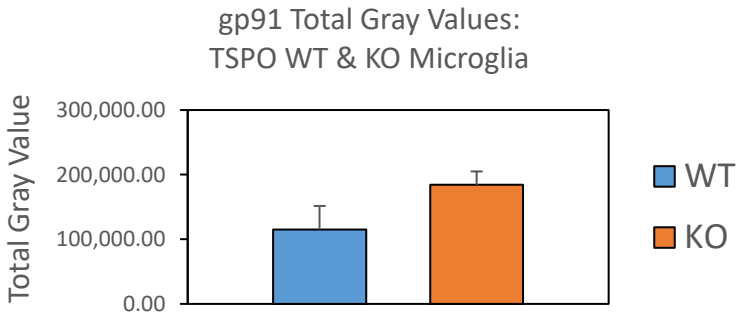

FIGURE 5. TSPO and gp91^{phox} Immunocytochemistry in TSPO WT & KO Microglia

Preliminary confocal imaging of TSPO WT and KO microglia at low magnification (A) and high magnification (B) confirms the deletion of TSPO. Quantification of the total gray value for gp91 indicates higher levels in TSPO KO microglia as compared to TSPO WT microglia. Scale bar = 20 um. n = 1 with 20+ cells imaged per genotype.

REFERENCES

Akira, S., & Takeda, K. (2004). Functions of toll-like receptors: lessons from KO mice. *C R Biol, 327*(6), 581-589.

Bae, K. R., Shim, H. J., Balu, D., Kim, S. R., & Yu, S. W. (2014). Translocator protein 18 kDa negatively regulates inflammation in microglia. *J Neuroimmune Pharmacol, 9*(3), 424-437. doi:10.1007/s11481-014-9540-6

Barron, A. M., Garcia-Segura, L. M., Caruso, D., Jayaraman, A., Lee, J. W., Melcangi, R. C., & Pike, C. J. (2013). Ligand for translocator protein reverses pathology in a mouse model of Alzheimer's disease. *J Neurosci, 33*(20), 8891-8897. doi:10.1523/JNEUROSCI.1350-13.2013

Beckers, L., Ory, D., Geric, I., Declercq, L., Koole, M., Kassiou, M., . . . Baes, M. (2018). Increased Expression of Translocator Protein (TSPO) Marks Pro-inflammatory Microglia but Does Not Predict Neurodegeneration. *Mol Imaging Biol, 20*(1), 94-102. doi:10.1007/s11307-017-1099-1

Block, M. L., Zecca, L., & Hong, J. S. (2007). Microglia-mediated neurotoxicity: uncovering the molecular mechanisms. *Nat Rev Neurosci, 8*(1), 57-69. doi:10.1038/nrn2038

Burgi, B., Lichtensteiger, W., & Schlumpf, M. (2000). Diazepam-binding inhibitor/acyl-CoA-binding protein mRNA and peripheral benzodiazepine receptor mRNA in endocrine and immune tissues after prenatal diazepam exposure of male and female rats. *J Endocrinol, 166*(1), 163-171.

Canat, X., Carayon, P., Bouaboula, M., Cahard, D., Shire, D., Roque, C., . . . Casellas, P. (1993). Distribution profile and properties of peripheral-type benzodiazepine receptors on human hemopoietic cells. *Life Sci, 52*(1), 107-118.

Chen, M. K., Baidoo, K., Verina, T., & Guilarte, T. R. (2004). Peripheral benzodiazepine receptor imaging in CNS demyelination: functional implications of anatomical and cellular localization. *Brain, 127*(Pt 6), 1379-1392. doi:10.1093/brain/awh161

Clayton, J. A., & Collins, F. S. (2014). Policy: NIH to balance sex in cell and animal studies. *Nature, 509*(7500), 282-283.

Colton, C., Wilt, S., Gilbert, D., Chernyshev, O., Snell, J., & Dubois-Dalcq, M. (1996). Species differences in the generation of reactive oxygen species by microglia. *Mol Chem Neuropathol, 28*(1-3), 15-20. doi:10.1007/BF02815200

Drugan, R. C., Holmes, P. V., & Stringer, A. P. (1991). Sexual dimorphism of stress-induced changes in renal peripheral benzodiazepine receptors in rat. *Neuropharmacology, 30*(4), 413-416.

Fairweather, D., Coronado, M. J., Garton, A. E., Dziedzic, J. L., Bucek, A., Cooper, L. T., Jr., . . . Guilarte, T. R. (2014). Sex differences in translocator protein 18 kDa (TSPO) in the heart: implications for imaging myocardial inflammation. *J Cardiovasc Transl Res, 7*(2), 192-202. doi:10.1007/s12265-013-9538-0

Garcia, E. F., & Woolley, D. E. (2008). Gender differences in brain peripheral benzodiazepine receptor (PBR) expression and seizures produced by heptachlor during development. *Proc West Pharmacol Soc, 51*, 18-22.

Gordon, R., Hogan, C. E., Neal, M. L., Anantharam, V., Kanthasamy, A. G., & Kanthasamy, A. (2011). A simple magnetic separation method for high-yield isolation of pure primary microglia. *J Neurosci Methods, 194*(2), 287-296. doi:10.1016/j.jneumeth.2010.11.001

Haynes, S. E., Hollopeter, G., Yang, G., Kurpius, D., Dailey, M. E., Gan, W. B., & Julius, D. (2006). The P2Y12 receptor regulates microglial activation by extracellular nucleotides. *Nat Neurosci, 9*(12), 1512-1519. doi:10.1038/nn1805

Kawashima, N., Tsuji, D., Okuda, T., Itoh, K., & Nakayama, K. (2009). Mechanism of abnormal growth in astrocytes derived from a mouse model of GM2 gangliosidosis. *J Neurochem, 111*(4), 1031-1041. doi:10.1111/j.1471-4159.2009.06391.x

Kopec, A., Smith, C. J., Ayre, N. R., Sweat, S. C., & Bilbo, S. D. (2017). Microglial elimination of dopamine D1 receptors defines sex-specific changes in nucleus accumbens development and social play behavior during adolescence. *bioRxiv*. doi:10.1101/211029

Kuhlmann, A. C., & Guilarte, T. R. (1999). Regional and temporal expression of the peripheral benzodiazepine receptor in MPTP neurotoxicity. *Toxicol Sci, 48*(1), 107-116.

Kuhlmann, A. C., & Guilarte, T. R. (2000). Cellular and subcellular localization of peripheral benzodiazepine receptors after trimethyltin neurotoxicity. *J Neurochem, 74*(4), 1694-1704.

Kuo, J., Hamid, N., Bondar, G., Dewing, P., Clarkson, J., & Micevych, P. (2010). Sex differences in hypothalamic astrocyte response to estradiol stimulation. *Biol Sex Differ, 1*(1), 7. doi:10.1186/2042-6410-1-7

Kyrkanides, S., Brouxhon, S. M., Tallents, R. H., Miller, J. N., Olschowka, J. A., & O'Banion, M. K. (2012). Conditional expression of human beta-hexosaminidase in the neurons of Sandhoff disease rescues mice from neurodegeneration but not neuroinflammation. *J Neuroinflammation, 9*, 186.

Lavisse, S., Guillermier, M., Herard, A. S., Petit, F., Delahaye, M., Van Camp, N., . . . Escartin, C. (2012). Reactive astrocytes overexpress TSPO and are detected by TSPO positron emission tomography imaging. *J Neurosci, 32*(32), 10809-10818. doi:10.1523/JNEUROSCI.1487-12.2012

Le Fur, G., Guilloux, F., Rufat, P., Benavides, J., Uzan, A., Renault, C., . . . Gueremy, C. (1983). Peripheral benzodiazepine binding sites: effect of PK 11195, 1-(2-chlorophenyl)-N-methyl-(1-methylpropyl)-3 isoquinolinecarboxamide. II. In vivo studies. *Life Sci, 32*(16), 1849-1856.

Liddelow, S. A., Guttenplan, K. A., Clarke, L. E., Bennett, F. C., Bohlen, C. J., Schirmer, L., . . . Barres, B. A. (2017). Neurotoxic reactive astrocytes are induced by activated microglia. *Nature, 541*(7638), 481-487. doi:10.1038/nature21029

Liu, M., Hurn, P. D., Roselli, C. E., & Alkayed, N. J. (2007). Role of P450 aromatase in sex-

specific astrocytic cell death. *J Cereb Blood Flow Metab, 27*(1), 135-141. doi:10.1038/sj.jcbfm.9600331

Liu, M., Oyarzabal, E. A., Yang, R., Murphy, S. J., & Hurn, P. D. (2008). A novel method for assessing sex-specific and genotype-specific response to injury in astrocyte culture. *J Neurosci Methods, 171*(2), 214-217. doi:10.1016/j.jneumeth.2008.03.002

Loth, M. K., Choi, J., McGlothan, J. L., Pletnikov, M. V., Pomper, M. G., & Guilarte, T. R. (2016). TSPO in a murine model of Sandhoff disease: presymptomatic marker of neurodegeneration and disease pathophysiology. *Neurobiol Dis, 85*, 174-186. doi:10.1016/j.nbd.2015.11.001

Maeda, J., Higuchi, M., Inaji, M., Ji, B., Haneda, E., Okauchi, T., . . . Suhara, T. (2007). Phase-dependent roles of reactive microglia and astrocytes in nervous system injury as delineated by imaging of peripheral benzodiazepine receptor. *Brain Res, 1157*, 100-111. doi:10.1016/j.brainres.2007.04.054

Mittelbronn, M., Dietz, K., Schluesener, H. J., & Meyermann, R. (2001). Local distribution of microglia in the normal adult human central nervous system differs by up to one order of magnitude. *Acta Neuropathol, 101*(3), 249-255.

Owen, D. R., Narayan, N., Wells, L., Healy, L., Smyth, E., Rabiner, E. A., . . . Moore, C. S. (2017). Pro-inflammatory activation of primary microglia and macrophages increases 18 kDa translocator protein expression in rodents but not humans. *J Cereb Blood Flow Metab, 37*(8), 2679-2690. doi:10.1177/0271678X17710182

Robert, R., Ghazali, D. A., Favreau, F., Mauco, G., Hauet, T., & Goujon, J. M. (2011). Gender difference and sex hormone production in rodent renal ischemia reperfusion injury and repair. *J Inflamm (Lond), 8*, 14. doi:10.1186/1476-9255-8-14

Rothhammer, V., Borucki, D. M., Tjon, E. C., Takenaka, M. C., Chao, C. C., Ardura-Fabregat, A., . . . Quintana, F. J. (2018). Microglial control of astrocytes in response to microbial metabolites. *Nature, 557*(7707), 724-728. doi:10.1038/s41586-018-0119-x

Ruff, M. R., Pert, C. B., Weber, R. J., Wahl, L. M., Wahl, S. M., & Paul, S. M. (1985). Benzodiazepine receptor-mediated chemotaxis of human monocytes. *Science, 229*(4719), 1281-1283.

Ryder, E., Doe, B., Gleeson, D., Houghton, R., Dalvi, P., Grau, E., . . . Ramirez-Solis, R. (2014). Rapid conversion of EUCOMM/KOMP-CSD alleles in mouse embryos using a cell-permeable Cre recombinase. *Transgenic Res, 23*(1), 177-185. doi:10.1007/s11248-013-9764-x

Santos-Galindo, M., Acaz-Fonseca, E., Bellini, M. J., & Garcia-Segura, L. M. (2011). Sex differences in the inflammatory response of primary astrocytes to lipopolysaccharide. *Biol Sex Differ, 2*, 7. doi:10.1186/2042-6410-2-7

Saura, J., Tusell, J. M., & Serratosa, J. (2003). High-yield isolation of murine microglia by mild trypsinization. *Glia, 44*(3), 183-189. doi:10.1002/glia.10274

Savchenko, V. L. (2013). Regulation of NADPH oxidase gene expression with PKA and cytokine IL-4 in neurons and microglia. *Neurotox Res, 23*(3), 201-213. doi:10.1007/s12640-012-9327-6

Skaper, S. D., Debetto, P., & Giusti, P. (2010). The P2X7 purinergic receptor: from physiology to neurological disorders. *FASEB J, 24*(2), 337-345. doi:10.1096/fj.09-138883

Veenman, L., Papadopoulos, V., & Gavish, M. (2007). Channel-like functions of the 18-kDa translocator protein (TSPO): regulation of apoptosis and steroidogenesis as part of the host-defense response. *Curr Pharm Des, 13*(23), 2385-2405.

Weizman, R., Lehmann, J., Leschiner, S., Allmann, I., Stoehr, T., Heidbreder, C., . . . Gavish, M. (1999). Long-lasting effect of early handling on the peripheral benzodiazepine receptor. *Pharmacol Biochem Behav, 64*(4), 725-729.

Woods, M. J., & Williams, D. C. (1996). Multiple forms and locations for the peripheral-type benzodiazepine receptor. *Biochem Pharmacol, 52*(12), 1805-1814.

Woods, M. J., Zisterer, D. M., & Williams, D. C. (1996). Two cellular and subcellular locations for the peripheral-type benzodiazepine receptor in rat liver. *Biochem Pharmacol, 51*(10), 1283-1292.

Zavala, F., & Lenfant, M. (1987). Benzodiazepines and PK 11195 exert immunomodulating activities by binding on a specific receptor on macrophages. *Ann N Y Acad Sci, 496*, 240-249.

Zavala, F., & Lenfant, M. (1987). Peripheral benzodiazepines enhance the respiratory burst of macrophage-like P388D1 cells stimulated by arachidonic acid. *Int J Immunopharmacol, 9*(3), 269-274.

Zavala, F., Taupin, V., & Descamps-Latscha, B. (1990). In vivo treatment with benzodiazepines inhibits murine phagocyte oxidative metabolism and production of interleukin 1, tumor necrosis factor and interleukin-6. *J Pharmacol Exp Ther, 255*(2), 442-450.

Zavala, F., Veber, F., & Descamps-Latscha, B. (1990). Altered expression of neutrophil peripheral benzodiazepine receptor in X-linked chronic granulomatous disease. *Blood, 76*(1), 184-188.

Zavala, F., Veber, F., Taupin, V., Nguyen, A. T., & Descamps-Latscha, B. (1990). Reconstitution of peripheral benzodiazepine receptor expression in X-linked chronic granulomatous disease by interferon-gamma. *Lancet, 336*(8717), 758-759.